Design and Synthesis of Allosteric Inhibitors against Dengue Virus Protease

Dissertation

Zur Erlangung des Doktorgrades
der Naturwissenschaften (Dr. rer. nat.)

dem
Fachbereich Pharmazie der Philipps-Universität Marburg
vorgelegt von

M. Sc. (Chemie) Kerstin Mark

aus
Waldbröl

Die Untersuchungen zur vorliegenden Arbeit wurden am Institut für Pharmazeutische Chemie des Fachbereichs Pharmazie der Philipps-Universität Marburg unter Anleitung von Frau Prof. Dr. Wibke E. Diederich in der Zeit von Februar 2018 bis Juli 2021 durchgeführt.

Abgabedatum: 21.10.2021

Tag der mündlichen Prüfung: 09.12.2021

Erstgutachter: Prof. Dr. Wibke E. Diederich

Zweitgutachter: Prof. Dr. Torsten Steinmetzer

Hochschulkennziffer: 1180

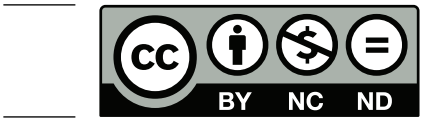
BY NC ND

„Nature is relentless and unchangeable, and it is indifferent as to whether its hidden reasons and actions are understandable to man or not.“

- Galileo Galilei

I Table of Contents

II Kurzzusammenfassung

Obwohl Denguefieber mit etwa 390 Millionen Infektionen pro Jahr die weltweit häufigste durch Arthropoden übertragene Krankheit ist, gibt es bisher keine zugelassene spezifische therapeutische Behandlung. Daher befasste sich diese Arbeit mit dem Design und der Synthese neuartiger allosterischer DENV-Proteaseinhibitoren als potenzielle Wirkstoffe gegen das Denguefieber. Als Ausgangspunkt wurde ein *in silico High Throughput Screening* (HTS) durchgeführt, das die allosterische Tasche der geschlossenen Konformation der DENV3-Protease als Rezeptor und die ZINC15 Lead-Like Bibliothek als Input für das Docking verwendete. Dies führte zu einer Auswahl von 15 Verbindungen, die gekauft und in einem fluoreszenzbasierten Enzym-Assay *in vitro* getestet wurden. Die wirksamste Verbindung aus diesem Set zeigte einen vielversprechenden IC_{50}-Wert von 136±16 μM gegen die DENV3-Protease sowie einen nicht-kompetitiven Bindungsmodus und wurde erfolgreich auf ein Leitfragment reduziert, das ebenfalls eine signifikante Hemmung der DENV-Protease zeigte. Dieses Leitfragment diente als Ausgangspunkt für einen *in silico Fragment growing*-Ansatz, der nach Docking und Bewertung zu einer Auswahl von 17 Verbindungen führte, die synthetisiert und ebenfalls *in vitro* getestet wurden. Vier dieser Verbindungen zeigten eine signifikant erhöhte Aktivität gegenüber der DENV3-Protease im fluoreszenzbasierten Assay im Vergleich zum initialen Screening-Hit, wobei die effektivste Verbindung einen IC_{50}-Wert von 28±7.9 μM gegenüber der DENV3 Protease zeigte. Ein allgemeines strukturelles Motiv, das den wirksamsten Inhibitoren gemeinsam ist, wurde identifiziert und als Vorlage für eine umfassende *Structure-Activity Relationship* (SAR) Studie verwendet, die wichtige Merkmale der Protein-Ligand-Interaktionen aufdeckte. Die wirksamste Verbindung in der SAR-Studie (IC_{50}(DENV3)=12.3±3.5 μM) zeigte auch eine hohe Wirksamkeit gegenüber einem binären DENV4-Proteasekonstrukt und gegen die ZIKV-Protease, mit einem IC_{50}-Wert gegen letztere im niedrigen mikromolaren Bereich. Der nicht-kompetitive Bindungsmodus wurde auch für die optimierten Ligandenstrukturen bestätigt, und es wurden erste Mutationsexperimente durchgeführt, um die tatsächliche Bindungsstelle in der Protease zu klären. Zellbasierte Experimente zeigten eine geringe Zytotoxizität der etablierten Ligandenserie bei Konzentrationen von bis zu 25 μM und eine relative Hemmung der ZIKV-Replikation von mehr als 50% bei Konzentrationen von 5-10 μM. Insgesamt bilden die in dieser Arbeit erzielten Ergebnisse eine gute Grundlage für die weitere Entwicklung potenter flaviviraler Proteaseinhibitoren.

III Abstract

Although dengue fever is the most common arthropod-borne disease worldwide, with approximately 390 million infections per year, no specific therapeutic treatment is available to date. Therefore, this thesis addressed the design and synthesis of novel allosteric DENV protease inhibitors as potential anti-dengue drugs. As a starting point, an *in silico* High Throughput Screening (HTS) was performed targeting the closed conformation allosteric pocket of DENV3 protease using the ZINC15 lead-like library as input for docking. This resulted in a selection of 15 compounds that were purchased and tested in a fluorescence-based enzyme assay *in vitro*. The most potent compound from this set showed a promising IC_{50} value of 136±16 μM against DENV3 protease as well as a non-competitive binding mode and was successfully simplified to a core fragment, which also showed significant inhibition of the DENV protease. This core fragment served as starting point for an *in silico* fragment growing approach, which after docking and evaluation resulted in a selection of 17 compounds to be synthesized and tested *in vitro*. Four of these compounds showed significantly increased activity toward DENV3 protease compared to the initial hit in the fluorescence-based assay, with an IC_{50} value of 28±7.9 μM against DENV3 protease for the most potent one. A general structural motif common to the most effective inhibitors was identified and used as a template for a comprehensive SAR study that revealed important features of the protein-ligand interactions. The most potent compound resulting from this study (IC_{50}(DENV3)=12.3±3.5 μM) also showed high potency against a binary DENV4 protease construct and against ZIKV protease, with an IC_{50} value against the latter in the low micromolar range. The non-competitive binding mode was also confirmed for the optimized ligand structures, and preliminary mutation experiments were conducted to clarify the actual binding site in the protease. Cell-based experiments revealed low cytotoxicity of the established ligand series at concentrations up to 25 μM and relative inhibition of ZIKV replication of more than 50% at concentrations of 5-10 μM. Overall, the results obtained in this thesis provide a good basis for further development of potent flaviviral protease inhibitors.

IV List of Abbreviations

AA amino acid

ADE antibody-dependent enhancement

ADT AutoDock Tools

AMC 7-amino-4-methylcoumarin

APCI atmospheric pressure chemical ionization

aq aqueous

Ar aromatic residue

Boc *tert*-butylcarbonate

BPTI bovine pancreatic Trypsin inhibitor

Bz benzoyl

Chaps 3-[dimethyl[3-(3α,7α,12α-trihydroxy-5β-cholan-24-amido)propyl]azaniumyl] propane-1-sulfonate

CPE (virus-induced) cytopathic effect

Cyhex cyclohexane

dba dibenzylideneacetone

DCM dichloromethane

DEE diethyl ether

DENV Dengue virus

DF Dengue fever

DHF Dengue hemorrhagic fever

DIPEA *N*-ethyl-*N*-(propan-2-yl)propan-2-amine

dist. distilled

DMAP 4-dimethylaminopyridine

DMF *N,N*-dimethylformamide

DMSO dimethylsulfoxide

DSS Dengue shock syndrome

DTT dithiothreitol

EA elemental analysis/combustion analysis

EDCI 1-ethyl-3-(3-dimethylaminopropyl)carbodiimide

EI electron ionization

eq equivalent(s)

ER endoplasmic reticulum

ESI electrospray ionization

Et ethyl

et al. et alia (lat.): and others

EtOAc ethyl acetate

EtOH ethanol

HBTU (2-(1*H*-benzotriazol-1-yl)-1,1,3,3-tetramethyluronium hexafluorophosphate

HOAc acetic acid

HOBt 1-hydroxybenzotriazole

HPLC high performance liquid chromatography

HPP *Hit Picking Party*, plenary discussion of docking results

HR-MS high-resolution mass spectrometry

HTS high-throughput screening

^{i}**PrOH** 2-propanol

L ligand

LC-MS liquid chromatography coupled with mass spectrometry

LLE lipophilic ligand efficiency

MD molecular dynamics

Me methyl

MeCN acetonitrile

MeOH methanol

M.P. melting point

MTBE methyl *tert*-butylether

MTT (3-(4,5-dimethylthiazol-2-yl)-2,5-diphenyltetrazolium bromide

NAD(P)H Nicotinamide adenine dinucleotide (phosphate)

NCI national cancer institute (USA)

n.d. not determined

NMR nuclear magnetic resonance (spectroscopy)

NS non-structural

Nu nucleophile

pdb protein data bank

prep preparative

PyBOP benzotriazol-1-yloxytripyrrolidinophosphonium hexafluorophosphate

RNA ribonucleic acid

RT room temperature

SAR structure-activity relationship

S-Phos dicyclohexyl(2',6'-dimethoxy[1,1'-biphenyl]-2-yl)phosphane

TBEV tick-borne encephalitis virus

TEA triethylamine

TFA trifluoroacetic acid

THF tetrahydrofuran

TLC thin layer chromatography

TOF time of flight

Tris tris(hydroxymethyl)aminomethane

Triton X-100 O-[4-(1,1,3,3-tetramethylbutyl)phenoxy]polyethoxyethanol

UV ultra violet light

WNV West Nile virus

wt weight

YFV yellow fever virus

ZIKV Zika virus

1 Introduction

1.1 Dengue Virus

1.1.1 Epidemiology and Clinical Disease

Dengue Virus (DENV) is a so-called arbovirus, as it is transmitted to humans by the mosquitoes *Aedes aegypti* and *Aedes albopictus* and is therefore endemic in tropical and subtropical regions.[1] Today, 3.6 billion people in more than 100 countries are at risk of infection, making DENV the leading arthropod-borne disease in the world.[2] But only about 25% of infected people develop symptomatic disease, so the number of infections can only be estimated at about 390 millions per year (2010 data).[3] If clinical symptoms develop, most patients suffer from a self-limiting fever, called Dengue Fever (DF), which is accompanied by headache, severe muscle and joint pain as well as rash.[2] However, some patients also develop severe manifestations, namely Dengue haemorrhagic fever (DHF) or Dengue shock syndrome (DSS), which are characterized by rapid onset of capillary leakage and may be fatal.[2]

1.1.2 Genetics and Replication Mechanism

DENV is a single-stranded (+)-sense RNA virus belonging to the genus *Flavivirus* within the family *Flaviviridae*. This genus also includes other human pathogens such as yellow fever virus (YFV), West Nile virus (WNV), tick-borne encephalitis virus (TBEV) and Zika virus (ZIKV).[4] The virions of DENV are approx. 50 nm spheres consisting of structural proteins C, E and prM/M, a lipid envelope, and a 10.7 kbp capped RNA and primarily infect monocytes, macrophages, dendritic cells, and mast cells in the human body.[2]
The basic life cycle of DENV in human cells is shown in Figure 1.1 and may be described as follows:[5]

1. The virus enters the host cell by receptor-mediated endocytosis.
2. The acidic conditions inside the endosome cause a trimerisation of the viral E-protein which leads to the release of the nucleocapsid into the cytoplasm.
3. At the endoplasmic reticulum (ER) membrane, the viral polyprotein is synthesized using the host cell machinery.
4. The polyprotein is cleaved into individual proteins by a viral and host-cell proteases.
5. The viral genome is also replicated at the ER and immature virions bud into the ER lumen.

6. The maturation of the viral particles takes place at the trans-golgi network and includes cleavage of the prM protein by the host protease furin.

7. The mature virus particles are released from the cell by exocytosis.

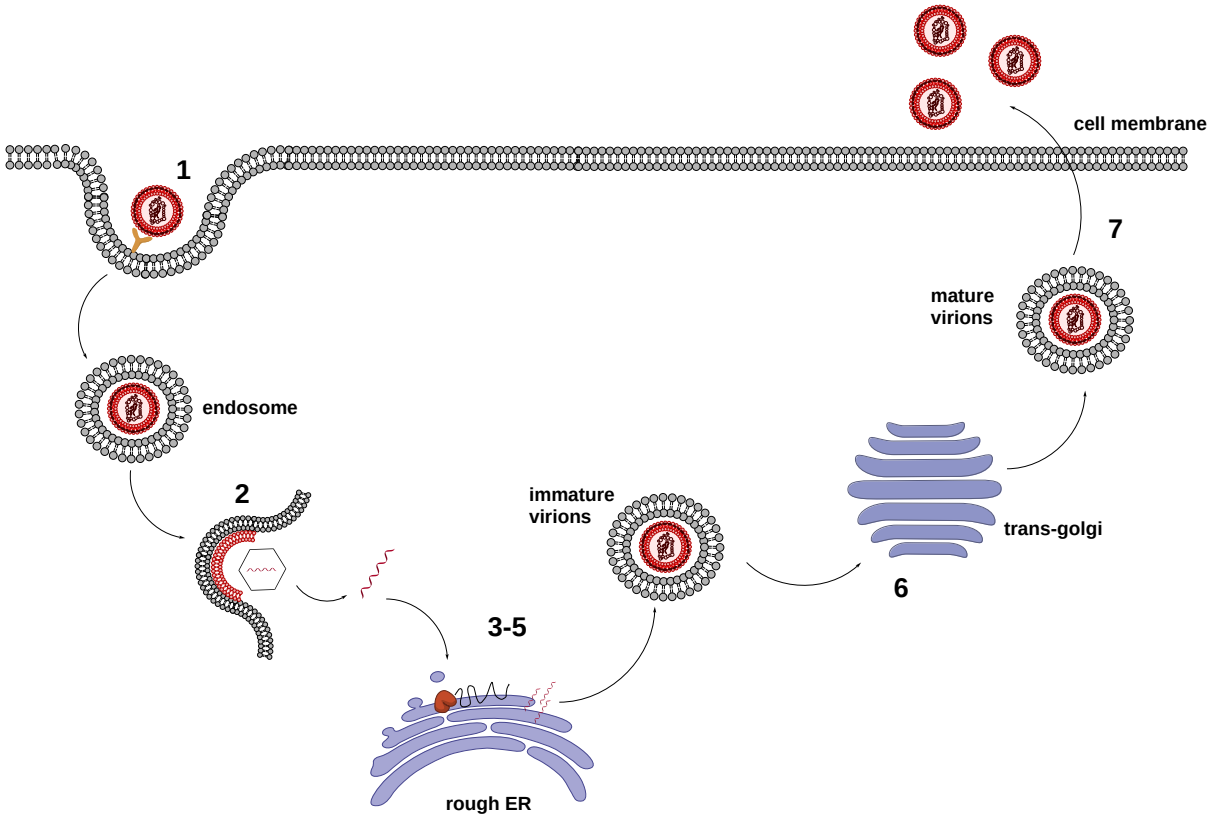

Fig. 1.1 The schematic life cycle of DENV in human host cells (data from [2]).

An essential step in the viral life cycle is the cleavage of the viral polyprotein, which is anchored to the ER membrane by numerous transmembrane domains in the replication complex (Figure 1.2).[3] From the ER lumen side, the polyprotein is cleaved by the host proteases signalase and furin, whereas cleavage from the cytoplasmic side is performed by the viral protease.[3] Cleavage results in three structural viral proteins (C, E, prM/M), which are mainly involved in virus entry, attachment, assembly, and secretion, as well as seven non-structural (NS) viral proteins (NS1, NS2A, NS2B, NS3, NS4A, NS4B, NS5).[2, 4] A clear role in the viral life cycle has not been elucidated for every NS protein, but several enzymatic activities are known by now: The *N*-terminal part of NS3 together with NS2B as cofactor acts as the viral protease, whereas the *C*-terminal part of NS3 functions as a helicase. It is also known that NS5 is a RNA polymerase and a RNA methyltransferase.[1] Other important functions of the NS proteins include immune evasion and favoring viral replication over host cell processes.[6]

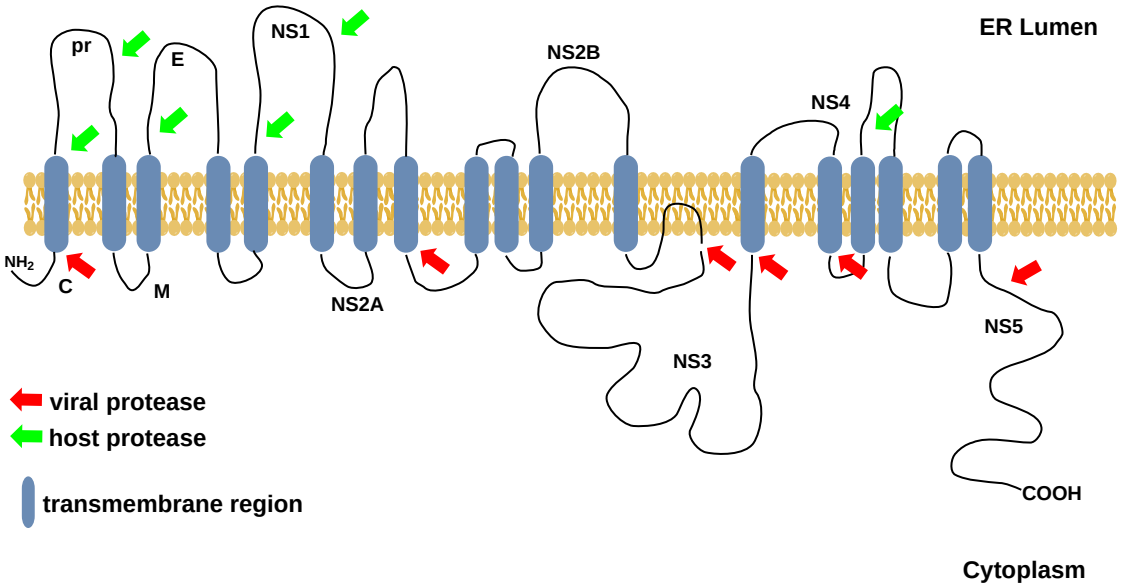

Fig. 1.2 The Dengue Virus polyprotein at the membrane of the rough endoplasmic reticulum (data from [3]).

Unlike other *Flaviviruses*, DENV consists of four distinct serotypes that differ between 25% - 40% at the amino acid level.[2] A primary infection with one of the serotypes results in lasting immunity against this serotype, but does not prevent a second infection with a different serotype.[7] This leads to a special feature of DENV infections called antibody-dependent enhancement (ADE): If a second infection by a heterologous serotype occurs, the risk of developing a severe dengue infection increases due to the presence of cross-reactive antibodies with low-affinity or poor neutralization.[7] This is also a major problem in the development of vaccines against DENV, as they must be highly effective against all four serotypes to avoid ADE. The only vaccine approved to date, Dengvaxia® (Sanofi-Pasteur), also suffers from this obstacle and is therefore recommended only for sero-positive patients aged 9 - 45 years.[8] A massive cluster of severe dengue infections has been reported in children under 9 years of age following vaccination.[8]

1.2 Dengue Virus Protease

1.2.1 General

As mentioned above, DENV has its own protease for cleaving the polyprotein from the cytoplasmic side. This protease consists of the *N*-terminal part of NS3 and NS2B as a cofactor. *In vivo*, NS2B is anchored to the rough ER by several transmembrane domains and thereby also fixes NS3 to it.[9] The proteolytic reaction is catalyzed by a triad consisting of residues His51, Asp75 and Ser135, so that the DENV protease belongs to the class of serine proteases.[9] Just like the human serine protease trypsin, it has a substrate specificity for basic residues (arginine, lysine) in P1 position and a tandem β-barrel architecture at the catalytic site.[10] The mechanism of the catalytic reaction (Figure 1.3) is also similar and can be described as follows:[10, 11]

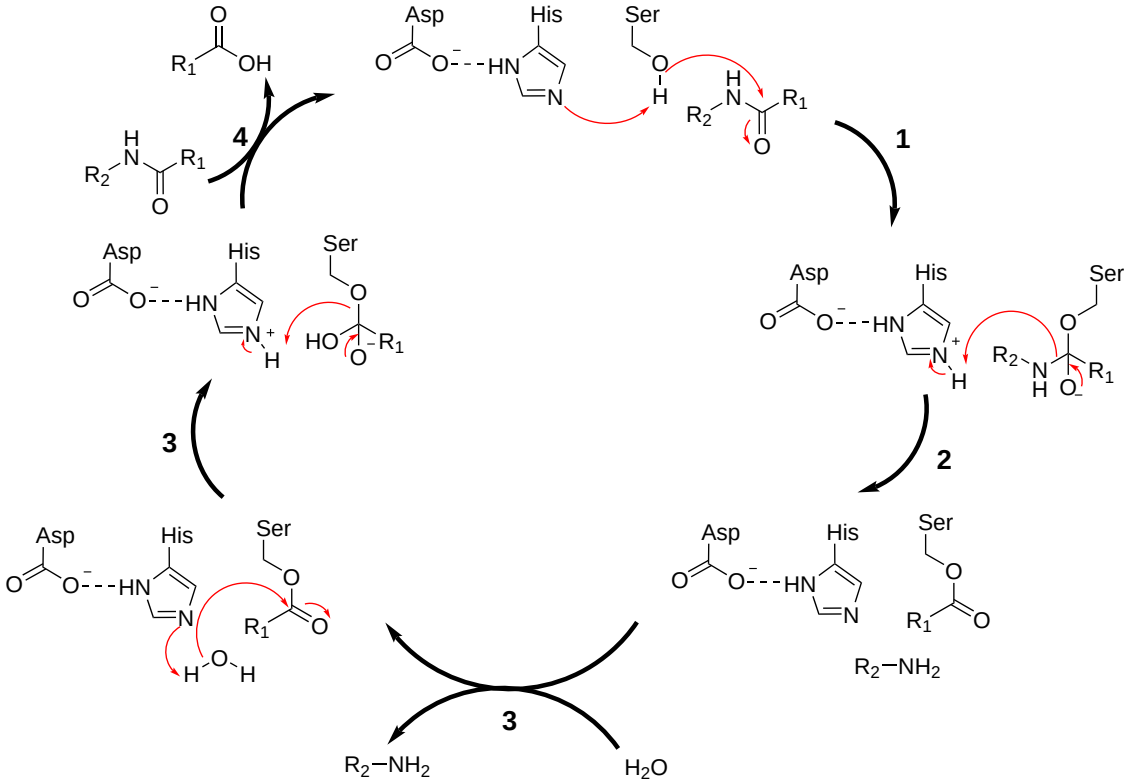

Fig. 1.3 The mechanism of the proteolysis catalyzed by the DENV protease (data from [11]).

1. An oligo-/polypeptide substrate binds to the active site of the enzyme. The nucleophilic serine of the catalytic triad attacks the carbonyl atom at the cleavage site forming a tetrahedral intermediate. The histidine residue acts as a base in this context and deprotonates the OH group of the serine. The resulting protonated histidine species is stabilized by a hydrogen bond to the aspartate of the catalytic

triad, while the oxyanion of the tetrahedral intermediate is stabilized by the positively charged oxyanion hole formed by main chain NH groups.

2. The collapse of the tetrahedral intermediate generates an acylenzyme complex and is catalyzed by the protonated histidine, which acts as an acid and stabilizes the newly formed *N*-terminus.

3. The *N*-terminal portion of the substrate is displaced by a water molecule, which then attacks the acylenzyme intermediate. Again, a tetrahedral intermediate stabilized by the oxyanion hole is formed.

4. Collapse of this intermediate generates the *C*-terminus of the substrate and restores the catalytic serine.

1.2.2 The Active Site

Compared to human trypsin-like serine proteases, the flaviviral NS2B/NS3 protease possesses some special properties, especially with regard to the active site. One example is the topology of the active site, which is flat and solvent-exposed with only shallow cavities in which the side chain residues of the substrate can reside.[12] Just like trypsin, the DENV protease cleaves peptide bonds following the amino acids arginine or lysine in P1 position, but the substrate specificity for the P2-P4 and P1'-P4' residues is very different.[13] Interestingly, although the sequence identity between the proteases of the four DENV serotypes is only about 60%, the proteases show a nearly identical substrate recognition pattern (Figure 1.4).[14]

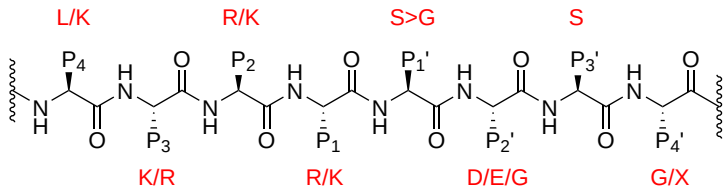

	Dengue 1	Dengue 2	Dengue 3	Dengue 4
NS2A/NS2B	WGRK SWPL	SKKR SWPL	LKRR SWPL	ASRR SWPL
NS2B/NS3	KKQR SGVL	KKQR AGVL	QTQR SGVL	KTQR SGAL
NS3/NS4A	AGRR SVSG	AGRK SLTL	AGRK SIAL	SGRK SITL
NS4B/NS5	GGRR GTGA	GGRR GTAQ	NTRR GTGN	TPRR GTGT

Fig. 1.4 Upper part: Substrate preference of DENV protease in synthetic peptides, lower part: Natural cleavage sites in DENV1-4 (adapted from [14]).

In P2 and P3 position, the DENV protease also shows a preference for arginine and lysine, but it was observed that this preference is much stronger for the P1 and P2 positions than for the P3 position.[14] For the P4 position, a weak preference for lysine and leucine was observed. The substrate specificity at the prime side proved to be much weaker - except for the P1' position, where small amino acids such as serine or glycine are strongly preferred.[15] The observed substrate specificity profile for synthetic peptides is also consistent with the natural cleavage sites in the polyprotein cleaved by the NS2B/NS3 protease (Figure 1.4).[14] Interestingly, the cleavage site between NS2B and NS3 possesses the suboptimal amino acid sequence glutamine-arginine in P2 and P1 position, respectively. This is thought to ensure a relatively late cleavage between NS2B and NS3 during polyprotein processing.[14]

1.2.3 Conformational Aspects

Conformational aspects of the DENV protease have been studied to date by several research groups using tools such as X-ray crystallography,[16–22] protein NMR[23–25] and cysteine disulfide traps.[26] The results of these studies varied slightly depending on the protease construct used and the assay conditions applied. Originally, a recombinant fusion protein consisting of the hydrophilic core region of NS2B and the *N*-terminal part of NS3 (protease part) was used, in which NS2B and NS3 are connected via a linker consisting of glycine and serine residues (GGGGSGGGG).[3]

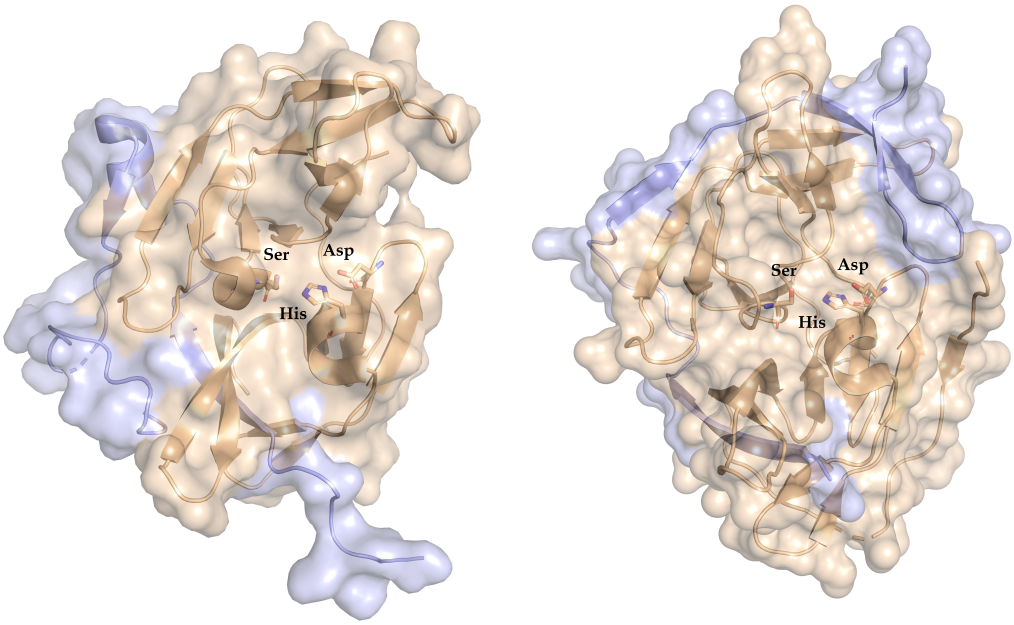

Fig. 1.5 Left side: open conformation of DENV protease (pdb code: 2FOM, DENV2),[16] right side: closed conformation of DENV protease (pdb code: 3U1I, DENV3).[17] The protein chains are shown as cartoon and surface, beige depicts NS3 and lightblue NS2B.

Recently, several research groups established "binary" constructs in which NS2B and NS3 exist as independent protein chains.[1] These constructs are thought to better represent the native state of DENV protease than the linked constructs.[9] The first crystal structure of the DENV protease was published in 2006 using a linked DENV2 protease construct in the absence of a substrate (pdb code 2FOM).[16] The obtained ligand-free structure was referred to as the "open" conformation of DENV protease.[16] The adjective "open" refers to the positioning of the cofactor NS2B: only the *N*-terminal part of NS2B interacts with NS3, while the *C*-terminal part forms a loop pointing away from NS3 (Figure 1.5, left side). The first ligand-bound structure of the DENV protease was published in 2012 (pdb code 3U1I).[17] For this, a linked construct of DENV3 protease was co-crystallized with an aldehyde-tetrapeptide inhibitor mimicking the substrate recognition pattern of the protease.[17] This crystal structure is now the archetype for the "closed" conformation of the DENV protease. It is considered to be the catalytically competent conformation of the protease, as NS2B complements NS3 to form the S_2 - S_4 subpockets in this structure (Figure 1.5, right side).[17] Although the assignment of structures to the open or the closed conformations is made by the arrangement of NS2B, both conformations also differ somewhat in the arrangement of NS3. The existence of both conformations in solution was confirmed by NMR studies[23–25] and the use of cystein disulfide traps,[26] but the relative abundance of both conformations varied from study to study.[9]

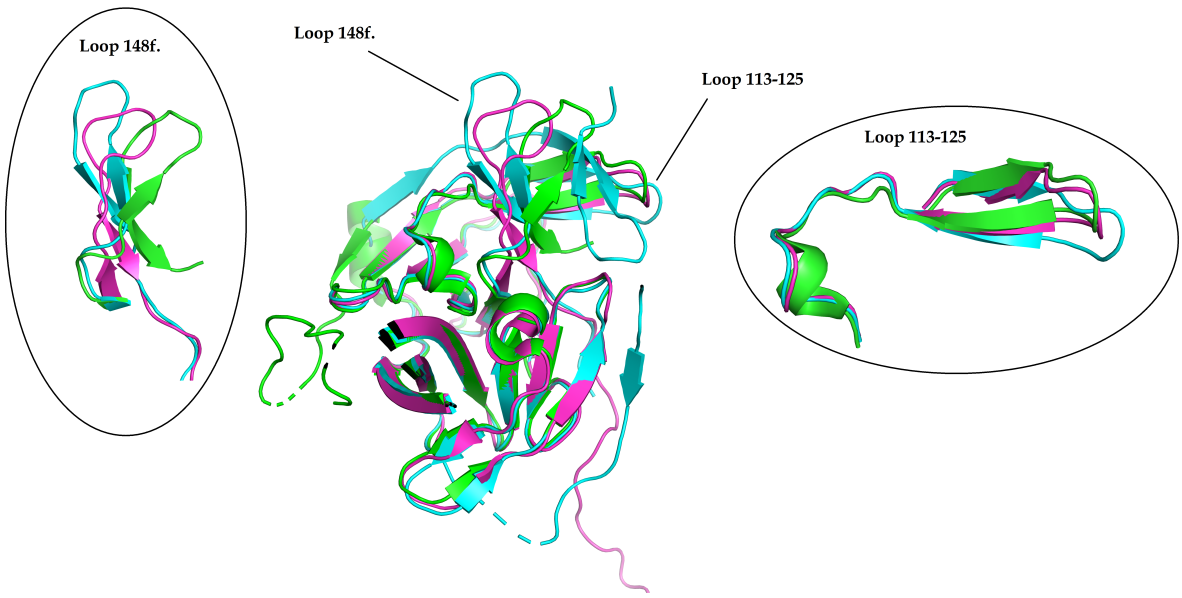

Fig. 1.6 A comparison of specific regions in different crystal structures of DENV protease (green: 2FOM,[16] cyan: 3U1I,[17] magenta: 2VBC[21]).

To date, several other crystal structures of the DENV protease and the related ZIKV protease have been published. A comparison of these structures shows that - although all structures have been assigned to either the closed or the open conformation - the exact orientation of NS2B and NS3 varies considerably between them.[9] A region of pronounced flexibility is found in NS3 segment 113-125 (Figure 1.6). Comparing the crystal structures with the pdb code 3U1I, 2FOM and 2VBC, different orientations of this loop are evident, which directly influence the shape of the active site. The flexibility of the protease in this region was also confirmed by mutagenesis studies and NMR analysis.[19, 23] Another important region in the protease with pronounced flexibility is the NS3 segment between residue 148 and the C-terminus (Figure 1.6). Of particular importance is that Asn152 of the conserved motif 148-153 (GLYGNG) can adopt different orientations, as can be seen in the X-ray structures of 2FOM, 3U1I and 2VBC.[9] This residue was found to be critical for enzymatic activity, although it is not part of the catalytic triad or the oxyanion hole. The N152A mutation resulted in complete loss of proteolytic activity.[27]
In summary, it can be stated that it is assumed that the NS2B/NS3 protease is present in an entire ensemble of conformations. The addition of a substrate or inhibitor then leads to a conformational selection, in which the ligand binds to one of the conformations, thereby shifting the equilibrium between the conformations.[9]

1.2.4 The Allosteric Site

Another result of the conformational analysis of flaviviral proteases was the discovery of a putative allosteric site within the NS2B/NS3 complex. To date, no native ligand for this site is known, but binding of small molecule as ligands to this site is thought to result in inhibition of the protease.[1, 3, 9, 19, 27, 28]
The allosteric site is located on the back of the active site and also shares several amino acid residues with the latter (see Figure 1.7). In contrast to the active site, the allosteric site is rather deep and hydrophobic. However, the exact shape of this pocket varies between crystal structures.[9, 16, 17] Until now, no crystal structure has been published with a ligand bound to the allosteric site, although one group claims this in a recent publication.[20] However, detailed analysis of the published electron density has revealed that the electron density assigned to the ligand most likely belongs to the *C*-terminus of the protein instead.[29, 30] Therefore, all published reports of allosteric inhibition of DENV protease are based on indirect methods, such as split-luciferase assays,[28] mutation experiments[27] and cysteine-reactive probes.[19] Nevertheless, two main points can be derived from these studies:

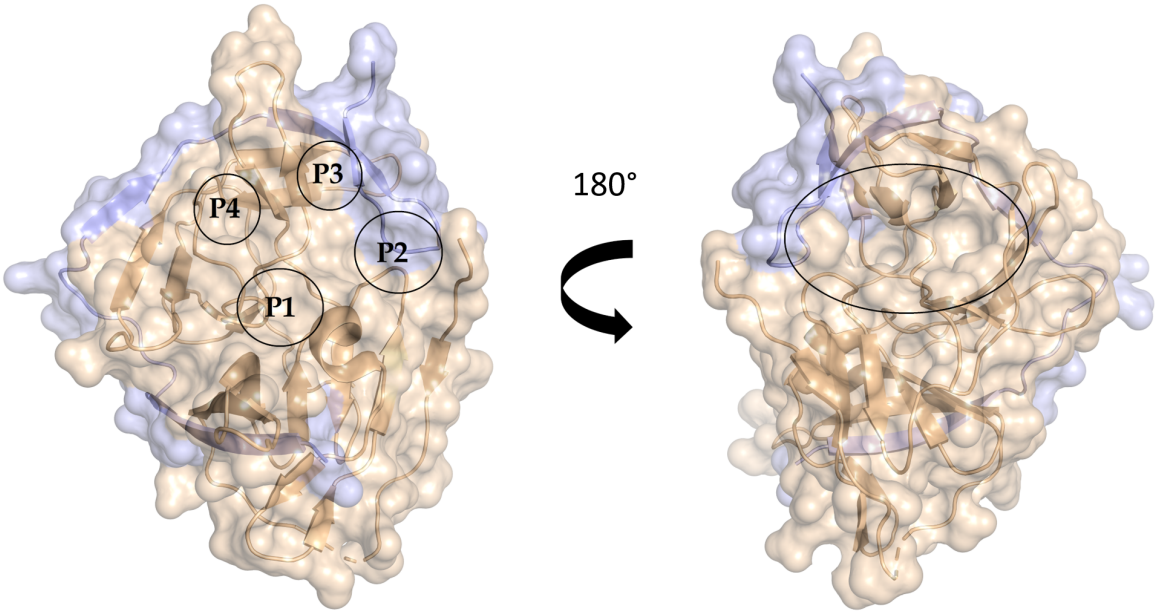

Fig. 1.7 The active (left) and the allosteric site (right) of DENV3 protease in the closed conformation. The binding pockets of the substrate residues are shown in circles in the active site. Beige: NS3, lightblue: NS2B.[17]

First, the allosteric site must be located between the 120s loop and the 150s loop, which corresponds to the cavity found on the back of the active site.[19, 28] Second, for the allosteric inhibition mechanism being observed, binding of a ligand to Asn152 - a residue that is also crucial for enzymatic activity of the protease - seems to be pivotal.[27]

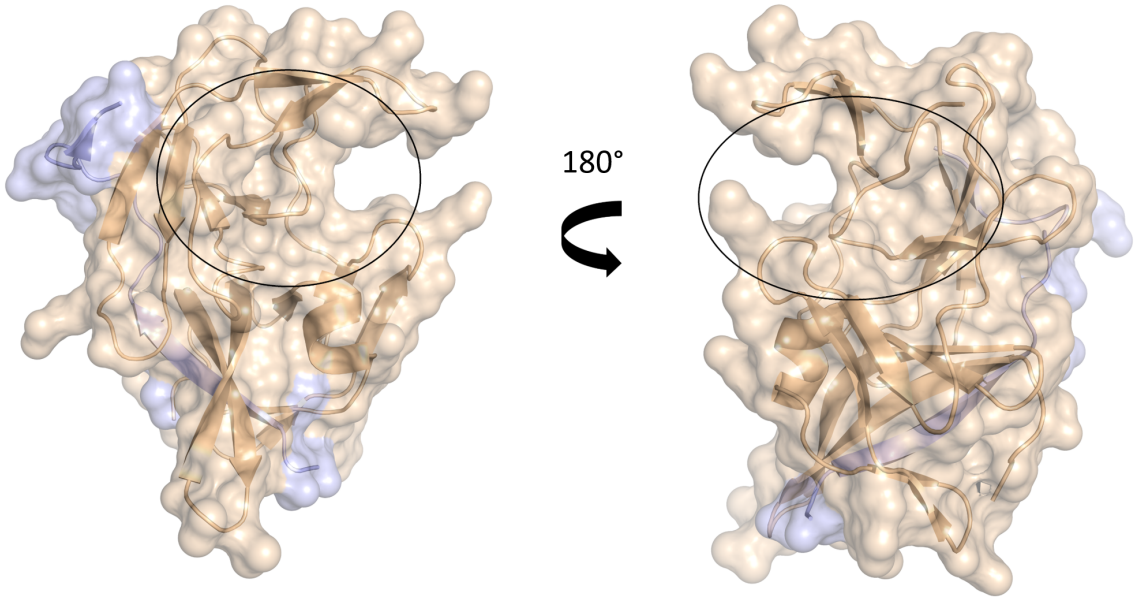

Fig. 1.8 The active (left) and the allosteric site (right) of ZIKV protease in the super-open conformation (pdb code: 6UM3). Beige: NS3, lightblue: NS2b.[31]

There is controversy in literature as to whether binding to the allosteric site in the open or closed conformation is responsible for the observed inhibition. On the one hand, binding to the allosteric site in the open conformation could stabilize the putatively catalytically inactive state;[28] on the other hand, binding to the allosteric site of the closed conformation could prevent the flexibility of the protease necessary for successful catalysis.[9]
Recently, the structure of a ZIKV protease described as a so-called "super open" conformation being stabilized by cysteine disulfide bridges was deposited in the pdb (pdb code: 6UM3).[31] In this structure, the active and allosteric sites are connected by a deep cavity created by rearrangements in the 120s loop and the 150s loop of NS3. It is also possible that ligand binding to this conformational state is responsible for the allosteric inhibition (Figure 1.8).[9] In summary, research regarding the allosteric site is still ongoing and several questions remain to be answered.

1.3 Development of Inhibitors targeting Dengue Virus Protease

First attempts to develop inhibitors of the DENV protease date back to the year 2001.[32] Since then, numerous different approaches have been published, resulting in more or less potent lead structures.[1, 3, 9] Despite these efforts, none of the reported inhibitors reached clinical trials, so treatment of DENV-infected patients remains symptomatic only.[33] The published inhibitors can be classified according to two different features: one is the binding site on the protease (either the active site or an allosteric site) and the other is the structural type of the inhibitor (peptide vs. small molecule).[3] In the following, active site inhibitors and allosteric inhibitors will be discussed separately.

1.3.1 Active Site Inhibitors

Peptide Inhibitors

The first described inhibitor of DENV protease was aprotinin (Bovine Pancreatic Trypsine Inhibitor, BPTI), a polypeptide known to inhibit many serine proteases.[34] Due to its high affinity for DENV protease (IC_{50} = 65 nM, DENV2), aprotinin is now often used as a positive control in DENV protease inhibition assays.[32]

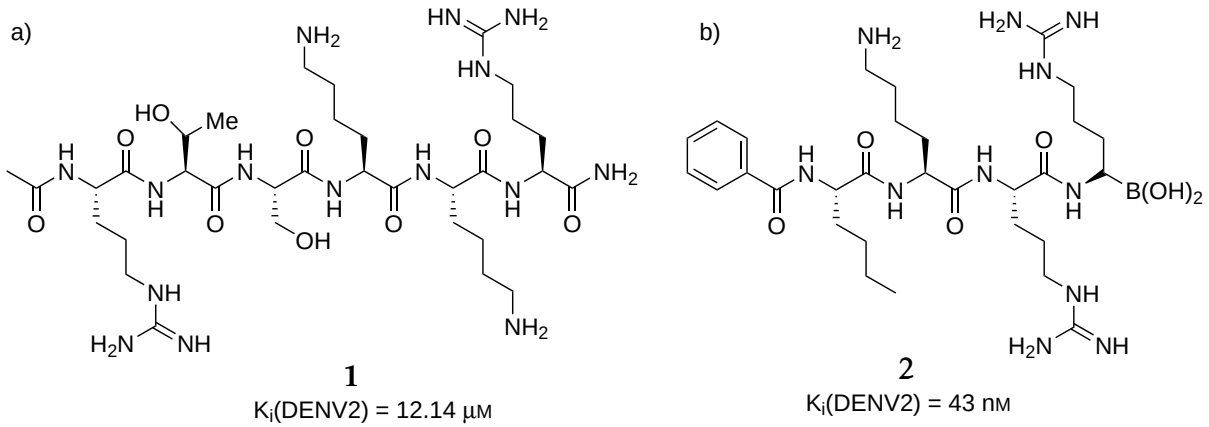

Fig. 1.9 Reported active site inhibitors of DENV protease mimicking polyprotein cleavage sites, a) a hexapeptide and b) a tetrapeptide with a boronic acid as nucleophilic warhead.[35, 36]

Initially, the design of active site inhibitors of DENV protease mostly focused on mimicking cleavage sites of the protease in the viral polyprotein with oligopeptides. With this approach, K_i-values in the low micromolar range could be achieved (see example in Figure 1.9, compound **1**).[35] A significant increase in affinity was achieved when nucleophilic warheads were introduced into these oligopeptides. These warheads (usually aldehydes or boronic acids) react with the serine of the catalytic triad resulting in a covalently bound intermediate.[36] Although these peptides have double-digit

nanomolar K_i-values (Figure 1.9, compound **2**), their applicability for clinical treatment is severely limited by cross-reactivity with many human serine proteases.[36]
Further progress in optimizing the affinity of petidic inhibitors has been made by cyclization approaches and by introducing non-natural amino acids.[37, 38] In the first case, the K_i-value of an octapeptide could be reduced by a factor of 20 by cyclization (K_i(linear)= 42 μM, K_i(cyclic) = 2.2 μM).[37] One reason for this change in affinity could be the reduced flexibility of the cyclic peptide and the resulting reduced loss of entropy upon binding. In the second case, the *C*-terminal and *N*-terminal positions of a tetrapeptide were systematically varied using non-natural amino acids.[38] A combination of the best residue in the *C*-terminal and in the *N*-terminal position led to an inhibitor with submicromolar affinity without the use of a nucleophilic warhead.[38] In addition, it showed only modest Thrombin inhibition (Figure 1.10, compound **3**).[38]

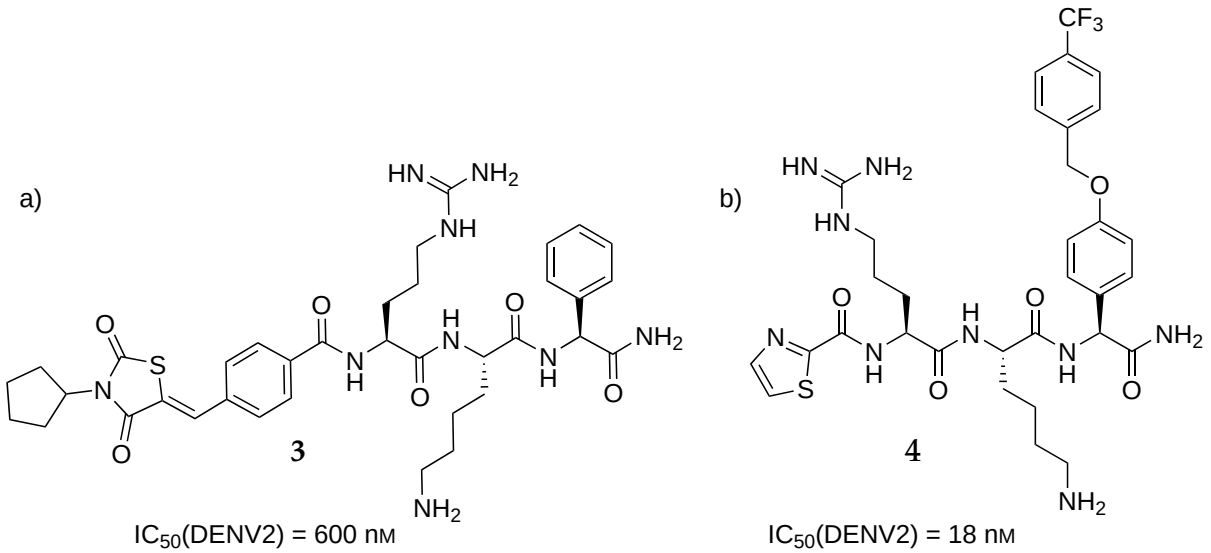

Fig. 1.10 Introduction of non-natural amino acids led to active site inhibitors with significantly increased affinity.[38, 39]

Further optimization of the inhibitor by the same research group resulted in a tetrapeptide with a double-digit nanomolar IC_{50}-value against DENV2 protease, making it the most potent inhibitor of DENV protease described to date (Figure 1.10, compound **4**).[39] While the optimized structures obtained are much more drug-like than the original structures derived from natural cleavage sites, their applicability for therapeutic use is limited by the low cell-permeability caused by the positively charged arginine and lysine side chains. All attempts to overcome this problem by using uncharged amino acid residues have had only limited success.[40, 41]

Small Molecule Inhibitors

The development of small molecule inhibitors of DENV protease cannot be described as a directed process. Rather, the literature contains many reports of a wide variety of approaches to find and improve small molecule inhibitors that target the active site, many of which were not further pursued.[3] As a result, there is a great structural diversity among the published inhibitors and a common structural motif is not apparent.[3] Some of the more successful approaches are described below.

One of the first reports of a small molecule that competitively inhibits DENV protease was published in 2005 by Ganesh *et al.*[42] As a starting point, the group searched a chemical database for compounds that mimic the guanidine-group of an arginine residue. The best resulting inhibitor was compound **5** (IC_{50}(DENV2) = 14 ±2 μM), which carries a phosphinic acid ester residue that forms a covalent bond with the catalytic serine (Figure 1.11).[42]

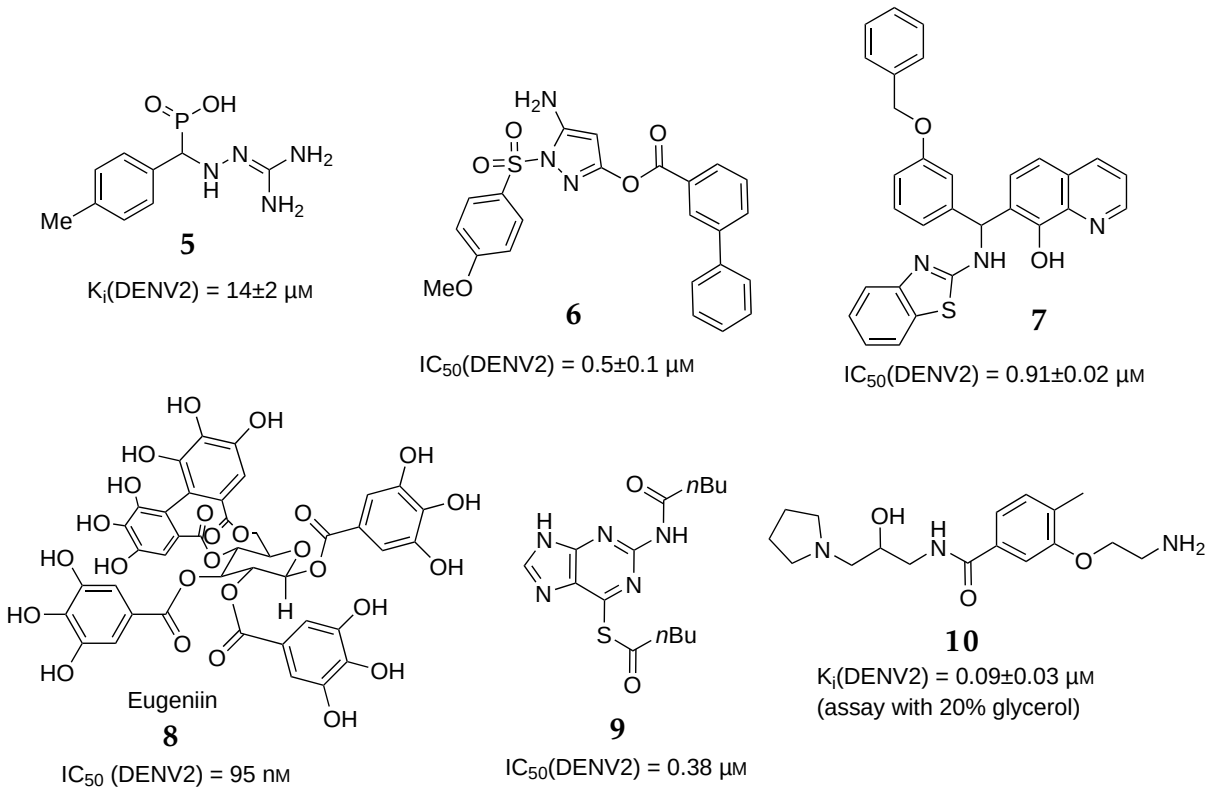

Fig. 1.11 Overview of selected small molecule inhibitors targeting the active site of DENV protease.[42–47]

The approach of using a covalent bond between the ligand and protease to increase affinity was also used by Koh-Stenta *et al.* 10 years later.[43] Here, a potent inhibitor of the WNV protease was used as a starting point, and variation of substituents resulted in compound **6**, which showed a submicromolar IC_{50}-value for the DENV protease (Figure 1.11).[43] The inhibition mechanism of the compound was elucidated by mass

spectrometry experiments: After binding of the ligand to the active site, the benzoyl residue of the pyrazole ester is pseudo-irreversibly transferred to the catalytic serine, thereby inhibiting the protease.[43] Although these results appeared quite promising, no follow-up study was published. A non-covalently binding small molecule inhibitor with submicromolar affinity was first described in 2013 by Lai *et al.*[44] Their initial hit resulted from an HTS against the WNV protease and was subsequently optimized for the DENV protease. An increase in affinity was achieved by introducing aminobenzothiazole substituents to the 8-hydroxyquinoline core (Figure 1.11, compound **7**). However, further studies of this class of compounds have been hampered by their poor solubility in aqueous medium.[44]
Natural product libraries were also tested for their potential to inhibit DENV protease. The most potent active site inhibitor discovered from this approach is eugeniin, a polyphenol extracted from cloves (Figure 1.11, compound **8**).[45] It has a double-digit nanomolar IC_{50}-value for DENV-protease and is highly soluble in water, so the authors announced further investigation into its potential as an anti-dengue drug.[45] Since virtual screening of large compound libraries has become very popular in recent years, this approach has also been pursued for the identification of active site inhibitors against DENV protease. One of the most successful examples was reported by Hariono *et al.* and was obtained by *in silico* docking of the NCI-diversity set and subsequent optimization of the first hit, which resulted in a thioguanine-based inhibitor **9** with a submicromolar IC_{50}-value for DENV protease (Figure 1.11).[46] A more advanced *in silico* modeling approach also led to the most potent active site inhibitor published to date. For this, Pach *et al.* used MD-based 3D pharmacophores as a starting point for virtual screening and subsequent docking.[47] The most promising hit from this search was compound **10** with a double-digit nanomolar affinity, which could be a promising lead due to its diverse structure.[47]

1.3.2 Allosteric Inhibitors

Since no native ligand of the allosteric site is known to date, the inhibitor design cannot be based on the mimicry of such a ligand. Instead, *in silico* or *in vitro* high-throughput screenings are usually used as starting point. Similar to the development of small molecule inhibitors for the active site, approaches leading to a wide variety of chemical scaffolds have been published.[3, 9] Optimization of these scaffolds resulted in inhibitors with IC_{50}-values in the low micromolar range, but inhibitors with nanomolar affinity have not been published even after almost 10 years of research in this field. Nevertheless, some of the most promising examples will be presented in the following.

One of the first groups to report on non-competitive inhibition of DENV protease were Yang *et al.* in 2011.[48] Based on an *in vitro* HTS of a compound library, they identified compound **11** as potent allosteric inhibitor (IC_{50}(DENV2)= 15.5±2.1 μM, Figure 1.12). Mutational analyses led the authors to conclude, that binding of the ligand disrupts the interaction between NS2B and NS3, but no precise binding location was suggested.[48] Another report by Deng *et al.* used an *in silico* HTS as a starting point for the study.[49] For docking, the allosteric pocket of DENV2 protease in the open conformation (pdb code 2FOM) was used as receptor. Optimization of the found hits by scaffold-hopping resulted in compound **12**, with a single-digit micromolar IC_{50}-value for DENV protease (Figure 1.12).[49] The binding site of the ligand remained somewhat uncertain in this case, as no further studies than docking were performed.

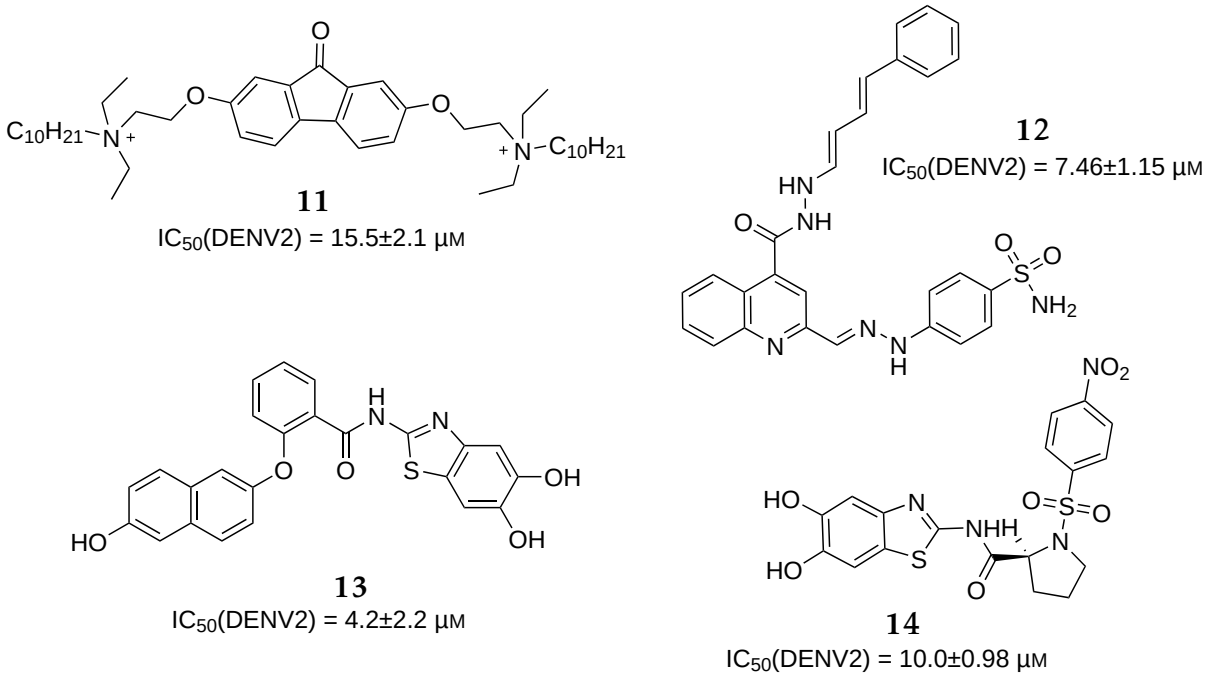

Fig. 1.12 Selected non-competitive inhibitors of DENV protease.[27, 48–50]

Another promising approach was published by Wu *et al.* in 2015, where *in vitro* screening of an in-house library identified compound **13** as a single-digit micromolar inhibitor of DENV protease (Figure 1.12).[27] To elucidate the binding mode of the inhibitor, docking to the allosteric site of the closed conformation (DENV3, pdb code 3U1I) was performed. The reported compound class of diaryl(thio)esters was further optimized in a subsequent publication by the same working group.[50] Within these studies, the water solubility of the compounds was improved by introducing a proline-scaffold. This did not improve the affinity for the DENV protease, but the most promising compound **14** showed a dramatically increased lipophilic ligand efficiency (LLE) (Figure 1.12).[50] Further mutational studies suggested binding of the inhibitors in the allosteric pocket of the open conformation, which was further supported by docking analyses.[50] From

these two publications, it is evident that identification of the exact binding mechanism for allosteric inhibitors of DENV protease is difficult due to the lack of suitable crystal structures.

In a study by Brecher *et al.*, an *in vitro* conformational-switch high-throughput assay was used to selectively screen for ligands that bind to the open conformation of DENV protease.[28] Using this approach, they were able to identify compound **15**, which was found to inhibit DENV protease effectively (IC_{50}(DENV2)= 1.8 μM, Figure 1.13). Docking studies suggested that binding of the ligand to the allosteric site was responsible for a shift in the conformational equilibrium of the protease towards the open conformation.[28] Although these results appear quite promising, no further optimization was published up to now. The same research group also used the developed conformational-switch assay to test existing drugs for their potential to inhibit DENV protease.[51] They found that temoporfin, nitazoxanid and niclosamid significantly inhibited DENV protease, with temoporfin (Figure 1.13, compound **16**) being the most effective one.[51] The authors confirmed the non-competitive binding mode by Dixon plot analysis. As binding site, the authors suggested the interaction region between NS2B and NS3, based on docking studies using the closed conformation (pdb code 3U1I) without the cofactor NS2B as a receptor.[51]

In summary, some promising approaches for the design of allosteric inhibitors of DENV protease have been published. However, affinity needs to be significantly improved and the binding site more precisely determined for potential candidates to enter clinical trials.

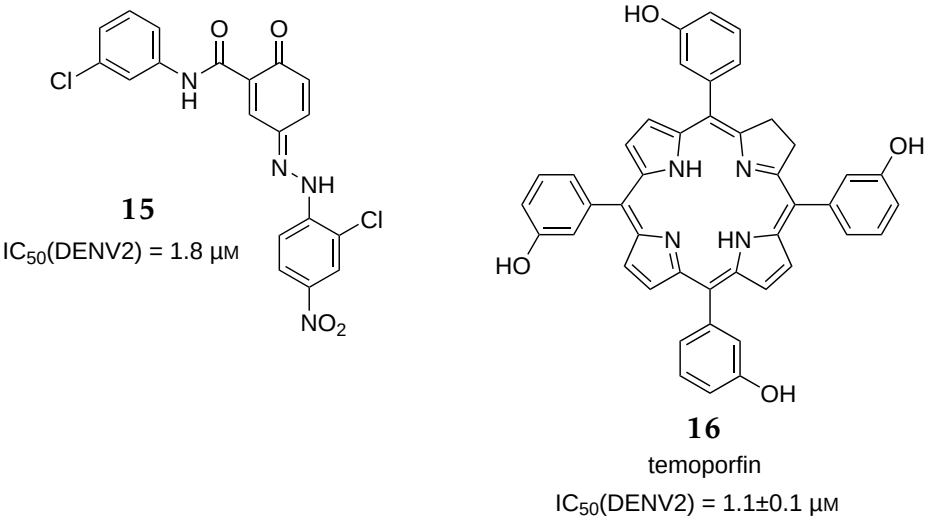

Fig. 1.13 Overview of allosteric inhibitors of DENV protease found using a conformational switch assay.[28, 51]

2 Scope of the Thesis

As discussed in the previous chapter, effective drugs for the therapy of DENV infections are urgently needed. Therefore, the aim of the present work was to find lead structures for the anti-dengue drug development. Since the DENV protease plays a crucial role in the viral life cycle and the allosteric pocket has a higher druggability compared to the active site, it was chosen as target structure for drug development.

Nowadays, expensive and costly *in vitro* high-throughput screenings to discover promising hits for a particular drug target can be avoided by *in silico* approaches. In this context, molecular docking, defined as computer-aided simulation of the conformation of a protein-ligand complex, has proven to be a powerful tool which should also be used in the present work for the discovery of initial hits from large *in silico* compound libraries.[52] The most promising *in silico* hits obtained from the docking process should then be purchased from commercial sources and validated by a fluorescence-based *in vitro* assay, which monitors the cleavage velocity of a tetrapeptide substrate by the DENV protease and thereby provides information about the inhibitory potency of a particular small molecule. Furthermore, biochemical tools such as Dixon-Plot analysis should be utilized to proof the allosteric binding mode.

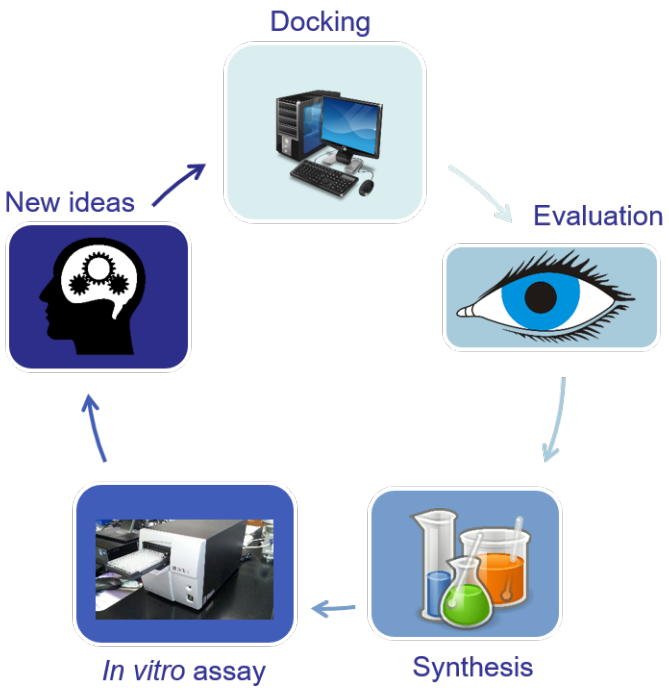

Fig. 2.1 Schematic representation of the applied drug design approach.

Hits that have been validated *in vitro* should be analyzed for their potential synthetic feasibility enabling the derivatization into more potent structures. The most promising hits should then be used as starting points for the design of new *in silico* compound libraries being used in a second docking process, which - after evaluation of the results - should lead to a list of compounds to be synthesized. The development of efficient synthetic approaches for the selected compounds as well as the execution of the syntheses should also be part of the present work. The compounds obtained should then be tested again in the *in vitro* assay.

The most potent compound resulting from this approach should then be further investigated by deducing a structure-activity relationship (SAR) in order to obtain information on the binding site properties and inhibition mechanism. Ideally, these studies should be complemented by X-ray structural data of the ligand-protein complex, which should be provided by J.H.W. Scanlan. Data for the *in cellulo* efficacy of the compounds should also be collected and discussed in collaboration with the group of E. Herker.

In summary, the aim of the present work was to utilize modern rational drug design methods such as molecular docking, X-ray crystallography and an *in vitro* assay system for the design of novel allosteric DENV protease inhibitors. Crucial part of the work was also the synthesis of the designed molecules using modern chemical approaches, such as transition metal catalyzed reactions and inert gas techniques, as well as the application of advanced purification techniques to obtain compounds with high purity (>95%) for *in vitro* and *in cellulo* testing.

3 Results and Discussion

3.1 Initial *in silico* High-Throughput Screening

Since a rational drug-design approach should be followed for the design of allosteric DENV protease inhibitors, an *in silico* high-throughput screening (HTS) approach using molecular docking was chosen as a tool for the identification of initial hits. As mentioned above, molecular docking is defined as a computer-aided simulation of the conformation of a protein-ligand complex and follows the classical "lock and key" principle, where the shape and the electrostatics of protein and ligand should be complementary.[52, 53] In addition, van der Waals interactions and hydrogen bond formation are also considered. The resulting poses are ranked by an affinity scoring function that calculates a so-called docking score for each pose. The docking score is an approximation to the free binding energy ΔG of the ligand-protein complex (in kcal/mol), with more or less severe simplifications implemented in the calculation process for reasons of efficiency.[53]

3.1.1 Selection and Preparation of the Protein Structure

In molecular docking, the quality of the result depends to a large extent on the correct selection and preparation of the three-dimensional structure of the protein.[53] Therefore, this step should be treated with great care. As described in the introduction, the published X-ray structures of DENV protease differ significantly in shape and properties of the allosteric site, so the selection of a crystal structure in this case has an even greater impact on the docking result. In this thesis, the X-ray structure with pdb-code 3U1I (DENV3, closed conformation) was selected for the following reasons:[17]

- The reported resolution of 2.5 Å is sufficient for molecular docking[17]
- All amino acids forming the allosteric pocket are well resolved
- The allosteric pocket is fully formed and accessible to a ligand
- Stabilization of the closed conformation should prevent the flexibility necessary for efficient catalysis
- The crucial amino acid Asn152 is part of the pocket and accessible for interactions

All other published X-ray structures (see introduction) did not fulfill one or more of the stated criteria, so no other structure was considered. For molecular docking the AutoDock Vina program[54] was used and therefore protein preparation was performed using the associated AutoDock Tools4 software (ADT4).[55] In ADT4, the following steps were executed using the X-ray structure 3U1I:

- Addition of all hydrogens and merging of all non-polar hydrogens (last step is specific for AutoDock Vina)
- Manual adjustment of the protonation state of all histidine nitrogens (according to the most probable protonation state at pH 9, NS2B: His72 (HD1), NS3: His47 (HD1), His51 (HD1), His60 (HE2))
- Check for missing residues or broken chains (none)
- Adding partial charges (Marsili-Gasteiger charges)[56, 57]

The protonation state of the histidine nitrogens was adjusted to pH 9, since the *in vitro* fluorescence-based assay for DENV protease is measured at this pH. An illustration of the resulting structure for the allosteric pocket of DENV protease is shown below.

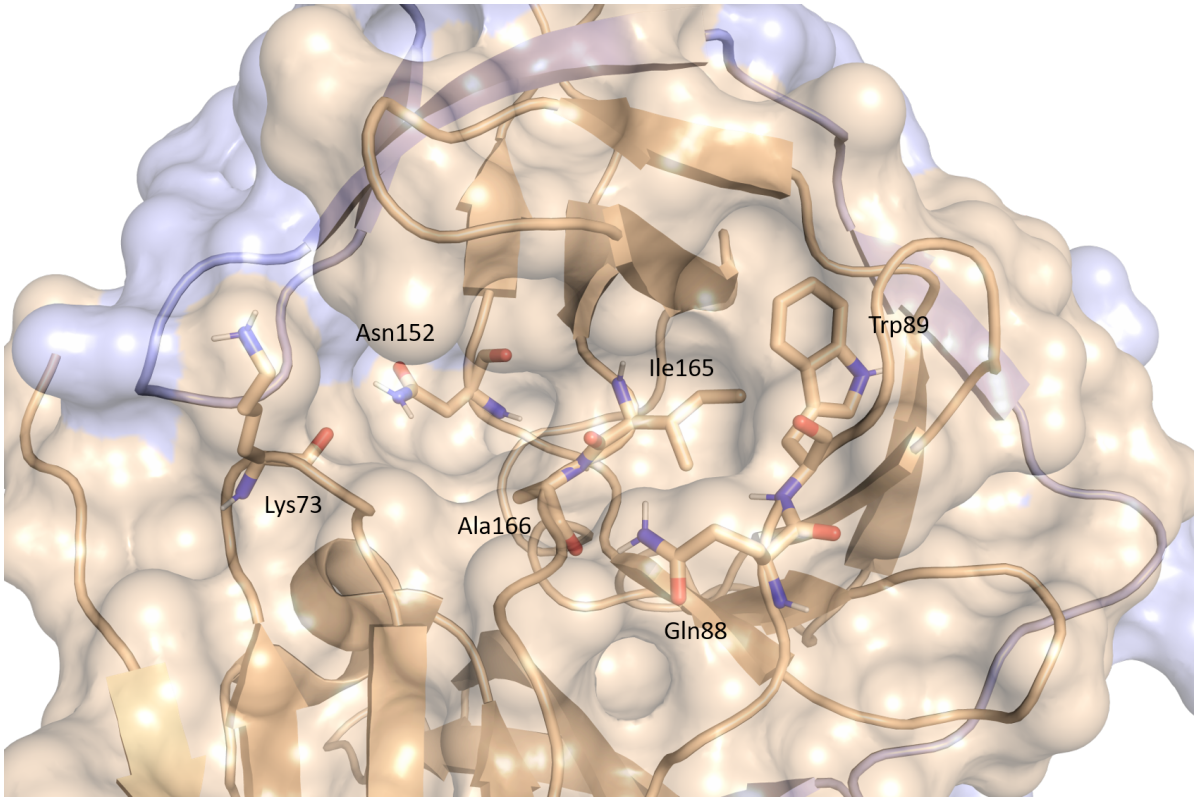

Fig. 3.1 Allosteric pocket of the closed conformation (pdb code 3U1I)[17] after protein preparation with ADT4. Beige: NS3, lightblue: NS2B, relevant amino acids are shown as sticks.

3.1.2 Selection of a Small Molecule Library

For the initial HTS, only commercially available small molecule compounds should be considered so that *in vitro* testing could be performed immediately after the most promising compounds were selected. One of the currently most comprehensive databases for chemical compounds is ZINC15,[58] therefore one of its subsets was also selected in this case. The following parameters were chosen to create the subset:

- A molecular weight of 300-350 g/mol, so that expansion to improve affinity was still possible without exceeding 500 g/mol.
- A clogP in the range of -1 to 3.5 to ensure adequate water solubility
- The availability was set to "agent" so that compounds were readily available
- The pH was set to medium (7) and high (9), as the assay was to be performed at pH 9
- The charge was not filtered (so -2 to +2 was allowed)

This resulted in a total number of approximately 4 million protomers (compounds in different protonation states), which were downloaded as 3D representations in the appropriate file format (.pdbqt for AutoDock Vina).

3.1.3 Set-up for AutoDock Vina

To understand why certain parameters were chosen for molecular docking with AutoDock Vina, it is necessary to discuss some of its unique features. First, unlike other docking programs, the scoring function of AutoDock Vina is rather empirical, so that the weights and terms for individual interactions (e.g. hydrogen bonds and van der Waals interactions) are a result of machine learning and are not derived directly from physical considerations.[54] Secondly, the search algorithm uses a stochastic global optimization approach, i.e. it starts with an arbitrary conformation and varies it until a local minimum of the scoring function is found.[54] It should be noted that the local minimum does not necessarily coincide with the global minimum of the scoring function. For this reason, multiple runs of AutoDock Vina with the same set-up can lead to different results depending on the starting point chosen by the program. In general, AutoDock Vina treats the receptor (i.e. protein) as rigid and the ligands as flexible molecules with 0 to 32 rotatable bonds. If necessary, some residues of the receptor can be also set as flexible.[54] A "search space" must be specified for the docking process. It is defined as a certain volume in the coordinate system of the receptor in which the different conformations of the ligand are to be taken into account.[54] The larger the

search space chosen, the higher the computational cost and thus the runtime of the program. In AutoDock Vina, the search space is a cuboid whose center and edge length are defined by the user.[54]
Considering the program properties discussed, the following parameters were chosen for the HTS:

- The center of the search space was set to (36.10/-8.30/9.13) and the edge lengths were defined as (22/18/24), which covers the entire volume of the allosteric pocket of 3U1I.
- The number of poses that should be stored for each compound was set to 3.
- The exhaustiveness of the pose optimization was set to auto, so that the program decided on the exhaustiveness required for each molecule.
- The HTS was set up on the Philipps-University Marburg cluster (MaRC2) with 4 cores and 2 GB RAM for each job (1000 jobs with about 4000 molecules each were submitted).

3.1.4 Evaluation of the HTS Results

After the entire library of small molecule had been docked with AutoDock Vina, the top 500 ranked molecules were visually examined. The following aspects were taken into account:

- Correctness of the given ligand structure: correct protonation state, molecule is not excessively distorted
- Complementarity of shape between receptor and ligand (no collisions)
- Possibility for the formation of hydrogen bonds or salt bridges
- Possible van der Waals or π-π interactions
- Number of stranded donors (and acceptors) of ligand and protein

Visual inspection resulted in a shortlist of 50 promising compounds, that were discussed and evaluated in plenary sessions, which eventually lead to the selection of 15 compounds that should finally be purchased and tested *in vitro* (see Figure 3.2). One criterion for the compilation of the compounds to be tested was also to achieve the greatest possible structural diversity between the compounds to increase the likelihood of finding active compounds in the *in vitro* assay.

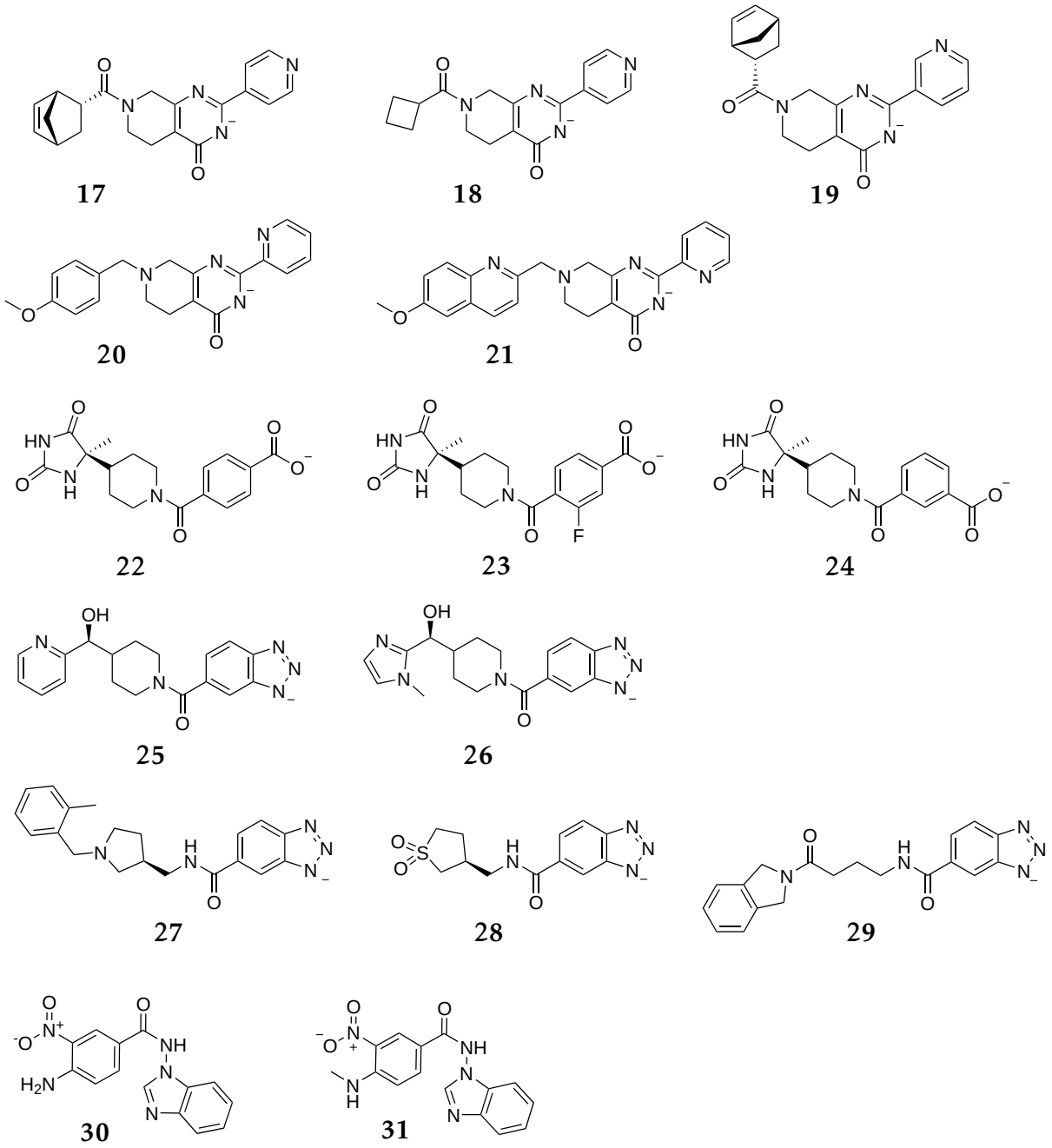

Fig. 3.2 Compounds selected from *in silico* HTS for *in vitro* tests. The protonation state is shown as the preferential one at pH 9 (calculated by ZINC15).[58]

3.1.5 *In vitro* Tests of the HTS Compounds

The 15 commercially available compounds shown in Figure 3.2 were tested in a fluorescence-based *in vitro* assay for their potential to inhibit the DENV3 protease. The general design of the assay system can be described as follows (for the exact assay composition, see Methods & Materials chapter and Ref. [27]): in this substrate-based enzyme assay, the cleavage rate of a tripeptide substrate by a glycine-linked construct of DENV3 protease (see Introduction) is determined. This is possible because the

tripeptide (PhAc-Lys-Arg-Arg↓AMC) contains 7-amino-4-methylcoumarin. In the uncleaved peptide, the fluorescence of coumarin **32** is quenched by the linked amino acids. After cleavage, coumarin **32** is released and can be detected by its fluorescence at 460 nm when excited at 380 nm. As the reaction proceeds, the fluorescence signal increases linearly, so that the recorded data can be fitted by a linear function. The percentage inhibition of an inhibitor at a given concentration is then calculated as the quotient between the slopes of the blank measurement (DMSO) and the inhibitor measurement.

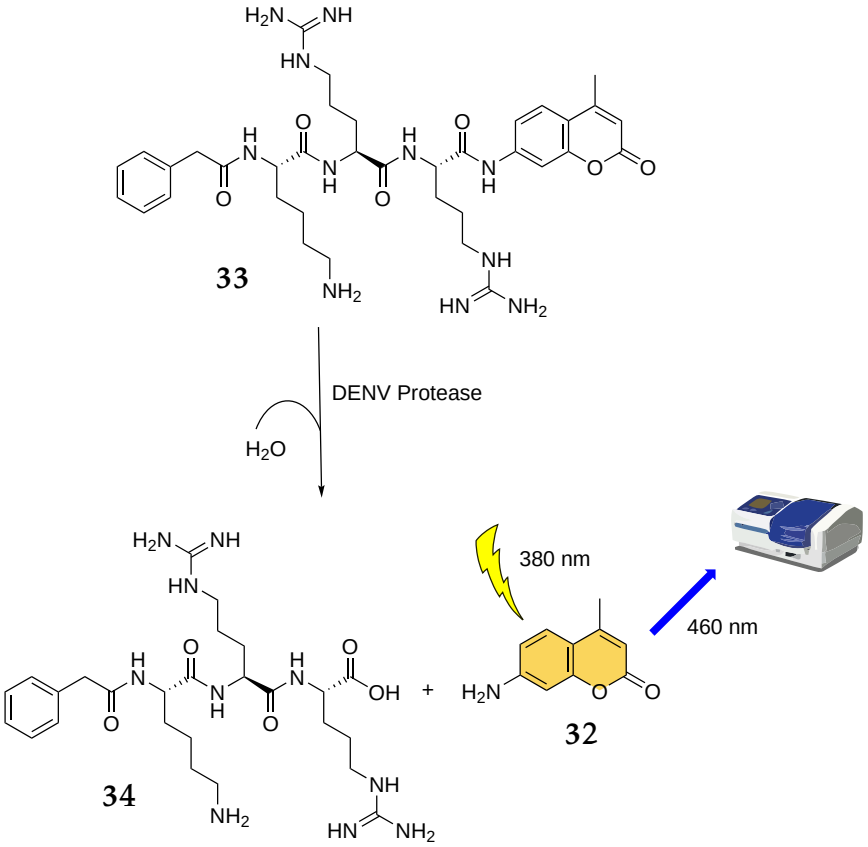

Scheme 3.1 In the employed *in vitro* assay system, the tripeptide PhAc-Lys-Arg-Arg-AMC is cleaved by DENV protease to release a tripeptide and 7-amino-4-methylcoumarin, which is fluorescent.

For the HTS compounds, the percentage inhibition was measured at 100 μM (see Figure 3.3). It can be clearly seen that the substances can be divided into three subgroups: Those showing negligible inhibition (<10% at 100 μM), those showing moderate inhibition (10%-25% inhibition at 100 μM) and those that show significant inhibition (>35% at 100 μM). Only the last group, which contains compounds **21**, **30** and **31**, is of interest for further drug development. Since **21** was poorly soluble in the assay buffer, it was also excluded from further consideration. The closely related analogues **30** and **31**,

differing only by a methyl group on the aniline nitrogen, showed similar inhibition of DENV protease, indicating specific inhibition. Furthermore, both compounds were very soluble in the assay buffer, so that aggregation has a negligible effect on DENV protease inhibition here. For this reason, compounds **30** and **31** were used as a starting point for further studies.

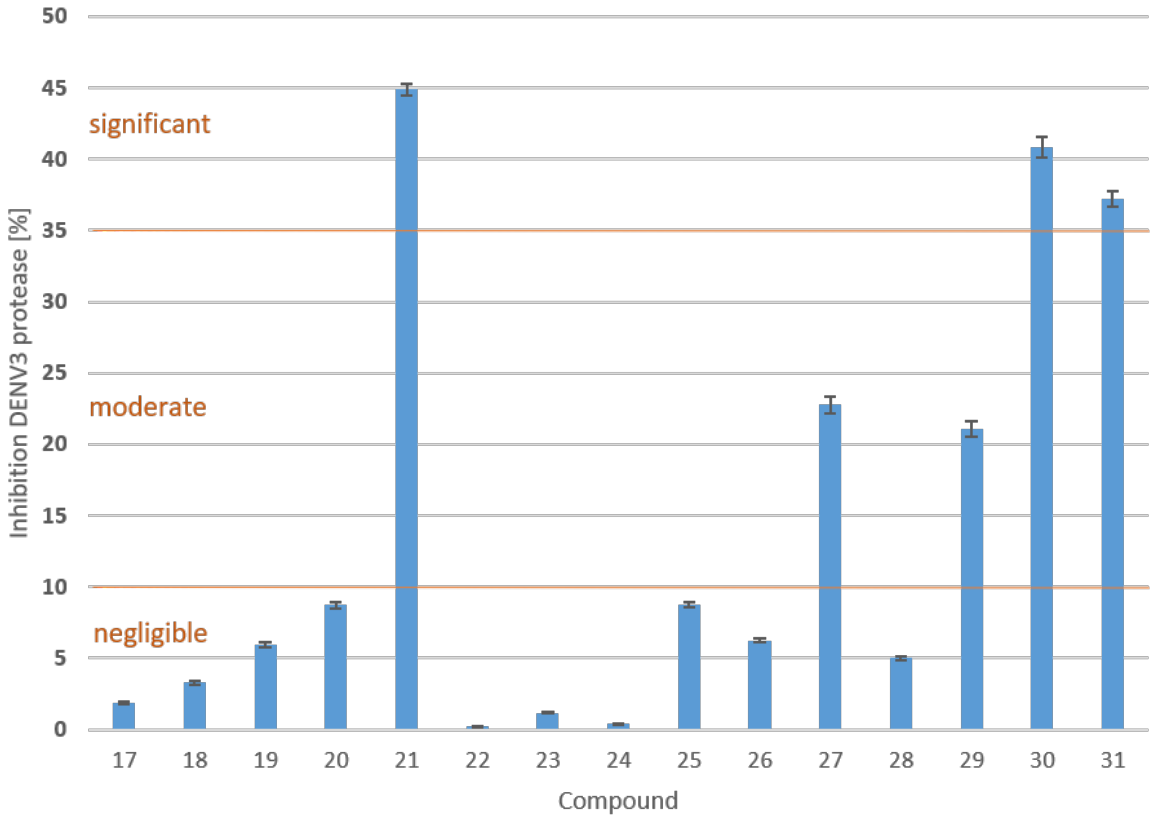

Fig. 3.3 Bar graph showing the percentage inhibition of HTS compounds against DENV3 protease in the fluorescence-based assay at 100 μM.

3.1.6 Further Investigation of the Initial Hit Compound 30

Both compounds **30** and **31** also showed an analogous docking pose as predicted by AutoDock Vina (see Figure 3.4). The nitro group points deep into the allosteric pocket and forms a hydrogen bond with Asn152, which - according to our hypothesis - is crucial for inhibition. Further hydrogen bonds are formed between the aniline amine and the carbonyl oxygen of Lys73, the amide nitrogen and the carbonyl oxygen of Ile165 and the nitrogen of the benzimidazole residue interacts with to Gln88. Moreover, the shape of the pocket is well complemented by the shape of the ligand. According to the predicted docking score, both compounds should significantly inhibit DENV3 protease. Therefore, the IC_{50} value of compound **30** was determined by measuring its percent inhibition of DENV3 at different concentrations (1 μM to 1000 μM). An IC_{50} curve was

then fitted to the data obtained (using GraphPad Prism 7.0), yielding an IC_{50} value of 136±16μM. Considering that compound **30** was a "first clue" from molecular docking, the obtained IC_{50} value seemed to be a good starting point for further optimization.

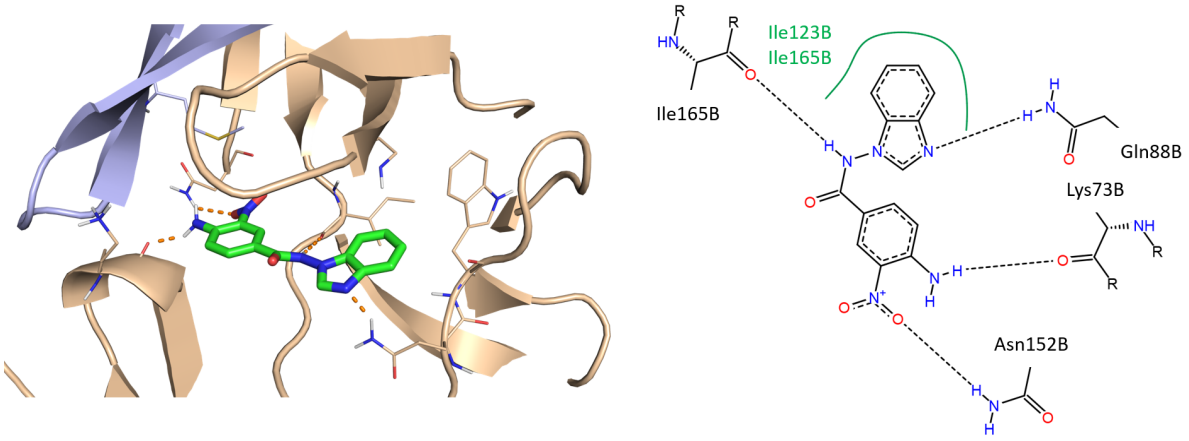

Fig. 3.4 Predicted docking pose of compound **30** in the allosteric pocket of DENV3 (docking was performed with AutoDock Vina)[54]. Left PyMOL image (beige: NS3, lightblue: NS2B, in sticks: compound **30**), right: PoseView image.

Since X-ray data for ligand-protein complexes of the DENV protease are difficult to obtain (see Introduction), an indirect method to detect the allosteric binding mode was needed. A well-known method for proofing non-competitive binding is the so-called Dixon plot.[59] In this plot, the reciprocal reaction rate of the enzyme of interest is plotted against the inhibitor concentration for different substrate concentrations. In this case, $\frac{v_{DMSO}}{v_0}$ was plotted to allow comparison between different measurements since the absolute reaction rates determined varied on the instrument used. As v_{DMSO} is a constant for a series of measurements, this does not change the result of the Dixon plot analysis.

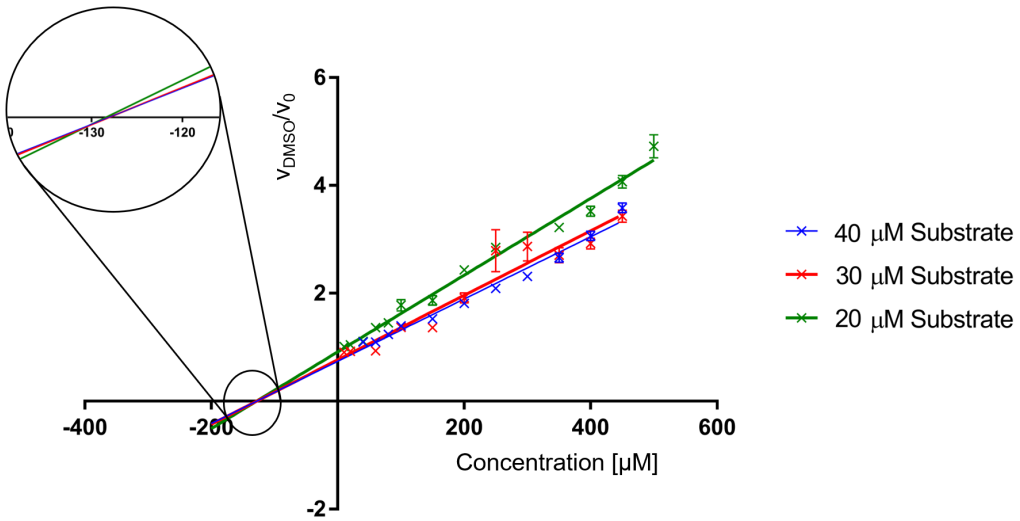

Fig. 3.5 Dixon plot-like analysis for compound **30** against DENV3 protease, using three different substrate concentrations (20, 30, and 40 μM).

In this case, reaction rates were measured for 20, 30, and 40 μM substrate concentrations. Then, when the inhibitor concentration is plotted against the reciprocal reaction rate for the different substrate concentrations, all lines should intersect at a point on the x-axis, if a non-competitive binding mode is present. Indeed, this intersection marks the -K_i value of the protein-ligand complex.[59] Here, all three lines crossed on the x-axis at -128 μM, so that a non-competitive binding mode can be assumed for compound **30** (see Figure 3.5).

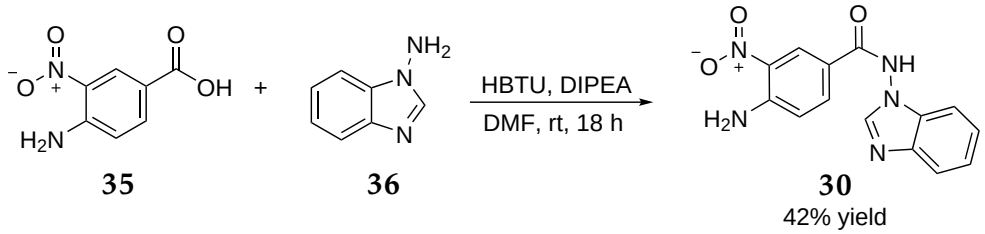

Scheme 3.2 One-step synthesis of compound **30** from 4-amino-3-nitrobenzoic acid (**35**) and 1-amino-benzimidazole (**36**).

Since for the initial tests compound **30** was only acquired in a small amount (10 mg) with limited purity (>90%), it was necessary to re-synthesize this compound on a larger scale and with improved purity to confirm the results shown above. Compound **30** was accessible in a one-step synthesis from 4-amino-3-nitrobenzoic acid (**35**) and 1-amino-benzimidazole (**36**) using standard amide coupling conditions (Scheme 3.2). Although the yield of the reaction was only moderate (42%), sufficient material with a higher purity (>95%) was obtained for further testing. An IC_{50} determination for this batch of compound **30** gave an IC_{50}-value of 189.5±20 μM, which was in reasonable agreement with the previously determined one.

3.2 Transferal of an Initial Hit into a Lead Fragment

With the discussed results in hand, the next question to be answered was which parts of compound **30** are essential for the observed DENV protease inhibition. In a first step answering this question, compound **37** was synthesized (Scheme 3.3). It contains the entire "left" part of compound **30** (orientation as seen in docking pose, Fig. 3.4 left), but the benzimidazole moiety is replaced by a cyclopropyl group, which represents the smallest possible substituent (besides a methyl group). Compound **38** was synthesized by transferring 4-amino-3-nitrobenzoic acid (**35**) into the corresponding acid chloride and subsequent reaction with cyclopropylamine. The reaction proceeded smoothly and furnished compound **37** in good yield (75%) and high purity, so that this type of reaction was used as a template for future similar reactions. Although compound **37** has nearly fragment size (<12 heavy atoms)[60] and thus was expected to show little or no

inhibition of DENV3 protease, its IC_{50} value against DENV3 protease was determined to be 226±30 μM, making it only slightly less potent than compound **30**, suggesting that the 1-amino-benzimidazole residue plays only a minor role in the affinity of compound **30**, which is supported by the docking pose shown above (Figure 3.4), where 3 of 4 hydrogen bonds are formed by the portion of the molecule retained in compound **37**. Indeed, when the structure of compound **37** was used as input for molecular docking, an analogous docking pose as for compound **30** was retrieved. The ligand efficiency (LE) of compound **37** was determined to be 0.32 using the approximation $LE = 1.4 \cdot pIC_{50} \cdot \frac{1}{N}$ (N is the number of heavy atoms, in this case 16).[60] This fits well with the often stated requirement that the LE of candidates in the drug design development process should always be greater than 0.3,[60] so that compound **37** is considered a good starting point for further drug development.

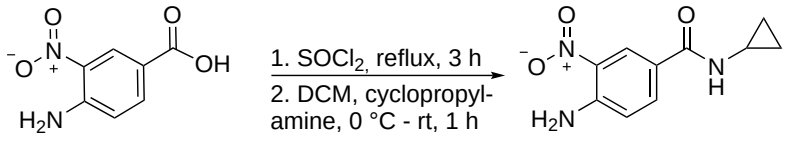

35 → **37** (75% yield)

Scheme 3.3 Synthesis of compound **37** by generation of an acid chloride from compound **35** and subsequent reaction with cyclopropylamine.

3.2.1 Efforts for the Replacement of the Nitro Group

Since drugs containing nitro groups have been associated with mutagenicity and genotoxicity,[61] usually within medicinal chemistry projects efforts are made to replace this residue. Here, due to the proposed docking pose of compound **37**, it would be important to maintain the hydrogen bond to amino acid Asn152 in case of replacing the nitro group. Since fluorine atoms can also act as (weak) hydrogen bond acceptors,[62] the nitro group was replaced by a fluorine (compound **39**) and a trifluoromethyl group (compound **40**) in a first attempt (Scheme 3.4).

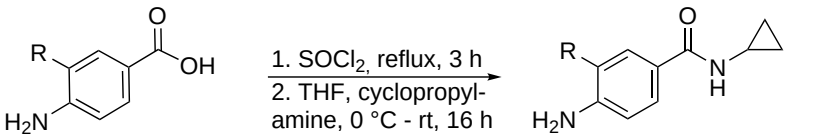

R = F **41**; R = CF_3 **42** → R = F **39** 96% yield; R = CF_3 **40** 93% yield

Scheme 3.4 Synthesis of two fluorine-containing compounds **39** and **40** in an first attempt to replace the potentially toxic nitro group.

Surprisingly, both compounds showed no activity against DENV3 protease, even at a concentration of 1000 μM, most likely due to the weaker hydrogen bond accepting properties of fluorine or maybe due to a changed binding mode. In an *in silico* approach, the nitro group was replaced by several other functional groups with hydrogen bond acceptor properties, such as carboxylic acid, ester, sulfonamide and methyl sulfoxide. The resulting virtual compounds were docked into the allosteric pocket of DENV3 protease with AutoDock Vina, but apart from the compound with a methyl sulfoxide substituent, all other compounds did not lead to promising docking poses. Therefore, only the synthesis of methyl sulfoxide derivative **43** was pursued. The required five-step synthetic route started from methyl 3-fluoro-4-nitro-benzoic acid (**44**), which was reacted in the first step with sodium thiomethylate in a nucleophilic aromatic substitution (Scheme 3.5). This step proved to be very temperature sensitive: at -78 °C, the reaction did not proceed at all, while at room temperature a 1:1 mixture was obtained between compound **45** and a di-methyl-sulfinyl substituted side product. Interestingly, the nitro group acted as a leaving group at room temperature. This is quite unusual but has been reported in the literature.[63] The most suitable reaction temperature was -42 °C, at which no by-product was formed and compound **45** could be isolated in 31% yield.

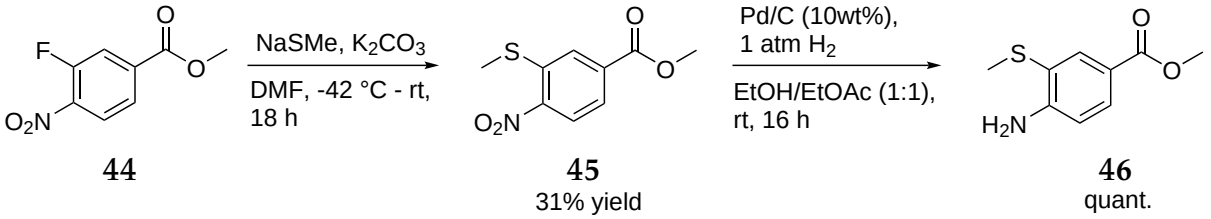

Scheme 3.5 First two steps in the synthetic route towards compound **43**.

In the second step, the nitro group of compound **45** was reduced to an amine via Pd/C-catalyzed hydrogenation, which proceeded smoothly in quantitative yield. The obtained product **46** proved to be slightly sensitive to air (formation of by-products within 3-4 days in air), so it was stored under argon atmosphere. The methylsulfinyl residue of compound **46** was subsequently converted to a methyl sulfoxide by oxidation.

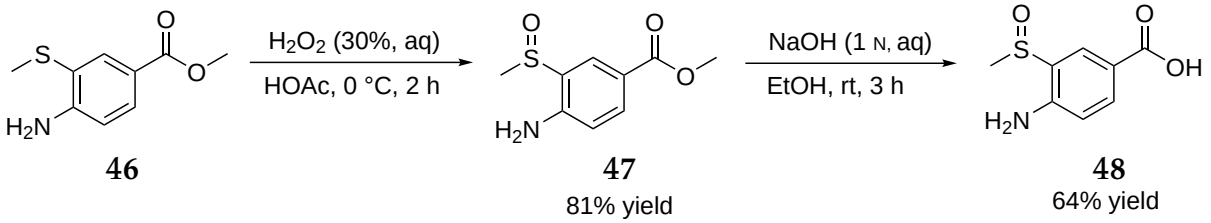

Scheme 3.6 Third and fourth step in the synthetic route towards compound **43**.

When using only one equivalent of hydrogen peroxide as oxidant, no overoxidation to the corresponding methyl sulfdioxide was observed and compound **47** was obtained in good yield (Scheme 3.6). Saponification of compound **47** with sodium hydroxide proceeded with only moderate yield due to the formation of a separable but not identifiable by-product. For the conversion of compound **48** to the final product, the established protocol of acid chloride formation followed by addition of cyclopropylamine was used. Interestingly, this approach led to the formation of several non-separable by-products, so this reaction path was not pursued further. Alternatively, compound **48** was reacted with cyclopropylamine under amide coupling conditions using HBTU as the coupling reagent (Scheme 3.7), giving rise to compound **43** in a moderate yield of 48%. However, as compound **43** was obtained in sufficient amount and purity for *in vitro* testing, the reaction conditions were not optimized further. Although compound **43** is itself a solid, its high hygroscopicity caused it to liquefy in air within minutes, so measuring a specific amount became a challenge.

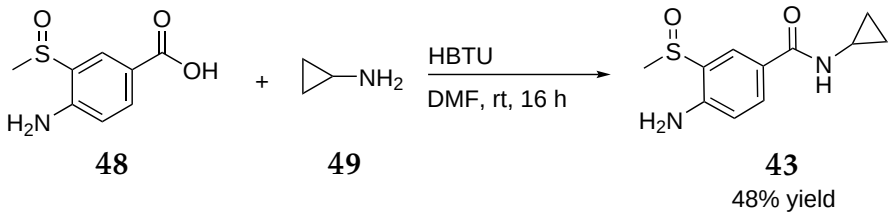

Scheme 3.7 Compound **43** was synthesized via amide coupling of compound **48** with cyclopropylamine.

As the docking pose of compound **43** looked quite promising, it was surprising that the compound showed no detectable inhibition of DENV3 protease in the fluorescence-based assay. From all these failed attempts to replace the nitro group, it was concluded that the nitro group was essential for the observed inhibition and would not be replaced in a suitable manner.

3.2.2 Further Structural Studies of the Lead Fragment

In additional molecular docking studies, both the substitution of the aniline amine and the substitution of the amide residue were investigated (same setup as before for docking). Two substitutions proved to be advantageous: first, the replacement of the aniline amine by a hydroxy group which preserved the proposed hydrogen bond to Lys73, but had the advantage of not having an additional stranded donor. Second, by replacing the amide residue with a sulfonamide, the hydrogen bond to Ile165 was retained, but offered more conformational freedom compared to an amide. Both substitutions were also synthesized to verify the *in silico* predictions with the help of *in vitro* experiments.

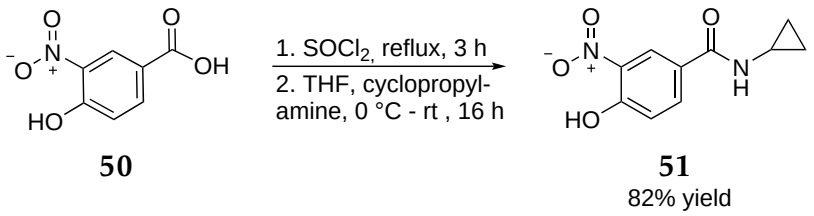

Scheme 3.8 Synthesis of the hydroxy-substituted compound **51** via acide chloride formation and subsequent reaction with cyclopropylamine.

The hydroxy-substituted derivative **51** was synthesized by forming the corresponding acid chloride from 4-hydroxy-3-nitrobenzoic acid (**50**) and subsequent reaction with cyclopropylamine, furnishing compound **51** in good yield and high purity (Scheme 3.8). The IC_{50} of compound **51** against DENV3 protease was determined by a fluorescence-based assay. With 241±25 μM it is comparable to the value determined for compound **37**. It can be concluded that the substitution of the aniline amine by a hydroxy group has only a weak effect on the inhibition of DENV3 protease.

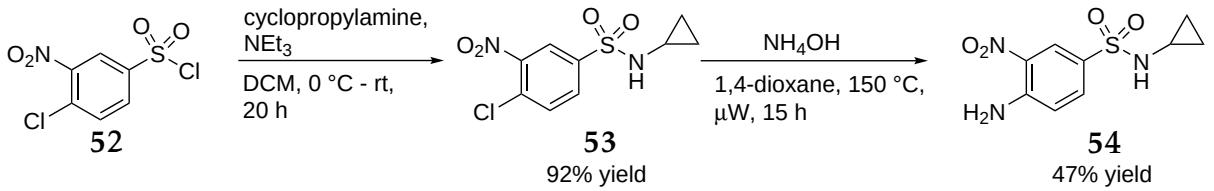

Scheme 3.9 Synthesis of sulfonamide **54** from 4-chloro-3-nitro-benzenesulfonyl chloride (**52**) in a two-step procedure.

The synthesis of sulfonamide **54** was accomplished in a two-step procedure (Scheme 3.9): first, 4-chloro-3-nitro-benzenesulfonyl chloride (**52**) was reacted with cyclopropylamine in a nucleophilic substitution of the sulfur-bound chlorine in very good yield. Subsequently, sulfonamide **53** was converted to compound **54** by reaction with ammonium hydroxide. Since this nucleophilic aromatic substitution required high temperatures to proceed, it was carried out in a microwave reactor at 150 °C. Due to the harsh reaction conditions, several unidentifiable side products were formed and compound **54** could only be isolated in moderate yield (47%). The IC_{50} value of compound **54** against DENV3 protease was determined to be 251±14 μM, which is in the same range as the value determined for the lead fragment **37**. Since the sulfonamide substitution did not result in any appreciable improvement in affinity and was more complicated to synthesize and low yielding compared to the amide, this strategy was not pursued further.

3.2.3 Investigation of Ester Derivatives

The starting material for the synthesis of compound **37**, 4-amino-3-nitrobenzoic acid (**35**), was also tested for its inhibition of DENV3 protease in the fluorescence-based assay. Surprisingly, its IC_{50} value was even lower than that for fragment **37**, namely 187±18 μM. Since the assay is measured at pH 9, the carboxylic acid of compound **35** should be deprotonated and thus negatively charged, preventing the formation of a hydrogen bond to Ile165.

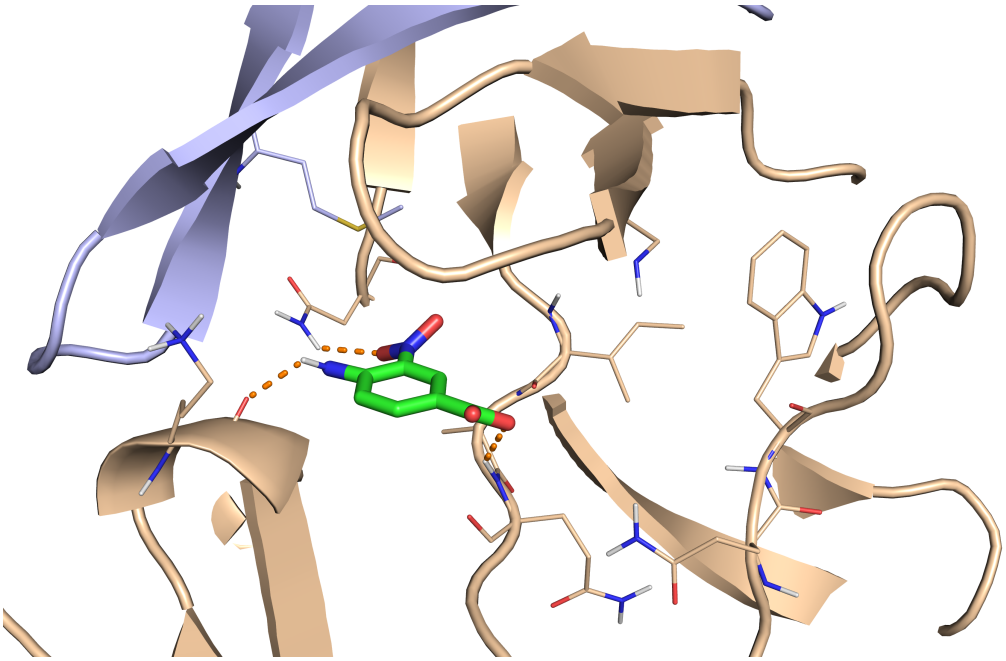

Fig. 3.6 Docking pose of compound **35** in the allosteric pocket of DENV3. Beige: NS3, lightblue: NS2B, in sticks: compound **35**.

To better understand the obtained IC_{50} value, the structure of 4-amino-3-nitrobenzoic acid (**35**) was also used as input for molecular docking. In the resulting docking pose, the hydrogen bonds to AAs Asn152 and Lys73 were retained, but the hydrogen bond to Ile165 was replaced by a hydrogen bond to Ala166 (Figure 3.6). Considering the determined IC_{50} value for compound **35**, this seems plausible.

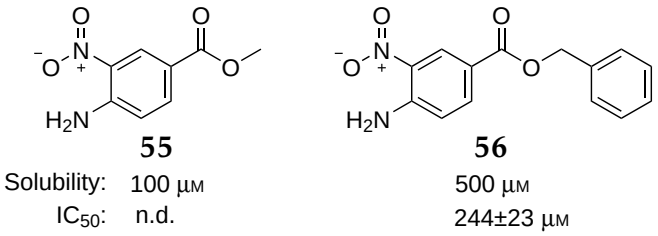

Fig. 3.7 The two esters **55** and **56** showed limited solubility in the fluorescence-based assay and did not perform better than the amide derivatives.

Since corresponding ester derivatives should also be able to form this hydrogen bond to Ala166, two ester derivatives, methyl 4-amino-3-nitrobenzoate (**55**) and benzyl 4-amino-3-nitrobenzoate (**56**), were synthesized to test this hypothesis (using standard esterification procedures, see Experimental section). The methyl ester **55** proved to be too insoluble in the buffer of the fluorescence-based assay to determine its IC_{50} value, but the benzyl derivative **56** was moderately soluble ($\approx 500\ \mu M$) allowing its IC_{50} value against DENV3 protease to be determined ($244 \pm 23\ \mu M$, Figure 3.7). Since the ester derivatives had limited solubility and did not perform significantly better than the amide derivatives, they were not investigated further.

3.3 Extension of the Lead Fragment into more Potent Structures

3.3.1 *In silico* Generation and Docking of a Library of Extended Compounds

Having established the essential structural requirements for the inhibition of DENV protease by examination of the lead fragment **37**, in the next step a library of compounds with hypothetically increased affinity was generated and evaluated by molecular docking. To maintain the interactions with the "left" part of the allosteric pocket, the core structure of lead compound **37** was retained, but the cyclopropyl residue was replaced by substituents with additional interactions (Figure 3.8).

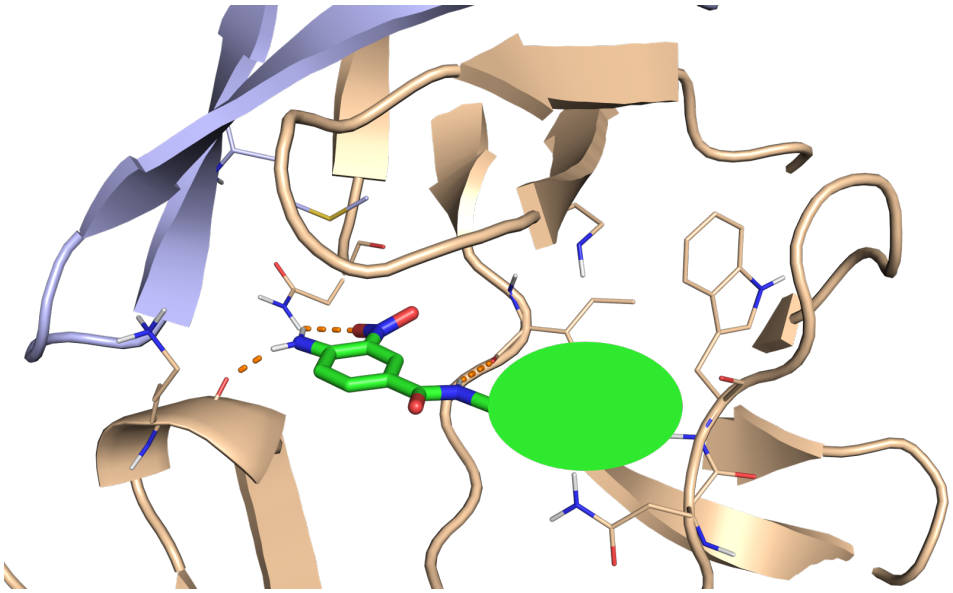

Fig. 3.8 Illustration of the envisaged extension of lead fragment **37** by molecular docking. Beige: NS3, lightblue: NS2B, in sticks: extended compound (oval pictures moiety to be varied).

To create a suitable *in silico* molecule library, two approaches were taken: first, the screening compound catalog of the vendor Enamine was searched for molecules that met the criteria described above. The reason for this search was that the original hit **30** was from this catalog, so Enamine was known to have this structural type of compounds in its portfolio. The search resulted in a total number of 1499 analogues, which were converted from SMILES-code to the required pdbqt format using the OpenBabel program.[64] In a second approach, the Pingui module, developed by the Kolb research group, was used to generate a suitable library. In Pingui, chemical reactions can be applied to a given starting material using a library of molecules as reaction partners.[65] In this case, 4-amino-3-nitrobenzoic acid was *in silico* coupled to all amines available from the supplier Molport in an amide coupling reaction, resulting in a virtual library of 37607 compounds that were also converted from SMILES-code to pdbqt format using

OpenBabel.[64] For molecular docking of both libraries, the same receptor file and set up of AutoDock Vina was used as for the HTS. The top 500 ranked molecules of each docking were visually inspected using the same criteria as previously described and two additional criteria: it was additionally checked whether the established interactions with the "left" part of the allosteric pocket were maintained and whether the respective extension offered additional favorable interactions. If any of the criteria were not met, the compound was discarded.

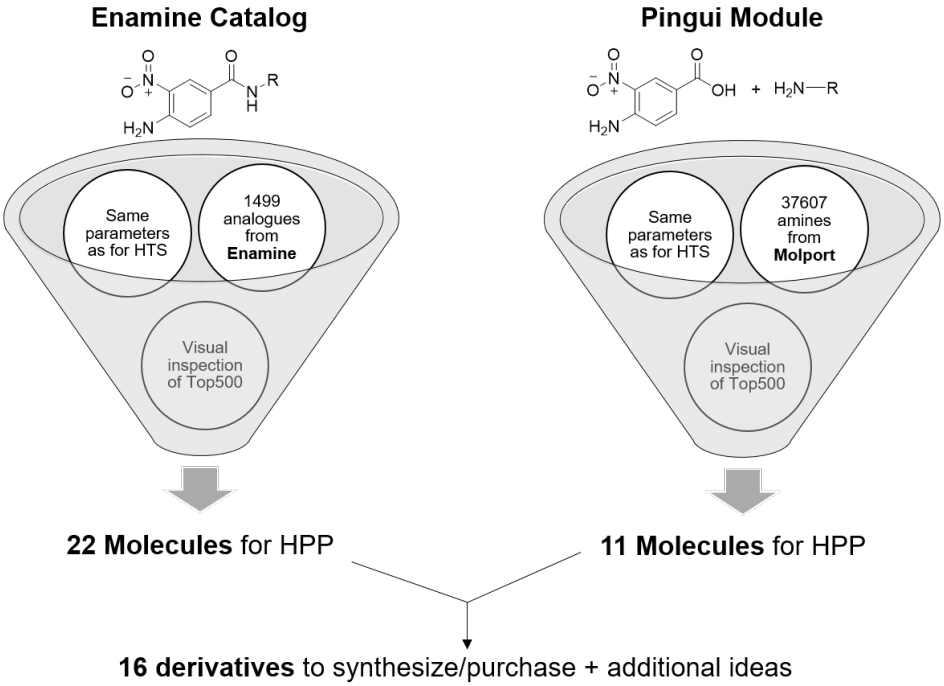

Fig. 3.9 Illustration of the two approaches taken for virtual screening of the extended compounds.

As illustrated in Figure 3.9, in case of the Enamine catalog library this approach resulted in 22 compounds with advantageous docking poses, and in the case of the Pingui module library, 11 compounds were retrieved. The docking poses of all selected compounds were further discussed and evaluated in plenary ("Hit Picking Party", HPP), resulting in a set of 16 compounds to be either synthesized or purchased for *in vitro* testing. One additional brainstormed idea was also added to this list. The list of compounds obtained covers a broad structural range, increasing the probability of finding one or more hits with improved affinity (Figure 3.10). For each compound, a synthetic route had to be established.

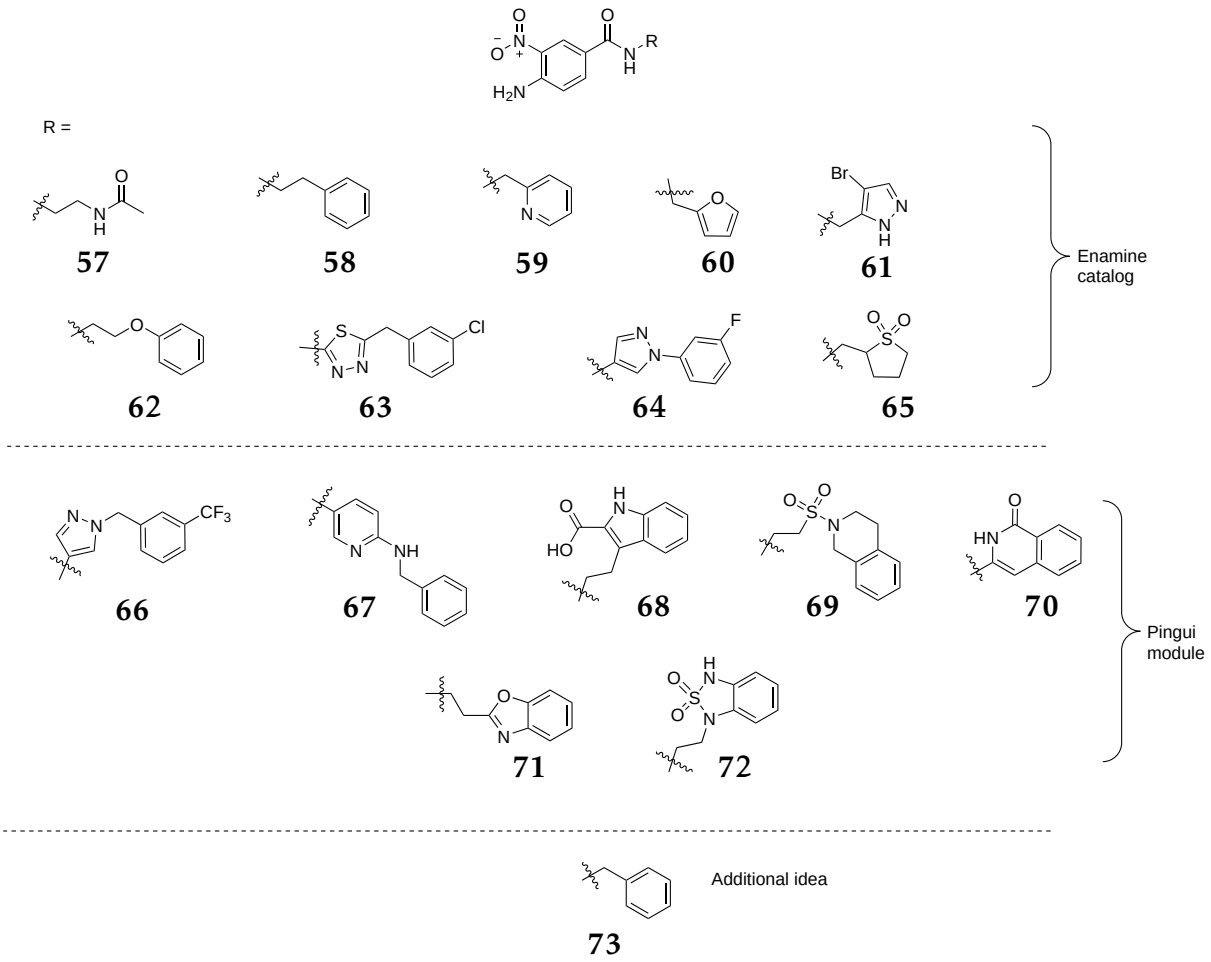

Fig. 3.10 Structure of the compounds selected for further investigations from the two docking processes.

3.3.2 Synthesis of the Extended Compounds

One-Step Syntheses

For the synthesis of 7 of the 17 compounds, only the amide coupling step of the commercially available amine with 4-amino-3-nitrobenzoic acid (**35**) was required. Since the conversion of the carboxylic acid to the corresponding acid chloride and subsequent reaction with an amine as nucleophile had already been successful for this structural motif, this method was also used here. In the case of cyclopropylamine, the amine acted as both nucleophile and base. However, since most of the seven amines were less basic (or more expensive), triethylamine (TEA) or DIPEA were used as the base, and the amine was added only in a slight excess (1.1-1.2 eq). In all cases, 4-amino-3-nitrobenzoic acid (**35**) was refluxed in thionyl chloride for 2-3 h to convert it to the corresponding acid chloride. After removal of the excess of thionyl chloride, the crude acid chloride was dissolved in THF, and amine and base were added at 0 °C. After stirring at RT overnight, complete conversion was observed in all cases. Although the

starting material 4-amino-3-nitrobenzoic acid (**35**) contains an (aniline) amine that could act as a nucleophile, the formation of by-products due to attack of the aniline amine has been detected only in trace amounts (1-5% according to LC-MS), which can most likely be attributed to the reduced nucleophilicity caused by the *ortho*-nitro group. Consequently, protecting group strategies did not appear to be necessary in this case.

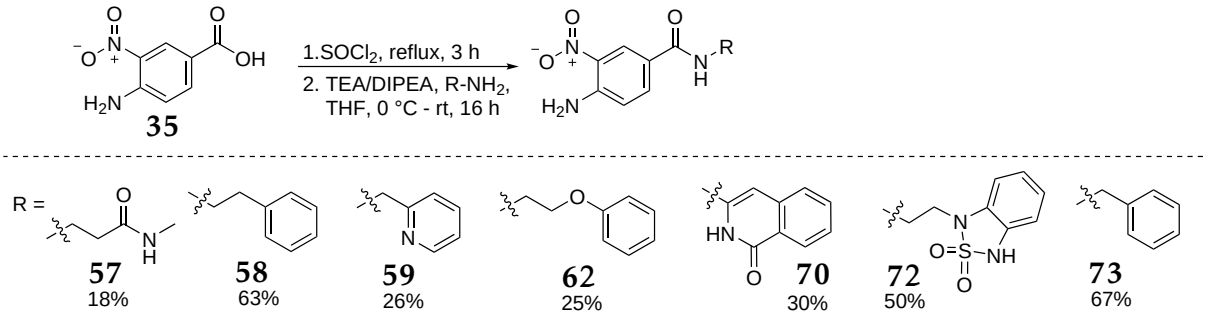

Scheme 3.10 One-step syntheses of target compounds from 4-amino-3-nitrobenzoic acid (**35**) via acid chloride generation and subsequent reaction with an amine as nucleophile.

As shown in Scheme 3.10, the yield varied considerably in the different reactions (from 18% to 67%). The main reason for this were the purification steps required to obtain the final products in sufficient purity for *in vitro* testing. For example, compound **57** proved to be highly polar and highly soluble in water, so that extraction with organic solvents was only possible to a limited extent and column chromatography under normal phase conditions was completely impossible. The product could only be purified by recrystallization from MTBE/^{i}PrOH (1:1), which resulted in a poor yield (18%). Other compounds, such as compound **70**, were poorly soluble in common organic solvents (and water) and incomplete product recovery was an issue in each purification step. In contrast, compound **73** was highly soluble in EtOAc and acetone, facilitating purification was eased and resulting in a good yield (67%).

Synthesis of thiadiazole 63

A retrosynthetic analysis revealed that thiadiazole **63** can be synthesized in a two-step procedure by first generating the required amine **74** in a cyclization reaction with thiosemicarbazide and then reacting it with 4-amino-3-nitrobenzoic acid (**35**) in an amide coupling. The appropriate reaction conditions for the first step have already been described in the literature,[66] and could be reproduced here. The proposed reaction mechanism for the cyclization can be described as follows:[67] first, the carboxylic acid is converted to the corresponding acid chloride by reaction with $POCl_3$. The activated intermediate is then nucleophilically attacked by the hydrazide moiety of the thiosemicarbazide to form intermediate I under HCl elimination. Protonation of

the carbonyl oxygen yields to intermediate II, which is intramolecularly attacked by the sulfur atom to form the five-membered intermediate III. This intermediate exists in three different mesomeric forms, as shown in Scheme 3.11. Deprotonation of the charged intermediate III leads to the formation of the uncharged intermediate IV, which, after protonation and subsequent water elimination, reacts to form intermediate VI, which again exists in three different mesomeric forms. Deprotonation of this intermediate then yields the 1,3,4-thiadiazole as final product.

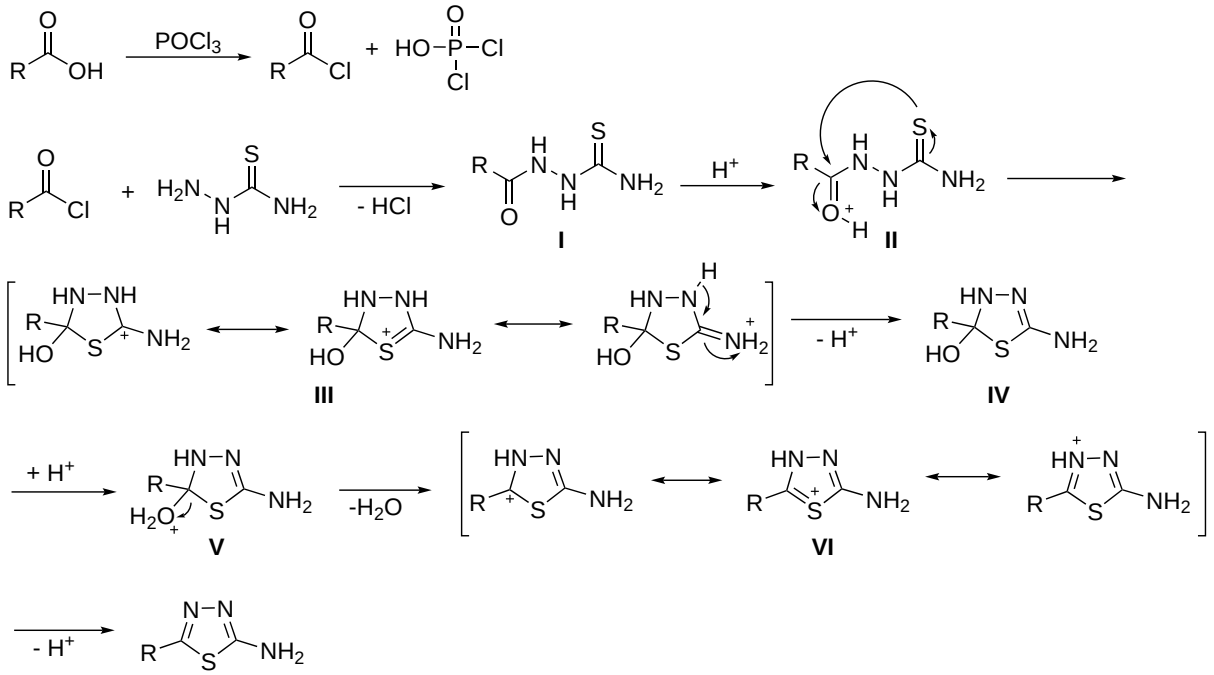

Scheme 3.11 Proposed reaction mechanism for the formation of 1,3,4-thiadiazoles from the corresponding carboxylic acids and thiosemicarbazide.[67]

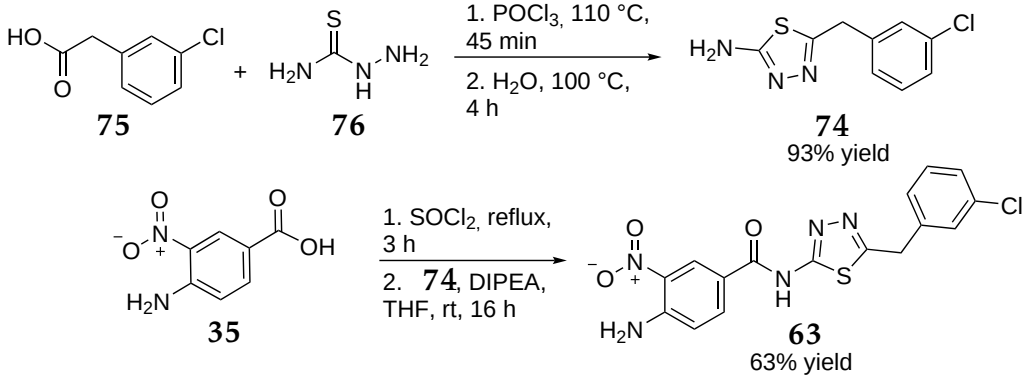

Scheme 3.12 Synthesis of 1,3,4-thiadiazole **63** in a two-step procedure by generating amine **74** by cyclization with thiosemicarbazide (**76**) and subsequent amide coupling.

Accordingly, 3-chlorophenylacetic acid (**75**) was refluxed with thiosemicarbazide (**76**) in $POCl_3$ for 45 min, after which water was added to quench the excess $POCl_3$ (Scheme 3.12). After neutralization and filtration, compound **74** was obtained in very good yield (93%). The step of the amide coupling was carried out under the same reaction conditions as in the one-step syntheses and gave the desired thiadiazole **63** in good yield (63%) and high purity.

Synthesis of Pyrazoles 66 and 64

Pyrazole **66** was synthesized following a three-step sequence: in the first step, 3-(trifluoromethyl)benzyl bromide (**77**) was reacted with 4-nitro-1*H*-pyrazole (**78**) in a nucleophilic substitution using K_2CO_3 as base (Scheme 3.13), which after workup gave the desired pyrazole **79** in nearly quantitative yield (96%). Iron powder was used as a reducing agent (under acidic conditions) for the subsequent reduction of the nitro group. Follow-up purification proved difficult because product **80** coordinated to the iron ions formed during the reaction. However, no alternative reducing agent (e.g. Pd/C) was tested since most other reducing agents would also cleave off the benzyl moiety. Decoordination of the iron ions could be achieved by transferring the amine to an HCl salt, which gave compound **80** in moderate yield (52%) and good purity.

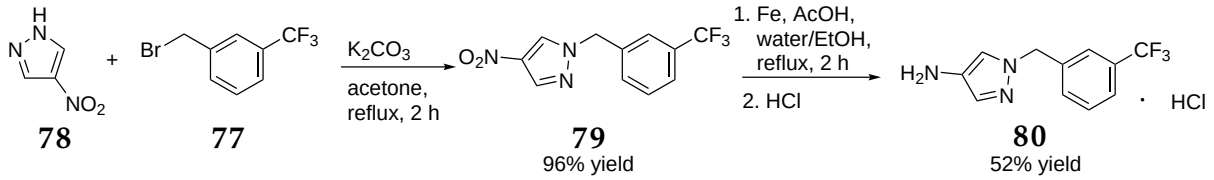

78 **77** **79** 96% yield **80** 52% yield

Scheme 3.13 Synthesis of amine **80** in a two-step procedure by nucleophilic substitution of 4-nitro-1*H*-pyrazole (**78**) and subsequent reduction of the nitro group.

The final amide coupling step was carried out under standard conditions giving rise to the desired pyrazole **66** in excellent (95%) yield and high purity (Scheme 3.14).
For the synthesis of pyrazole **64**, the order of the synthesis steps had to be reversed: first, 1*H*-pyrazol-4-amine (**81**) was reacted with 4-amino-3-nitrobenzoic acid (**35**) under the usual amide coupling conditions (Scheme 3.15). During the reaction, a side product was formed due to the nucleophilic attack of the pyrazole-NH instead of the -NH_2 group, which significantly decreased the yield (20%). However, the desired product **82** was obtained in sufficient purity after column chromatography and additional washing steps.

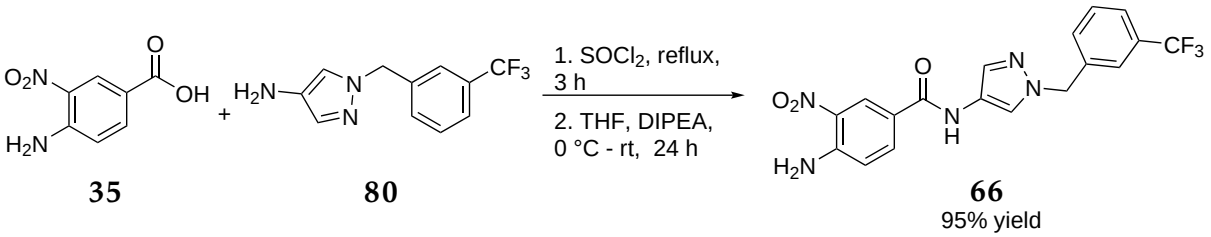

Scheme 3.14 The final step in the synthesis of pyrazole **66** was the amide coupling of 4-amino-3-nitrobenzoic acid (**35**) with amine **80**.

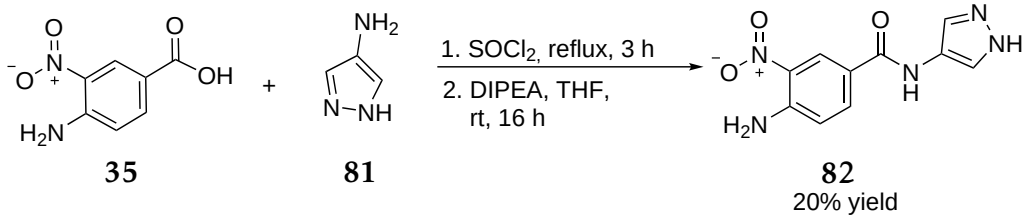

Scheme 3.15 Synthesis of compound **82** by amide coupling of 1*H*-pyrazol-4-amine (**81**) with 4-amino-3-nitrobenzoic acid (**35**).

In the second step, compound **82** was reacted in an Ullmann-type coupling with 3-bromo-fluorobenzene (**83**) using a system consisting of copper(I) iodide and *trans*-*N*,*N*'-dimethyl cyclohexane-1,2-diamine (**84**) as catalyst (Scheme 3.16). This reaction furnished the desired pyrazole **64** in acceptable yield (41%) and high purity. In this case, the two synthesis steps had to be reversed because the Ullmann coupling of 1*H*-pyrazol-4-amine (**81**) with 3-bromo-fluorobenzene (**83**) was unsuccessful (no conversion). Possibly, 1*H*-pyrazol-4-amine (**81**) as a bidentate ligand coordinates strongly to the copper center, thereby blocking the catalytic cycle.

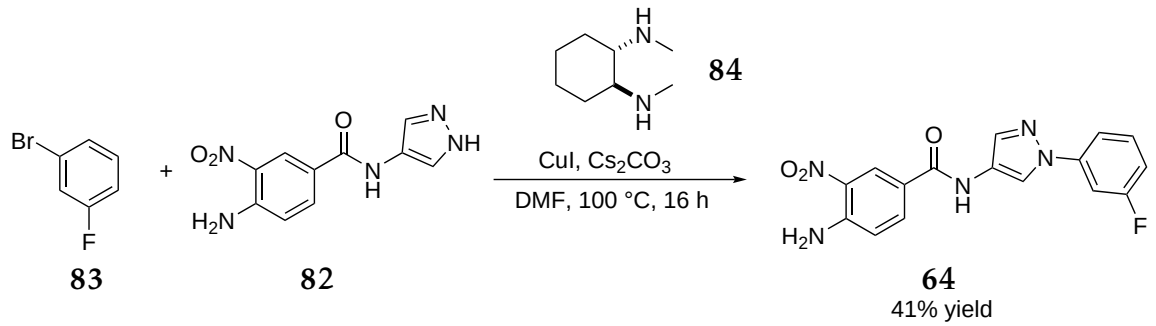

Scheme 3.16 Ullmann-type reaction for the synthesis of pyrazole **64** from compound **82** and 3-bromo-fluorobenzene (**83**).

The catalytic mechanism of Ullmann-type reactions has for a long time controversially been discussed in the literature, but it is now most commonly assumed that the reaction proceeds in the following manner:[68] in the first step, an aromatic amine coordinates to copper(I) species I, which is formed from a copper(I)-halogen salt (usually CuI) and a (bidentate) ligand. This step is reversible and leads to intermediate II. The amine of intermediate II is deprotonated by a base (e.g. Cs_2CO_3), resulting formally in an HX elimination and formation of intermediate III. This intermediate undergoes oxidative addition to aryl halide Ar'X forming intermediate IV. Since Cu(III)-species are quite unstable, this intermediate undergoes rapid reductive elimination by releasing the product Ar'Nu and re-forming the catalytically active copper-species I.

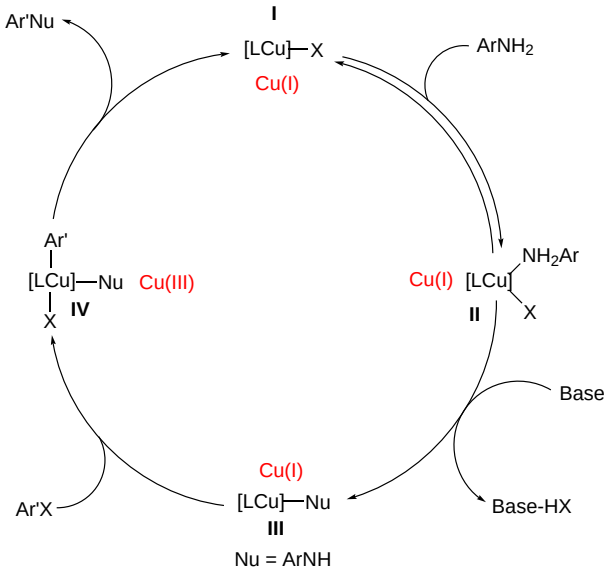

Scheme 3.17 Most probable catalytic mechanism for Ullmann-type reactions using an aromatic amine as nucleophile.[68]

Synthesis of Pyridine 67

For the synthesis of pyridine **67**, a similar approach was taken as for pyrazole **66**: first, 2-chloro-5-nitropyridine (**85**) was reacted with benzylamine in a nucleophilic substitution, giving compound **86** in excellent yield (94%) (Scheme 3.18). Subsequently, the nitro group was reduced to the corresponding amine using iron powder as reducing agent. Although coordination of the formed iron ions by product **87** also occurred here, a sufficiently pure product was obtained by column chromatography (72% yield). Obviously, the amine-iron complex was much less stable in this case.
Again, the final product **67** was obtained by amide coupling of amine **87** with 4-amino-3-nitrobenzoic acid (**35**) (Scheme 3.19). Since no side reaction occurred and the final product **67** was readily soluble in common organic solvents, the purification step proceeded without complications and afforded pyridine **67** in almost quantitative yield.

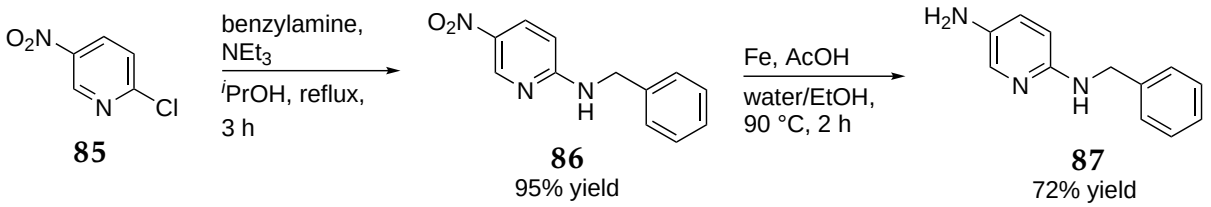

Scheme 3.18 Two-step synthesis of amine **87** by nucleophilic substitution of 2-chloro-5-nitropyridine (**85**) with benzylamine and subsequent reduction of the nitro group.

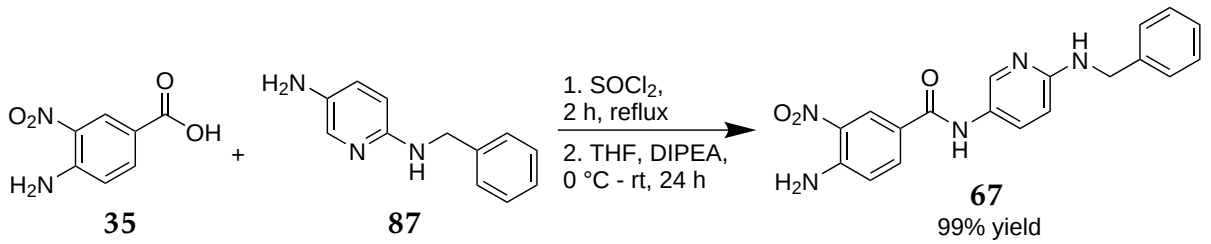

Scheme 3.19 Final step in the synthesis of pyridine **67**: Amide coupling of amine **87** with 4-amino-3-nitrobenzoic acid (**35**).

Synthesis of Compounds 69 and 71

The synthetic pathway for both compound **69** and compound **74** began with phthalimide-protected starting materials, so that their synthesis was quite analogous and can be described in one section. In the first step of the synthetic pathway towards compound **69**, sulfonyl chloride **88** was reacted with isoquinoline **89**, 3.5 eq of which were added so that it acted as both base and nucleophile (Scheme 3.20).

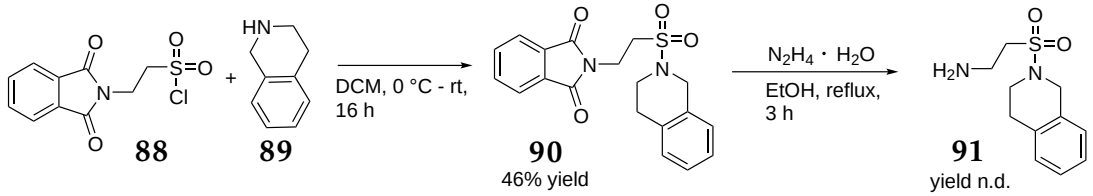

Scheme 3.20 Synthesis of amine **91** starting from 2-(1,3-dioxoisoindolin-2-yl)ethane-1-sulfonyl chloride (**88**) and subsequent deprotection with hydrazine hydrate.

Since the obtained product **90** did not prove stable on column chromatography, it was purified by recrystallization from ^{i}PrOH, resulting in an acceptable yield of 46%. The second step involved deprotection of the phthalimid-protected amine using hydrazine hydrate. Although the general procedure is frequently described in the literature, in this case it resulted in the formation of many by-products that could only partially be separated from the desired product **91**. Therefore, the yield of amine **91** was not determined and it was used directly for the next step.

In the last step, crude amine **91** was reacted with 4-amino-3-nitrobenzoic acid (**35**) in an amide coupling reaction (Scheme 3.21). Since only a crude mixture of compound **91** could be used, it was not surprising that the reaction yielded many side-products that had to be separated by column chromatography followed by prep-HPLC (reversed phase, water/MeCN as eluent). However, it was possible to synthesize the desired compound **69** in low yield (19% over two steps) but high purity.

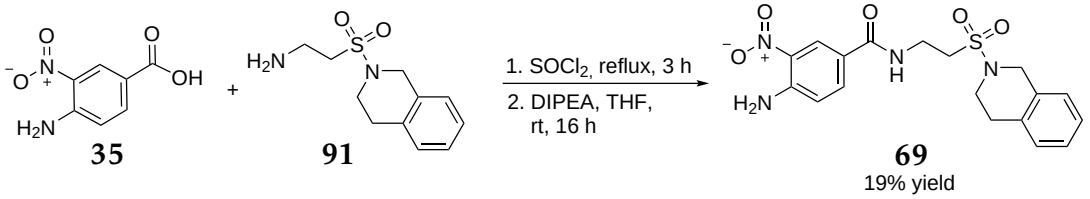

Scheme 3.21 Final step in the synthesis of compound **69**: amide coupling of amine **91** with 4-amino-3-nitrobenzoic acid (**35**) (yield is given over two steps).

The general approach to the synthesis of compound **71** was quite similar, with the first stepbeing slightly modified: first, the phthalimide-protected starting material **92** was reacted with 2-aminophenol (**93**) in a cyclization reaction (Scheme 3.22). Acidic conditions and high temperatures were required for this cyclization, so it was carried out in polyphosphoric acid at 180 °C.[69]

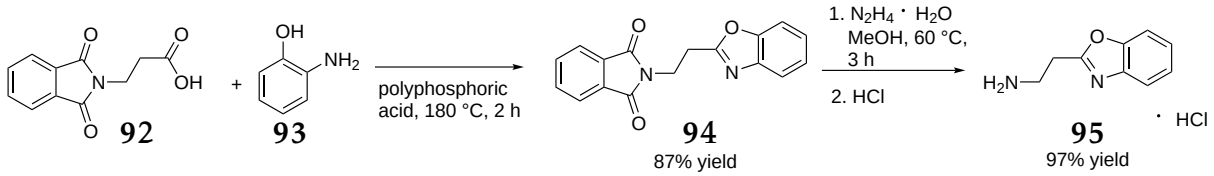

Scheme 3.22 The synthesis of amine **95** was conducted in a two-step procedure by cyclization and subsequent deprotection of the phthalimide-protected amine.

After collection of the product by filtration and washing/extraction, compound **94** was obtained in high yield (87%) and good purity. Analogous to the previously described synthetic route, the phthalimide-protected amine **94** was deprotected by use of hydrazine hydrate. In this case, however, the reaction proceeded smoothly and gave the desired amine **95** in nearly quantitative yield (97%) after conversion to the corresponding HCl salt.

Finally, amine **95** was reacted to the final compound **71** by amide coupling with 4-amino-3-nitrobenzoic acid (**35**) (Scheme 3.23). As described previously, the HCl salt was deprotonated prior to reaction with DIPEA. Although the reaction conversion was complete and no side-product formation was detected, the desired compound **71** was obtained in only 33% yield after column chromatography.

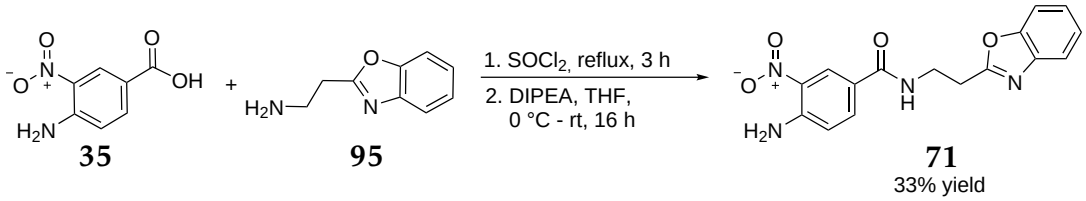

Scheme 3.23 Final step in the synthesis of compound **71**: amide coupling of amine **95** with 4-amino-3-nitrobenzoic acid (**35**).

Non-Synthesized Compounds

In the case of the compounds discussed above, it was possible to find a short synthetic approach, which proved to be more favorable than purchasing the corresponding substances. In principle, self-synthesis of the substances always offers the advantage of supplying larger quantities in higher purity than would be possible with commercial purchase. However, for compounds **60**, **61** and **65**, no reasonable synthetic approach could be identified, so they were purchased directly from the supplier Enamine in sufficient quantity and purity for *in vitro* testing (10 mg each, >90% purity). For compound **68**, a literature search for a useful synthetic approach was also unsuccessful, but it was also not available for purchase from the usual suppliers, so it had to be excluded from the list of compounds to be tested for activity against DENV3 protease (Figure 3.11).

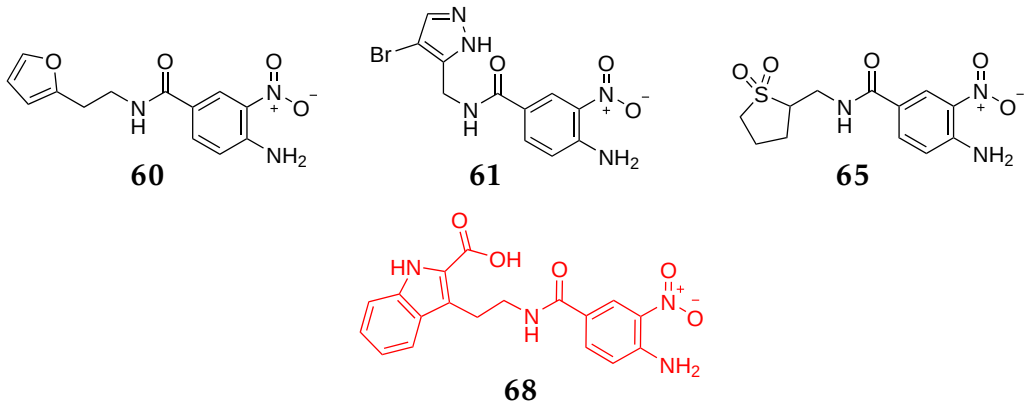

Fig. 3.11 Structure of the compounds that were not synthesized. Compounds **60**, **61** and **65** were purchased from the supplier Enamine, compound **68** was excluded from further considerations.

3.3.3 *In vitro* Testing of the Extended Compounds

Having presented the synthesis of the extended compounds in detail in the previous section, this section focuses on the discussion of their activity in the fluorescence-based DENV3 protease assay. Initially, the percentage inhibition of each compound was tested at a concentration of 100 μM to determine if the compounds performed better than the lead fragment **37**.

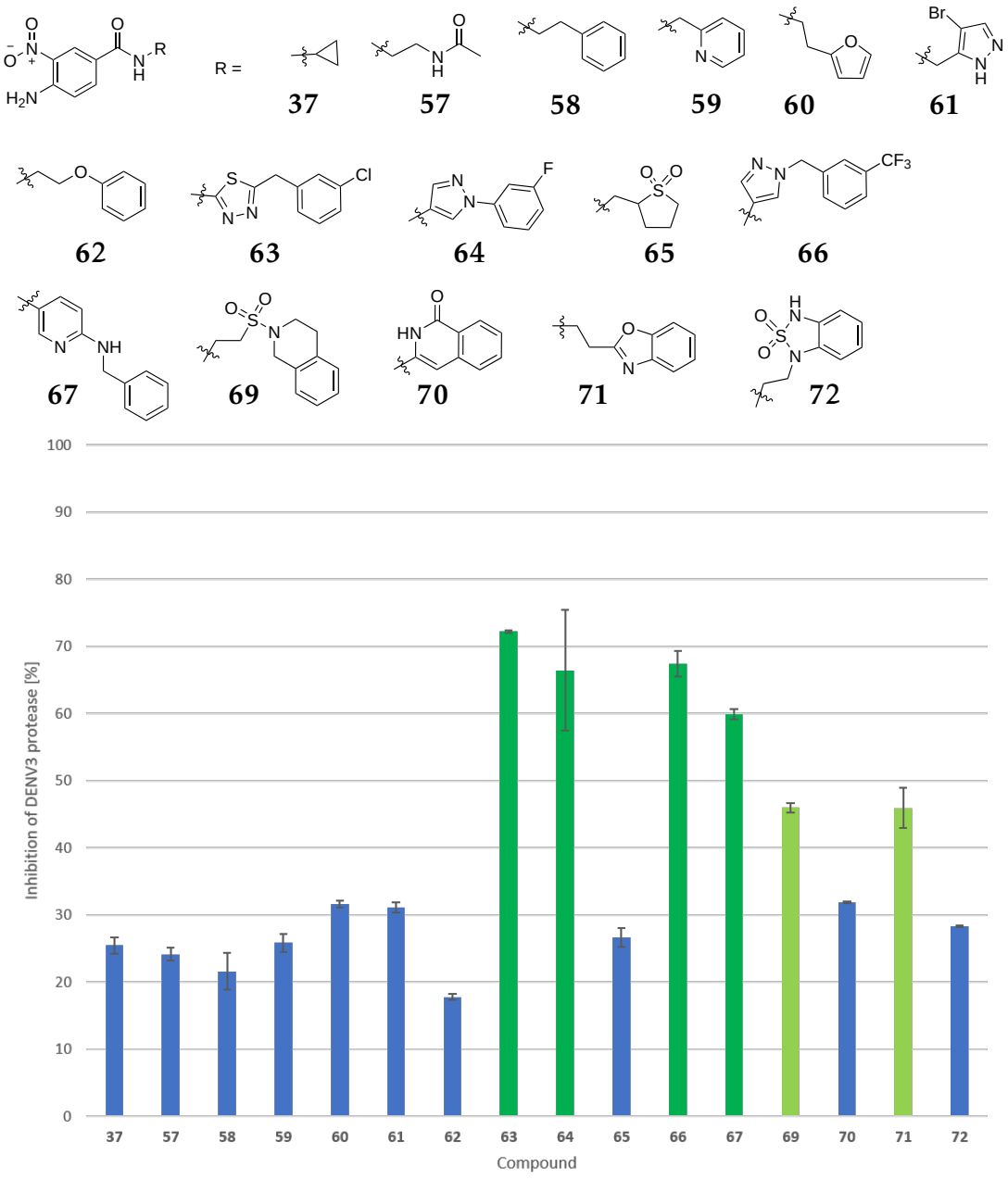

Fig. 3.12 Bar graph showing the percentage inhibition of the extended compounds against DENV3 protease in the fluorescence-based assay at 100 μM inhibitor concentration.

All compounds were sufficiently soluble in the assay buffer to quantify their percentage inhibition at 100 μM, except for compound **73**, which precipitated at this concentration and was therefore excluded from further testing. Analyzing the bar graph shown in Figure 3.12, the extended compounds can be divided into three groups: Those that show only slightly better inhibition than fragment **37** (blue), those showing moderately improved inhibition (compounds **69** and **71**, light green) and those that show significantly improved inhibition (compounds **63**, **64**, **66** and **67**, green). Subsequently, the IC_{50} values of the compounds of the second and third group against DENV2 and DENV3 protease were determined to gain more information about their potential as DENV protease inhibitors. In the measurements, it was found that compounds **64** and **69** were not sufficiently soluble in the assay buffer for IC_{50} determination, since they precipitated at concentrations above 125 μM. Therefore, they had to be excluded from further experiments. The successfully determined IC_{50} values of compounds **63**, **66**, **67** and **71** are shown in Table 3.1.

Table 3.1 Determined IC_{50} values against DENV2 and DENV3 protease in the fluorescence-based enzyme assay.

Compound no.	IC_{50}(DENV3) [μM]	IC_{50}(DENV2) [μM]
63	28.2±7.9	35.2±6.8
66	34.7±8.5	54.1±4.8
67	47.1±17.4	77.8±9.6
71	80.7±11.7	n.d.

Comparing the values obtained for the DENV2 and DENV3 proteases, it is noteworthy that although they follow the same trend, all compounds inhibit the DENV2 protease more weakly than the DENV3 protease. This might be attributed to the fact that for docking a DENV3 X-ray structure was used and thus all inhibitors are "optimized" for inhibition of the DENV3 protease. For both serotypes, compound **63** is the most potent inhibitor, with an IC_{50} value of approximately 30 μM. Only slightly higher IC_{50} values were determined for the structurally related compound **66**. However, the difference between the two values for DENV2 and DENV3 is slightly higher for compound **66** than for compound **63**. Compound **67**, which - in contrast to compounds **63** and **66** - consists of a six-membered heterocycle bound to the amide, shows a slightly worse IC_{50} value of about 50 μM (for DENV3). For compound **71**, only the IC_{50} value against DENV3 protease was recorded, since it was anticipated that the IC_{50} value for DENV2 protease would be approximately 100 μM and thus the compound was not of interest for further studies.

The docking poses of the three best-performing compounds are shown in Figure 3.13. It can be seen that the predicted interactions are similar for all three compounds: In addition to the hydrogen bonds predicted for the 4-amino-3-nitro-benzamide residue, all compounds form a hydrogen bond to AA Gln88 via a heterocyclic nitrogen atom, which acts as an acceptor.

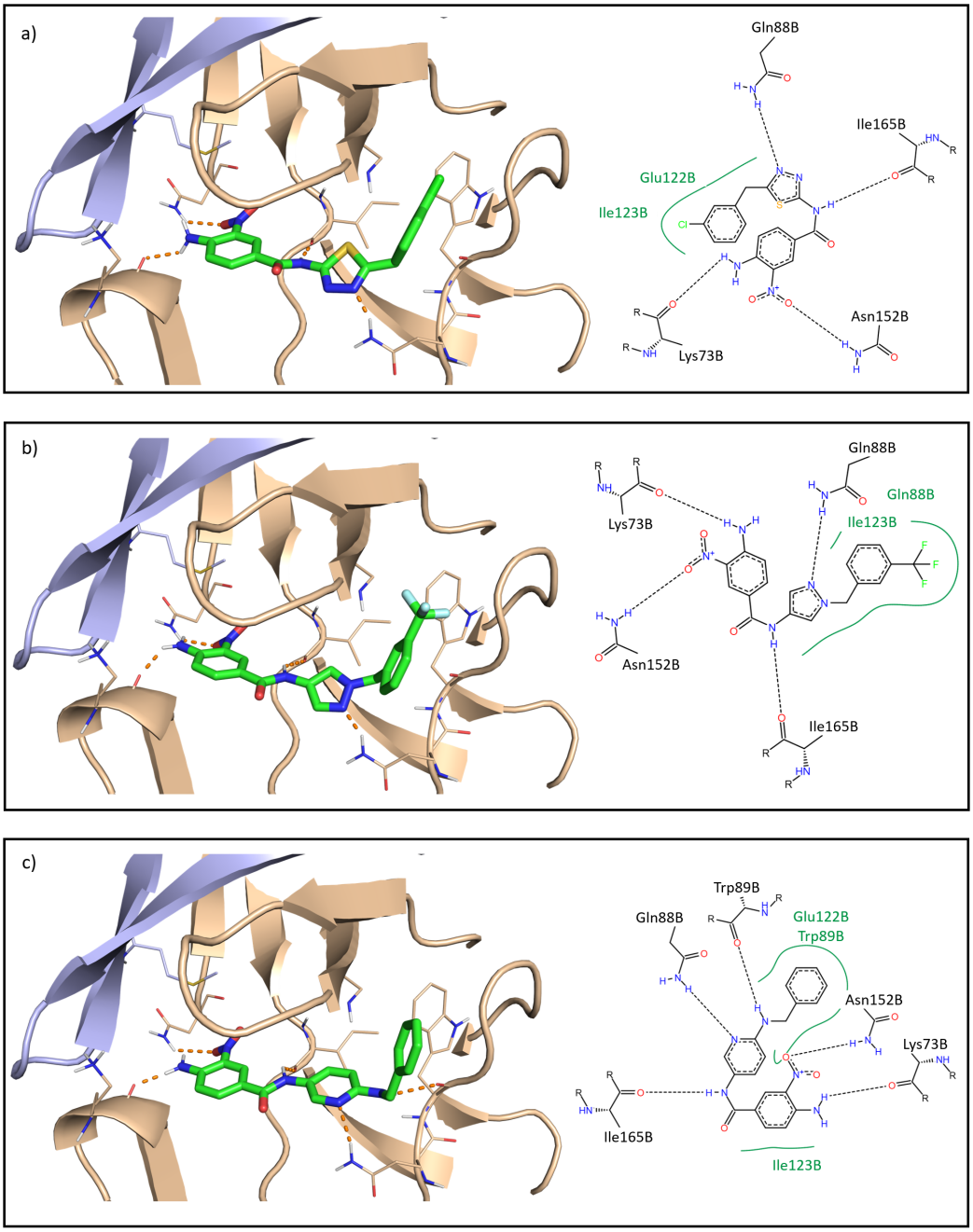

Fig. 3.13 Docking poses generated by AutoDock Vina for compounds a) **63**, b) **66** and c) **67** in the allosteric pocket of DENV3. On the left side, a 3D-representation of the predicted binding mode in PyMOL is shown, on the right side the proposed interactions between ligand and protein are shown in PoseView.

The (substituted) benzyl residue is located in a hydrophobic pocket formed by AAs Trp89 and Ile123. For compound **67**, an additional hydrogen bond to the carbonyl oxygen of AA Trp89 is predicted, but it is questionable to what extent this interaction occurs in reality, since the IC_{50} of compound **67** was the highest of all three. It is possible that more energy would be required at this location for desolvation than would be released by the formation of a hydrogen bond.

Comparing the structural features of the most active compounds, a general motif for potent allosteric DENV protease inhibitors can be derived (Figure 3.14). The "left" part of the inhibitor bears a 4-amino-3-nitro-benzamide residue, which has already been established as lead fragment core in previous studies. The fragment core is then directly linked to a five- or six-membered heterocycle that has at least one hydrogen bond acceptor enabling the interaction with the carbonyl oxygen of Gln88. Attached to this central heterocycle via a one- or two-atom linker, a *meta*-substituted phenyl ring was found to be well suited. The *meta*-substitution of the phenyl ring was predicted in the docking to be more advantageous than *ortho*- or *para*-substitution for sterical reasons. All compounds deviating from this general motif showed significantly decreased potency in the DENV protease assay, with the exception of compound **64**, which lacks the linker between the heterocycle and the phenyl residue. Although for compound **64** a high percentage inhibition at 100 μM was determined, its limited solubility in the assay buffer prevented further experiments. With this general motif in hand, starting from the most active inhibitor **63**, a third design-cycle was undertaken to further optimize the affinity.

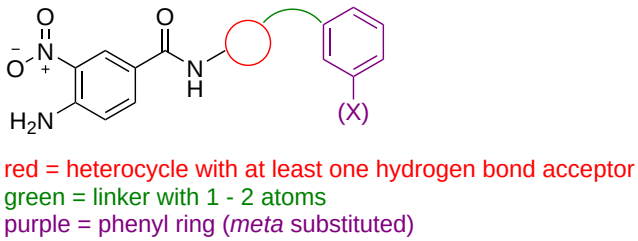

Fig. 3.14 Schematic representation of the derived general motif for potent DENV protease inhibitors.

3.4 SAR-Study Starting from Compound 63

In the following SAR-study, three positions of the most potent compound **63** (labeled as A, B, C in Figure 3.15) were varied in order to gather more information about the requirements for effective allosteric inhibition of DENV protease.

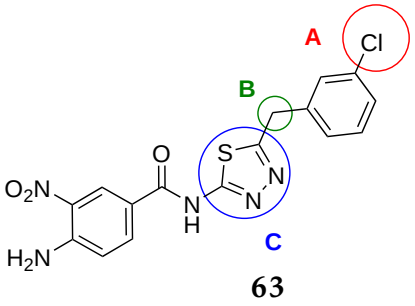

Fig. 3.15 Schematic representation of the positions to be varied starting from compound **63** for the SAR-studies.

3.4.1 Variation of Position A

First, the chlorine atom of compound **63**, located in *meta*-position of the phenyl ring, was systematically replaced by other halogens or alkyl substituents (position A). For the halogen-substituted derivatives **96**, **97**, and **98**, the same synthetic sequence could be used as for chloro derivative **63**, starting from the corresponding carboxylic acid (Scheme 3.24).

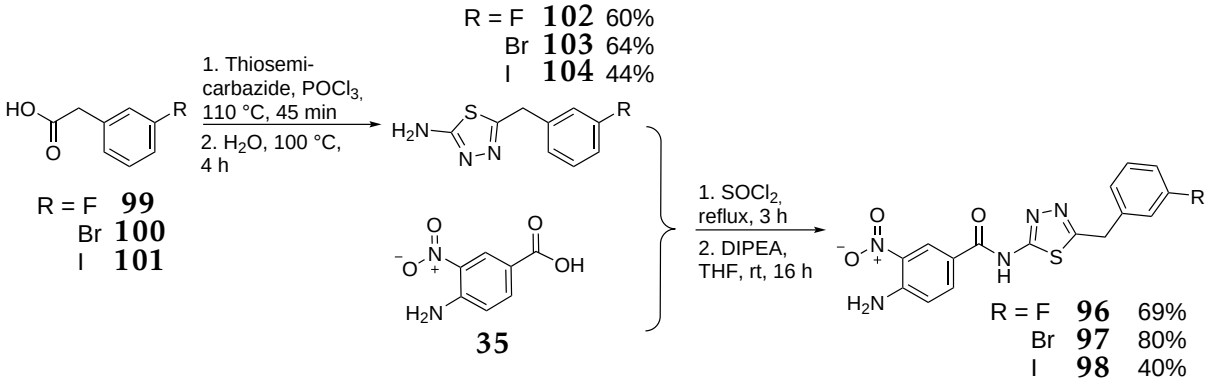

Scheme 3.24 Syntheses of the halogen-substituted compounds **96**, **97**, and **98**.

The cyclization step proceeded in moderate to good yields for all halogen-substituted carboxylic acids (44-64%), while the range of yields was broader for the amide coupling reaction (40-80%). Interestingly, in both steps, reaction yields for the iodine-substituted derivative were the lowest, probably due to its lower solubility compared to the fluorinated and brominated derivative. In all cases, the target compounds were obtained in sufficient amount and purity for *in vitro* testing.

Table 3.2 Determined IC_{50} values of halogen-substituted compounds against DENV3 protease in the fluorescence-based enzyme assay.

Compound no.	Halogen Substituent	IC_{50}(DENV3) [μM]
96	F	127.7±11.8
63	Cl	28.2±7.9
97	Br	22.5±3.0
98	I	33.9±3.8

All three compounds were sufficiently soluble to determine their IC_{50} values against DENV3 protease in the fluorescence-based assay. As shown in Table 3.2, the fluorine-substituted compound **96** shows an IC_{50} value almost 5-fold higher than the other three compounds. All other halogen-substituted compounds showed similar IC_{50} values, with the bromine derivative **97** being the most potent one. Apparently, the strong negative partial charge on the relatively small fluorine atom is detrimental to the protein-ligand interactions in this case. As suggested by the docking, the *meta*-substituent resides in a hydrophobic part of the protein.
Furthermore, alkyl substituents were introduced in position A, namely an isopropyl, a *tert*-butyl, a methyl, and a trifluoro-methyl substituent, following the same synthetic approach as for the halogen-derivatives. The corresponding carboxylic acids for the synthesis of the isopropyl and the *tert*-butyl derivatives were, however, not commercially available, so they had to be prepared in-house. For the *tert*-butyl-derivative, a retrosynthetic analysis revealed a two-step synthesis in which carboxylic acid **105** should be accessible by Suzuki cross-coupling of 1-bromo-3-(*tert*-butyl)benzene (**106**) with vinylboronic acid pinacol ester (**107**) and subsequent regioselective oxidation of the vinyl double bond in the terminal position.

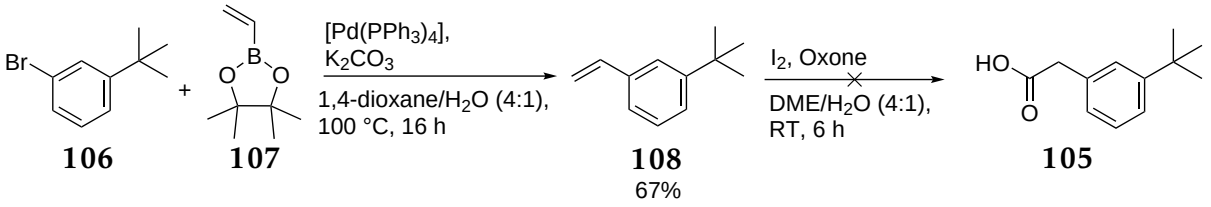

Scheme 3.25 Attempted synthesis of carboxylic acid **105** by Suzuki cross-coupling and subsequent oxidation of the vinyl double bond in terminal position.[70]

The Suzuki cross-coupling afforded the desired styrene derivative **108** in good yield (67%), although the product proved to be slightly sensitive to air and had to be stored under argon to prevent decomposition over time (Scheme 3.25). The subsequent terminal oxidation of styrene derivatives has been reported in the literature, but was

not reproducible here.[70] Under the given reaction conditions, only an inseparable mixture of different reaction products was obtained (Scheme 3.25). Since no other efficient synthetic route to the *tert*-butyl-derivative was feasible, the preparation of this compound was discarded, as was the synthesis of an isopropyl derivative, as this would have had to be synthesized by the same route. For the methyl-substituted derivative **109** and the trifluoro-substituted derivative **110**, the corresponding carboxylic acid was commercially available, so that the same synthetic route as described for the halogen-derivatives could be followed (Scheme 3.26).

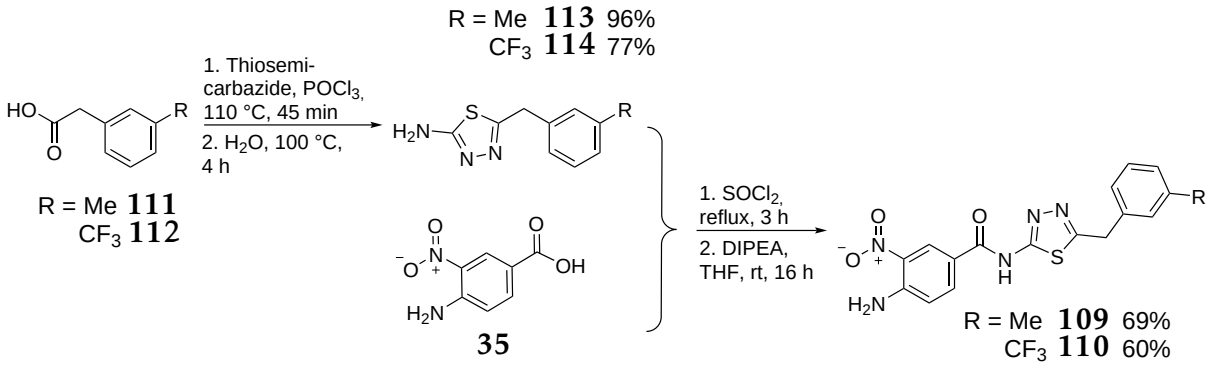

Scheme 3.26 Syntheses of the alkyl-substituted compounds **109** and **110**.

For both alkyl derivatives, cyclization and amide coupling proceeded well (60-96%), and purification was not hampered by the occurrence of side products. The determined IC_{50} vales for compounds **109** and **110** against the DENV3 protease are shown in Table 3.3. It can be seen that both derivatives showed very similar potency against DENV3 protease, with the methyl derivative **109** being slightly more active. However, both derivatives have a 1.5-fold increased IC_{50} value compared to the halogen-substituted derivatives (except fluorine).

Table 3.3 Determined IC_{50} values of alkyl-substituted compounds against DENV3 protease in the fluorescence-based enzyme assay.

Compound no.	Alkyl Substituent	IC_{50}(DENV3) [μM]
109	Me	41.1±3.6
110	CF_3	45.8±3.8

It can be hypothesized that additional effects, such as weak halogen-π interactions or halogen bonding, take place in the interaction between protein and the halogen-substituted inhibitors, which are not present in the case of alkyl substituents.
Since a chloro- or bromo-substituent proved to perform best in *meta*-position of the phenyl ring, it was tested if a 3,5-dichloro or 3,5-dibromo substitution would increase

the activity of the inhibitors against DENV3 protease even more. Both compounds **115** and **116** were synthesized analogously to the mono-halogenated compounds (Scheme 3.27).

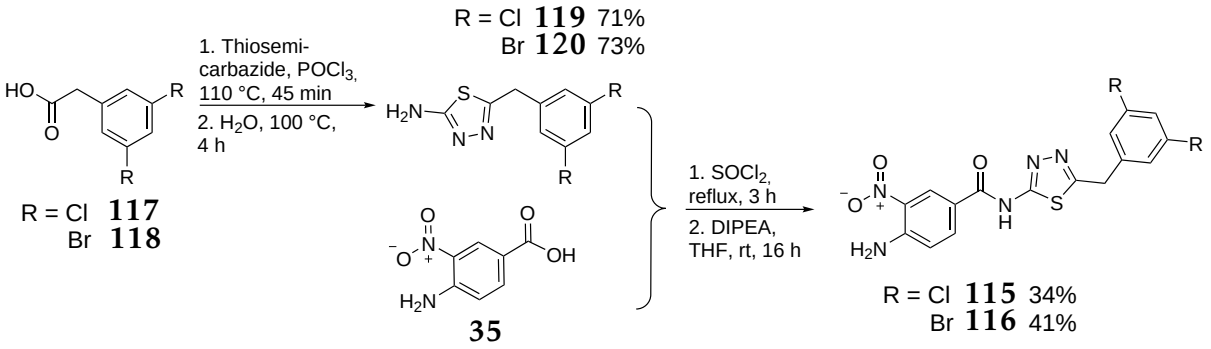

Scheme 3.27 Syntheses of the 3,5-di-halogenated compounds **115** and **116**.

Although the cyclization step afforded the desired compounds **119** and **120** in similar yields as for the monosubstituted compounds (71% and 73%), the amide coupling step proceeded with significantly lower yields (34% and 41%). The main problem occurred during the chromatographic purification, as both compounds precipitated in course of the chromatographic work-up and could only be partially recovered. Nevertheless, sufficient material for *in vitro* tests could be obtained.

Table 3.4 Determined IC_{50} values of di-halogen-substituted compounds against DENV3 protease in the fluorescence-based enzyme assay.

Compound no.	Substituents	IC_{50}(DENV3) [μM]
115	3,5-di-chloro	19.9±3.7
116	3,5-di-bromo	12.3±3.5

Both 3,5-di-substitutions resulted in an improvement of the IC_{50} value by about 10 μM compared to the corresponding mono-substituted derivatives (Table 3.4). This finding might be a consequence of the reduction of possible rotamers by increasing the symmetry of the compounds. However, this slight increase in affinity might also be attributed to the increase in molecular weight.

3.4.2 Variation of Position C

In parallel to the synthesis of the compounds described above with different substituents in position A, compounds with different heterocycles in position C and different linker lengths (position B) were synthesized. Since pyrazole derivatives (e.g. compound **66**) had also proved to be potent inhibitors, two additional pyrazoles **121** and **122** with

different substituents in region A were synthesized. Since it was not known at the time of the synthesis of the pyrazoles that a fluorine substituent in position A has a negative effect on the affinity, compound **121** was synthesized. The synthetic route followed was analogous to that previously described for pyrazole **66**. In the case of the 3,5-dichloro-substituted derivative, the required starting material (3,5-dichlorobenzyl bromide (**123**)) was not commercially available, so it was synthesized (see Experimental section).

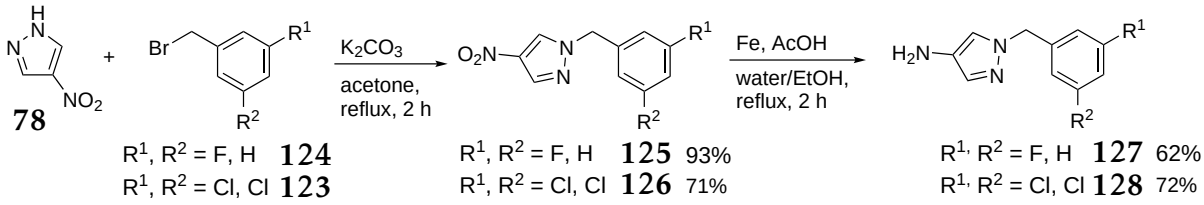

Scheme 3.28 Synthesis of pyrazoles **127** and **128** via a two-step protocol consisting of nucleophilic substitution and subsequent reduction of the nitro group.

For both pyrazoles, the corresponding benzyl bromide derivative was reacted in a nucleophilic substitution with 4-nitro-1*H*-pyrazole (**78**) yielding compounds **125** and **126** in excellent to good yields (Scheme 3.28). Reduction of the nitro group with iron powder proceeded smoothly for both compounds and afforded the corresponding amines **127** and **128** in good yields. Amine **127** had to be converted to an HCl salt to remove residual iron traces. In the final step, carboxylic acid **35** was reacted with the corresponding amines in an amide coupling reaction, giving the final compounds **121** and **122** in good yields (Scheme 3.29). In this case, amine **127** · 2 HCl was added directly to the reaction mixture along with six equivalents DIPEA to ensure complete deprotonation of the amine, which worked as well as deprotonating the amine before adding it to the reaction mixture.

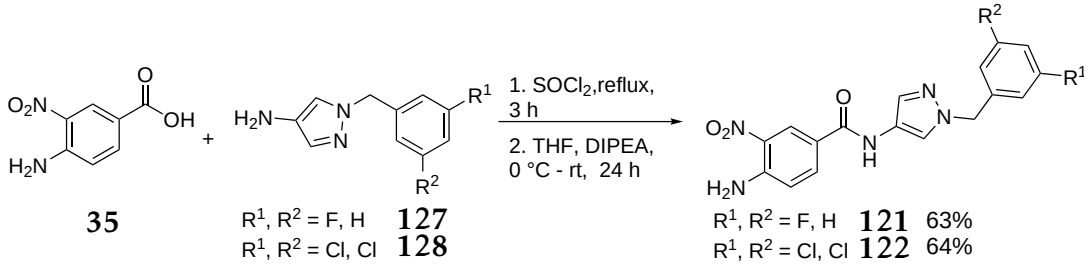

Scheme 3.29 Final step in the synthesis of pyrazoles **121** and **122**: amide coupling with 4-amino-3-nitro-benzoic acid (**35**).

Both pyrazoles were tested for their activity against DENV3 protease in the fluorescence-based assay (Table 3.5). As expected retrospectively, the fluorine-substituted derivative **121** exhibited significantly lower activity compared to the trifluoromethyl-substituted

derivative **66**. It seems that fluorine is an unfavorable substituent in region A, regardless of the chosen heterocycle in position C. Surprisingly, the 3,5-dichloro-substituted pyrazole **122** did not show increased activity compared to pyrazole **66**, although the 3,5-dichloro-substitution had been shown to be beneficial in case of the thiadiazole compound. Apparently, the interaction between ligand and protein is somewhat different in the case of pyrazoles, so that 3,5-dichloro-substitution is not advantageous in the former case but is in the latter.

Table 3.5 Determined IC_{50} values of the pyrazole derivatives against DENV3 protease in the fluorescence-based enzyme assay.

Compound no.	Substituents (3,5-position)	IC_{50}(DENV3) [μM]
66	CF_3, H	34.7±8.5
121	F, H	112.3±9.7
122	Cl, Cl	35.2±7.4

In a second approach, position C was substituted with an 1,3,4-oxadiazole and an 1,3-oxazole respectively, in order to test the effect of a smaller and more polar atom in the 5-membered heterocycle (S vs. O) and to test the importance of the second nitrogen in the heterocycle, since according to docking only the nitrogen in 3-position should form a hydrogen bond to AA Gln88. The synthesis of oxadiazole **129** was analogous to the synthesis of thiadiazole **63**, except that the cyclization reagent was exchanged for semicarbazide (**130**) as shown in Scheme 3.30.

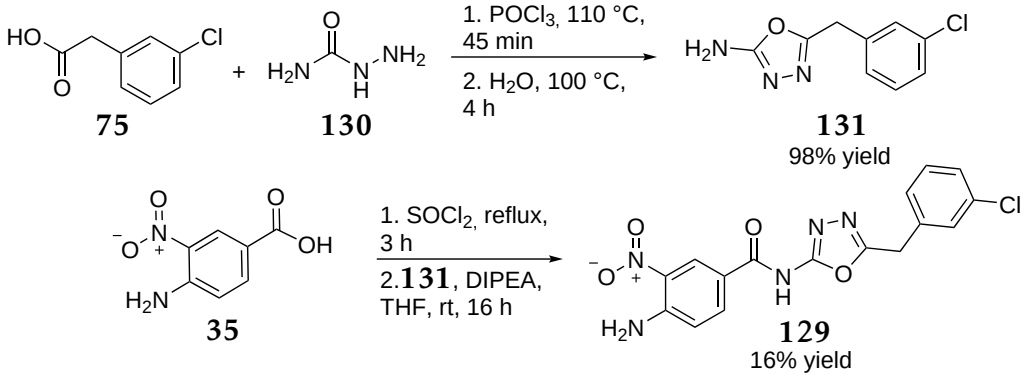

Scheme 3.30 Synthesis of oxadiazole **129** in a two-step procedure consisting of cyclization and subsequent amide coupling.

The cyclization reaction worked very well with semicarbazide rendering compound **131** in nearly quantitative yield (Scheme 3.30). The subsequent amide coupling reaction however, resulted in the formation of several side products that were difficult to separate from the desired oxadiazole **129**, which was obtained after recrystallization from MeCN

in only 16% yield. Apparently, the S/O exchange at the heterocycle has a strong influence on the selectivity of the amide coupling reaction, although the reasons for this remain unclear. Nevertheless, compound **129** could be obtained in sufficient amount and purity for *in vitro* tests.

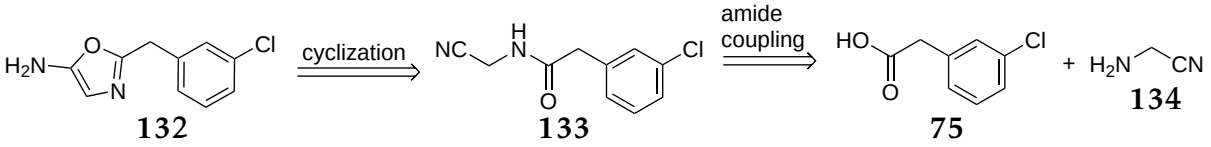

Scheme 3.31 Retrosynthetic approach selected for the synthesis of oxazole **132**.

For the synthesis of a 3-oxazole derivative, the retrosynthetic approach shown in Scheme 3.31 was chosen (only the first two steps are shown, amine **132** should then be coupled to **35** applying the standard coupling protocol).

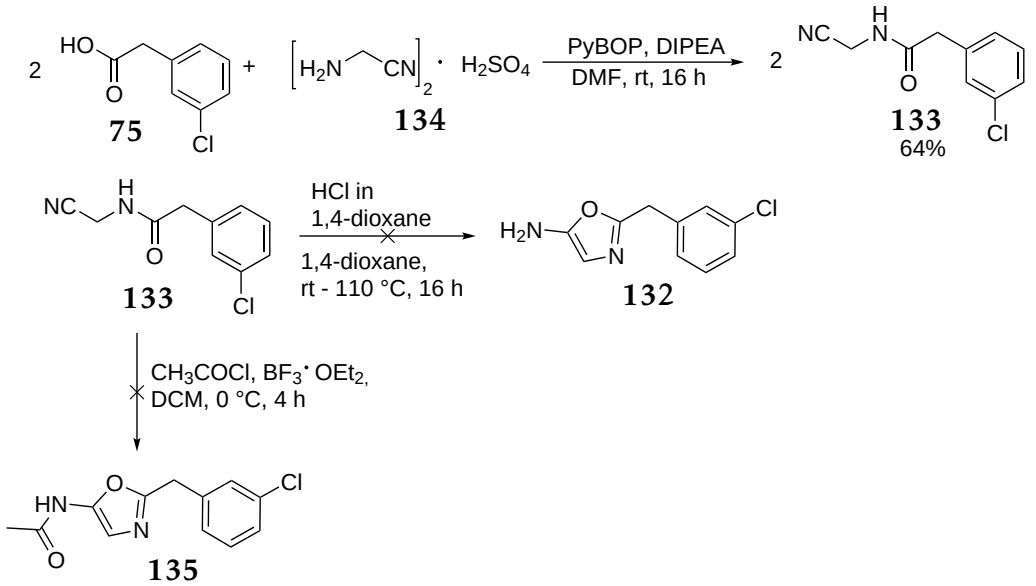

Scheme 3.32 Attempted synthesis of 3-oxazole **132** via amide coupling and subsequent cyclization.

In the first step, 3-chloro-phenylacetic acid (**136**) was reacted with aminoacetonitrile sulfate (**134**) in an amide coupling reaction using PyBOP as the coupling reagent, which was chosen after other attempts with more common coupling reagents such as EDCI/HOBt had failed. Three equivalents of DIPEA were added to ensure complete deprotonation of aminoacetonitrile. The desired coupling product was obtained in good yield (64%) after column chromatography (Scheme 3.32). The cyclisation of compound **137** turned out to be the key reaction step: A first attempt under acidic conditions using HCl in 1,4-dioxane as acid failed, even after prolonged heating to reflux.[71] In a second attempt, $BF_3{\cdot}OEt_2$ was used as a Lewis acid. Although these reaction conditions were

also described in the literature,[72] no conversion could be detected. Based on these results, the synthesis of a 3-oxazole derivative was discarded.
Since pyridine derivative **67** showed good activity against DENV3 protease, a pyrimidine derivative was also synthesized. The symmetric substitution of the heterocycle in regard to the nitrogen atoms reduces the number of possible rotamers and thus the entropy loss during binding. Since a Negishi cross-coupling was used to link the pyrimidine core to the benzyl moiety, a methyl group was chosen as the substituent in region A to avoid the risk of side reactions. First, pyrimidine **138** was double BOC-protected using a standard reaction protocol (Scheme 3.33), giving compound **139** in very good yield (83%).

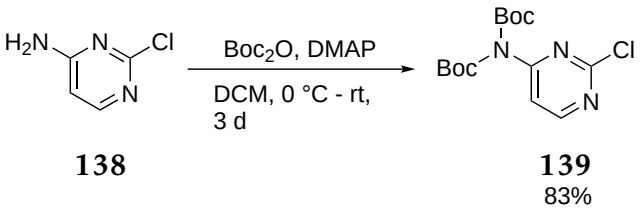

138 **139** 83%

Scheme 3.33 First step in the synthesis towards pyrimidine **140**: Double BOC-protection of compound **138** using standard reaction conditions.

Then, compound **139** was reacted with 3-methyl-benzyl bromide in a Negishi cross-coupling. For this purpose, 3-methyl-benzyl bromide (**141**) was *in situ* converted into the corresponding zinc organyl by adding iodine and zinc powder (Scheme 3.34).

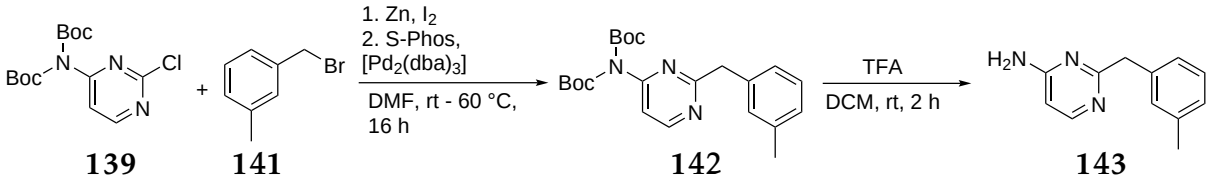

139 **141** **142** 47% **143** 80%

Scheme 3.34 Synthesis of amine **143** by Negishi cross-coupling and subsequent deprotection with TFA.

A catalyst system consisting of $[Pd_2(dba)_3]$ and S-Phos was used, since it is known that the resulting catalyst performs cross-coupling efficiently even for the relatively unreactive benzylzinc organyls.[73] The desired compound **142** was obtained after column chromatography in an acceptable yield of 47%. Obviously, homo-coupling of the pyrimidine also occurred to some extent, decreasing the yield. Subsequently, double Boc-protected compound **142** was deprotected with TFA as a strong acid, giving amine **143** in good yield (80%).
In the final step, amine **143** was reacted with 4-amino-3-nitrobenzoic acid (**35**) in an amide coupling as previously described (Scheme 3.35), providing pyrimidine **140** in good yield (61%) and high purity after recrystallization from ^{i}PrOH.

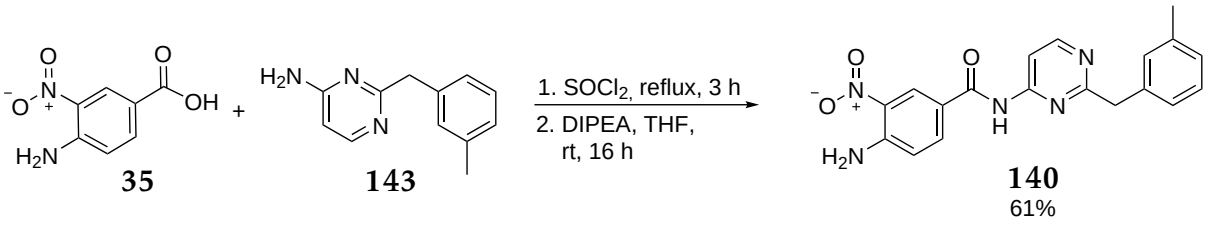

Scheme 3.35 Final step in the synthesis of pyrimidine **140**: amide coupling of 4-amino- 3-nitrobenzoic acid (**35**) with compound **143**.

Up to this point, only aromatic ring systems had been synthesized and tested as substituents in the C-position. To clarify whether aliphatic rings are also tolerated in the C-position, the piperidinyl-substituted inhibitor **144** was synthesized. Since 4-amino-1-benzyl piperidine **145** is commercially available, it was directly converted into the desired compound **144** by reaction with 4-amino-3-nitrobenzoic acid (**35**) in an amide coupling (Scheme 3.36). Due to the high basicity and nucleophilicity of amine **145**, the reaction proceeded very smoothly and with higher yield than with aromatic amines (89%).

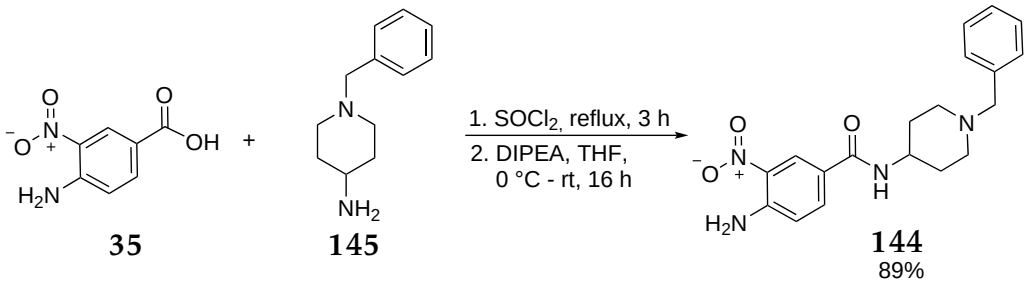

Scheme 3.36 Synthesis of piperidinyl-substituted inhibitor **144** by amide coupling reaction of 4-amino-1-benzyl piperidine **145** and 4-amino-3-nitrobenzoic acid (**35**).

The results of the IC_{50} value determination for compounds **129**, **140**, and **144** against the DENV3 protease are shown in Table 3.6. It is easy to see that all of the C-position substitutions tested are not beneficial. The S/O substitution at the five-membered heterocycle (compound **63** vs. compound **129**) resulted in an decrease in affinity by almost a factor of two. Apparently, the smaller and more polar oxygen atom is not well tolerated at this position, probably due to desolvation effects. Moreover, the S/O atom of the ring could act as a hydrogen bond acceptor, although the docking does not suggest this. In this case, however, the sulfur atom would be a much stronger acceptor than the oxygen atom. Substitution of the 1,3,4-thiadiazole residue with a pyrimidine also resulted in an increase in the IC_{50} value by almost a factor of two (compound **109** vs. compound **140**).

Table 3.6 Determined IC_{50} values of the compounds with varied ring system in the C-position against DENV3 protease in the fluorescence-based enzyme assay.

Compound no.	Ring system	Substituent *meta*-position	IC_{50}(DENV3) [μM]
63	1,3,4-thiadiazole	Cl	28.2±7.9
129	1,3,4-oxadiazole	Cl	53.9±12.3
109	1,3,4-thiadiazole	Me	41.1±3.6
140	pyrimidine	Me	72.8±7.2
144	piperidine	-	238±27

This observation can be explained by the docking pose generated by AutoDock Vina for compound **140** (Figure 3.16): in the other compounds in this series, a hydrogen bond is formed between the amide nitrogen and AA Ile165. This is not possible for compound **140** due to a distortion of the pose to accommodate the six-membered heterocycle. Moreover, the hydrogen bond distances between compound **140** and AAs Asn152 and Lys73 are larger, making the interactions weaker. These effects could contribute to the fact that five-membered heterocycles are better suited than six-membered heterocycles to address this region of the allosteric pocket.

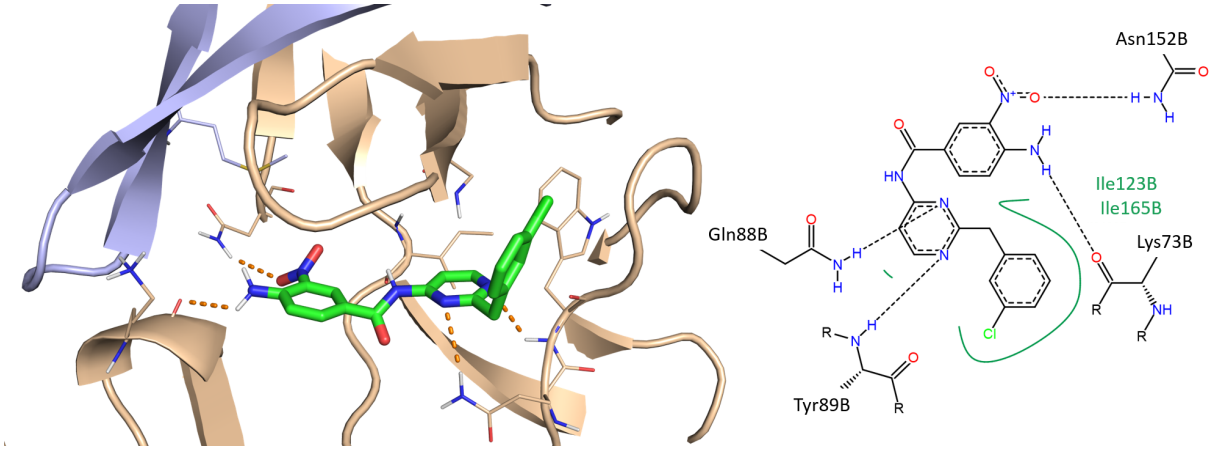

Fig. 3.16 Docking pose of compound **140** in the allosteric pocket of DENV3. On the left side, a 3D-representation in PyMOL is shown, on the right side proposed interactions between ligand and protein are shown in PoseView.

An even stronger decrease in affinity was observed when the aromatic ring system was replaced by an aliphatic one: for compound **144**, the IC_{50} value against the DENV3 protease increased almost tenfold compared to compound **63**. This could be due either to the higher entropy loss upon binding of the piperidine scaffold (more rotatable bonds need to be fixed) or to steric issues, as an aliphatic cycle has a higher steric demand than an aromatic one. Based on this finding, no further aliphatic ring systems were tested in the C-position.

3.4.3 Variation of Position B

Finally, the influence of the linker between the heterocycle and the phenyl ring on the affinity of the resulting inhibitors was investigated (position B). For this purpose, a series of compounds was synthesized with an ethylene instead of a methylene linker. To compare the results with previous findings, three compounds with previously tested substituents in the C-position were selected (compounds **146**, **147**, and **148**).
For the synthesis of compounds **146** and **147**, the corresponding phenylpropionic acids were reacted with thiosemicarbazide (Scheme 3.37), giving the amines **149** and **150** in yields similar to those obtained in previous cyczlization reactions. The final amide coupling afforded the desired compounds **146** and **147** in moderate to good yield (55% and 64%).

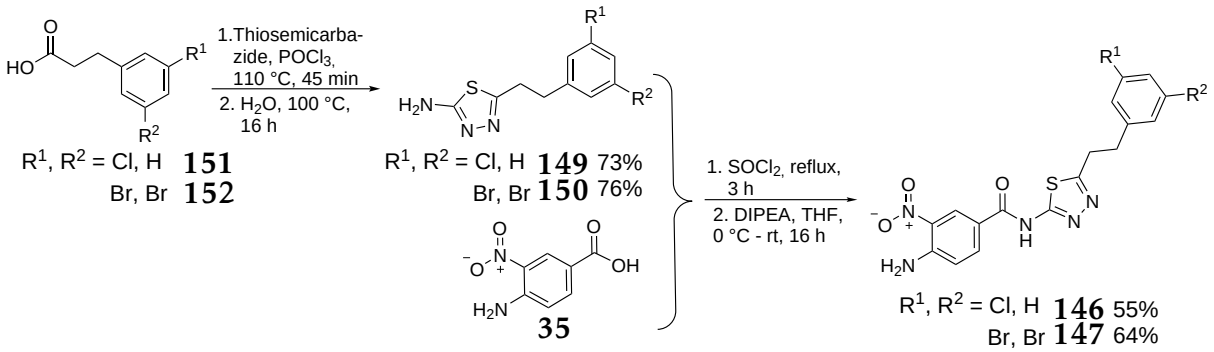

Scheme 3.37 Synthesis of the compounds **146** and **147**, bearing an ethylene linker.

The synthesis of piperidine derivative **148** was carried out in a three-step procedure, starting from Boc-protected 4-amino-piperidine (**153**), which was reacted with (2-bromoethyl)benzene (**154**) in a nucleophilic substitution (Scheme 3.38).

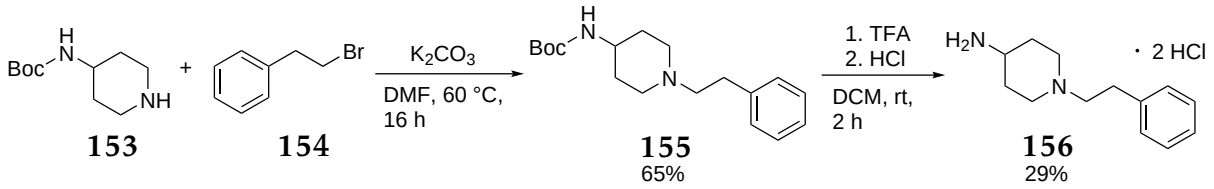

Scheme 3.38 First two steps in the synthesis of compound **148**: Nucleophilic substitution and subsequent Boc-deprotection.

The desired product was obtained directly from the reaction mixture by precipitation and filtration. Although the reaction proceeded smoothly, only a moderate yield of 65% was achieved, probably due to incomplete recovery of the compound during the filtration step. The subsequent Boc-deprotection with the strong acid TFA led to the formation of several side products, which could only be separated by converting the desired amine into the corresponding HCl salt, accompanied by yield loss (29%).

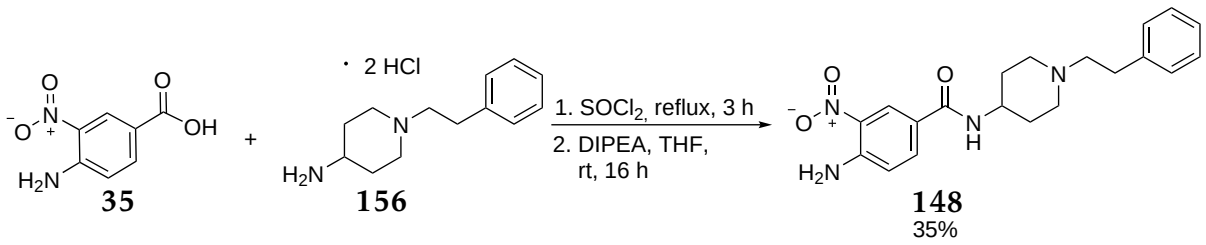

Scheme 3.39 Amide coupling of 4-amino-3-nitrobenzoic acid (**35**) with amine **156**, which afforded the final compound **148**.

For the subsequent amide coupling reaction, compound **156** · 2 HCl was deprotonated by adding an excess of DIPEA, which had worked well in previous reactions with other HCl salts (Scheme 3.39). In this case however, several by-products were formed and the yield of the final product **148** was rather low (35%). Probably, the basicity of DIPEA was not high enough to completely deprotonate amine **156**, so its nucleophilicity was significantly reduced. Nevertheless, compound **148** was obtained in sufficient amount and purity for *in vitro* testing.

Table 3.7 Determined IC_{50} values of the compounds with varied linker length in the B-position against DENV3 protease in the fluorescence-based enzyme assay.

Cmpd. no.	No. C-atoms linker	Region C	Substituent A	IC_{50}(DENV3) [μM]
63	1	thiadiazole	Cl	28.2±7.9
146	2	thiadiazole	Cl	21.1±3.3
116	1	thiadiazole	Br,Br	12.3±3.5
147	2	thiadiazole	Br,Br	14.1±3.1
144	1	piperidine	-	238±27
148	2	piperidine	-	121±11

The results of the IC_{50} value determination for the compounds with an ethylene linker are shown in Table 3.7. For the thiadiazole derivatives **146** and **147**, the effect of the linker variation is neglectable (**63** vs. **146** and **157** vs. **147**). Apparently, for both ethylene derivatives, the effects of increased entropy loss upon binding and the improved possibility of optimal residue accommodation balance each other out. In contrast, the IC_{50} value for the C2-piperidine derivative **148** is reduced by almost a factor of two compared to its C1-analog **144**. In this case, the increased flexibility seems to improve the accommodation of the sub-optimal piperidine residue.

In summary, starting from compound **63** in the third design cycle, a first structure-activity relationship was derived that led to some surprising and unanticipated results. Some of the findings could be explained by analyzing the respective docking poses, while other findings can only be speculated about. The most potent inhibitor in the series was thiadiazole **116**, but other thiadiazoles proved to be similarly potent.

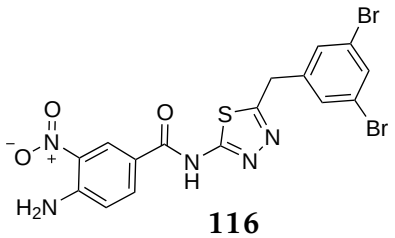

116

Fig. 3.17 Structure of the most potent inhibitor of the series, thiadiazole **116** (IC_{50}(DENV3)=12.3±3.5 μM).

3.5 Further Biochemical Investigations

In this chapter, the results of additional biochemical investigations are discussed. The aim of these studies was to obtain a deeper understanding of the mode of action of the designed ligand series and to gain initial insights into the general suitability of the inhibitors as anti-Dengue drugs.

3.5.1 Investigation of the Ligand Potency towards a Binary DENV4 Protease Construct

As discussed in the Introduction, recombinant fusion proteins consisting of the hydrophilic core region of NS2B and the *N*-terminal part of NS3 are most commonly used for enzyme-based flaviviral assays.[3] Such a construct was also used to obtain affinity data via a fluorescence-based DENV2 and DENV3 enzyme assay as discussed in the previous sections. Because there is an ongoing debate in the literature as to whether "linked" constructs correctly represent the native state of the flaviviral protease,[9] a binary (= unlinked) construct of the DENV4 protease was also used to determine the affinity of the inhibitors in the fluorescence-based enzyme assay for comparison. This construct (termed bDENV4), was expressed and purified by Dr. A. Nguyen. First, the enzyme kinetic parameters for the expressed bDENV4 construct were determined using a Lineweaver-Burk plot. To generate this plot, the reaction rate of the enzyme-catalyzed reaction (in this case, proteolysis) is measured at different concentrations of the substrate of interest.[74] If the enzyme kinetics follow ideal second-order kinetics, the double reciprocal plot of the values obtained yield a linear curve with the following equation (3.1, derived from the Michaelis-Menten equation):[74]

$$\frac{1}{V} = \frac{K_m}{V_{max}} \cdot \frac{1}{[S]} + \frac{1}{V_{max}} \tag{3.1}$$

where V is the reaction velocity, V_{max} is the maximum reaction velocity, $[S]$ is the substrate concentration and K_m is the Michaelis-Menten constant. The resulting Lineweaver-Burk plot for the bDENV4 construct is shown in Figure 3.18. The linear regression curve applied has an R^2 value of 0.9955, so the reaction catalyzed by the bDENV4 protease follows second-order kinetics quite well. Inserting the calculated parameters of the regression curve yields the following values for V_{max} and K_m of the bDENV4 protease:

$$V_{max} = 61.35\ a.u./s,\ K_m = 24.66\ \mu M$$

The determined K_m value is in good agreement with the ones determined for the linked DENV2 (21.8 μM) and DENV3 (41.5 μM) protease constructs in earlier experiments with the same substrate (PhAc-KRR-AMC), since the substrate specificity differs slightly

among the different serotypes.[75] Regarding the enzyme kinetics, linked and binary constructs of the DENV protease seem to behave similarly.

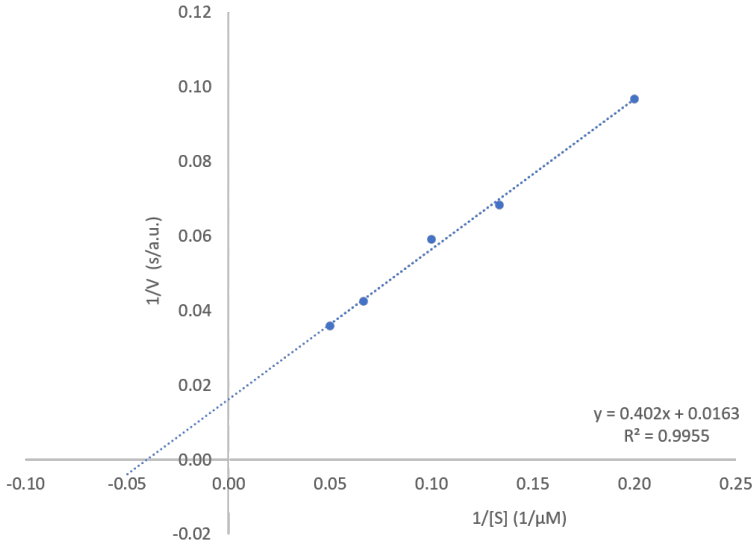

Fig. 3.18 Lineweaver-Burk plot for the bDENV4 construct. V is the reaction velocity and $[S]$ is the substrate concentration.

Once the activity of the bDENV4 construct had been confirmed, it was used in further assays. To get a first impression of the potency of the ligand series against this "more native" construct, the IC_{50} value of the most potent inhibitor **116** was determined. As shown in Figure 3.19, compound **116** also inhibited the bDENV4 protease in a dose-dependent manner with an IC_{50} value of 17.1±2.4 µM, which is similar to the value determined for the linked DENV3 protease (12.3±3.5 µM). Apparently, the linked constructs mimic the natural state as well as the binary constructs, at least as far as the determination of the IC_{50} values for this ligand series in concerned.

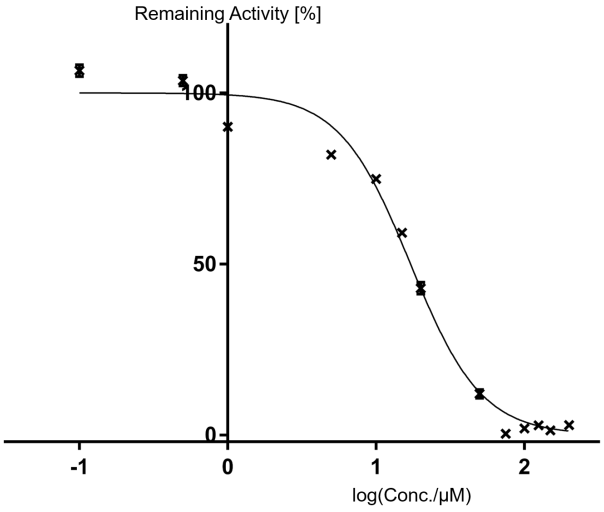

Fig. 3.19 Compound **116** inhibits the bDENV4 protease in a dose-dependent manner (IC_{50}=17.1±2.4 µM).

3.5.2 Investigation of the Ligand Potency towards bZIKV protease

Since Zika Virus also belongs to the genus *Flavivirus*, its protease has a high sequence and structural homology with the DENV protease.[4] Therefore, many of the reported DENV protease inhibitors also show high potency against the ZIKV protease, and often the potency against the latter is even higher.[50] In this context, the efficacy of the established ligand series against ZIKV protease was also tested. The binary ZIKV protease construct used for the fluorescence-based enzyme assay was kindly provided by the Steinmetzer research group.

To obtain a first overview of the extent of inhibition of the bZIKV protease by the established ligand series, the parent compound **63** of the SAR study and the most potent compound **116** were tested. Both ligands inhibited the bZIKV protease in a dose-dependent manner with IC_{50} values significantly lower than those obtained for the DENV3 protease (Figure 3.20). For compound **116** an IC_{50} value in the single-digit micromolar range was determined (Table 3.8).

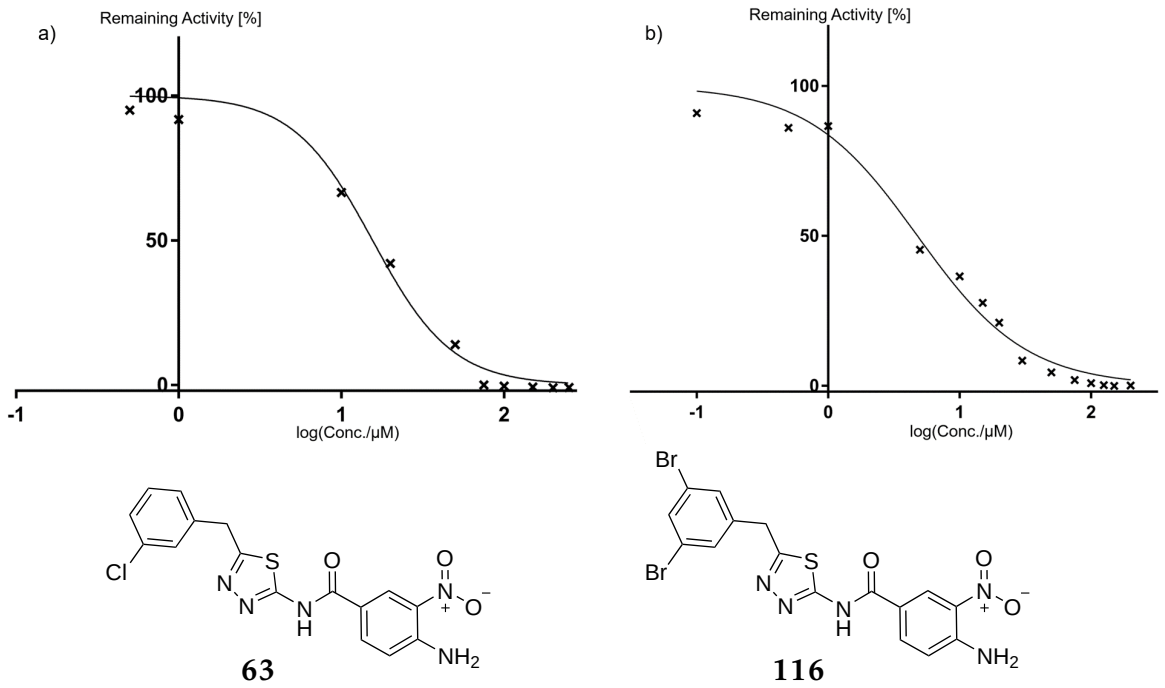

Fig. 3.20 Upper part: dose-response curves for the inhibition of bZIKV protease by compound **63** (a) and **116** (b), lower part: chemical structures of **63** and **116**.

The obtained findings could not be rationalized by docking. All attempts with different X-ray structures of the ZIKV protease as input failed, although the structural and sequential identity for the allosteric pocket region between the two flaviviruses is quite high.

Table 3.8 Determined IC_{50} values for compounds **63** and **116** against bZIKV protease and DENV3 protease.

Compound no.	IC_{50}(DENV3) [μM]	IC_{50}(bZIKV) [μM]
63	28.2±7.9	15.5±2.8
116	12.3±3.5	4.8±1.1

One possible reason for this finding is exemplified for pdb-ID 6Y3B in Figure 3.21:[41] compared to the DENV3 protease, a Gly164Ala mutation is present in the ZIKV protease. This additional methyl group is in close contact (<2 Å between heavy atoms) to the ligand **97** when its docking pose for the DENV3 protease is aligned with the ZIKV protease. If this combination of ligand **97** and ZIKV protease was used as input for docking, the software would place the ligand far outside the pocket to avoid close contact with Ala164. In reality however, the protease is flexible and can adapt its conformation upon ligand binding (induced fit), but this process cannot be described by docking. Further investigations with MD-simulations would be necessary here, but are not the subject of this project.

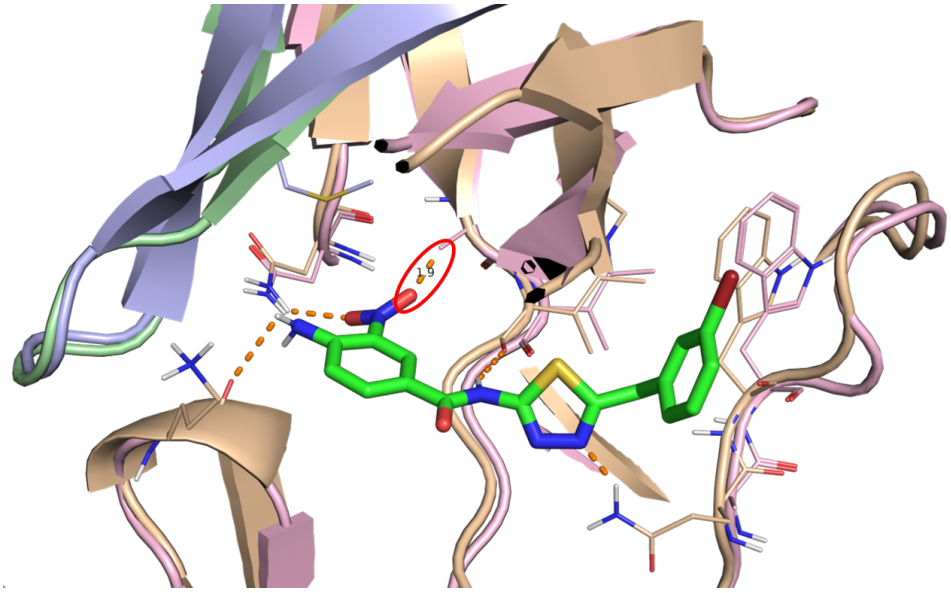

Fig. 3.21 Alignment of the docking pose of ligand **97** in the allosteric pocket of DENV3 protease and the corresponding region of ZIKV protease (pdb-ID: 6Y3B).[41] Beige: NS3 of DENV3, rose: NS3 of ZIKV, lightblue: NS2B of DENV3, light green: NS2B of ZIKV, sticks: ligand **97**, red circle: close contact between ligand and the methyl group of Ala164 of the ZIKV protease.

3.5.3 Dixon-Plot Analysis for Compound 147

The non-competitive binding mode was already confirmed for the first hit **30**, but examples are known from the literature in which the binding mode changes during ligand optimization.[76] Therefore, Dixon-plot analysis was also performed for compound **147**, which is an example of the optimized ligand set. As can be seen in Figure 3.22, all lines cross on the x-axis of the plot, so a non-competitive binding mode can also be assumed for compound **147**. The K_i-value of this ligand for DENV3 protease was determined to be 8.4±0.4 μM, which is in the same range as the IC_{50}-value of the compound (14.1±3.1 μM). It can be argued that the measured values deviate more from the regression line than was the case with the Dixon-plot of the first hit **30**, but this is mainly due to pipetting accuracy, which affects the measured values more significantly for more potent compounds. To improve accuracy, higher dilutions would be needed so that larger volumes are pipetted.

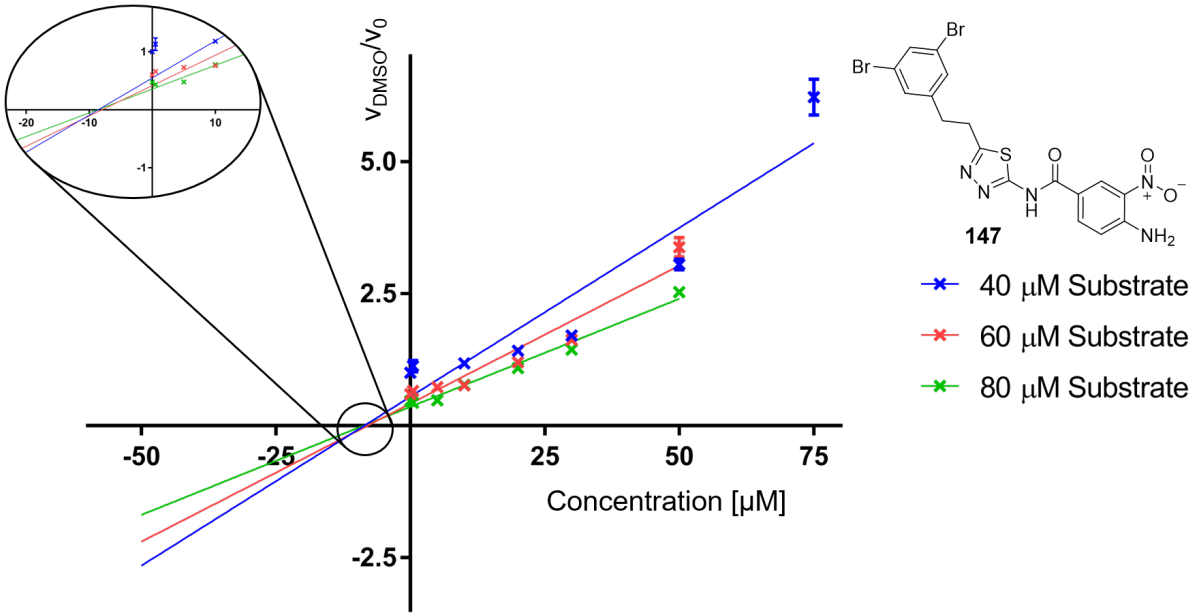

Fig. 3.22 Dixon-Plot analysis for compound **147** against DENV3 protease, using three different substrate concentrations (40, 60, and 80 μM).

3.5.4 Mutation Studies to Confirm the Binding Location

Since all attempts to crystallize a ligand-protein complex consisting of either DENV or ZIKV protease and a compound from the optimized ligand series have failed so far, alternative methods were required to study the binding mode and site. Mutation studies are a common tool for confirmation of the binding mode,[50] so it was also applied here. First, *in silico* mutation with PyMOL was used to investigate which mutations would block the putative ligand binding site (allosteric pocket). To this end, several amino

acids were mutated from either NS2B or NS3 to Phe/Trp *in silico*, using the docking pose of **147** in the allosteric pocket of the DENV3 protease as a template. The most effective blockade of the binding site was achieved with mutations I123F and I123W in the NS3 chain (see Figure 3.23). Both mutations were designed to prevent the ligand from binding by dividing the allosteric pocket in two smaller pockets.

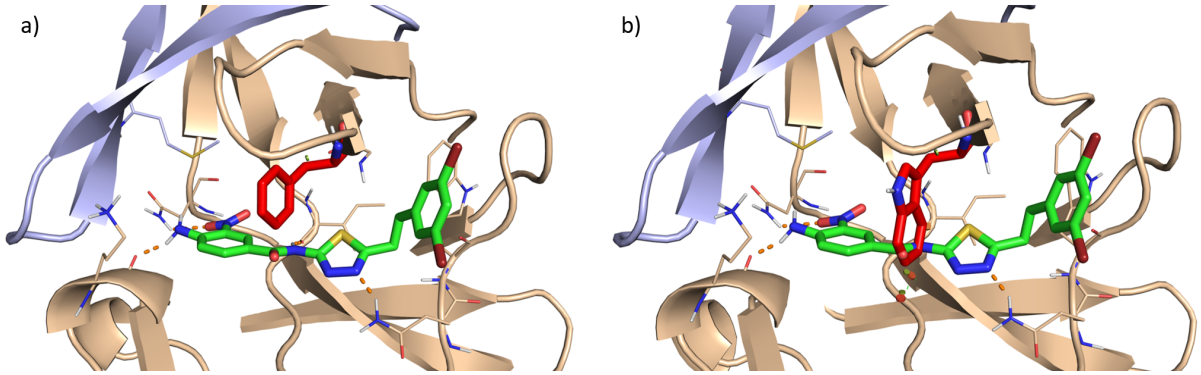

Fig. 3.23 Result of the *in silico* mutation study: Mutations I123F (a) and I123W (b) are most effective for blocking the allosteric pocket. Beige: NS3, light-blue: NS2B, green: **147**, red: mutation I123F/I123W.

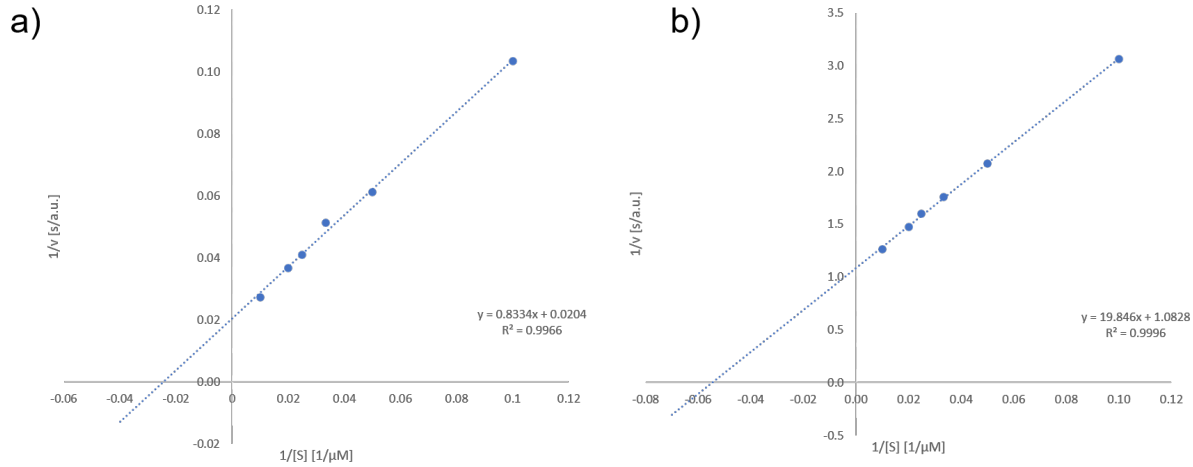

Fig. 3.24 Lineweaver-Burk-plot for the DENV3-I123F protease (a) and DENV3-I123W protease (b). V is the reaction rate and $[S]$ the substrate concentration.

The introduction of the mutations into the sequence of the DENV3 protease and the over expression as well as the purification of the resulting proteins was performed by Dr. A. Nguyen. To asses the extent to which the introduced mutations affect protein folding and reactivity, Lineweaver-Burk plot analysis was conducted for both proteins (Figure 3.24). For both proteins, the R^2-value of the corresponding regression curves is >0.99, so that second-order kinetics of the catalyzed reaction can be assumed. Obviously, the I123F mutation does not affect proteolysis catalyzed by the protease significantly,

since the K_m value determined is almost identical to that of the wild type (Table 3.9). This is not the case for the I123W mutant, which has a significantly lower K_m-value and a drastically lower v_{max}-value than the I123F mutant. The residual activity of the I123W mutant can be estimated to be 2% compared to the wild type/I123F mutant. Apparently, the I123W mutation leads to significant structural changes that impair proteolytic activity of the protease. It is therefore questionable to what extent the I123W mutant is still a representative model for the study of ligand binding.

Table 3.9 Determined kinetic parameters for DENV3-I123F and DENV3-I123W protease in comparison to the wildtype.

Protease	K_m [μM]	v_{max} [a.u./s]
DENV3-WT	41.50[75]	-
DENV3-I123F	40.85	49.02
DENV3-I123W	18.26	0.92

Subsequently, the efficacy of three different inhibitors (**63**, **116**, and **146**) against DENV3-I123F protease was determined. Surprisingly, the mutant was even slightly more strongly inhibited by the compounds than the wild type (Figure 3.25). There are three different explanations for this observation:

1. The phenyl ring of the introduced I123F mutation might rotate out of the allosteric site due to an adaption of the protease conformation upon binding (induced fit). Although it is known that the DENV protease is quite flexible with respect to its conformation, such a strong conformational change upon binding does not seem very likely.

2. The binding hypothesis is incorrect and binding does not occur into the closed[17] conformation. It is possible that the ligands bind in the open[16] or super-open[9] conformation instead. As mentioned in the Introduction, the shape of the allosteric pocket varies significantly between these conformations, so the I123F mutation may not block the allosteric pocket of one of the latter conformations.

3. The binding of the ligands occurs at a completely different allosteric site on the protein. This is theoretically possible, but there is no further evidence to support this assumption.

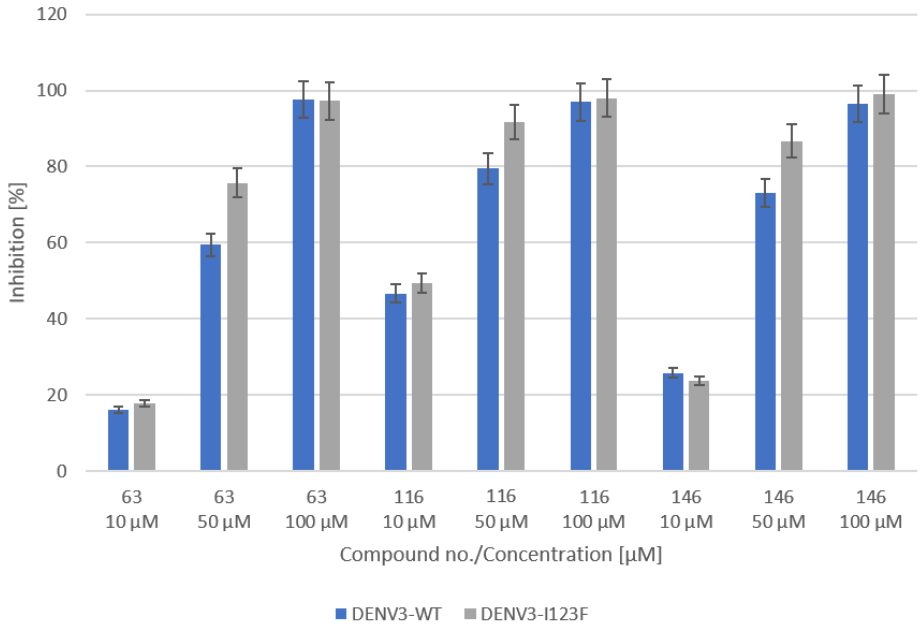

Fig. 3.25 Comparison of the percentage inhibition of DENV3-WT and DENV3-I123F by three different inhibitors (**63**, **116** and **146**).

Unfortunately, the performed mutation study did not provide further insight into the binding mode of the established ligand series, so that further studies with this approach were not conducted.

3.5.5 Tryptophan Quenching Assay

Another indirect method to obtain information about the binding site of a ligand is the so-called tryptophan quenching assay. This assay takes advantage of the inherent fluorescence of tryptophan residues when excited at 280 nm.[77] Since the absorption of other residues at this wavelength is low, the tryptophan residues can be selectively excited at this wavelength and the resulting emission measured at a peak wavelength of 340 nm.[77]

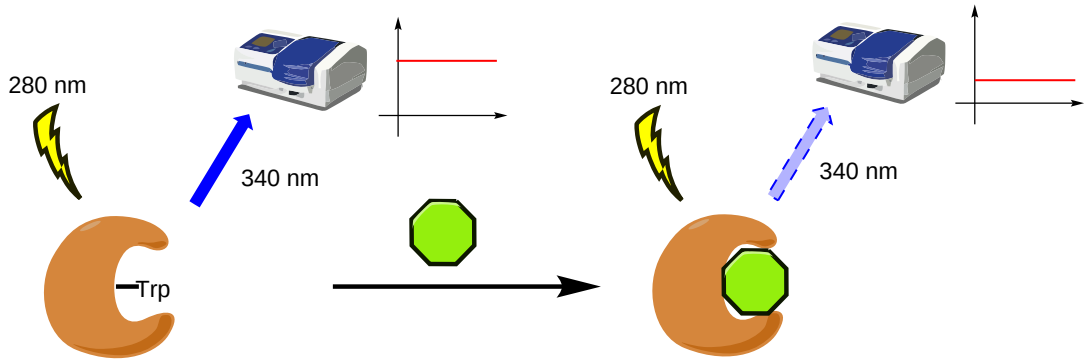

Fig. 3.26 General principle of the tryptophan quenching assay, orange: protein, green: ligand.

When a ligand binds to the protein in close proximity to a tryptophan residue, the emission signal is often significantly reduced due to Foerster resonance energy transfer (FRET) between the tryptophan residue and the ligand. For efficient energy transfer, the absorption maximum of the ligand must be in the range of the emission maximum of tryptophan and the distance between the two must be in the range of 0.5 to 10 nm.[78] If the emission intensity of a protein in solution decreases after the addition of a particular ligand, it is likely that the ligand binds near one of the tryptophan residues of the protein (see Figure 3.26). If one subsequently mutates all of the protein's tryptophan residues to alanine and measures the tryptophan quenching assay for each of the mutants, one can deduce which tryptohan residue is near the ligand binding site.[79]
For this assay to work, two requirements must be met: first, the protein must have at least one tryptophan residue in its sequence. Second, the ligand must have significant absorbance at 340 nm. Both requirements are met for the combination of DENV3 protease and compound **147**: the protease sequence contains six tryptophan residues and the ligand exhibits a pronounced absorption at the indicated wavelength (the absorption spectrum is shown in Figure 3.27).

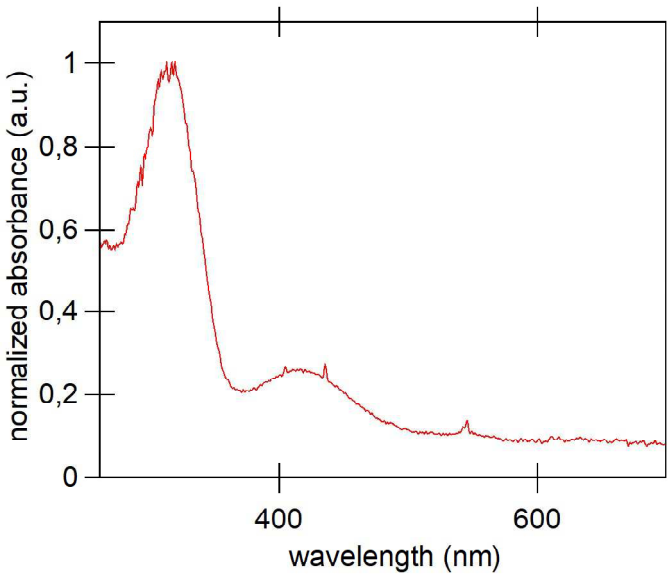

Fig. 3.27 Normalized UV-Vis spectrum of compound **147** at 150 μM concentration measured in the assay buffer used for the tryptophan quenching assay (2% DMSO concentration). The absorption maximum was determined to be at 318 nm.

Tryptophan fluorescence after addition of ligand **147** was measured at three different concentrations (10, 50, and 100 μM). As can be seen in Table 3.11, the tryptophan fluorescence of DENV3 protease was significantly and dose-dependently quenched by the addition of the ligand, indicating that the binding of ligand **147** occurs near a

tryptophan residue of the protease. After this measurement, aprotinin was added to the protein-ligand solution. Since aprotinin is a potent active site inhibitor of DENV3 protease,[32] its addition should restore tryptophan fluorescence if the ligand also binds in the active site (competitive binding mode).[79] This is not the case here: addition of aprotinin does not restore the initial tryptophan fluorescence, which is another indicator of a non-competitive binding of the established ligand series to the DENV3 protease.

Table 3.10 Results of the tryptophan quenching assay for addition of compound **147** to DENV3 protease.

Conc. [μM] **147**	Relative Fluorescence after **147** addition [%]	Relative Fluorescence **147** + aprotinin [%]
0	100.0	100.0
10	87.8	90.3
50	63.5	66.4
100	34.5	36.5

To gain further insights into the binding mode of the ligands to the DENV3 protease, all six tryptophan residues must each be mutated to alanine, so the following mutants must be prepared and tested in the tryptophan quenching assay: W61A (NS2B), W5A (NS3), W50A (NS3), W69A (NS3), W83A (NS3) and W89A (NS3). This work is currently being done by G. Bach in our research group, but is not the scope of this project.

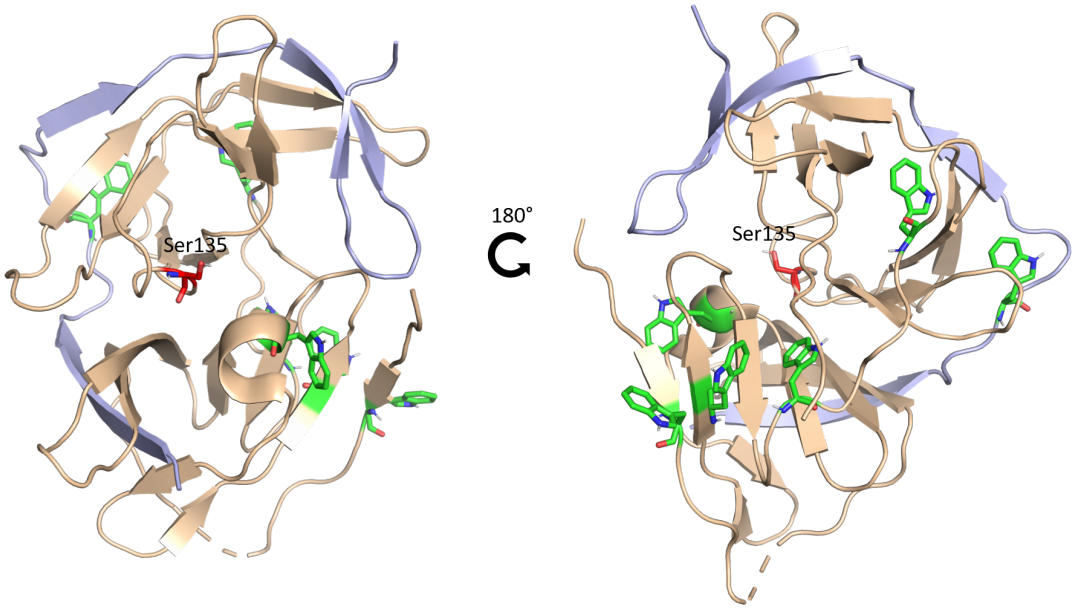

Fig. 3.28 Overview of the location of the trytophan residues in the DENV3 protease (pdb code: 3U1I). Lightblue: NS2B, beige: NS3, green sticks: trytophan residues, red sticks: serine residue of the catalytic triad.

3.5.6 Selectivity of the Established Ligand Series

So far, the activity of the established series of ligands has only been determined for two flaviviral proteases, so no conclusions can be drawn about their selectivity profile. To obtain a first overview whether the observed inhibition is selective for flaviviral proteases or whether serine proteases are inhibited in general, two exemplary compounds (**63** and **116**) were tested for their activity against the human serine protease trypsin. The necessary experiments were performed in U. Bauer's research group by S.Salehipour using a fluorescence-based enzyme assay similar to that described in detail for DENV and Zika protease.[80] In this case, the fluorogenic substrate is Bz-Arg-AMC, which also releases AMC after cleavage by trypsin. The compounds to be tested were added to the assay buffer (50 mM Tris, 150 mM NaCl, pH 8, 25 μM substrate) as solutions in DMSO so that the final assay concentration was 100 μM of the compound and 1% DMSO. The assay was started by adding trypsin and the fluorescence intensity (λ_{ex} = 485 nm, λ_{em} = 525 nm) was recorded over 1 h at RT.[80] The trypsin inhibitor gabexate mesylate was used as a positive control. The results of the experiments are shown in Figure 3.29. Apparently, compounds **63** and **116** did not inhibit the protease at any of the trypsin concentrations tested, whereas gabexate mesylate significantly inhibited the protease at concentrations <4.3 μM.

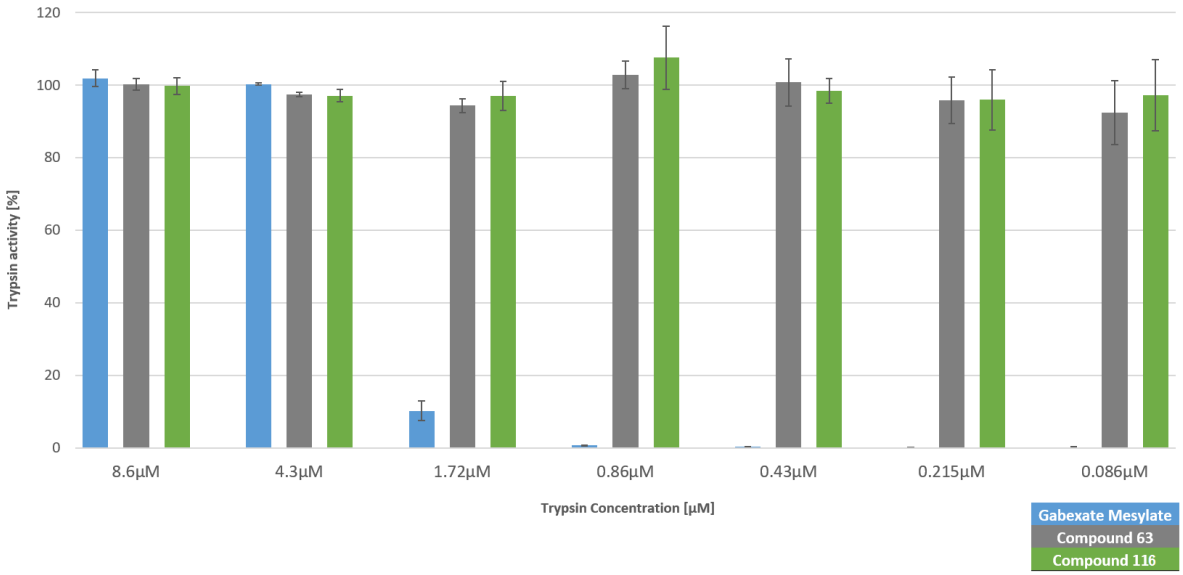

Fig. 3.29 Determination of the trypsin inhibition (%) of compounds **63** and **116** in comparison to Gabexate Mesylate at 100 μM inhibitor concentration and varying trypsin-concentrations.

These results are a strong evidence that the established ligand series selectively inhibits flaviviral proteases and not serine proteases in general. Further experiments with additional serine proteases (and other targets) are necessary to further determine the selectivity profile of the compounds.

3.5.7 Cell-based Experiments

Although assays with isolated enzymes are a useful tool for initial testing of potential inhibitors, they cannot replace *in cellulo* experiments. Many inhibitors that show promising activity against isolated enzymes fail in cell-based experiments due to low cell permeability or high cell toxicity.[81] There are many reports in the literature of promising NS2B/NS3 protease inhibitors that showed no activity in cell-based flaviviral replication assays.[81] To investigate if this problem exists here as well, the most potent inhibitors of the established ligand set were tested for their toxicity to Huh7 cells and for their inhibitory potential of ZIKV replication. The corresponding experiments were performed by Dr. A. Schöbel in E. Herker's research group.
To determine the cell-toxicity of the compounds, a so-called MTT assay was performed in Huh7 cells. This assay records cellular metabolic activity as an indicator of cell viability, proliferation and cytotoxicity.[82] It is a colometric assay using a yellow tetrazolium salt (MTT, **158**) which is reduced to purple formazan (**159**) by NAD(P)H-dependent oxidoreductase enzymes of metabolically active cells (Scheme 3.40).[83] The number of metabolically active cells is determined by the absorption intensity at 500 nm, the absorption maximum of the reduced formazan.

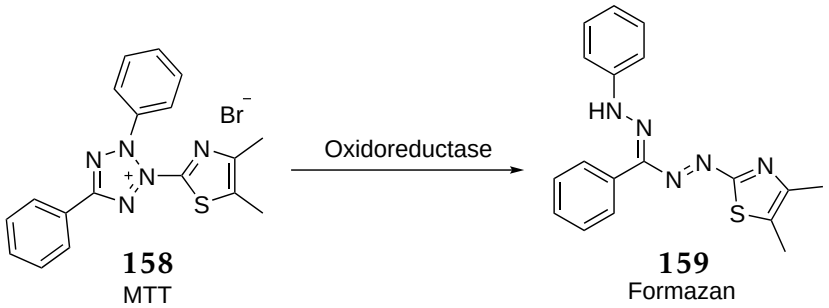

Scheme 3.40 In the MTT-assay, the cell viability is monitored by the reduction of MTT to formazan by NAD(P)H-dependent oxidoreductase enzymes.[84]

In the experimental set-up, Huh7.5 cells were seeded in a 96-well plate and treated with three different concentrations (5, 10, 25 μM) of each of the compounds (**63**, **66**, **115**, **97**, **98**, **122**, **116**, and **146**). After 4 h incubation, MTT was added and the increase in absorbance intensity over 240 min was measured. All tested compounds were well tolerated by the cells at a concentration of 5 μM and 10 μM respectively, as the determined curves did not deviate from the positive control (0.1% DMSO). At a concentration of 25 μM, most compounds showed significant cell toxicity as indicated by a decrease in the absorption intensity. The only compounds that did not exhibit detectable toxicity at 25 μM were ligands **115** and **116**. Two example MTT-reduction curves are shown in Figure 3.30 (measurements were performed in duplicates). For compound **122**, the absorption intensity at 25 μM decreases significantly compared to

the positive control, while for compound **115** there is no deviation from the positive control at this concentration. The same observation can be made for compounds **66** (pyrazole residue, cell-toxicity at 25 μM) and **116** (thiadiazole, no cell-toxicity at 25 μM). Apparently, a thiadiazole substitution in the C-position is less toxic to cells than a pyrazole substitution.

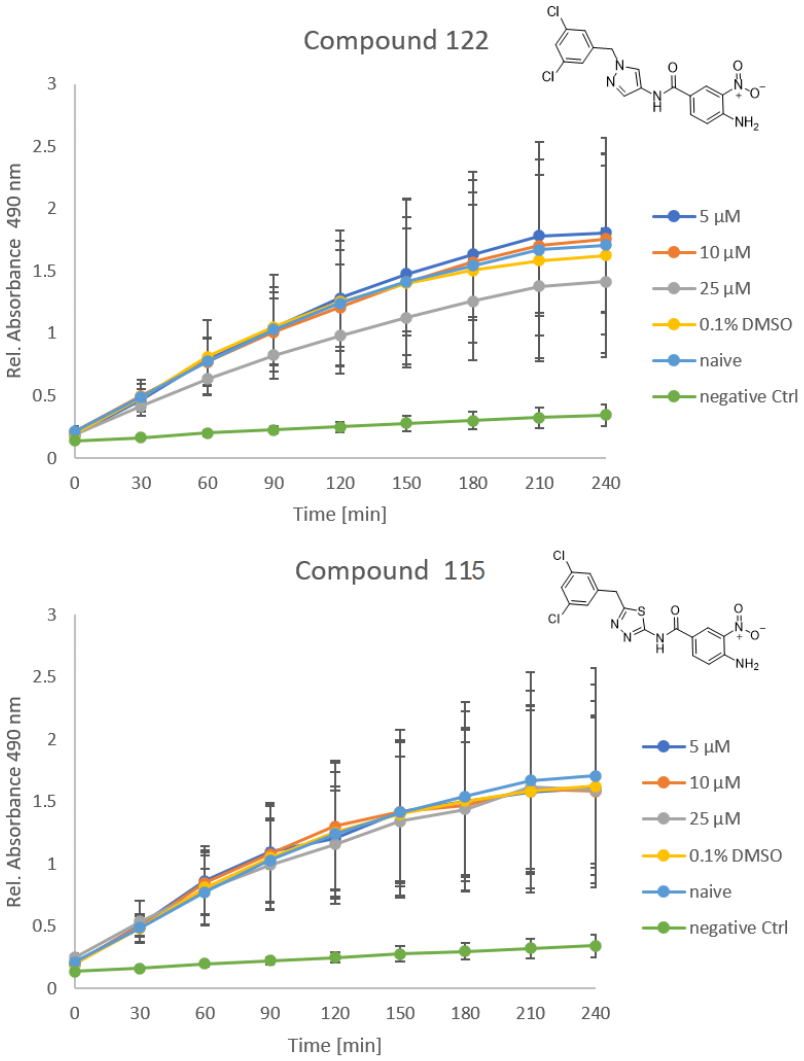

Fig. 3.30 MTT-reduction curves for compounds **122** and **115**.

To evaluate whether the established ligands are able to inhibit ZIKV replication *in cellulo*, the following general experimental setup was used (see Figure 3.31): Huh7.5 cells were infected with a ZIKV strain for 1 h and treated with different concentrations of each inhibitor for 48 h after removal of the virus inocolum. DMSO (0.1%) served as a negative control. The supernatants were harvested after this time and used to infect BHK21 cells showing a virus-induced cytopathic effect (CPE) after ZIKV infection.
For this purpose, BHK21 cells were seeded into a 96-well plate and infected with serial dilutions of viral supernatants for 1 h. After removal of the inoculum, the cells were

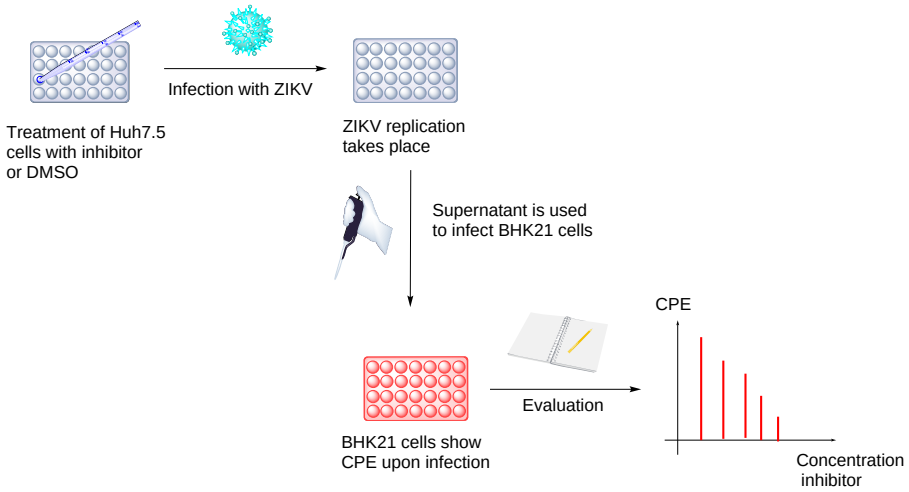

Fig. 3.31 Procedure to determine ZIKV replication inhibition by the established ligands.

incubated for 6 days. The amount of CPE that occurred was determined by crystal violet staining as a measure of the amount of viral particles transferred from the infected Huh7.5 cells to the BHK21 cells. When the compounds added to the Huh7.5 cells inhibit ZIKV replication, the amount of viral particles transferred from the Huh7.5 cells to the BHK21 cells decreases and so does the CPE that occurs. All inhibitors were tested at a concentration of 5 μM and 10 μM, as they were found to be non-toxic in this range.

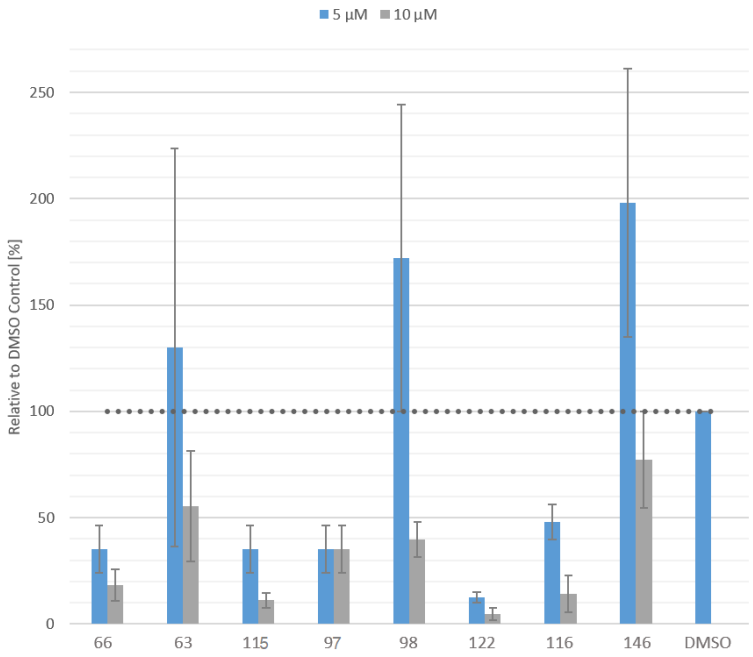

Fig. 3.32 Results of the ZIKV replication assay. Measurements were performed relative to a DMSO-control.

The obtained ZIKV replication inhibition by the compounds compared to the DMSO-control is shown in Figure 3.32 (the measurements were performed in triplicate). Except for **63**, **98**, and **146**, all compounds show a relative inhibition of ZIKV replication of more than 50% at a concentration of 5 μM. At a concentration of 10 μM, compounds **115** and **116** even show a relative inhibition of replication of more than 80%. Compound **122** showed the strongest relative inhibition of replication, but BHK21 cells treated with this compound showed a shape change, probably indicating toxicity of this compound. Overall, the results suggest that most of the ligands tested are indeed cell-permeable and can significantly inhibit ZIKV replication at concentrations that are not toxic to cells. Further experiments to investigate replication inhibition of other flaviviruses are currently underway.

4 Summary and Outlook

The aim of this project was the design and synthesis of novel non-competitive DENV protease inhibitors, as there is currently no drug available to treat DENV infection and the protease of this virus is a promising target for drug development.
As a starting point for further studies, an *in silico* HTS was performed using the allosteric site of the closed conformation of DENV3 protease as receptor. A library of small molecules derived from the ZINC15 database, which consisted of approx. 4 million compounds, was used as ligand input, and the docking process was performed using the AutoDock Vina software. The top 500 ranked molecules were visually inspected and discussed in a *Hit Picking Party* (plenary discussion of docking results, HPP), resulting in a list of 15 compounds to be purchased and tested *in vitro*. For *in vitro* evaluation, a fluorescence-based enzyme assay was used to measure the cleavage rate of a tripeptide substrate by DENV3 protease as a function of the concentration of inhibitor added. Three compounds showed significant inhibition of DENV3 protease (>35% at 100 μM), with compound **30** being the most effective (Figure 4.1a). The IC_{50} value of this compound was determined to be 136±16 μM, and the non-competitive binding mode was confirmed by Dixon plot analysis (Figure 4.1b).

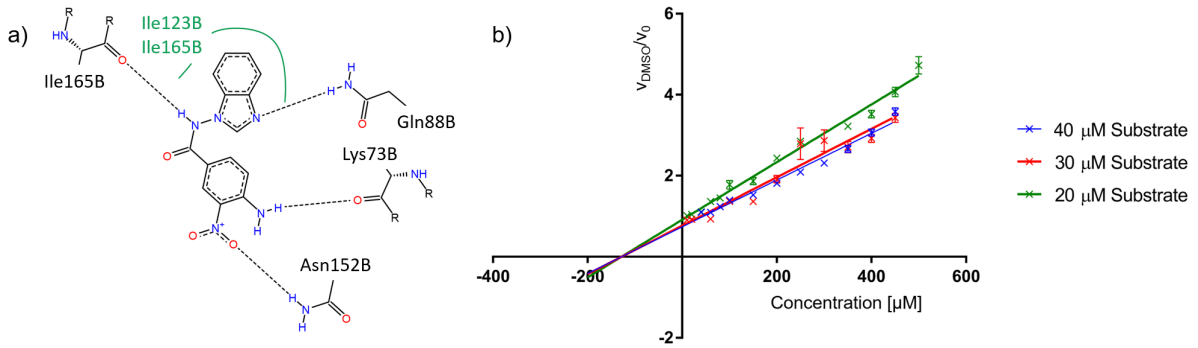

Fig. 4.1 a) PoseView image for the docking pose of compound **30** in the allosteric pocket of DENV3 protease, b) Dixon plot analysis for compound **30** against DENV3 protease, using three different substrate concentrations.

Compound **30** was successfully reduced to the lead fragment **37**, which retained the "left" part of the initial hit and showed a promising IC_{50} value of 226±30 μM. In a first SAR study, it was shown that the nitro group of compound **37** is essential for the observed activity and cannot be replaced in a suitable way, while the amino group can be substituted by a hydroxy group without decreasing affinity. Replacement of the amide moiety with a sulfonamide resulted in a slightly less effective inhibitor, and ester derivatives showed limited solubility in aqueous medium, so the amide structure was considered most promising (Figure 4.2).

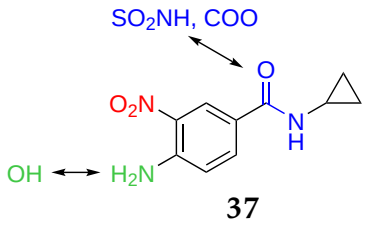

37

Fig. 4.2 Results obtained in the SAR study starting from the lead fragment **37**. Red: cannot be replaced without loss of affinity, blue: replacement results in decreased efficacy, green: can be replaced while retaining the affinity.

To obtain compounds with potentially increased affinity, extensions of the lead fragment **37** were created *in silico* taking two different approaches (Enamine catalog and Pingui module). The resulting library was used as input for docking, using the same setup as before. After visual inspection and plenary discussion, a list of 17 compounds remained for synthesis and *in vitro* testing. Thirteen of the 17 selected compounds were synthesized via self-developed pathways, consisting of one to three steps, while three compounds were purchased from the supplier Enamine and one compound was discarded due to lack of synthesizability (Scheme 4.1).

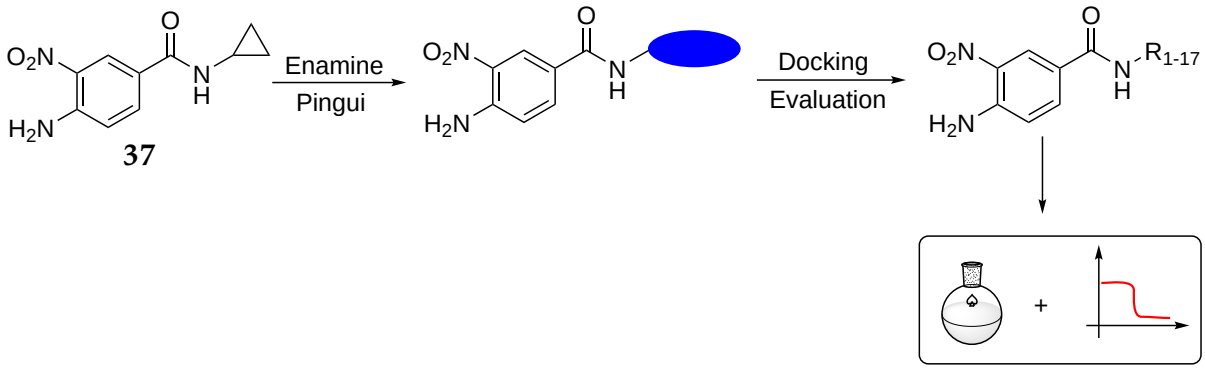

Scheme 4.1 Procedure to create a series of potentially more efficient inhibitors.

Four of the 17 compounds tested *in vitro* in the fluorescence-based assay showed significantly enhanced activity toward DENV3 protease (>60% inhibition at 100 μM). Their IC_{50} values were determined to be in the range of 28-81 μM against DENV2 and DENV3 protease respectively, with compound **63** being the most potent one (IC_{50}(DENV3) = 28±7.9 μM, Figure 4.3a). From these findings, a common motif of all potent allosteric DENV protease inhibitors was deduced: the fragment core of **37** has to be attached directly to a five- or six-membered heterocycle which is connected to a (*meta*-substituted) phenyl ring via a one- or two-atom linker (Figure 4.3b).
The most potent compound so far, **63**, was used as starting point for a comprehensive SAR study in which the substituents in positions A, B, and C were systematically varied (Figure 4.4a). In position A, bromine was found to be the optimal substituent, while

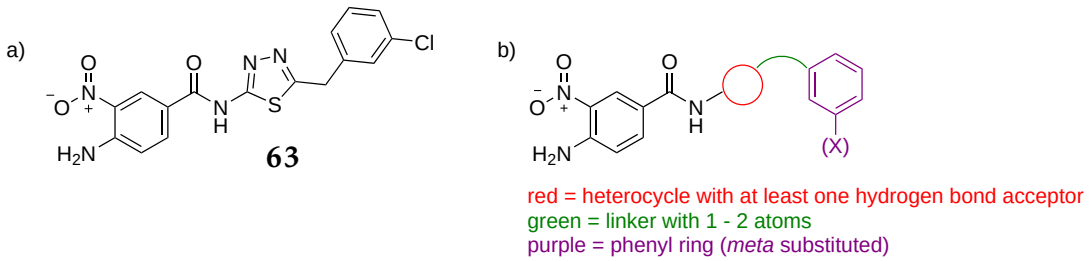

Fig. 4.3 a) Compound **63** turned out to be the most potent inhibitor from the fragment extension approach. b) Common structural motif of all potent DENV protease inhibitors.

fluorine increased the IC_{50} value by almost a factor of five. It was also found that a 3,5-disubstitution pattern was beneficial for affinity, at least in combination with a thiadiazole residue in the C position. Compounds with a pyrazole residue in the C position proved to be almost as effective as those with a thiadiazole residue, but all other substituents were not that effective. Varying the linker length in the B position (methylene vs. ethylene linker) had only a little effect on the activity of the resulting compounds, at least for the compounds with an aromatic residue in the C position. For compounds with an aliphatic ring in the C position, the ethylene linker proved to be better suited. Overall, the SAR study revealed that the substituent combination in compound **116** is the most effective so far (IC_{50}(DENV3)=12.3±3.5 μM, Figure 4.4b).

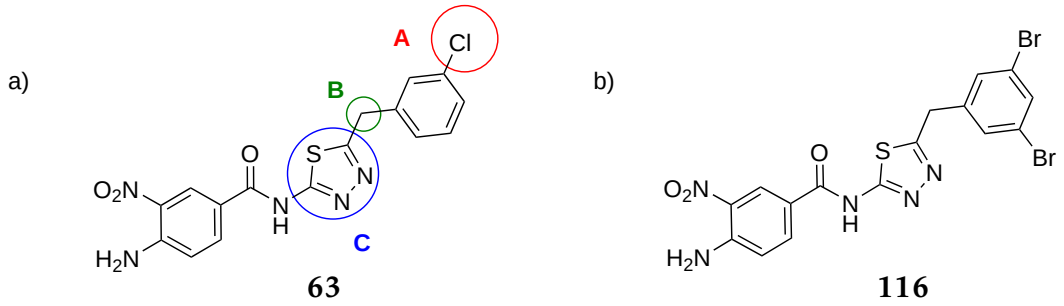

Fig. 4.4 a) Positions varied in the SAR study starting from compound **63**, b) Structure of the most potent compound **116** from the SAR study.

The activity of compound **116** was also tested against a binary DENV4 protease, which is thought to correspond better to the native state of the DENV protease than the glycine-linked protease constructs. Noteworthy, this protease construct was inhibited by compound **116** as strongly as the linked constructs, so it can be assumed that the IC_{50} values obtained with the linked construct are representative. Interestingly, compounds **63** and **116** proved to be even more potent inhibitors of the related ZIKV protease than of the DENV protease, with IC_{50} values of 15.5±2.8 μM and 4.8±1.1 μM, respectively. This result could not be explained by docking as the G164A mutation in the ZIKV protease hindered all docking attempts most likely due to clashes of the ligand in

the predefined receptor. The non-competitive binding mode initially confirmed for compound **30** was also confirmed for compound **147**, so it can be assumed that the binding mode of the established ligand series did not change during the optimization process.
Mutation studies were carried out to investigate the binding site of the established ligand series, since all attempts to crystallize the corresponding ligand-protein complexes had previously failed. An I123F mutant of DENV3 protease, designed to block the allosteric pocket for ligand binding, was surprisingly as susceptible to inhibition by the established ligands as the wild type. Possible reasons for this result have been discussed, but further experiments are needed to clarify this finding.

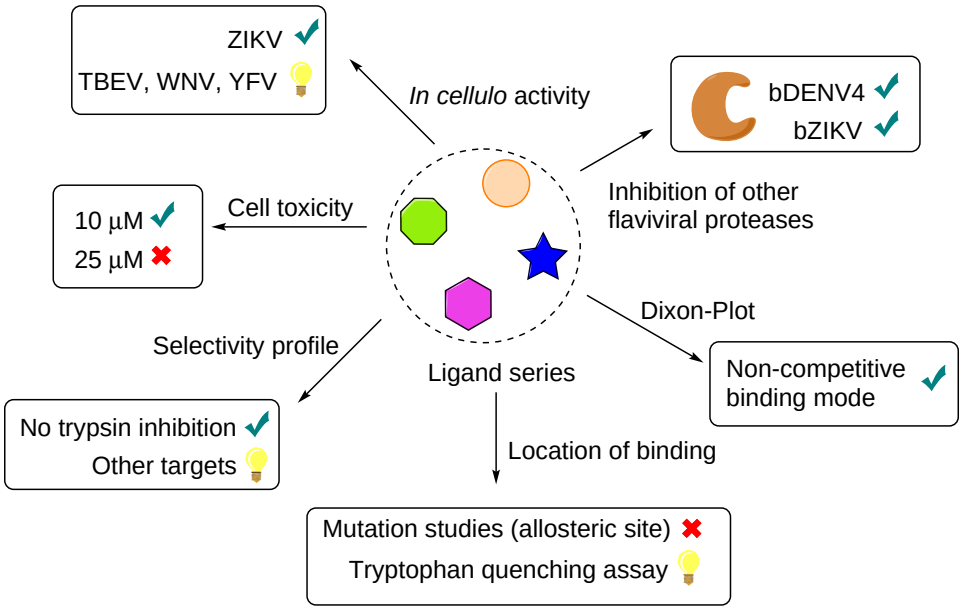

Fig. 4.5 Overview of the assays performed to investigate the properties of the established ligand series.

In a tryptophan quenching assay, compound **147** was shown to bind close to one or more tryptophan residues of the DENV3 protease. This information can be used as a starting point for further studies in which the corresponding tryptophan residues are sequentially mutated to alanine, thus providing information which of the tryptophan residues is in close proximity to the ligand binding site. In a collaborative project with the group of U. Bauer, it was shown that the established ligands do not inhibit the human serine protease trypsin, which is a strong indication of a selective inhibition of flaviviral proteases by the established ligands. Further experiments including additional targets are needed to more accurately determine the selectivity profile of the compounds.

Cell-based experiments with the established ligands were performed by the group of E. Herker. The compounds were found to be non-toxic to Huh7.5 cells at concentrations up to 10 μM-25 μM, depending on the ligand. The thiadiazole derivatives were found to be less toxic than the pyrazole derivatives in this context. Most of the tested compounds inhibited ZIKV replication more than 50% at 5 μM concentration in an *in cellulo* assay, indicating that the established ligands are indeed cell permeable and can effectively inhibit ZIKV replication. In future experiments the activity profile of the most potent compounds against other flaviviruses, such as TBEV, WNV or YFV will be determined.

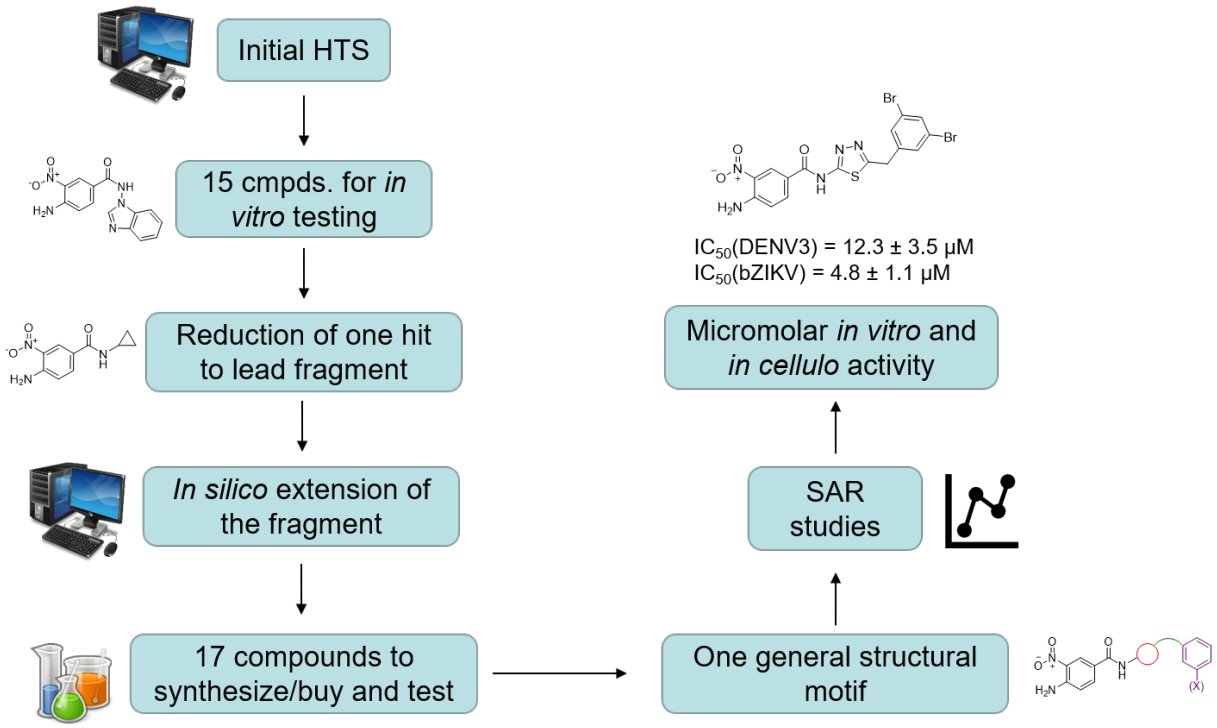

Fig. 4.6 Flowchart visualizing the milestones achieved in this project.

5 Experimental Part

5.1 Materials and Methods

Reactions: All reactions were carried out using standard glass equipment with teflon-coated stirring bars and magnetic stirrers. Reactions involving oxygen- and/or water-sensitive substances were carried-out in oven-dried vessels under argon atmosphere (*argon N50 Air Liquide*) using Schlenck techniques. Fine vacuum conditions were generated with a rotary vane oil pump (*RZ 2.5 Vacuubrand*). All used syringes and cannulas were flushed with argon before use.

Starting materials and reagents: Unless otherwise noted, all starting materials and reagents were taken from the working group's inventory or bought by *ABCR*, *Acros Organics*, *Alfa Aesar*, *BLD Pharma*, *Fluorochem*, *J&K*, *Sigma Aldrich* or *TCI* and used without further purification. If necessary, reagents were dried before use utilizing standard techniques.

Solvents: All solvents used were either purchased in HPLC-grade quality or, for water-sensitive reactions, as dry solvents stored under argon atmosphere over molecular sieves and used without further purification.

Yield determination: The determination of the product yield was carried out gravimetically and the determination of the product purity was achieved either by combustion analysis or by q-^{1}H-NMR spectroscopy.

Microwave assisted reactions were performed in closed, pressure-stable glass ware using a *Discover (CEM)* microwave oven coupled with an *Explorer (CEM)* auto sampler.

Thin layer chromatography (TLC) was used to monitor the reaction progress and selectivity and for a rough estimation of product purity during purification. Commercial plates on the basis of silica coated alumina plates (*MERCK*, *silicagel F60*, *F254*) were used. Fluorescence absorption was detected with a UV-lamp (λ=254 nm). Alternatively, the plate was stained using Cer(IV)- or $KMnO_4$-staining solution followed by heating.

Column Chromatography: Purification steps via column chromatography were performed using silica 60 (0.063 - 0.04 mm, *Macherey-Nagel*) for the adsorption of the crude material. Prepacked columns from different vendors (*FlashPure (Büchi)*, *Reveleris (Grace)*, *PuriFlash (Interchim)*) were used for the separation on two different MPLC-systems:

- *Reveleris X2* (*Grace*, now *Büchi*)
- Pump module *C-601 (X2)*, pump manager *C-615*, UV-detector *C-630* and fraction collector *C-660 (Büchi)*

Preparative high-performance liquid chromatography (prep-HPLC): If needed, the product was further purified using preparative HPLC. The purification was performed on a *C-850 Flashprep (Büchi)* using a *PrepPure C18* (100 Å, 10 μm, 250 x 20 mm, *Büchi*) column.

High-performance liquid chromatography coupled with mass spectrometry (HPLC-MS) was used to monitor the reaction progress and selectivity and for estimation of product purity during purification. The spectra were recorded on a *1260 Infinity (Agilent)* HPLC-system coupled with an *Expression S CMS (Advion)* mass spectrometer.

NMR spectroscopy: ^{1}H-NMR spectra for in-process control were measured automatically at the NMR-facilitiy of the Chemistry Department using either a *Bruker AV III HD* (250 MHz) or a *Bruker AV III* (300 MHz). All NMR-spectra for the collection of analytical data of the respective compounds were either measured on a *Jeol ECX400* (400 MHz) or a *Jeol ECA500* (500 MHz) by the staff of the NMR-facilities of the Pharmacy Department. The chemical shifts are given in *ppm* on the δ-scale referenced to the residual solvent signal as follows:[85]

- $CDCl_3$: 7.26 ppm (^{1}H), 77.16 ppm (^{13}C)
- DMSO-d_6: 2.50 ppm (^{1}H), 39.52 ppm (^{13}C)
- acetone-d_6: 2.05 ppm (^{1}H), 29.84, 206.26 ppm (^{13}C)
- MeOD-d_4: 3.31 ppm (^{1}H), 49.00 ppm (^{13}C)

The multiplicities caused by coupling are abbreviated as follows: br (broad), s (singlet), d (doublet), t (triplet), q (quartet), quint (quintet), dd (doublet of a doublet), dt (doublet of a triplet), ddd (doublet of a doublet of a doublet), m (multiplet) and sm (symmetric multiplet). The coupling constants are given in *Hertz* (Hz). For quantitative ^{1}H-NMR spectroscopy an appropriate internal standard was used to quantify the purity of the respective compound.

- Maleic acid: Product No. 92816, *Sigma Aldrich* (99.94 ± 0.16% purity)
- Dimethyl sulfon: Product No. 41867, *Sigma Aldrich* (99.73 ± 0.09% purity)

The editing and evaluation of the spectra was made with the software *Delta* from *Jeol* (version 5.2.1 and 5.3.1).

High resolution mass spectrometry (HR-MS): All mass spectra were recorded by the staff of the mass spectrometry facility of the Chemistry department. HR-EI spectra were recorded with an *AccuTOF GCv 4G (Jeol)* Time of Flight (TOF) spectrometer. An internal or external standard was used for time drift correction. HR-ESI and HR-APCI mass spectra were acquired with a *LTQ-FT Ultra (Thermo Fisher Scientific)* mass spectrometer. The resolution was set to 100.000. The relation between mass and charge (*m/z*) is noted.

Combustion Analysis (EA): All combustion analyses were performed by the staff of the elemental analysis facility of the Chemistry department with a *vario MICRO CUBE (Elementar)* and are given in percent.

Melting Point (MP): All melting points were measured on a *M 3000* and a *M 5000 (Krüss)* and are uncorrected.

5.2 Synthesis of DENV protease inhibitors

In the following chapter, synthesis instructions are arranged in ascending order according to the number of the respective final stage. The synthesis of the precursors always precedes the synthesis of the corresponding final stage.

5.2.1 Synthesis of 4-amino-*N*-(1*H*-benzo[*d*]imidazol-1-yl)-3-nitrobenzamide (30)

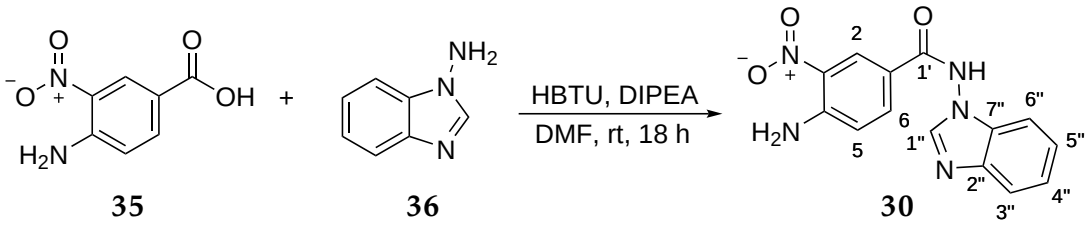

35 **36** **30**

Dry solvents were used and the reaction was carried out under Ar atmosphere.
In a 10 mL N_2-flask, 4-amino-3-nitrobenzoic acid (**35**) (250 mg, 1.37 mmol, 1.00 eq) and HBTU (622 mg, 1.64 mmol, 1.20 eq) were dissolved in DMF (3.5 mL). After stirring for 30 min at room temperature, 1-amino-benzimidazole (**36**) (201 mg, 1.51 mmol, 1.10 eq) and DIPEA (0.35 mL, 2.06 mmol, 1.50 eq) were added. The resulting dark orange solution was stirred until complete conversion could be detected via TLC (18 h). Water (50 mL) was cooled to 0 °C and the reaction mixture was poured onto it. A yellow solid precipitated and was collected by filtration, washed with water and DEE and finally dried *in vacuo*. The crude product was adsorbed onto silica and purified by column chromatography (silica, DCM/MeOH (+NH_3) 100:0 → 90:10) to give rise to 4-amino-*N*-(1*H*-benzo[*d*]imidazol-1-yl)-3-nitrobenzamide (**30**) (171 mg, 0.58 mmol, 42%) as a yellow solid.

^{1}**H-NMR:** 500 MHz, DMSO-d_6, δ_H = 7.15 (d, $^3J_{H,H}$=9.2 Hz, 1H, H-C5), 7.27 (ddd, $^3J_{H,H}$=7.6 Hz, 7.6 Hz, $^4J_{H,H}$=1.4 Hz, 1H, H-C5”), 7.30 (ddd, $^3J_{H,H}$= 7.6 Hz, 7.6 Hz, $^4J_{H,H}$=1.4 Hz, 1H, H-C4”), 7.41 (dd, $^3J_{H,H}$=6.9 Hz, $^4J_{H,H}$=1.4 Hz, 1H, H-C3”), 7.72 (dd, $^3J_{H,H}$=7.0 Hz, $^4J_{H,H}$=1.4 Hz, 1H, H-C6”), 7.97 (br, s, 2H, NH_2), 7.88 (d, $^4J_{H,H}$=2.0 Hz, 1H, H-C6), 8.35 (s, 1H, H-C1’), 8.79 (d, $^4J_{H,H}$=2.0 Hz, 1H, H-C2), 12.00 (s, 1H, CONH) ppm.

^{13}C-NMR: 125 MHz, DMSO-d_6, δ_C = 109.4 (1C, C3”), 117.6 (1C, C_{quart}), 119.4 (1C, C5), 119.8 (1C, C6”), 122.1 (1C, C4” or C5”), 123.2 (1C, C4” or C5”), 126.5 (1C, C2), 129.6 (1C, C_{quart}), 133.5 (1C, C_{quart}), 134.0 (1C, C6), 141.0 (1C, C_{quart}), 144.3 (1C, C1”), 148.5 (1C, C_{quart}), 164.4 (1C, C1’) ppm.

HR-MS: ESI(+), *m/z* = 298.0931 ($[M+H]^+$, calcd. for $C_{14}H_{12}N_5O_3$: 298.0935).

EA-CHN: 55.87% C, 3.79% H, 23.50% N
(calcd. for $C_{14}H_{11}N_5O_3 \cdot 0.25\ H_2O$: 55.72% C, 3.84% H, 23.21% N).

M.P.: Decomposition at 225 °C.

5.2.2 Synthesis of 4-amino-*N*-cyclopropyl-3-nitrobenzamide (37)

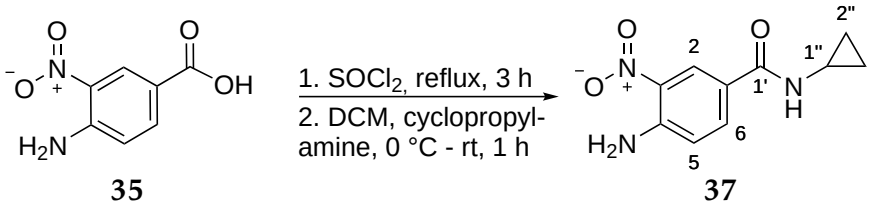

35 **37**

Dry solvents were used and the reaction was carried out under Ar atmosphere.
In a 50 mL N_2-flask, 4-amino-3-nitrobenzoic acid (**35**) (196 mg, 1.00 mmol, 1.00 eq) was suspended in thionyl chloride (3 mL). The reaction mixture was heated to reflux for 3 h. Thereafter, excess thionyl chloride was removed under reduced pressure and the orange residue was dried *in vacuo*. After suspending the intermediate in DCM (5 mL), cyclopropylamine (172 mg, 3.00 mmol, 3.00 eq) was added at 0 °C. The suspension was stirred at room temperature for 1 h. Complete conversion was determined via HPLC-MS after that time. The solvent was removed under reduced pressure and the residue was taken up in water (20 mL) and extracted with EtOAc (3x 30 mL). The combined organic layers were washed with sat. NaCl-solution, dried over $MgSO_4$, filtered and the solvent was removed under reduced pressure. The crude product was adsorbed onto silica and purified by column chromatography (silica, Cyhex/EtOAc 75:25 → 25:75), which resulted in 4-amino-*N*-cyclopropyl-3-nitrobenzamide (**37**) (165 mg, 0.75 mmol, 75%) as a yellow solid.

^{1}H-NMR: 500 MHz, DMSO-d_6, δ_H = 0.54-0.57 (m, 2H, H-C2"), 0.67 (sm, 2H, H-C2"), 2.81 (sm, 1H, H-C1"), 7.01 (d, $^3J_{H,H}$=8.9 Hz, 1H, H-C5), 7.71 (br, s, 2H, NH_2), 7.83 (dd, $^3J_{H,H}$=8.9 Hz, $^4J_{H,H}$=2.0 Hz, 1H, H-C6), 8.38 (d, $^4J_{H,H}$=3.7 Hz, 1H, CONH), 8.53 (d, $^4J_{H,H}$=2.0 Hz, 1H, H-C2) ppm.

^{13}C-NMR: 125 MHz, DMSO-d_6, δ_C = 5.6 (2C, C2"), 22.9 (1C, C1"), 118.7 (1C, C5), 121.3 (1C, C1), 125.2 (1C, C2), 129.5 (1C, C3), 138.9 (1C, C6), 147.6 (1C, C4), 165.6 (1C, CO) ppm.

HR-MS: APCI(+), *m/z* = 222.0869 ($[M+H]^+$, calcd. for $C_{10}H_{12}N_3O_3$: 222.0873).

EA-CHN: 53.37% C, 4.80% H, 18.50% N
(calcd. for $C_{10}H_{11}N_3O_3 \cdot 0.25\ H_2O$: 53.21% C, 5.14% H, 18.62% N).

M.P.: 203.2 °C.

5.2.3 Synthesis of 4-amino-*N*-cyclopropyl-3-fluorobenzamide (39)

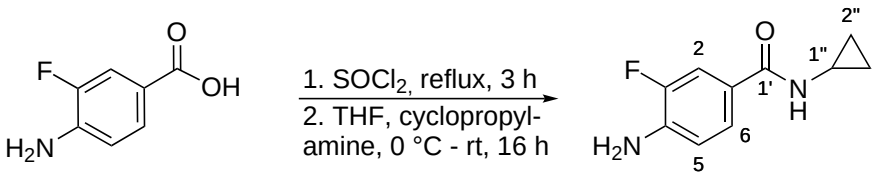

41 **39**

Dry solvents were used and the reaction was carried out under Ar atmosphere.
In a 25 mL N_2-flask, 4-amino-3-fluorobenzoic acid (**41**) (388 mg, 2.50 mmol, 1.00 eq) was suspended in thionyl chloride (7 mL). The reaction mixture was stirred for 3 h and the residual thionyl chloride removed by distillation. The intermediate was dried *in vacuo* and thereafter dissolved in THF (7.5 mL). The solution was cooled to 0 °C and cyclopropylamine (429 mg, 7.50 mL, 1.00 eq) was added dropwise at the given temperature. Complete conversion could be observed by HPLC-MS after stirring for 16 h at room temperature. The reaction mixture was washed with water (30 mL) and the aqueous layer extracted with EtOAc (3x 15 mL). The combined organic layers were dried over $MgSO_4$, filtered and the solvent removed under reduced pressure. The crude material was adsorbed onto silica and purified by column chromatography (silica, Cyhex/EtOAc 60:40 → 50:50). The desired 4-amino-*N*-cyclopropyl-3-fluorobenzamide (**39**) (464 mg, 2.39 mmol, 96%) could be obtained as a white solid.

^{1}H-NMR: 500 MHz, DMSO-d_6, δ_H = 0.50-0.53 (m, 2H, H-C2"), 0.63-0.66 (m, 2H, H-C2"), 2.78 (m, 1H, H-C1"), 5.63 (br, s, 2H, NH_2), 6.72 (ddd, $^3J_{H,H}$=8.8 Hz, $^4J_{H,F}$=8.3 Hz, $^5J_{H,H}$=1.9 Hz, 1H, H-C5), 7.42 (dd, $^3J_{H,H}$=8.6 Hz, $^4J_{H,H}$=2.0 Hz, 1H, H-C6), 7.47 (dd, $^3J_{H,F}$=12.9 Hz, $^4J_{H,H}$=1.7 Hz, 1H, H-C2), 8.04 (d, $^3J_{H,H}$=3.7 Hz, 1H, CONH) ppm.

^{13}C-NMR: 125 MHz, DMSO-d_6, δ_C = 5.7 (s, 2C, C2"), 22.9 (s, 1C, C1"), 113.8 (d, $^2J_{C,F}$=19.2 Hz, 1C, C2), 114.6 (d, $^3J_{C,F}$=4.8 Hz, 1C, C5), 121.6 (d, $^3J_{C,F}$=4.8 Hz, 1C, C1), 124.2 (d, $^4J_{C,F}$=2.4 Hz, 1C, C6), 139.4 (d, $^2J_{C,F}$=13.2 Hz, 1C, C4), 149.4 (d, $^1J_{C,F}$=236.2 Hz, 1C, C3), 166.4 (s, 1C, C1') ppm.

^{19}F-NMR: 470 MHz, DMSO-d_6, δ_F = -135.97 ppm.

HR-MS: ESI(+), *m/z* = 195.0929 ($[M+H]^+$, calcd. for $C_{10}H_{12}FN_2O$: 195.0928).

EA-CHN: 61.81% C, 5.66% H, 14.29% N
(calcd. for $C_{10}H_{11}FN_2O$: 61.85% C, 5.71% H, 14.42% N).

M.P.: 105.4 °C.

5.2.4 Synthesis of 4-amino-*N*-cyclopropyl-3-(trifluoromethyl)benzamide (40)

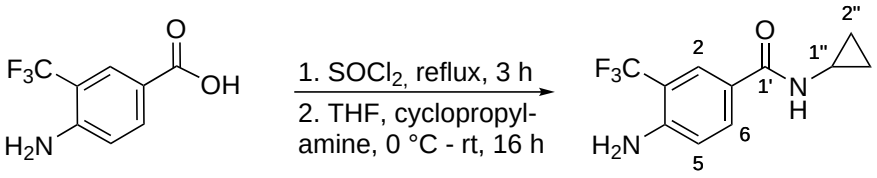

42 **40**

Dry solvents were used and the reaction was carried out under Ar atmosphere.
A 25 mL N_2-flask was charged with 4-amino-3-(trifluoromethyl)benzoic acid (**42**) (513 mg, 2.50 mmol, 1.00 eq) and thionyl chloride (7 mL). The reaction mixture was heated to reflux for 3 h, concentrated under reduced pressure and the resulting residue was dried *in vacuo*. The *in situ* generated acid chloride was dissolved in THF (7.5 mL) and cooled to 0 °C. Cyclopropylamine (429 mg, 7.50 mmol, 3.00 eq) was added at this temperature slowly and after stirring at room temperature for 16 h complete conversion was determined by HPLC-MS. The reaction mixture was diluted with EtOAc (15 mL), washed with water (30 mL) and the aqueous layer extracted with EtOAc (3x 10 mL). The combined organic layers were dried over $MgSO_4$, filtered and the solvent was removed under reduced pressure. The crude material was purified by column chromatography (DCM/MeOH (+NH_3) 100:0 → 96:4) to afford 4-amino-*N*-cyclopropyl-3-(trifluoromethyl)benzamide (**40**) (563 mg, 2.31 mmol, 93%) as a beige solid.

^{1}H-NMR: 500 MHz, DMSO-d_6, δ_H = 0.51-0.54 (m, 2H, H-C2”), 0.64-0.68 (m, 2H, H-C2”), 2.79 (sm, 1H, H-C1”), 6.06 (br, s, 2H, NH_2), 6.80 (d, $^3J_{H,H}$=8.9 Hz, 1H, H-C5), 7.75 (dd, $^3J_{H,H}$=8.9 Hz, $^4J_{H,H}$=2.0 Hz, 1H, H-C6), 7.87 (d, $^4J_{H,H}$=2.0 Hz, 1H, H-C2), 8.19 (d, $^3J_{H,H}$=3.7 Hz, 1H, CONH) ppm.

^{13}C-NMR: 125 MHz, DMSO-d_6, δ_C = 5.6 (s, 2C, C2”), 22.9 (s, 1C, C1”), 109.4 (q, $^2J_{C,F}$=30.0 Hz, 1C, C3), 115.8 (s, 1C, C5), 120.8 (s, 1C, C1), 124.9 (q, $^1J_{C,F}$=272.3 Hz, 1C, CF_3), 125.8 (q, $^3J_{C,F}$=4.8 Hz, 1C, C2), 132.0 (s, 1C, C6), 148.4 (s, 1C, C4), 166.3 (s, 1C, C1’) ppm.

^{19}F-NMR: 470 MHz, DMSO-d_6, δ_F = -61.57 ppm.

HR-MS: ESI(+), *m/z* = 245.0896 ([M+H]$^+$, calcd. for $C_{11}H_{12}F_3N_2O$: 245.0896).

EA-CHN: 53.87% C, 4.54% H, 11.15% N
(calcd. for $C_{11}H_{11}F_3N_2O$: 54.10% C, 4.54% H, 11.47% N).

M.P.: 113.4 °C.

5.2.5 Synthesis of methyl 3-(methylthio)-4-nitrobenzoate (45)

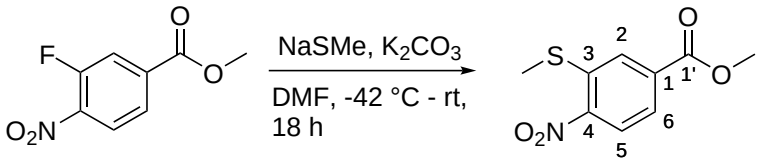

44 **45**

Dry solvents were used and the reaction was carried out under Ar atmosphere.
In a 50 mL N_2-flask, K_2CO_3 (821 mg, 5.94 mmol, 2.00 eq) was dried *in situ*. Afterwards, methyl 3-fluoro-4-nitro-benzoic acid (**44**) (500 mg, 2.97 mmol, 1.00 eq) was added and both solids were suspended in DMF (10 mL) and cooled to -42 °C. In a second flask, sodium thiomethylate (292 mg, 4.16 mmol, 1.40 eq) was dissolved in DMF (10 mL) and the solution was slowly added to the first flask at -42 °C. The reaction mixture was allowed to warm to RT over night. After detection of complete conversion by TLC, EtOAc (30 mL) was added and the mixture was washed with LiCl-solution (5% wt, aq, 30 mL). The aqueous layer was extracted with EtOAc (3x 30 mL) and the combined organic layers dried over $MgSO_4$, filtered and evaporated to dryness. The residue was adsorbed onto silica and purified by column chromatography (silica, Cyhex/EtOAc 97:3 → 75:25) to afford methyl 3-(methylthio)-4-nitrobenzoate (**45**) as a yellow solid (212 mg, 0.93 mmol, 31%).

^{1}H-NMR: 500 MHz, $CDCl_3$, δ_H = 2.57 (s, 3H, SMe), 3.98 (s, 3H, COOMe), 7.86 (dd, $^3J_{H,H}$=8.5 Hz, $^4J_{H,H}$=1.6 Hz, 1H, H-C6), 8.05 (d, $^4J_{H,H}$=1.4 Hz, 1H, H-C2), 8.28 (d, $^3J_{H,H}$=8.7 Hz, 1H, H-C5) ppm.

^{13}C-NMR: 125 MHz, $CDCl_3$, δ_C = 16.2 (1C, SMe), 53.1 (1C, COOMe), 125.1 (1C, C5), 126.4 (1C, C2), 127.3 (1C, C6), 134.5 (1C, C3), 139.9 (1C, C1), 147.8 (1C, C4), 165.4 (1C, C1') ppm.

HR-MS: EI(+), *m/z* = 227.02561 ($[M]^+$, calcd. for $C_9H_9NO_4S$: 227.02523).

M.P.: 110.1 °C.

5.2.6 Synthesis of methyl 4-amino-3-(methylthio)benzoate (46)

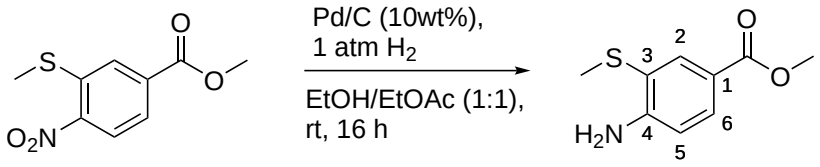

45 **46**

The reaction was carried out under Ar atmosphere.

A 50 mL three-necked-flask was charged with compound **45** (200 mg, 0.88 mmol, 1.00 eq), Pd/C (10% wt, 47.0 mg, 0.044 mmol, 0.05 eq), and EtOH/EtOAc (1:1, 6 mL). The atmosphere of the flask was exchanged to H_2 (1 atm) and the reaction mixture was stirred at RT for 16 h, after which complete conversion was detected by TLC. Afterwards, Pd/C was removed by filtration over Celite® and the filtrate was evaporated to dryness. After drying *in vacuo*, methyl 4-amino-3-(methylthio)benzoate (**46**) was obtained as a pale yellow solid (178 mg, 0.90 mmol, quantitative yield).

^{1}H-NMR: 500 MHz, $CDCl_3$, δ_H = 2.38 (s, 3H, SMe), 3.86 (s, 3H, COOMe), 6.75 (d, $^3J_{H,H}$=8.2 Hz, 1H, H-C5), 7.77 (dd, $^3J_{H,H}$=8.4 Hz, $^4J_{H,H}$=2.1 Hz, 1H, H-C6), 8.06 (d, $^4J_{H,H}$=2.1 Hz, 1H, H-C2) ppm.

^{13}C-NMR: 125 MHz, $CDCl_3$, δ_C = 17.9 (1C, SMe), 51.9 (1C, COOMe), 114.1 (br, 1C, C5), 120.5 (br, 1C, C3), 125.8 (br, 1C, C1), 130.9 (1C, C2 or C6), 135.6 (1C, C2 or C6), 150.8 (br, 1C, C4), 166.9 (1C, C1') ppm.

HR-MS: APCI(+), *m/z* = 198.0588 ($[M+H]^+$, calcd. for $C_9H_{12}NO_2S$: 198.0583).

M.P.: 48.5 °C.

All recorded spectral data are in accordance to literature.[86]

5.2.7 Synthesis of methyl 4-amino-3-(methylsulfinyl)benzoate (47)

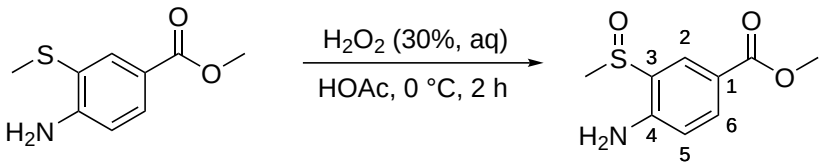

46 **47**

In a 50 mL round-bottomed flask, compound **46** (592 mg, 3.00 mmol, 1.00 eq) was dissolved in HOAc (15.0 mL) and cooled to 0 °C. At this temperature, H_2O_2-solution (30% wt, aq, 0.30 mL, 3.00 mmol, 1.00 eq) was added dropwise. After stirring for 2 h at 0 °C, complete conversion was detected by TLC, so that the reaction was quenched by addition of sodium thiosulfate-solution (10% wt, aq, 10 mL). The pH-value was adjusted to pH=7 by addition of NaOH and then EtOAc (30 mL) was added. The mixture was washed with water (15 mL) and the aqueous layer extracted with EtOAc (3x 30 mL). The combined organic layers were dried over $MgSO_4$, filtered and the solvent removed under reduced pressure. The crude material was adsorbed onto silica and purified by column chromatography (silica, Cyhex/EtOAc 65:35 → 10:90), which afforded methyl 4-amino-3-(methylsulfinyl)benzoate (**47**) as a yellow solid (516 mg, 2.42 mmol, 81%).

^{1}H-NMR: 500 MHz, DMSO-d_6, δ_H = 2.74 (s, 3H, SMe), 3.78 (s, 3H, COOMe), 6.46 (br, s, 2H, NH_2), 6.77 (d, $^3J_{H,H}$=8.5 Hz, 1H, H-C5), 7.76 (dd, $^3J_{H,H}$=8.5 Hz, $^4J_{H,H}$=2.1 Hz, 1H, H-C6), 8.00 (d, $^4J_{H,H}$=2.1 Hz, 1H, H-C2) ppm.

^{13}C-NMR: 125 MHz, DMSO-d_6, δ_C = 39.6 (1C, SMe), 51.5 (1C, COOMe), 115.3 (1C, C5), 116.8 (1C, C2), 124.8 (1C, C1), 126.6 (1C, C6), 132.6 (1C, C3), 150.0 (1C, C4), 165.6 (1C, C1') ppm.

HR-MS: EI(+), *m/z* = 213.04528 ($[M]^+$, calcd. for $C_9H_{11}NO_3S$: 213.04596).

M.P.: 133.4 °C.

5.2.8 Synthesis of 4-amino-3-(methylsulfinyl)benzoic acid (48)

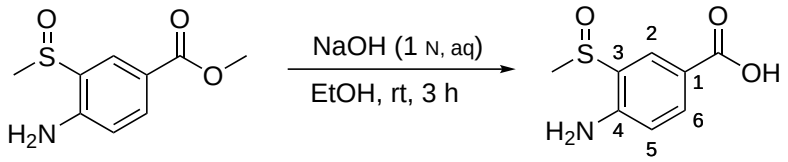

47 **48**

In a 100 mL round-bottomed flask, compound **47** (400 mg, 1.88 mmol, 1.00 eq) was dissolved in EtOH (20 mL) and NaOH-solution (1 N, aq, 20 mL) was added. After stirring at RT for 3 h, complete conversion was detected by TLC, so that EtOH was removed under reduced pressure. Afterwards, the pH-value was adjusted to pH=1 by addition of HCl-solution (4 M, aq) and then EtOAc (30 mL) was added. The mixture was washed with sat. NaCl-solution (20 mL) and the aqueous layer extracted with EtOAc (3x 30 mL). The combined organic layers were dried over $MgSO_4$, filtered and evaporated to dryness. The residue was adsorbed onto silica and purified by column chromatography (silica, DCM/MeOH 95:5 → 90:10), which afforded 4-amino-3-(methylsulfinyl)benzoic acid (**48**) as a pale yellow solid (239 mg, 1.20 mmol, 64%).

^{1}H-NMR: 500 MHz, DMSO-d_6, δ_H = 2.74 (s, 3H, SMe), 6.39 (br, s, 2H, NH_2), 6.75 (d, $^3J_{H,H}$=8.5 Hz, 1H, H-C5), 7.73 (dd, $^3J_{H,H}$=8.5 Hz, $^4J_{H,H}$=2.1 Hz, 1H, H-C6), 7.96 (d, $^4J_{H,H}$=2.1 Hz, 1H, H-C2), 12.4 (br, s, 1H, COOH) ppm.

^{13}C-NMR: 125 MHz, DMSO-d_6, δ_C = 39.6 (1C, SOMe), 115.2 (1C, C5), 118.0 (1C, C2), 124.5 (1C, C1), 126.8 (1C, C6), 132.8 (1C, C3), 149.8 (1C, C4), 166.7 (1C, C1') ppm.

HR-MS: ESI(+), *m/z* = 200.0381 ($[M+H]^+$, calcd. for $C_8H_{10}NO_3S$: 200.0376).

M.P.: 191.7 °C.

5.2.9 Synthesis of 4-amino-*N*-cyclopropyl-3-(methylsulfinyl)benzamide (43)

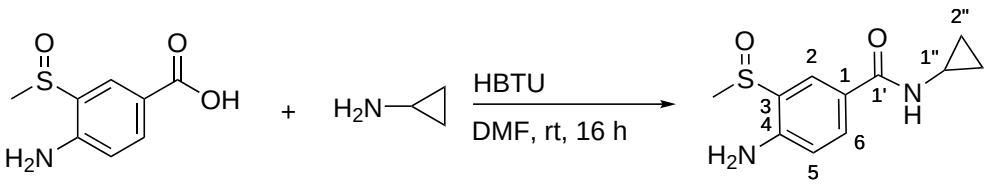

48 **49** **43**

Dry solvents were used and the reaction was carried out under Ar atmosphere.
In a 10 mL Schlenck-tube, compound **48** (180 mg, 0.90 mmol, 1.00 eq) and HBTU (410 mg, 1.08 mmol, 1.20 eq) were dissolved in DMF (3.5 mL) and stirred at RT for 30 min. Afterwards, cyclopropylamine (**49**) (0.15 mL, 3.00 mmol 3.00 eq) was added dropwise. The reaction mixture was stirred for 16 h at RT (detection of complete conversion by TLC). Afterwards, EtOAc (15 mL) was added and the mixture was washed with LiCl-solution (5% wt, aq, 15 mL) and the aqueous layer extracted with EtOAc (3x 15 mL). The combined organic layers were dried over $MgSO_4$, filtered and the solvent removed under reduced pressure. The crude product was adsorbed onto silica and purified by column chromatography (silica, DCM/MeOH ($+NH_3$) 100:0 → 95:5) to give the desired 4-amino-*N*-cyclopropyl-3-(methylsulfinyl)benzamide (**43**) as a very hygroscopic, beige solid (102 mg, 0.43 mmol, 48%).

^{1}H-NMR: 500 MHz, DMSO-d_6, δ_H = 0.52-0.54 (m, 2H, H-C2”), 0.65-0.67 (m, 2H, H-C2”), 2.76 (m, 4H, SOMe, H-C1”), 6.72 (d, $^3J_{H,H}$=8.6 Hz, 1H, H-C5), 7.67 (dd, $^3J_{H,H}$=8.9 Hz, $^4J_{H,H}$=2.0 Hz, 1H, H-C6), 7.86 (d, $^4J_{H,H}$=2.0 Hz, 1H, H-C2), 7.92 (br, s, 2H, NH_2), 8.16 (d, $^3J_{H,H}$=4.0 Hz, 1H, CONH) ppm.

^{13}C-NMR: 125 MHz, DMSO-d_6, δ_C = 3.3; 5.7 (two conformations, 2C, C2”), 22.3; 22.9 (two conformations, 1C, C1”), 39.6 (1C, SOMe), 115.2 (1C, C5), 122.1 (1C, C2), 123.9 (1C, C1), 124.7 (1C, C6), 130.8 (1C, C3), 148.9 (1C, C4), 166.6 (1C, C1’) ppm.

HR-MS: ESI(+), *m/z* = 239.0855 ($[M+H]^+$, calcd. for $C_{11}H_{15}N_2O_2S$: 239.0849).

q-^{1}H-NMR: 500 MHz, DMSO-d_6, maleic acid as internal standard: 95.8% ± 0.4% purity.

M.P.: Decomposition at 120 °C.

5.2.10 Synthesis of *N*-cyclopropyl-4-hydroxy-3-nitrobenzamide (51)

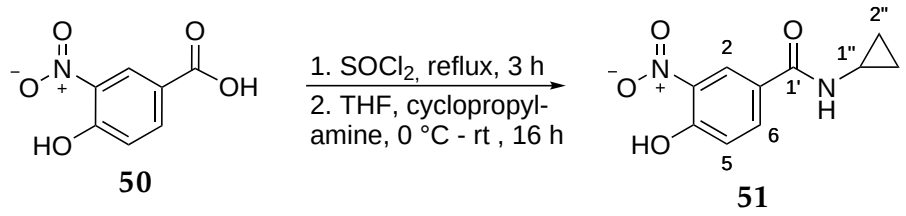

50 **51**

Dry solvents were used and the reaction was carried out under Ar atmosphere.
A 25 mL N_2-flask was charged with 4-hydroxy-3-nitrobenzoic acid (**50**) (458 mg, 2.50 mmol, 1.00 eq) and thionyl chloride (6 mL). After stirring for 3 h at reflux, the excess thionyl chloride was removed under reduced pressure, the remaining residue further dried *in vacuo* and afterwards dissolved in THF (7.5 mL). The solution was cooled to 0 °C and cyclopropylamine (429 mg, 7.50 mmol, 3.00 eq) was added slowly at this temperature. The resulting yellow suspension was stirred for 16 h at room temperature, whereupon complete conversion could be detected by HPLC-MS. The suspension was taken up in EtOAc (50 mL), washed with water (30 mL) and the aqueous phase extracted with EtOAc (3x 30 mL). The combined organic layers were dried over $MgSO_4$, filtered and the solvent was removed under reduced pressure. The crude product was adsorbed onto silica and purified by column chromatography (silica, Cyhex/EtOAc 80:20 → 0:100) which afforded *N*-cyclopropyl-4-hydroxy-3-nitrobenzamide (**51**) (455 mg, 2.05 mmol, 82%) as a pale yellow solid.

^{1}H-NMR: 500 MHz, DMSO-d_6, δ_H = 0.55-0.58 (m, 2H, H-C2”), 0.69 (sm, 2H, H-C2”), 2.83 (sm, 1H, H-C1”), 7.16 (d, $^3J_{H,H}$=8.6 Hz, 1H, H-C5), 8.00 (dd, $^3J_{H,H}$=8.6 Hz, $^4J_{H,H}$=2.3 Hz, 1H, H-C6), 8.38 (d, $^4J_{H,H}$=2.3 Hz, 1H, H-C2), 8.49 (d, $^3J_{H,H}$=4.0 Hz, 1H, CONH), 11.51 (br, s, 1H, OH) ppm.

^{13}C-NMR: 125 MHz, DMSO-d_6, δ_C = 5.6 (2C, C2”), 23.0 (1C, C1”), 118.8 (1C, C5), 124.3 (1C, C2), 125.2 (1C, C1), 133.7 (1C, C6), 136.3 (1C, C3), 154.1 (1C, C4), 165.2 (1C, C1’) ppm.

HR-MS: ESI(+), *m/z* = 223.0715 ($[M+H]^+$, calcd. for $C_{10}H_{11}N_2O_4$: 223.0713).

EA-CHN: 53.77% C, 4.57% H, 12.33% N
(calcd. for $C_{10}H_{10}N_2O_4$: 54.05% C, 4.54% H, 12.61% N).

M.P.: 174.3 °C.

5.2.11 Synthesis of 4-chloro-*N*-cyclopropyl-3-nitrobenzenesulfonamide (53)

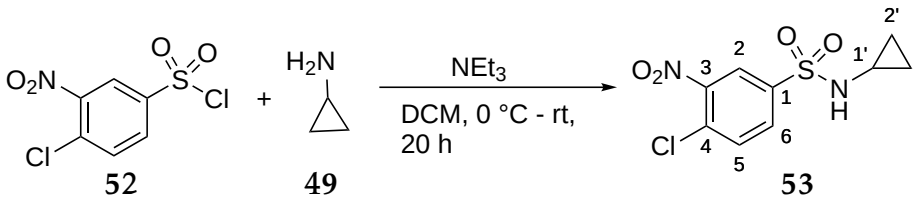

Dry solvents were used and the reaction was carried out under Ar atmosphere.
In a 25 mL N_2-flask, 4-chloro-3-nitro-benzenesulfonyl chloride (**52**) (640 mg, 2.50 mmol, 1.00 eq) was dissolved in DCM (6 mL) and cooled to 0 °C. In another flask, cyclopropylamine (**49**) (0.20 mL, 2.75 mmol 1.10 eq) and NEt_3 (0.38 mmol, 2.75 mmol, 1.10 eq) were dissolved in DCM (2 mL) and the resulting solution was added dropwise to the first flask. The reaction mixture was stirred for 30 min at 0 °C and for 10 h at RT (detection of complete conversion by TLC). Afterwards, the reaction mixture was washed with sat. NH_4Cl-solution (40 mL) and the aqueous layer extracted with DCM (3x 30 mL). The combined organic layers were dried over $MgSO_4$, filtered and the solvent removed under reduced pressure. The crude product was adsorbed onto silica and purified by column chromatography (silica, Cyhex/EtOAc 95:5 → 80:20) to give the desired 4-chloro-*N*-cyclopropyl-3-nitrobenzenesulfonamide (**53**) as a pale yellow solid (639 mg, 2.31 mmol, 92%).

^{1}H-NMR: 500 MHz, DMSO-d_6, δ_H = 0.39-0.43 (m, 2H, H-C2'), 0.49-0.56 (m, 2H, H-C2'), 2.22 (sm, 1H, H-C1'), 8.03-8.08 (m, 2H, H-C5 + H-C6), 8.27 (s, 1H, NH), 8.43 (d, $^4J_{H,H}$=1.8 Hz, 1H, H-C2) ppm.

^{13}C-NMR: 125 MHz, DMSO-d_6, δ_C = 5.1 (2C, C2'), 24.1 (1C, C1'), 124.1 (1C, C2), 129.4 (1C, C5), 131.5 (1C, C4), 133.1 (1C, C6), 140.4 (1C, C1), 147.4 (1C, C3) ppm.

HR-MS: EI(+), *m/z* = 275.99488 ([M]$^+$, calcd. for $C_9H_9ClN_2O_4S$: 275.99715).

M.P.: 106.2 °C.

5.2.12 Synthesis of 4-amino-*N*-cyclopropyl-3-nitrobenzenesulfonamide (54)

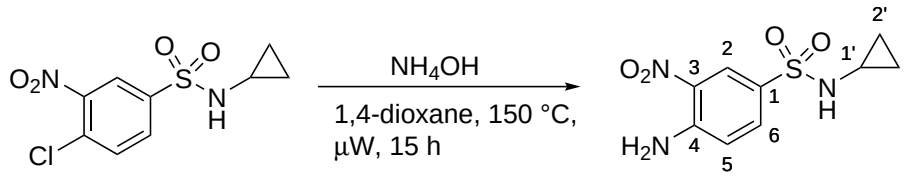

53 **54**

In a 20 mL microwave-tube, **53** (400 mg, 1.45 mmol, 1.00 eq) was dissolved in 1,4-dioxane (3.5 mL) and NH_4OH (30% wt in water, 5.0 mL). The resulting solution was heated in a microwave reactor (300 W, 300 psi max.) at 150 °C for 15 h, after which complete conversion was detected by TLC. Water (50 mL) and EtOAc (50 mL) were added to the reaction mixture and the aqueous layer was extracted with EtOAc (3x 30 mL). The combined organic layers were dried over $MgSO_4$, filtered and the solvent removed under reduced pressure. The crude material was adsorbed onto silica and purified by column chromatography (silica, Cyhex/EtOAc 80:20 → 40:60), which afforded 4-amino-*N*-cyclopropyl-3-nitrobenzenesulfonamide (**54**) as a yellow solid (176 mg, 0.68 mmol, 47%).

^{1}H-NMR: 500 MHz, DMSO-d_6, δ_H = 0.35-0.38 (m, 2H, H-C2'), 0.47-0.50 (m, 2H, H-C2'), 2.13 (sm, 1H, H-C1'), 7.15 (d, $^3J_{H,H}$=9.2 Hz, 1H, H-C5), 7.68 (dd, $^3J_{H,H}$=8.9 Hz, $^4J_{H,H}$=2.3 Hz, 1H, H-C6), 7.78 (br, s, 1H, SO_2NH), 7.98 (br, s, 2H, NH_2), 8.38 (d, $^4J_{H,H}$=2.3 Hz, 1H, H-C2) ppm.

^{13}C-NMR: 125 MHz, DMSO-d_6, δ_C = 5.0 (2C, C2'), 24.0 (1C, C1'), 120.0 (1C, C5), 125.8 (1C, C2), 126.1 (1C, C1), 128.9 (1C, C6), 132.6 (1C, C3), 148.2 (1C, C4) ppm.

HR-MS: ESI(+), *m/z* = 258.0542 ($[M+H]^+$, calcd. for $C_9H_{12}N_3O_4S$: 258.0543).

EA-CHN: 40.76% C, 4.33% H, 15.55% N (calcd. for $C_9H_{11}N_3O_4S \cdot H_2O$: 40.60% C, 4.54% H, 15.78% N).

M.P.: 154.8 °C.

5.2.13 Synthesis of methyl 4-amino-3-nitrobenzoate (55)

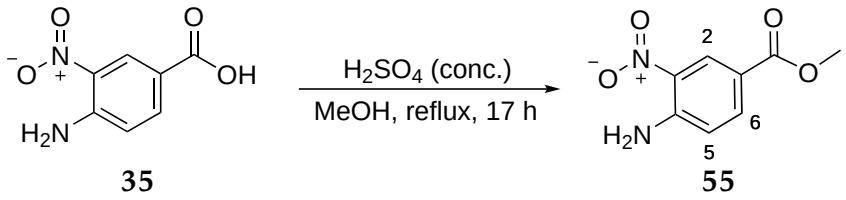

35 **55**

A 250 mL two-necked flask was charged with 4-amino-3-nitrobenzoic acid (**35**) (1.00 g, 5.50 mmol, 1.00 eq) and the solid was suspended in methanol (75 mL). Concentrated sulfuric acid (3.36 g, 34.25 mmol, 6.23 eq) was slowly added and the suspension was heated to reflux for 17 h until complete conversion was indicated by TLC. The reaction was quenched by the addition of sodium bicarbonate until a pH = 7-8 was reached. Afterwards, the solvent was evaporated under removed pressure. The residue was taken up in water (80 mL) and extracted with EtOAc (3x 75 mL). The combined organic layers were dried over $MgSO_4$, filtered, and evaporated to dryness. The crude material was adsorbed onto silica and purified by column chromatography (silica, Cyhex/EtOAc 95:5 → 65:35). The desired methyl 4-amino-3-nitrobenzoate (**55**) (919 mg, 4.68 mmol, 85%) was obtained as a yellow solid.

^{1}H-NMR: 500 MHz, DMSO-d_6, δ_H = 3.81 (s, 3H, OCH_3), 7.06 (d, $^3J_{H,H}$=8.9 Hz, 1H, H-C5), 7.85 (dd, $^3J_{H,H}$=8.9 Hz, $^4J_{H,H}$=2.0 Hz, 1H, H-C6), 7.98 (br, s, 2H, NH_2), 8.55 (d, $^4J_{H,H}$=2.0 Hz, 1H, H-C2) ppm.

^{13}C-NMR: 125 MHz, DMSO-d_6, δ_C = 51.9 (1C, OCH_3), 116.1 (1C, C1), 119.3 (1C, C5), 128.0 (1C, C2), 129.6 (1C, C3), 134.7 (1C, C6), 148.8 (1C, C4), 164.8 (1C, CO) ppm.

HR-MS: EI(+), *m/z* = 196.04743 ([M]$^+$, calcd. for $C_8H_8N_2O_4$: 196.04841).

EA-CHN: 48.80% C, 4.14% H, 14.21% N
(calcd. for $C_8H_8N_2O_4$: 48.98% C, 4.11% H, 14.28% N).

All recorded spectral data are in accordance to literature.[87]

5.2.14 Synthesis of benzyl 4-amino-3-nitrobenzoate (56)

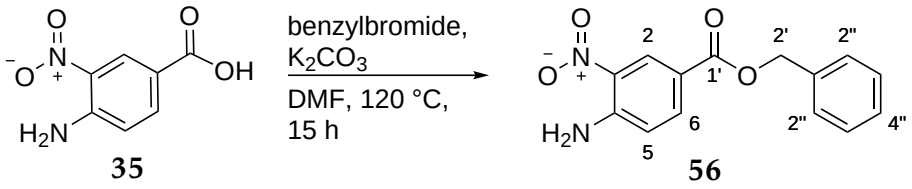

In a 25 mL round-bottomed flask, 4-amino-3-nitrobenzoic acid (**35**) (455 mg, 2.50 mmol, 1.00 eq) and potassium carbonate (691 mg, 5.00 mg, 2.00 eq) were suspended in DMF (12 mL). Benzylbromide (0.30 mL, 2.50 eq, 1.00 eq) was added and the reaction mixture was stirred at reflux for 15 h. After that time, complete conversion was observed by HPLC-MS, so that the suspension was diluted with EtOAc (20 mL), washed with LiCl-solution (5% wt, 30 mL) and the aqueous layer extracted with EtOAc (3x 20 mL). The combined organic layers were dried over $MgSO_4$, filtered and evaporated to dryness. The crude product was adsorbed onto silica and purified via column chromatography (Cyhex/EtOAc 100:0 → 80:20) providing benzyl 4-amino-3-nitrobenzoate (**56**) (515 mg, 1.89 mmol, 76%) as a yellow solid.

^{1}**H-NMR:**	500 MHz, DMSO-d_6, δ_H = 5.31 (s, 2H, H-C2'), 7.07 (d, $^3J_{H,H}$=9.2 Hz, 1H, H-C5), 7.33-7.46 (m, 5H, H-C2" - H-C4"), 7.88 (dd, $^3J_{H,H}$=8.9 Hz, $^4J_{H,H}$=2.0 Hz, 1H, H-C6), 7.97 (br, s, 2H, NH_2), 8.57 (d, $^4J_{H,H}$=2.0 Hz, 1H, H-C2) ppm.
^{13}**C-NMR:**	125 MHz, DMSO-d_6, δ_C = 66.0 (1C, C2'), 116.1 (1C, C1), 119.4 (1C, C5), 128.0 (2C, C2" or C3"), 128.0 (1C, C4"), 128.1 (1C, C2), 128.5 (2C, C2" or C3"), 129.7 (1C, C1"), 134.8 (1C, C6), 136.2 (1C, C3), 148.9 (1C, C4), 164.2 (1C, C1') ppm.
HR-MS:	APCI(+), *m/z* = 273.0877 ($[M+H]^+$, calcd. for $C_{14}H_{13}N_2O_4$: 273.0870).
EA-CHN:	61.61% C, 4.45% H, 10.27% N (calcd. for $C_{14}H_{12}N_2O_4$: 61.76% C, 4.44% H, 10.29% N).
M.P.:	123.1 °C.

All recorded spectral data are in accordance to literature.[88]

5.2.15 Synthesis of *N*-(2-acetamidoethyl)-4-amino-3-nitrobenzamide (57)

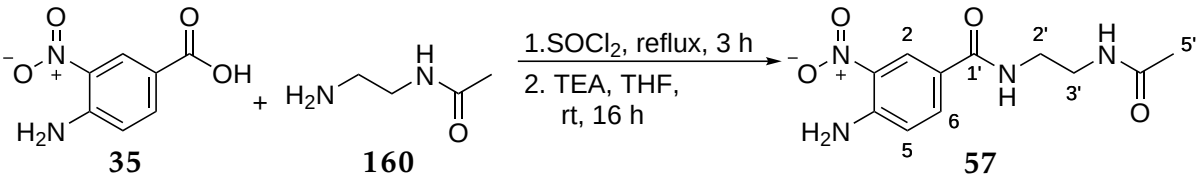

35 **160** **57**

Dry solvents were used and the reaction was carried out under Ar atmosphere.
In a 25 mL N_2-flask, 4-amino-3-nitrobenzoic acid (**35**) (455 mg, 2.50 mmol, 1.00 eq) was suspended in thionyl chloride (12.5 mL) and one drop of DMF was added. The suspension was stirred at reflux for 3 h and then the excess thionyl chloride was removed by distillation. The residue was taken up in THF (5 mL) and was slowly added to a solution of *N*-(2-aminoethyl)acetamide (**160**) (297 mg, 2.75 mmol, 1.10 eq) and triethylamine (0.52 mL, 3.75 mmol, 1.50 eq) in THF (5 mL) at room temperature. After stirring at room temperature for 16 h, complete conversion was detected via TLC. The reaction mixture was washed with water (30 mL) and the aqueous layer extracted with EtOAc (3x 30 mL). The combined organic layers were washed with sat. $NaHCO_3$-solution, sat. NaCl-solution, dried over $MgSO_4$, filtered and the solvent removed under reduced pressure. The crude product was recrystallized from MTBE/^{i}PrOH (1:1) to afford *N*-(2-acetamidoethyl)-4-amino-3-nitrobenzamide (**57**) (120 mg, 0.45 mmol, 18%) as a yellow solid.

^{1}H-NMR: 500 MHz, DMSO-d_6, δ_H = 1.80 (s, 3H, H-C5'), 3.15-3.20 (m, 2H, H-C2' or H-C3'), 3.26-3.30 (m, 2H, H-C2' or H-C3'), 7.03 (d, $^3J_{H,H}$=8.9 Hz, 1H, H-C5), 7.73 (br, s, 2H, NH_2), 7.85 (dd, $^3J_{H,H}$=8.9 Hz, $^4J_{H,H}$=2.0 Hz, 1H, H-C6), 7.92 (t, $^3J_{H,H}$=5.4 Hz, 1H, CONH), 8.47 (t, $^3J_{H,H}$=5.4 Hz, 1H, CONH), 8.56 (d, $^4J_{H,H}$=2.0 Hz, 1H, H-C2) ppm.

^{13}C-NMR: 125 MHz, DMSO-d_6, δ_C = 22.1 (1C, C5'), 38.2 (1C, C2' or C3'), 39.1 (1C, C2' or C3'), 118.8 (1C, C5), 121.3 (1C, C1), 125.3 (1C, C2), 129.5 (1C, C3), 133.8 (1C, C6), 147.6 (1C, C4), 164.6 (1C, C1'), 169.4 (1C, C4') ppm.

HR-MS: ESI(+), *m/z* = 267.1090 ($[M+H]^+$, calcd. for $C_{11}H_{15}N_4O_4$: 267.1088).

EA-CHN: 49.50% C, 5.37% H, 20.79% N
(calcd. for $C_{11}H_{14}N_4O_4$: 49.62% C, 5.30% H, 21.04% N).

M.P.: 231.5 °C.

5.2.16 Synthesis of 4-amino-3-nitro-*N*-phenethylbenzamide (58)

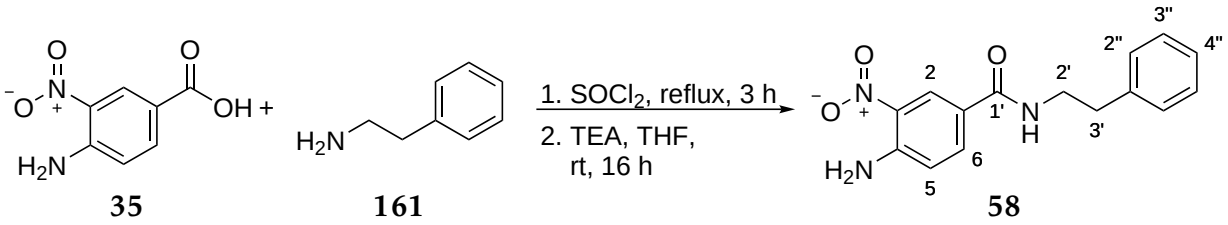

35 **161** **58**

Dry solvents were used and the reaction was carried out under Ar atmosphere.
In a 25 mL N_2-flask 4-amino-3-nitrobenzoic acid (**35**) (455 mg, 2.50 mmol, 1.00 eq) was suspended in thionyl chloride (12.5 mL) and one drop of DMF was added. The suspension was stirred at reflux for 3 h, which after the excess thionyl chloride was removed by distillation. The residue was taken up in THF (5 mL) and was slowly added to a solution of 2-phenylethan-1-amine (**161**) (333 mg, 2.75 mmol, 1.10 eq) and triethylamine (0.52 mL, 3.75 mmol, 1.50 eq) in THF (5 mL) at room temperature. After stirring at room temperature for 16 h, complete conversion was detected via TLC. The reaction mixture was washed with water (30 mL) and the aqueous layer extracted with EtOAc (3x 30 mL). The combined organic layers were washed with sat. $NaHCO_3$-solution, sat. NaCl-solution, dried over $MgSO_4$, filtered and the solvent removed under reduced pressure. The crude product was adsorbed onto silica and purified by column chromatography (silica, Cyhex/EtOAc 90:10 → 60:40) to give 4-amino-3-nitro-*N*-phenethylbenzamide (**58**) (451 mg, 1.58 mmol, 63%) as a yellow solid.

^{1}H-NMR: 500 MHz, DMSO-d_6, δ_H = 2.82 (t, $^3J_{H,H}$=7.7 Hz, 2H, H-C3'), 3.44-3.48 (m, 2H, H-C2'), 7.03 (d, $^3J_{H,H}$=8.9 Hz, 1H, H-C5), 7.18-7.31 (m, 5H, H-C2" - H-C4"), 7.72 (br, s, 2H, NH_2), 7.84 (dd, $^3J_{H,H}$=8.9 Hz, $^4J_{H,H}$= 2.3 Hz, 1H, H-C6), 8.51-8.53 (m, 1H, CONH), 8.54 (d, $^4J_{H,H}$=2.0 Hz, 1H, H-C2) ppm.

^{13}C-NMR: 125 MHz, DMSO-d_6, δ_C = 35.1 (1C, C3'), 40.8 (1C, C2'), 118.8 (1C, C5), 121.4 (1C, C1), 125.2 (1C, C2), 126.1 (1C, C4"), 128.3 (2C, C2" or C3"), 128.6 (2C, C2" or C3"), 129.5 (1C, C1"), 133.9 (1C, C6), 139.5 (1C, C3), 147.6 (1C, C4), 164.4 (1C, C1') ppm.

HR-MS: ESI(+), *m/z* = 286.1186 ($[M+H]^+$, calcd. for $C_{15}H_{16}N_3O_3$: 286.1186).

EA-CHN: 62.95% C, 5.36% H, 14.64% N
(calcd. for $C_{15}H_{15}N_3O_3$: 63.15% C, 5.30% H, 14.73% N).

M.P.: 178.9 °C.

5.2.17 Synthesis of 4-amino-3-nitro-*N*-(pyridin-2-ylmethyl)benzamide (59)

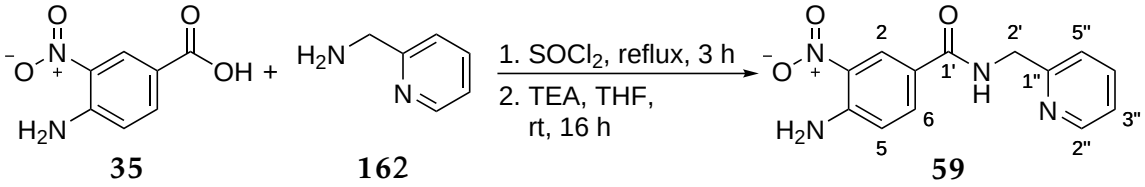

35 **162** **59**

Dry solvents were used and the reaction was carried out under Ar atmosphere.
In a 25 mL N_2-flask, 4-amino-3-nitrobenzoic acid (**35**) (455 mg, 2.50 mmol, 1.00 eq) was suspended in thionyl chloride (12.5 mL) and one drop of DMF was added. The suspension was stirred at reflux for 3 h and then the excess thionyl chloride was removed by distillation. The residue was taken up in THF (5 mL) and was slowly added to a solution of pyridin-2-ylmethanamine (**162**) (379 mg, 2.75 mmol, 1.10 eq) and triethylamine (0.52 mL, 3.75 mmol, 1.50 eq) in THF (5 mL) at room temperature. After stirring at room temperature for 16 h, complete conversion was detected via TLC. The reaction mixture was washed with water (30 mL) and the aqueous layer extracted with EtOAc (3x 30 mL). The combined organic layers were washed with sat. $NaHCO_3$-solution, sat. NaCl-solution, dried over $MgSO_4$, filtered and the solvent removed under reduced pressure. The crude product was adsorbed onto silica and purified by column chromatography (silica, DCM/MeOH (+NH_3) 100:0 → 90:10). Since the product still contained impurities afterwards, it was recrystallized from Cyhex/EtOAc (2:1) to give 4-amino-3-nitro-*N*-(pyridin-2-ylmethyl)benzamide (**59**) (177 mg, 0.65 mmol, 26%) as a yellow solid.

^{1}H-NMR: 500 MHz, DMSO-d_6, δ_H = 4.54 (d, $^3J_{H,H}$=5.7 Hz, 2H, H-C2'), 7.05 (d, $^3J_{H,H}$=9.2 Hz, 1H, H-C5), 7.25 (ddd, $^3J_{H,H}$=7.5 Hz, $^3J_{H,H}$=4.9 Hz, $^4J_{H,H}$=1.2 Hz, 1H, H-C3"), 7.31 (d, $^3J_{H,H}$=7.7 Hz, H-C5"), 7.74 (dd, $^3J_{H,H}$=7.7 Hz, $^4J_{H,H}$=2.0 Hz, 1H, H-C4"), 7.76 (br, s, 2H, NH_2), 7.92 (dd, $^3J_{H,H}$=8.9 Hz, $^4J_{H,H}$=2.0 Hz, 1H, H-C6), 8.50 (ddd, $^3J_{H,H}$=4.9 Hz, $^4J_{H,H}$=1.7 Hz, $^5J_{H,H}$=0.9 Hz, 1H, H-C2"), 8.65 (d, $^4J_{H,H}$=2.0 Hz, 1H, H-C2), 9.07 (t, $^3J_{H,H}$=5.7 Hz, 1H, CONH) ppm.

^{13}C-NMR: 125 MHz, DMSO-d_6, δ_C = 44.7 (1C, C2'), 118.9 (1C, C5), 120.9 (1C, C3"), 121.0 (1C, C1), 122.0 (1C, C2), 125.5 (1C, C5"), 129.6 (1C, C3), 133.9 (1C, C6), 136.6 (1C, C4"), 147.7 (1C, C4), 148.8 (1C, C2"), 158.8 (1C, C1"), 164.6 (1C, C1') ppm.

HR-MS: ESI(+), *m/z* = 273.0981 ([M+H]$^+$, calcd. for $C_{13}H_{13}N_4O_3$: 273.0982).

EA-CHN: 57.13% C, 4.46% H, 20.44% N
(calcd. for $C_{13}H_{12}N_4O_3$: 57.35% C, 4.44% H, 20.58% N).

M.P.: 205.5 °C.

5.2.18 Synthesis of 4-amino-3-nitro-*N*-(2-phenoxyethyl)benzamide (62)

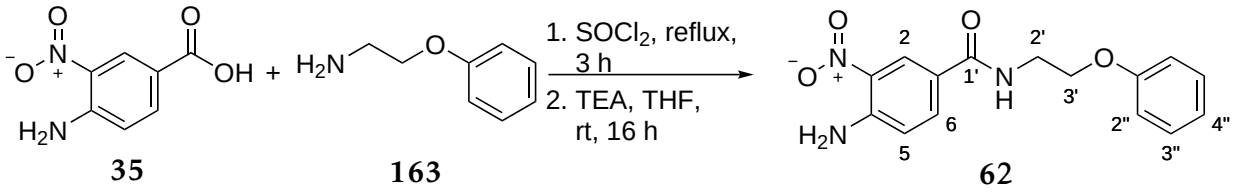

35 **163** **62**

Dry solvents were used and the reaction was carried out under Ar atmosphere.
In a 25 mL N_2-flask, 4-amino-3-nitrobenzoic acid (**35**) (500 mg, 2.75 mmol, 1.00 eq) was suspended in thionyl chloride (5.0 mL) and one drop of DMF was added. The suspension was stirred at reflux for 3 h and then the excess thionyl chloride was removed by distillation. The residue was taken up in THF (5 mL) and was slowly added to a solution of 2-phenoxyethan-1-amine (**163**) (415 mg, 3.03 mmol, 1.10 eq) and triethylamine (0.57 mL, 4.13 mmol, 1.50 eq) in THF (5 mL) at room temperature. After stirring at room temperature for 16 h, complete conversion was detected via TLC. The reaction mixture was washed with water (30 mL) and the aqueous layer extracted with EtOAc (3x 30 mL). The combined organic layers were washed with sat. $NaHCO_3$-solution, sat. NaCl-solution, dried over $MgSO_4$, filtered and the solvent removed under reduced pressure. The crude product was adsorbed onto silica and purified by column chromatography (silica, DCM/MeOH (+NH_3) 100:0 → 90:10). The desired 4-amino-3-nitro-*N*-(pyridin-2-ylmethyl)benzamide (**59**) (205 mg, 0.68 mmol, 25%) was obtained as a yellow solid.

^{1}H-NMR: 500 MHz, DMSO-d_6, δ_H = 3.60 (dt, $^3J_{H,H}$=5.7 Hz, 5.7 Hz, 2H, H-C2'), 4.10 (t, $^3J_{H,H}$=6.0 Hz, 2H, H-C3'), 6.88-7.00 (m, 3H, H-C2" + H-C4"), 7.03 (d, $^3J_{H,H}$=8.9 Hz, 1H, H-C5), 7.24-7.33 (m, 2H, H-C3"), 7.74 (br, s, 2H, NH_2), 7.89 (dd, $^3J_{H,H}$=8.9 Hz, $^4J_{H,H}$=2.0 Hz, 1H, H-C6), 8.59 (d, $^4J_{H,H}$=2.0 Hz, 1H, H-C2), 8.66 (t, $^3J_{H,H}$=5.4 Hz, 1H, CONH) ppm.

^{13}C-NMR: 125 MHz, DMSO-d_6, δ_C = 38.8 (1C, C2'), 65.9 (1C, C3'), 114.4 (2C, C2"), 118.8 (1C, C5), 120.6 (1C, C4"), 121.1 (1C, C1), 125.4 (1C, C2), 129.4 (2C, C3"), 129.5 (1C, C6), 133.8 (1C, C3), 147.7 (1C, C4), 158.4 (1C, C1"), 164.7 (1C, C1') ppm.

HR-MS: ESI(+), *m/z* = 324.0957 ($[M+Na]^+$, calcd. for $C_{15}H_{15}N_3O_4Na$: 324.0955).

EA-CHN: 59.63% C, 5.00% H, 13.70% N (calcd. for $C_{15}H_{15}N_3O_4$: 59.80% C, 5.02% H, 13.95% N).

M.P.: 166.8 °C.

5.2.19 Synthesis of 5-(3-chlorobenzyl)-1,3,4-thiadiazol-2-amine (74)

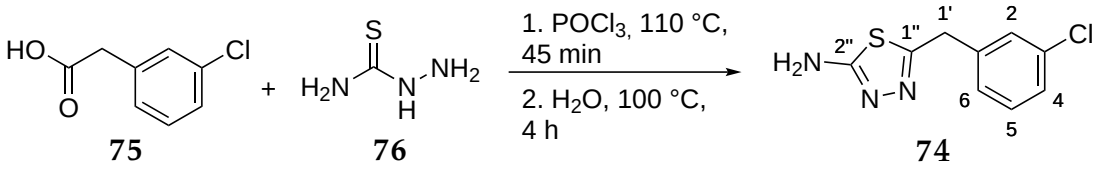

75 **76** **74**

The reaction was carried out under Ar atmosphere.
A 50 mL three-necked-flask was charged with 3-chlorophenylacetic acid (**75**) (682 mg, 4.00 mmol, 1.00 eq) and thiosemicarbazide (**76**) (366 mg, 4.00 mmol, 1.00 eq). After addition of $POCl_3$ (2 mL), the resulting suspension was heated to reflux for 45 min, upon which the solids dissolved completely. After the given time, the solution was cooled to 0 °C and water (6 mL) was added slowly. After stirring for 30 min at 0 °C, the reaction mixture was heated again to reflux for 3 h. Afterwards, the hot suspension was filtered and the filtrate was adjusted with sat. NaOH solution to pH=9-10, whereupon a white solid precipitated. The solid was collected by filtration and washed with water and DEE. Drying *in vacuo* afforded 5-(3-chlorobenzyl)-1,3,4-thiadiazol-2-amine (**74**) (838 mg, 3.71 mmol, 93%) as a white solid.

^{1}H-NMR: 500 MHz, DMSO-d_6, δ_H = 4.17 (s, 2H, H-C1'), 7.05 (br, s, 2H, NH_2), 7.25 (d, $^3J_{H,H}$=7.3 Hz, 1H, H-C6), 7.31-7.28 (m, 3H, H-C2, H-C4, H-C5) ppm.

^{13}C-NMR: 125 MHz, DMSO-d_6, δ_C = 34.7 (1C, C1'), 126.8 (1C, C4), 127.4 (1C, C6), 128.4 (1C, C2), 130.4 (1C, C5), 133.1 (1C, C3), 140.4 (1C, C1), 156.5 (1C, C1"), 168.8 (1C, C2") ppm.

HR-MS: ESI(+), *m/z* = 226.0206 ($[M+H]^+$, calcd. for $C_9H_9ClN_3S$: 226.0200).

M.P.: 192.2 °C.

All recorded spectral data are in accordance to literature.[66]

5.2.20 Synthesis of 4-amino-*N*-(5-(3-chlorobenzyl)-1,3,4-thiadiazol-2-yl)-3-nitrobenzamide (63)

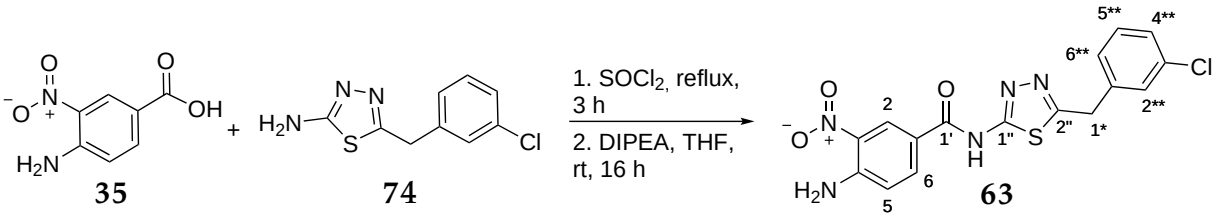

35 74 63

Dry solvents were used and the reaction was carried out under Ar atmosphere.
In a 50 mL Schlenck-tube, 4-amino-3-nitrobenzoic acid (**35**) (392 mg, 2.00 mmol, 1.00 eq) was suspended in thionyl chloride (6 mL) and heated to reflux for 3 h. The excess thionyl chloride was removed by distillation and the residue was dried *in vacuo*. Afterwards, it was dissolved in THF (10 mL) and the solution was cooled to 0 °C. At this temperature, compound **74** (542 mg, 2.40 mmol, 1.20 eq) and DIPEA (0.68 mL, 4.00 mmol, 2.00 eq) were added. Complete conversion could be obtained after stirring for 16 h at room temperature (determined via TLC). The reaction mixture was washed with water (75 mL) and the aqueous layer extracted with EtOAc (3x 50 mL). The combined organic layers were dried over $MgSO_4$, filtered and evaporated to dryness. The residue was adsorbed onto silica and purification was performed via column chromatography (silica, Cyhex/Acetone 95:5 → 0:100). The desired 4-amino-*N*-(5-(3-chlorobenzyl)-1,3,4-thiadiazol-2-yl)-3-nitrobenzamide (**63**) (491 mg, 1.26 mmol, 63%) was obtained as a yellow solid.

^{1}H-NMR: 500 MHz, DMSO-d_6, δ_H = 4.40 (s, 2H, H-C1*), 7.08 (d, $^3J_{H,H}$=9.2 Hz, 1H, H-C5), 7.32-7.45 (m, 4H, H-C2**, H-C4**, H-C5**, H-C6**), 7.95 (br, s, 2H, NH_2), 8.04 (dd, $^3J_{H,H}$=9.0 Hz, $^4J_{H,H}$=2.2 Hz, 1H, H-C6), 8.89 (d, $^4J_{H,H}$=2.0 Hz, 1H, H-C2), 12.90 (br, s, 1H, CONH) ppm.

^{13}C-NMR: 125 MHz, DMSO-d_6, δ_C = 34.3 (1C, C1*), 117.9 (br, 1C, C3), 119.1 (1C, C5), 126.9 (1C, either C4** or C5** or C6**), 127.5 (1C, either C4** or C5** or C6**), 127.6 (1C, C2), 128.7 (1C, C2**), 129.7 (1C, C1), 130.5 (1C, either C4** or C5** or C6**), 133.1 (1C, C3**), 134.3 (1C, C6), 140.1 (1C, C1**), 148.6 (1C, C4), 159.9 (br, 1C, C1"), 162.6 (br, 1C, C2"), 163.2 (br, 1C, C1') ppm.

HR-MS: APCI(+), *m/z* = 390.0432 ([M+H]$^+$, calcd. for $C_{16}H_{13}ClN_5O_3S$: 390.0422).

EA-CHN: 49.28% C, 3.29% H, 17.56% N (calcd. for $C_{16}H_{12}ClN_5O_3S$: 49.30% C, 3.10% H, 17.97% N).

M.P.: 253.7 °C.

5.2.21 Synthesis of 4-amino-3-nitro-*N*-(1*H*-pyrazol-4-yl)benzamide (82)

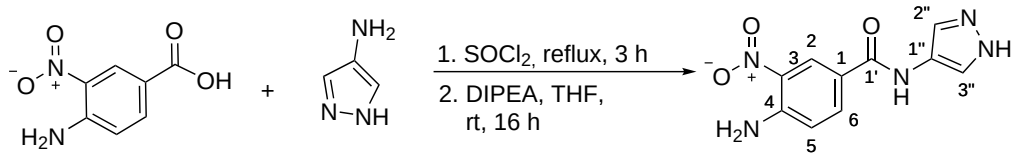

35 **81** **82**

Dry solvents were used and the reaction was carried out under Ar atmosphere.
In a 100 mL three-necked flask, 4-amino-3-nitrobenzoic acid (**35**) (2.95 g, 15.04 mmol, 1.00 eq) was suspended in thionyl chloride (30 mL) and heated to reflux for 3 h. Excess thionyl chloride was removed by distillation and the residue was dried *in vacuo*. Afterwards, it was dissolved in THF (30 mL) and the solution was cooled to 0 °C. At this temperature, 1*H*-pyrazol-4-amine (**81**) (1.50 g, 18.05 mmol, 1.20 eq) and DIPEA (5.1 mL, 30.1 mmol, 2.00 eq) were added. Complete conversion could be obtained after stirring for 16 h at room temperature (determined via TLC). Afterwards, the reaction mixture was evaporated to dryness, adsorbed onto silica and purified via column chromatography (silica, Cyhex/acetone 65:35 → 0:100). The product was washed with Cyhex and DCM and dried *in vacuo*, giving rise to 4-amino-3-nitro-*N*-(1*H*-pyrazol-4-yl)benzamide (**82**) as a yellow solid (728 mg, 2.95 mmol, 20%).

^{1}**H-NMR:**	500 MHz, DMSO-d$_6$, δ_H = 7.08 (d, $^{3}J_{H,H}$=8.9 Hz, 1H, H-C5), 7.80 (br, s, 2H, NH$_2$), 7.82 (s, 2H, H-C2" + H-C3"), 7.96 (dd, $^{3}J_{H,H}$=8.9 Hz, $^{4}J_{H,H}$=2.3 Hz, 1H, H-C6), 8.70 (d, $^{4}J_{H,H}$=2.3 Hz, 1H, H-C2), 10.34 (s, 1H, CONH), 12.54 (br, s, 1H, NH) ppm.
^{13}**C-NMR:**	125 MHz, DMSO-d$_6$, δ_C = 119.0 (1C, C5), 121.0 (1C, C3), 121.3 (1C, C1"), 125.4 (1C, C2), 129.6 (1C, C1), 134.0 (1C, C6), 147.8 (1C, C4), 161.7 (1C, C1') ppm, C2" + C3" are missing.
HR-MS:	ESI(+), *m/z* = 248.0785 ([M+H]$^+$, calcd. for $C_{10}H_{10}N_5O_3$: 248.0778).
M.P.:	> 300 °C.

5.2.22 Synthesis of 4-amino-*N*-(1-(3-fluorophenyl)-1*H*-pyrazol-4-yl)-3-nitro-benzamide (64)

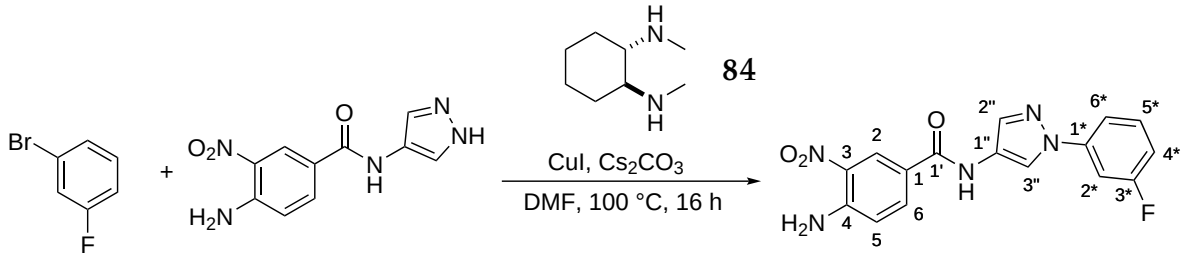

83 **82** **64**

Dry solvents were used and the reaction was carried out under Ar atmosphere.
In a 50 mL N_2-flask, Cs_2CO_3 (1.58 g, 4.86 mmol, 3.00 eq) was dried *in situ*. Compound **82** (400 mg, 1.62 mmol, 1.00 eq) was added and both solids were suspended in DMF (15 mL). 3-Bromo-fluorobenzene (**83**) (567 mg, 3.24 mmol, 2.00 eq), copper iodide (61.0 mg, 0.32 mmol, 0.20 eq) and *trans-N,N'*-dimethyl cyclohexane-1,2-diamine (**84**) (0.10 mL, 0.64 mmol, 0.40 eq) were added. The suspension was heated to 100 °C for 16 h (detection of complete conversion by TLC). Afterwards, EtOAc (30 mL) was added and the mixture was washed with LiCl-solution (5% wt, aq, 50 mL). The aqueous layer was extracted with EtOAc (3x 30 mL), the combined organic layers were dried with $MgSO_4$, filtered and the solvent removed under reduced pressure. The crude material was adsorbed onto silica and purified via column chromatography (silica, Cyhex/EtOAc 70:30 → 40:60) to afford 4-amino-*N*-(1-(3-fluorophenyl)-1*H*-pyrazol-4-yl)-3-nitro-benzamide (**64**) as a yellow solid (227 mg, 0.66 mmol, 41%).

^{1}H-NMR: 500 MHz, DMSO-d_6, δ_H = 7.07-7.15 (m, 2H, H-C5 + H-C2*), 7.50-7.55 (m, 1H, H-C4*), 7.68-7.71 (m, 2H, H-C5* + H-C6*), 7.85 (br, s, NH_2), 7.93 (s, 1H, H-C3"), 7.99 (dd, $^3J_{H,H}$=8.9 Hz, $^4J_{H,H}$=2.0 Hz, 1H, H-C6), 8.71 (s, 1H, H-C2"), 8.75 (d, $^4J_{H,H}$=2.3 Hz, 1H, H-C2), 10.59 (s, 1H, CONH) ppm.

^{13}C-NMR: 125 MHz, DMSO-d_6, δ_C = 105.2 (d, $^2J_{C,F}$=27.6 Hz, 1C, C2*), 112.4 (d, $^2J_{C,F}$=20.4 Hz, 1C, C4*), 113.7 (d, $^4J_{C,F}$=2.4 Hz, 1C, C6*), 117.9 (s, 1C, C3"), 119.1 (s, 1C, C5), 120.4 (s, 1C, C3), 124.3 (s, 1C, C2), 125.6 (s, 1C, C1), 129.6 (s, 1C, C6), 131.3 (d, $^3J_{C,F}$=9.6 Hz, 1C, C5*), 133.97 (s, 1C, C1" or C2"), 134.03 (s, 1C, C1" or C2"), 141.2 (d, $^3J_{C,F}$=10.8 Hz, 1C, C1*), 148.0 (s, 1C, C4), 162.1 (s, 1C, C1'), 162.6 (d, $^1J_{C,F}$=243.5 Hz, 1C, C3*) ppm.

^{19}F-NMR: 377 MHz, DMSO-d_6, δ_F = -111.17 ppm.

HR-MS: APCI(+), *m/z* = 342.1006 ($[M+H]^+$, calcd. for $C_{16}H_{13}FN_5O_3$: 342.0997).

EA-CHN: 53.16% C, 3.99% H, 19.38% N (calcd. for $C_{16}H_{12}FN_5O_3 \cdot H_2O$: 53.48% C, 3.93% H, 19.49% N).

M.P.: 243.1 °C.

5.2.23 Synthesis of 4-nitro-1-(3-(trifluoromethyl)benzyl)-1*H*-pyrazole (79)

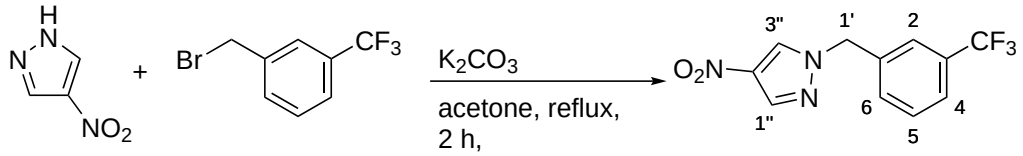

77 **79**

A 100 mL round-bottomed flask was charged with 4-nitro-1*H*-pyrazole (**78**) (1.50 g, 13.3 mmol, 1.00 eq), 3-(trifluoromethyl)benzyl bromide (**77**) (3.17 g, 13.3 mmol, 1.00 eq) and K_2CO_3 (9.16 g, 66.3 mmol, 5.00 eq). Upon addition of acetone (40 mL), the reaction mixture was heated to 60 °C for 2 h. After this time, complete conversion was detected by TLC, so that DCM (20 mL) was added to the reaction mixture. The suspension was washed with water (30 mL) and the aqueous layer extracted with DCM (3x 30 mL). The combined organic layers were dried over $MgSO_4$, filtered and the solvent removed under reduced pressure. The residue was adsorbed onto silica and purified by column chromatography (Cyhex/EtOAc 95:5 → 85:15), yielding 4-nitro-1-(3-(trifluoromethyl)benzyl)-1*H*-pyrazole (**79**) (3.47 g, 12.8 mmol, 96%) as a white solid.

^{1}H-NMR: 500 MHz, DMSO-d_6, δ_H = 5.52 (s, 2H, H-C1'), 7.58-7.75 (m, 4H, H-C2, H-C4 - H-C6), 8.29 (s, 1H, H-C1"), 9.08 (s, 1H, H-C3") ppm.

^{13}C-NMR: 125 MHz, DMSO-d_6, δ_C = 55.0 (1C, C1'), 124.0 (q, $^1J_{C,F}$=272.3 Hz, 1C, CF_3), 124.8 (q, $^3J_{C,F}$=3.6 Hz, 1C, C2 or C4), 124.9 (q, $^3J_{C,F}$=3.6 Hz, 1C, C2 or C4), 129.3 (q, $^2J_{C,F}$=32.4 Hz, 1C, C3), 129.8 (1C, C5 or C6), 130.9 (1C, C5 or C6), 132.2 (1C, C3"), 135.1 (1C, C2"), 136.2 (1C, C1"), 137.0 (1C, C1) ppm.

^{19}F-NMR: 470 MHz, DMSO-d_6, δ_F = -61.07 ppm.

HR-MS: APCI(+), *m/z* = 272.0641 ($[M+H]^+$, calcd. for $C_{11}H_9F_3N_3O_2$: 272.0641).

M.P.: 59.1 °C.

5.2.24 Synthesis of 1-(3-(trifluoromethyl)benzyl)-1*H*-pyrazol-4-amine (80)

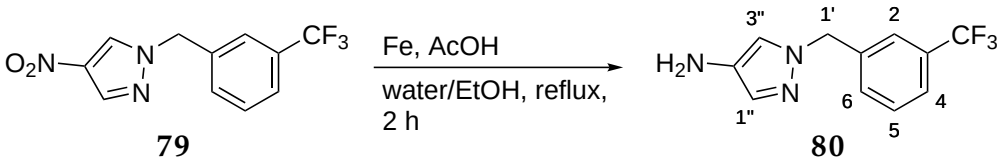

79 **80**

In a 100 mL round-bottomed flask, compound **79** (1.50 g, 5.53 mmol, 1.00 eq) was dissolved in water (20 mL) and EtOH (25 mL). Acetic acid (0.331 g, 5.53 mmol, 1.00 eq) and iron powder (0.927 g, 16.6 mmol, 3.00 eq) were added. The suspension was heated to 95 °C for 2 h, after which complete conversion was detected by TLC. The reaction mixture was filtered over Celite®, the filtrate was adjusted to pH=12 with NaOH-solution (2 M) and EtOAc was added (20 mL). The solution was washed with with water (30 mL) and the aqueous phase extracted with DCM (3x 25 mL). The combined organic layers were dried over $MgSO_4$, filtered and evaporated to dryness. The crude material was adsorbed onto silica and purified by column chromatography (DCM/MeOH (+NH_3) 100:0 → 98:2). Afterwards, the obtained product was dissolved in 1,4-dioxane (5 mL) and HCl (4 M in 1,4-dioxane, 1.5 mL, 2.10 eq) was added, which afforded 1-(3-(trifluoromethyl)benzyl)-1*H*-pyrazol-4-amine · 2 HCl (**80**) (687 mg, 2.85 mmol, 52%) as a beige solid.

^{1}H-NMR: 500 MHz, $CDCl_3$, δ_H = 5.47 (s, 2H, H-C1'), 6.94 (br, s, 1H, NH^+), 7.54-7.68 (m, 5H, H-C1", H-C2, H-C4 - H-C6), 8.17 (s, 1H, H-C3"), 10.35 (br, s, 3H, NH_3^+) ppm.

^{13}C-NMR: 125 MHz, $CDCl_3$, δ_C = 54.4 (1C, C1'), 113.4 (1C, C3"), 124.0 (q, $^1J_{C,F}$=272.2 Hz, 1C, CF_3), 124.2 (q, $^3J_{C,F}$=3.8 Hz, 1C, C2 or C4), 124.5 (q, $^3J_{C,F}$=3.8 Hz, 1C, C2 or C4), 125.8 (1C, C1"), 129.2 (q, $^2J_{C,F}$=31.6 Hz, 1C, C3), 129.7 (1C, C5 or C6), 131.9 (1C, C1), 134.2 (1C, C5 or C6), 138.5 (1C, C2") ppm.

^{19}F-NMR: 470 MHz, $CDCl_3$, δ_F = -61.06 ppm.

HR-MS: ESI(+), *m/z* = 242.0899 ($[M+H]^+$, calcd. for $C_{11}H_{11}F_3N_3$: 242.0900).

M.P.: Decomposition at 156 °C.

5.2.25 Synthesis of 4-amino-3-nitro-*N*-(1-(3-(trifluoromethyl)benzyl)-1*H*-pyrazol-4-yl)benzamide (66)

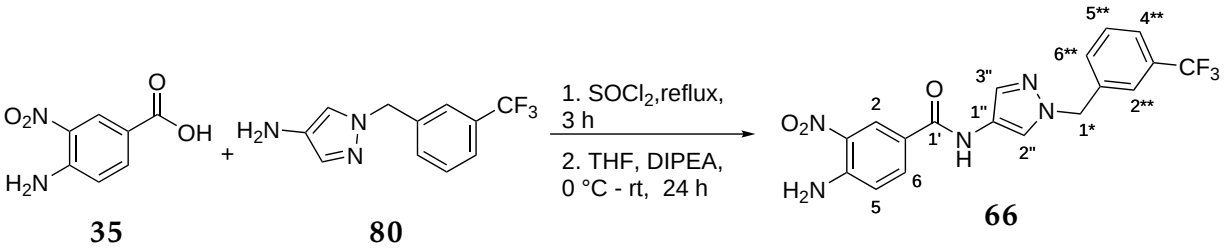

35 **80** **66**

Dry solvents were used and the reaction was carried out under Ar atmosphere.

A 25 mL N_2-flask was charged with 4-amino-3-nitrobenzoic acid (**35**) (0.500 g, 2.55 mmol, 1.00 eq) and thionyl chloride (7.5 mL). The suspension was heated to reflux for 3 h and afterwards the solvent was removed by distillation. The acid chloride was dried *in vacuo* and thereafter dissolved in THF (10 mL). The solution was cooled to 0 °C and compound **80** (0.690 g, 2.86 mmol, 1.12 eq) and DIPEA (0.87 mL, 5.10 mmol, 2.00 eq) were added at this temperature. Complete conversion was observed after stirring for 24 h at room temperature. The reaction mixture was taken up in water (30 mL) and the aqueous layer extracted with EtOAc (3x 25 mL). The combined organic layers were dried over $MgSO_4$, filtered and the solvent removed under reduced pressure. The residue was adsorbed onto silica and purified by column chromatography (silica, DCM/MeOH (+NH_3 in MeOH) 100:0 → 94:6) to afford 4-amino-3-nitro-*N*-(1-(3-(trifluoromethyl)benzyl)-1*H*-pyrazol- 4-yl)benzamide (**66**) (977 mg, 2.41 mmol, 95%) as a yellow solid.

^{1}H-NMR: 500 MHz, DMSO-d_6, δ_H = 5.43 (s, 2H, H-C1*), 7.08 (d, $^3J_{H,H}$=8.9 Hz, 1H, H-C5), 7.52-7.67 (m, 5H, H-C2", H-C2**, H-C4** - H-C6**), 7.81 (br, s, 2H, NH_2), 7.95 (dd, $^3J_{H,H}$=8.9 Hz, $^4J_{H,H}$=2.1 Hz, 1H, H-C6), 8.19 (s, 1H, H-C3"), 8.69 (d, $^4J_{H,H}$=2.1 Hz, 1H, H-C2), 10.40 (s, 1H, CONH) ppm.

^{13}C-NMR: 125 MHz, DMSO-d_6, δ_C = 54.1 (1C, C1*), 119.0 (1C, C5), 120.8 (1C, C1), 121.2 (1C, C3"), 122.2 (1C, C1"), 124.0 (q, $^3J_{C,F}$=3.8 Hz, 1C, C2** or C4**), 124.1 (q, $^1J_{C,F}$=272.3 Hz, 1C, CF_3), 124.3 (q, $^3J_{C,F}$=3.8 Hz, 1C, C2** or C4**), 125.5 (1C, C2), 129.2 (q, $^2J_{C,F}$=31.6 Hz, 1C, C3**), 129.6 (1C, C2"), 129.7 (1C, C5**), 131.1 (1C, C1**), 131.7 (1C, C6**), 134.0 (1C, C6), 139.1 (1C, C3), 147.8 (1C, C4), 161.7 (1C, C1') ppm.

^{19}F-NMR: 470 MHz, DMSO-d_6, δ_F = -60.60 ppm.

HR-MS: ESI(+), *m/z* = 406.1124 ($[M+H]^+$, calcd. for $C_{18}H_{15}F_3N_5O_3$: 406.1122).

EA-CHN: 53.23% C, 3.56% H, 17.09% N (calcd. for $C_{18}H_{14}F_3N_5O_3$: 53.34% C, 3.48% H, 17.28% N).

M.P.: 191.8 °C.

5.2.26 Synthesis of *N*-benzyl-5-nitropyridin-2-amine (86)

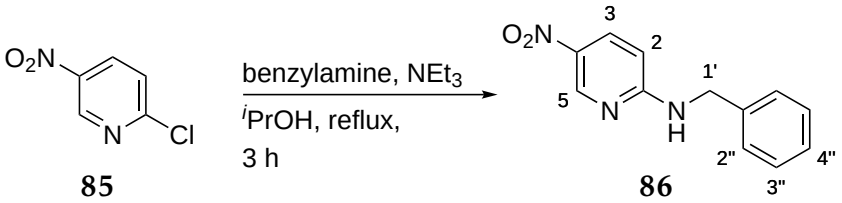

85 **86**

In a 100 mL round-bottomed flask, 2-chloro-5-nitropyridine (**85**) (1.50 g, 9.46 mmol, 1.00 eq) was dissolved in ^{i}PrOH (26 mL). Benzylamine (1.22 g, 11.4 mol, 1.20 eq) and NEt_3 (1.44 g, 14.2 mmol, 1.50 eq) were added and the solution was heated to reflux for 3 h. Complete conversion was detected by TLC, so that the reaction mixture was diluted with water (50 mL) and EtOAc (50 mL) and the aqueous layer was extracted with EtOAc (3x 25 mL). The combined organic layers were dried over $MgSO_4$, filtered and evaporated to dryness. The crude product was adsorbed onto silica and purified by column chromatography (silica, Cyhex/EtOAc 95:5 → 75:25). The desired *N*-benzyl-5-nitropyridin-2-amine (**86**) (2.04 g, 9.81 mmol, 94%) was obtained as a yellow solid.

^{1}H-NMR: 500 MHz, DMSO-d_6, δ_H = 4.63 (s, 2H, H-C1'), 6.63 (d, $^{3}J_{H,H}$=7.3 Hz, 1H, H-C2), 7.23-7.40 (m, 5H, H-C2" - H-C4"), 8.13 (dd, $^{3}J_{H,H}$=9.4 Hz, $^{4}J_{H,H}$=2.7 Hz, 1H, H-C3), 8.57 (br, s, 1H, NH), 8.92 (d, $^{4}J_{H,H}$=3.0 Hz, 1H, H-C5) ppm.

^{13}C-NMR: 125 MHz, DMSO-d_6, δ_C = 44.2 (1C, C1'), 108.5 (1C, C2), 127.0 (2C, C2"), 127.3 (1C, C4"), 128.4 (2C, C3"), 131.8 (1C, C4), 134.6 (1C, C3), 138.8 (1C, C1"), 146.7 (1C, C5), 161.2 (1C, C1) ppm.

HR-MS: APCI(+), *m/z* = 230.0923 ($[M+H]^+$, calcd. for $C_{12}H_{12}N_3O_2$: 230.0924).

M.P.: 131.3 °C.

All recorded spectral data are in accordance to literature.[89]

5.2.27 Synthesis of N^2-benzylpyridine-2,5-diamine (87)

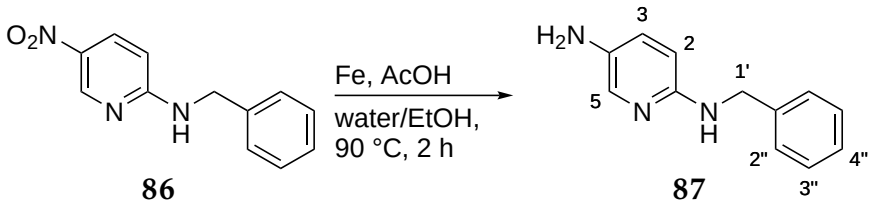

86 **87**

In a 25 mL round-bottomed flask, compound **86** (200 mg, 0.867 mmol, 1.00 eq) was dissolved in water (2.5 mL) and EtOH (3 mL). Acetic Acid (60.1 mg, 0.867 mmol, 1.00 eq) and iron powder (146 mg, 2.61 mmol, 3.00 eq) were added and the suspension was heated to 90 °C for 2 h. After this time, complete conversion could be detected by TLC. The excess iron powder was removed by filtration over Celite® and the filtrate was adjusted to pH=12 by NaOH-solution (1 M). Water (30 mL) was added and extraction was performed with DCM (3x 30 mL). The combined organic layers were dried over $MgSO_4$, filtered and the solvent removed under reduced pressure. Adsorption onto silica followed by column chromatography (silica, DCM/MeOH (+NH_3) 100:0 → 94:6) gave N^2-benzylpyridine-2,5-diamine (**87**) (124 mg, 0.624 mmol, 72%) as a beige solid.

^{1}H-NMR: 500 MHz, $CDCl_3$, δ_H = 4.26 (br, s, 2H, NH_2), 4.25 (d, $^3J_{H,H}$=6.0 Hz, 2H, H-C1'), 6.08 (t, $^3J_{H,H}$=6.0 Hz, 1H, NH), 6.33 (dd, $^3J_{H,H}$=8.7 Hz, $^5J_{H,H}$=0.7 Hz, 1H, H-C2), 6.82 (dd, $^3J_{H,H}$=8.6 Hz, $^4J_{H,H}$=2.9 Hz, 1H, H-C3), 7.19 (sm, 1H, H-C4"), 7.26-7.32 (m, 4H, H-C2", H-C3"), 7.46 (dd, $^4J_{H,H}$=2.9 Hz, $^5J_{H,H}$=0.6 Hz, 1H, H-C5) ppm.

^{13}C-NMR: 125 MHz, $CDCl_3$, δ_C = 45.1 (1C, C1'), 108.3 (1C, C2), 125.3 (1C, C3), 126.2 (1C, C4"), 127.2 (2C, C2"), 128.0 (2C, C3"), 133.1 (1C, C5), 135.4 (1C, C4), 145.4 (1C, C1"), 151.6 (1C, C1) ppm.

HR-MS: ESI(+), *m/z* = 200.1180 ($[M+H]^+$, calcd. for $C_{12}H_{14}N_3$: 200.1182).

M.P.: 83.3 °C.

All recorded spectral data are in accordance to literature.[89]

5.2.28 Synthesis of 4-amino-*N*-(6-(benzylamino)pyridin-3-yl)-3-nitro-benzamide (67)

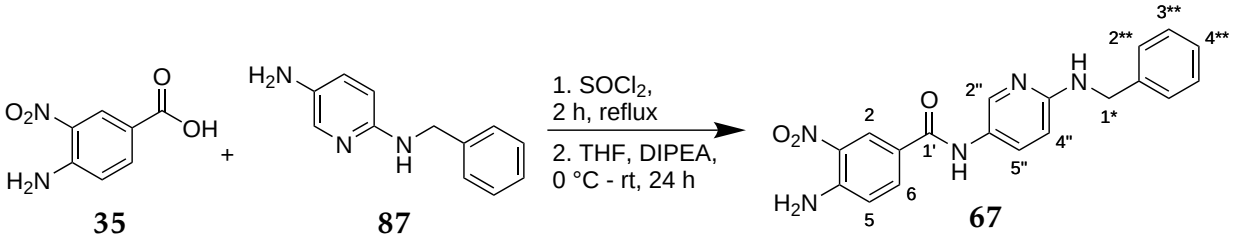

35 **87** **67**

Dry solvents were used and the reaction was carried out under Ar atmosphere.
A 50 mL N_2-flask was charged with 4-amino-3-nitrobenzoic acid (**35**) (500 mg, 2.55 mmol, 1.00 eq) and thionyl chloride (7.5 mL). The suspension was heated to reflux for 2 h and the excess thionyl chloride was removed under reduced pressure thereafter. The residue was dried *in vacuo* and afterwards dissolved in THF (13 mL). The solution was cooled to 0 °C and compound **164** (610 mg, 3.06 mmol, 1.20 eq) and DIPEA (0.87 mL, 5.10 mmol, 2.00 eq) were added at this temperature. The resulting solution was stirred at room temperature for 24 h. Complete conversion was then detected via TLC. The reaction mixture was washed with water (30 mL) and the aqueous layer extracted with EtOAc (3x 30 mL). The combined organic layers were dried over $MgSO_4$, filtered and evaporated to dryness. The residue was adsorbed onto silica and purified by column chromatography (silica, DCM/MeOH (+NH_3) 100:0 → 94:6) to afford 4-amino-*N*-(6-(benzylamino)pyridin-3-yl)-3-nitro-benzamide (**67**) (978 mg, 2.69 mmol, 99%) as a yellow solid.

^{1}H-NMR: 500 MHz, $DMSO_6$, δ_H = 4.47 (d, $^3J_{H,H}$=6.3 Hz, 2H, H-C1*), 6.62 (d, $^3J_{H,H}$=9.2 Hz, 1H, H-C4"), 6.92 (t, $^3J_{H,H}$=6.2 Hz, 1H, NH), 7.07 (d, $^3J_{H,H}$=8.9 Hz, 1H, H-C5). 7.20-7.22 (m, 1H, H-C4**), 7.29-7.34 (m, 4H, H-C2**, H-C3**), 7.67 (dd, $^3J_{H,H}$=8.0 Hz, $^4J_{H,H}$=2.6 Hz, 1H, H-C5"), 7.80 (br, s, 2H, NH_2), 7.95 (dd, $^3J_{H,H}$=9.0 Hz, $^4J_{H,H}$=2.2 Hz, 1H, H-C6), 8.22 (d, $^4J_{H,H}$=2.6 Hz, 1H, H-C2"), 8.68 (d, $^4J_{H,H}$=2.3 Hz, 1H, H-C2), 9.94 (s, 1H, CONH) ppm.

^{13}C-NMR: 125 MHz, $DMSO_6$, δ_C = 44.4 (1C, C1*), 107.4 (1C, C4"), 118.9 (1C, C5), 121.3 (1C, C1), 125.2 (1C, C3), 125.7 (1C, C2), 126.4 (1C, C4**), 127.1 (2C, C2** or C3**), 128.1 (2C, C2** or C3**), 129.6 (1C, C1**), 131.5 (1C, C5"), 134.1 (1C, C6), 140.69 (1C, C4 or C2"), 140.71 (1C, C4 or C2"), 147.8 (1C, C3"), 155.6 (1C, C1"), 163.2 (1C, C1') ppm.

HR-MS: ESI(+), *m/z* = 364.1403 ($[M+H]^+$, calcd. for $C_{19}H_{18}N_5O_3$: 364.1404).

EA-CHN: 62.08% C, 4.94% H, 18.90% N (calcd. for $C_{19}H_{17}N_5O_3 \cdot 0.25\ H_2O$: 62.03% C, 4.79% H, 19.04% N).

M.P.: 219.5 °C.

5.2.29 Synthesis of 2-(2-((3,4-dihydroisoquinolin-2(1*H*)-yl)sulfonyl)ethyl) isoindoline-1,3-dione (90)

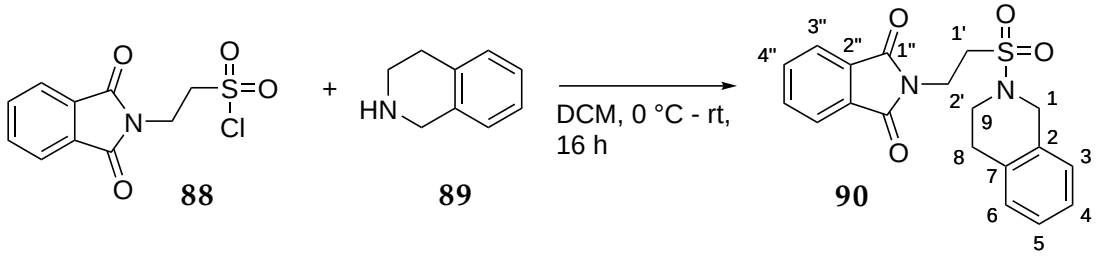

88 89 90

Dry solvents were used and the reaction was carried out under Ar atmosphere.
In a 50 mL N_2-flask, 2-(1,3-dioxoisoindolin-2-yl)ethane-1-sulfonyl chloride (**88**) (1.00 g, 3.66 mmol, 1.00 eq) was dissolved in DCM (15.0 mL). At 0 °C, 1,2,3,4-tetrahydroisoquinoline (**89**) (1.60 mL, 12.8 mmol, 3.50 eq) was added dropwise. The obtained solution was stirred at 0 °C for 30 min and afterwards stirred at RT overnight (detection of complete conversion via TLC). The reaction mixture was washed with HCl-solution (0.5 M, 30 mL) and the aqueous layer extracted with DCM (3x 25 mL). The combined organic layers were washed with sat. NaCl-solution, dried over $MgSO_4$, filtered and evaporated to dryness. The obtained residue was triturated with DEE and afterwards recrystallized from ^{i}PrOH affording 2-(2-((3,4-dihydroisoquinolin-2(1*H*)-yl)sulfonyl)ethyl)isoindoline-1,3-dione (**90**) as a white solid (525 mg, 1.68 mmol, 46%).

^{1}H-NMR: 500 MHz, DMSO-d_6, δ_H = 2.87 (sm, 2H, H-C8), 3.48-3.51 (m, 4H, H-C9 + H-C1'), 3.97 (t, $^{3}J_{H,H}$=6.9 Hz, 2H, H-C2'), 4.41 (s, 2H, H-C1), 7.13-7.18 (m, 4H, H-C3 - H-C6), 7.82-7.87 (m, 4H, H-C3" + H-C4") ppm.

^{13}C-NMR: 125 MHz, DMSO-d_6, δ_C = 28.2 (1C, C8), 32.0 (1C, C2'), 42.7 (1C, C1 or C9), 45.9 (1C, C1 or C9), 46.4 (1C, C1'), 123.0 (2C, C3"), 126.1 (1C, C3 or C4 or C5), 126.2 (1C, C3 or C4 or C5), 126.5 (1C, C3 or C4 or C5), 128.8 (1C, C6), 131.5 (2C, C2"), 132.1 (1C, C2 or C7), 133.2 (1C, C2 or C7), 134.4 (2C, C4"), 167.3 (2C, C1") ppm.

HR-MS: APCI(+), *m/z* = 371.1069 ($[M+H]^+$, calcd. for $C_{19}H_{19}N_2O_4S$: 371.1060).

M.P.: 120.2 °C.

5.2.30 Synthesis of 2-((3,4-dihydroisoquinolin-2(1*H*)-yl)sulfonyl)ethan-1-amine (91)

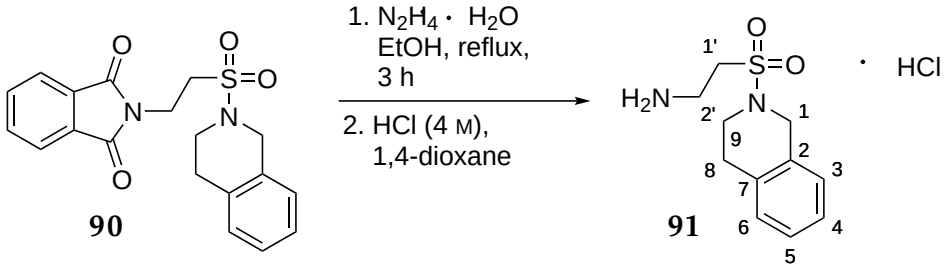

In a 50 mL two-necked flask, compound **90** (450 mg, 1.21 mmol, 1.00 eq) was dissolved in EtOH (10 mL). Hydrazine hydrate (50-60% wt, 0.17 mL, 2.66 mmol, 2.20 eq) was added dropwise and the solution was stirred at reflux for 3 h (detection of complete conversion by TLC). Afterwards, the reaction mixture was adsorbed onto Celite® and purified by column chromatography (silica, EtOAc/MeOH (+NH_3) 100:0 → 88:12). The obtained product was dissolved in 1,4-dioxane (10 mL) and HCl-solution (4 N in 1,4-dioxane, 0.30 mL, 1.21 mmol, 1.00 eq) was added dropwise. The obtained solid was collected by filtration, washed with DEE and dried *in vacuo*, giving rise to 2-((3,4-dihydroisoquinolin-2(1*H*)-yl)sulfonyl)ethan-1-amine (**91**) · HCl as a white solid. It still contained an inseparable side product, so that the yield was not determined (ca. 65% purity, determined via LC-MS).

^{1}H-NMR: 500 MHz, DMSO-d_6, δ_H = 2.88-2.93 (m, 4H, H-C8 + H-C9), 3.16-3.20 (m, 2H, H-C2'), 3.47-3.50 (m, 2H, H-C1'), 4.41 (s, 2H, H-C1), 7.18 (br, s, 3H, NH_3^+), 7.87-7.90 (m, 2H, H-C5 + H-C6), 8.06-8.09 (m, 2H, H-C3 + H-C4) ppm.

^{13}C-NMR: 125 MHz, DMSO-d_6, δ_C = 28.3 (1C, C8), 36.2 (1C, C2'), 42.7 (1C, C9), 46.5 (1C, C1), 51.9 (1C, C1'), 125.1 (1C, C4), 126.1 (1C, C3 or C5), 126.3 (1C, C3 or C5), 127.2 (1C, C6), 128.1 (1C, C2 or C7), 132.4 (1C, C2 or C7), ppm.

HR-MS: ESI(+), *m/z* = 241.1012 ([M+H]$^+$, calcd. for $C_{11}H_{17}N_2O_2S$: 241.1005).

5.2.31 Synthesis of 4-amino-*N*-(2-((3,4-dihydroisoquinolin-2(1*H*)-yl)sulfonyl)ethyl)-3-nitrobenzamide (69)

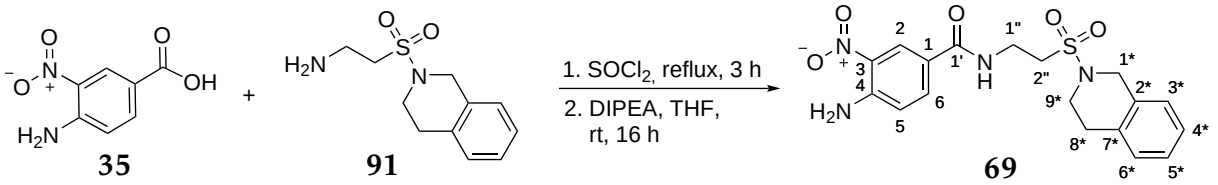

35 91 69

Dry solvents were used and the reaction was carried out under Ar atmosphere.
In a 50 mL three-necked flask, 4-amino-3-nitrobenzoic acid (**35**) (102 mg, 0.52 mmol, 1.00 eq) was suspended in thionyl chloride (5 mL) and heated to reflux for 3 h. Excess thionyl chloride was removed by distillation and the residue was dried *in vacuo*. Afterwards, it was dissolved in THF (5 mL) and the solution was cooled to 0 °C. At this temperature, compound **91** (150 mg, 0.62 mmol, 1.20 eq) and DIPEA (0.20 mL, 1.04 mmol, 2.00 eq) were added. Complete conversion was achieved by stirring for 16 h at room temperature (determined via TLC). The reaction mixture was washed with water (30 mL) and the aqueous layer extracted with EtOAc (3x 25 mL). The combined organic layers were washed with sat. NaCl-solution, dried over $MgSO_4$, filtered and evaporated to dryness. The residue was adsorbed onto silica and purification was performed via column chromatography (silica, DCM/MeOH (+NH_3) 100:0 → 93:7). The obtained residue was triturated with Cyhex and afterwards further purified by prep-HPLC (Water/MeCN 80:20 → 5:95), yielding the desired 4-amino-*N*-(2-((3,4-dihydroisoquinolin-2(1*H*)-yl)sulfonyl)ethyl)-3-nitrobenzamide (**69**) (40 mg, 0.1 mmol, 19%) as a yellow solid.

^{1}H-NMR: 500 MHz, DMSO-d_6, δ_H = 2.88 (sm, 2H, H-C8*), 3.36 (t, $^3J_{H,H}$=7.3 Hz, 2H, H-C2”), 3.49 (t, $^3J_{H,H}$=6.0 Hz, 2H, H-C9*), 3.62 (dt, $^3J_{H,H}$=7.1 Hz, 5.3 Hz, 2H, H-C1”), 4.42 (s, 2H, H-C1*), 7.01 (d, $^3J_{H,H}$=8.9 Hz, 1H, H-C5), 7.16 (br, s, 4H, H-C3* - H-C6*), 7.76 (br, s, 2H, NH_2), 7.81 (dd, $^3J_{H,H}$=8.9 Hz, $^4J_{H,H}$=2.1 Hz, 1H, H-C6), 8.52 (d, $^4J_{H,H}$=1.8 Hz, 1H, H-C2), 8.64 (t, $^3J_{H,H}$=5.3 Hz, 1H, CONH) ppm.

^{13}C-NMR: 125 MHz, DMSO-d_6, δ_C = 28.4 (1C, C8*), 34.0 (1C, C1”), 42.8 (1C, C1* or C9*), 46.4 (1C, C1* or C9*), 47.8 (1C, C2”), 118.9 (1C, C3), 120.8 (1C, C5), 125.3 (1C, C2), 126.1 (1C, C3* or C4 or C5* or C6*), 126.3 (1C, C3* or C4 or C5* or C6*), 126.5 (1C, C3* or C4 or C5* or C6*), 128.8 (1C, C3* or C4 or C5* or C6*), 129.5 (1C, C1), 132.2 (1C, C2* or C7*), 133.3 (1C, C2* or C7*), 133.7 (1C, C6), 147.7 (1C, C4), 164.5 (1C, C1’) ppm.

HR-MS: ESI(+), m/z = 427.1057 ($[M+Na]^+$, calcd. for $C_{18}H_{20}N_4O_5SNa$: 427.1047).

q-^{1}H-NMR: 500 MHz, DMSO-d_6, maleic acid as internal standard: 95.0% ± 1.5% purity.

M.P.: 184.5 °C.

5.2.32 Synthesis of 4-amino-3-nitro-*N*-(1-oxo-1,2-dihydroisoquinolin-3-yl)-benzamide (70)

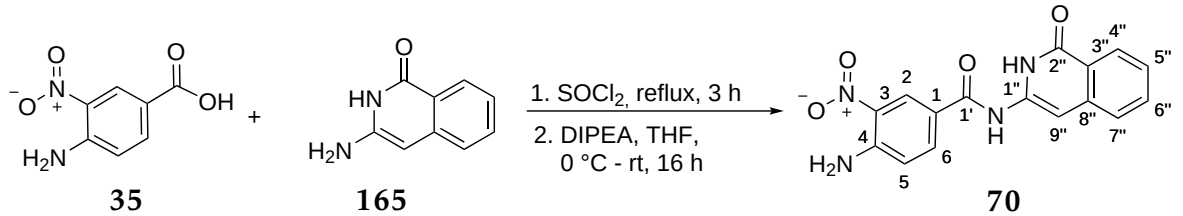

35 **165** **70**

Dry solvents were used and the reaction was carried out under Ar atmosphere.
In a 25 mL N_2-flask, 4-amino-3-nitrobenzoic acid (**35**) (255 mg, 1.30 mmol, 1.00 eq) was suspended in thionyl chloride (5 mL) and heated to reflux for 3 h. Excess thionyl chloride was removed by distillation and the residue was dried *in vacuo*. Afterwards, it was dissolved in THF (7.5 mL) and the solution was cooled to 0 °C. At this temperature, 3-aminoisoquinolin-1(2*H*)-one (250 mg, 1.56 mmol, 1.20 eq) and DIPEA (0.70 mL, 3.90 mmol, 3.00 eq) were added. Complete conversion was achieved by stirring for 16 h at room temperature (determined via TLC). The reaction mixture was washed with HCl-solution (0.5 M, aq, 30 mL) and the aqueous layer extracted with EtOAc (3x 25 mL). The combined organic layers were washed with sat. NaCl-solution, dried over $MgSO_4$, filtered and evaporated to dryness. The residue was adsorbed onto Celite® and purification was performed via column chromatography (silica, DCM/MeCN ($+NH_3$) 70:30 → 50:50), which afforded 4-amino-3-nitro-*N*-(1-oxo-1,2-dihydroisoquinolin-3-yl)-benzamide (**70**) (82 mg, 0.25 mmol, 30%) as an orange solid.

^{1}H-NMR: 500 MHz, DMSO-d_6, δ_H = 6.87 (s, 1H, H-C9”), 7.13 (d, $^3J_{H,H}$=8.9 Hz, 1H, H-C5), 7.37 (sm, 1H, H-C5” or H-C6”), 7.59-7.67 (m, 2H, H-C5” or H-C6” + H-C7”), 7.95-7.97 (m, 3H, H-C6 + NH_2), 8.11 (dd, $^3J_{H,H}$=7.5 Hz, $^4J_{H,H}$=0.7 Hz, 1H, H-C4”), 8.75 (d, $^4J_{H,H}$=2.3 Hz, 1H, H-C2), 10.36 (br, s, 1H, (C1’)ONH), 11.28 (br, s, 1H, (C2”)ONH) ppm.

^{13}C-NMR: 125 MHz, DMSO-d_6, δ_C = 92.4 (1C, C9”), 119.3 (1C, C5), 119.5 (1C, C3), 122.9 (1C, C2), 124.8 (1C, C3”), 126.0 (1C, C4” or C5” or C7”), 126.2 (1C, C4” or C5” or C7”), 126.6 (1C, C4” or C5” or C7”), 129.5 (1C, C1”), 132.7 (1C, C6”), 134.0 (1C, C1), 136.7 (1C, C8”), 138.7 (1C, C6), 148.4 (1C, C4), 161.1 (1C, C2”), 164.0 (1C, C1’) ppm.

HR-MS: APCI(+), *m/z* = 325.0940 ($[M+H]^+$, calcd. for $C_{16}H_{13}N_4O_4$: 325.0931).

q-^{1}H-NMR: 500 MHz, DMSO-d_6, dimethylsulfone as internal standard: 97.8% ± 0.7% purity.

M.P.: 223.4 °C.

5.2.33 Synthesis of 2-(2-(benzo[d]oxazol-2-yl)ethyl)isoindoline-1,3-dione (94)

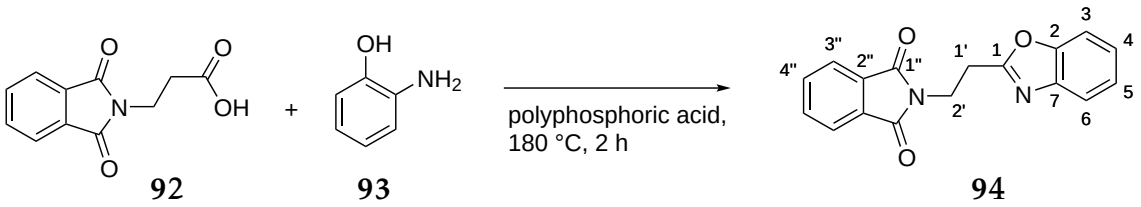

92 **93** **94**

In a 50 mL two-necked flask, 3-(1,3-dioxoisoindolin-2-yl)propanoic acid (**92**) (3.01 g, 13.7 mmol, 2.00 eq) and 2-aminophenol (**93**) (750 mg, 6.87 mmol, 1.00 eq) were dissolved in polyphosphoric acid (15.0 g) and heated to 180 °C for 2 h (complete conversion detected via TLC). The solution was left to stand at RT for 16 h, whereby a beige solid precipitated. The solid was collected by filtration, dissolved in DCM (25 mL) and the organic phase was washed with NaOH-solution (1 M, 25 mL). The aqueous layer was extracted with DCM (3x 20 mL) and the combined organic layers were dried over $MgSO_4$, filtered and the solvent removed under reduced pressure. The obtained solid was dried *in vacuo* to afford 2-(2-(benzo[d]oxazol-2-yl)ethyl)isoindoline-1,3-dione (**94**) as a beige solid (1.75 g, 5.98 mmol, 87%).

^{1}**H-NMR:**	500 MHz, DMSO-d_6, δ_H = 3.30 (sm, 2H, H-C1', overlayed by water), 4.06 (t, $^3J_{H,H}$=7.1 Hz, 2H, H-C2'), 7.33 (sm, 2H, H-C3 + H-C6), 7.61-7.65 (m, 2H, H-C4 + H-C5), 7.82-7.88 (m, 4H, H-C3" + H-C4") ppm.
^{13}**C-NMR:**	125 MHz, DMSO-d_6, δ_C = 27.0 (1C, C1'), 34.9 (1C, C2'), 110.5 (1C, C3), 119.3 (1C, C6), 123.1 (2C, C4"), 124.2 (1C, C4 or C5), 124.8 (1C, C4 or C5), 131.5 (2C, C2"), 134.4 (2C, C3"), 140.8 (1C, C7), 150.3 (1C, C2), 163.8 (1C, C1), 167.5 (2C, C1") ppm.
HR-MS:	APCI(+), *m/z* = 293.0924 ($[M+H]^+$, calcd. for $C_{17}H_{13}N_2O_3$: 293.0921).
M.P.:	174.0 °C.

All recorded spectral data are in accordance to literature.[69]

5.2.34 Synthesis of (benzo[d]oxazol-2-yl)ethan-1-amine (95)

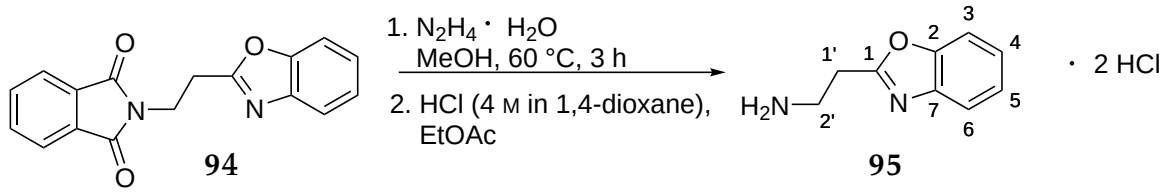

94 **95**

The reaction was carried out under Ar atmosphere.
In a 50 mL N_2-flask, compound **94** (200 mg, 0.68 mmol, 1.00 eq) was dissolved in MeOH (5.0 mL). Hydrazine hydrate (50-60% wt, 0.15 mL, 2.05 mmol, 3.00 eq) was added and the solution was stirred at 60 °C for 2 h. After the given time, complete conversion was detected via LC-MS, so that the solution was evaporated to dryness. The residue was taken up in EtOAc (25 mL) and washed with NaOH-solution (1 M, 35 mL). The aqueous layer was extracted with EtOAc (3x 25 mL) and the combined organic layers washed with sat. NaCl-solution, dried over $MgSO_4$, filtered and the solvent removed under reduced pressure. The residue was dissolved in EtOAc (10 mL) and HCl-solution (4 N in 1,4-dioxane, 0.70 mL, 4.00 eq) was added. The formed solid was collected by filtration, washed with EtOAc and dried *in vacuo* to afford (benzo[d]oxazol-2-yl)ethan-1-amine (**95**) · 2 HCl as a rose solid (132 mg, 0.66 mmol, 97%).

^{1}**H-NMR:**	500 MHz, DMSO-d_6, δ_H = 2.80 (t, $^3J_{H,H}$=6.9 Hz, 2H, H-C1'), 3.06 (dt, $^3J_{H,H}$=6.9 Hz, 6.9 Hz, 2H, H-C2'), 6.76 (sm, 1H, H-C3 or H-C6), 6.89-6.96 (m, 2H, H-C4 + H-C5), 7.74 (d, $^3J_{H,H}$=8.9 Hz, H-C3 or H-C6), 7.96 (br, s, 3H, NH_3^+), 9.51 & 9.76 (br, s, 1H, NH^+) ppm.
^{13}**C-NMR:**	125 MHz, DMSO-d_6, δ_C = 32.9 (1C, C1'), 35.1 (1C, C2'), 115.7 (1C, C3), 118.8 (1C, C6), 122.7 (1C, C4 or C5), 124.8 (1C, C4 or C5), 125.8 (1C, C7), 148.1 (1C, C2), 168.7 (1C, C1) ppm.
HR-MS:	ESI(+), *m/z* = 163.0870 ($[M+H]^+$, calcd. for $C_9H_{11}N_2O$: 163.0866).
M.P.:	113.0 °C.

5.2.35 Synthesis of 4-amino-*N*-(2-(benzo[d]oxazol-2-yl)ethyl)-3-nitrobenzamide (71)

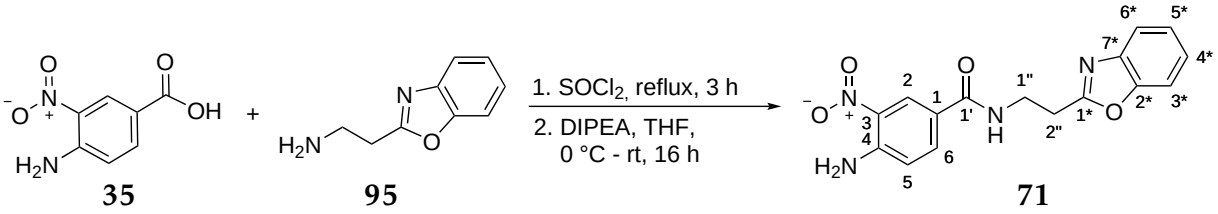

35 **95** **71**

Dry solvents were used and the reaction was carried out under Ar atmosphere.
In a 25 mL N_2-flask, 4-amino-3-nitrobenzoic acid (**35**) (242 mg, 2.00 mmol, 1.00 eq) was suspended in thionyl chloride (5 mL) and heated to reflux for 3 h. Excess thionyl chloride was removed by distillation and the residue was dried *in vacuo*. Afterwards, it was dissolved in THF (6 mL) and the solution was cooled to 0 °C. At this temperature, compound **95** (200 mg, 2.40 mmol, 1.20 eq) and DIPEA (0.42 mL, 4.00 mmol, 2.00 eq) were added. Complete conversion was achieved by stirring for 16 h at room temperature (determined via TLC). The reaction mixture was washed with water (50 mL) and the aqueous layer extracted with EtOAc (3x 30 mL). The combined organic layers were washed with sat. NaCl-solution, dried over $MgSO_4$, filtered and evaporated to dryness. The residue was adsorbed onto silica and purification was performed via column chromatography (silica, DCM/MeOH (+NH_3) 100:0 → 95:5). The desired 4-amino-*N*-(2-(benzo[d]oxazol-2-yl)ethyl)-3-nitrobenzamide (**71**) (213 mg, 0.65 mmol, 33%) was obtained as a yellow solid.

^{1}H-NMR: 500 MHz, DMSO-d_6, δ_H = 3.21 (t, $^3J_{H,H}$=6.9 Hz, 2H, H-C2”), 3.71 (dt, $^3J_{H,H}$=6.9 Hz, 5.7 Hz, 2H, H-C1”), 7.02 (d, $^3J_{H,H}$=8.9 Hz , 1H, H-C5), 7.35 (sm, 2H, H-C3* + H-C6*), 7.64-7.69 (m, 2H, H-C4* + H-C5*), 7.74 (s, 2H, NH_2), 7.82 (dd, $^3J_{H,H}$=8.9 Hz, $^4J_{H,H}$=2.1 Hz, 1H, H-C6), 8.53 (d, $^4J_{H,H}$=2.1 Hz, 1H, H-C2), 8.67 (t, $^3J_{H,H}$=5.5 Hz, 1H, CONH) ppm.

^{13}C-NMR: 125 MHz, DMSO-d_6, δ_C = 28.3 (1C, C2”), 36.9 (1C, C1”), 110.5 (1C, C4* or C5*), 118.8 (1C, C5), 119.2 (1C, C4* or C5*), 121.1 (1C, C3), 124.1 (1C, C3* or C6*), 124.6 (1C, C3* or C6*), 125.3 (1C, C2), 129.5 (1C, C1), 133.8 (1C, C6), 140.9 (1C, C7*), 147.7 (1C, C4), 150.3 (1C, C2*), 164.6 (1C, C1’), 164.9 (1C, C1*) ppm.

HR-MS: ESI(+), *m/z* = 327.1097 ([M+H]$^+$, calcd. for $C_{16}H_{15}N_4O_4$: 327.1098).

EA-CHN: 57.34% C, 4.27% H, 16.47% N (calcd. for $C_{16}H_{14}N_4O_4 \cdot 0.5\ H_2O$: 57.31% C, 4.51% H, 16.71% N).

M.P.: 135.2 °C.

5.2.36 Synthesis of 4-amino-*N*-(2-(2,2-dioxidobenzo[c][1,2,5]thiadiazol-1(3*H*)-yl)ethyl)-3-nitrobenzamide (72)

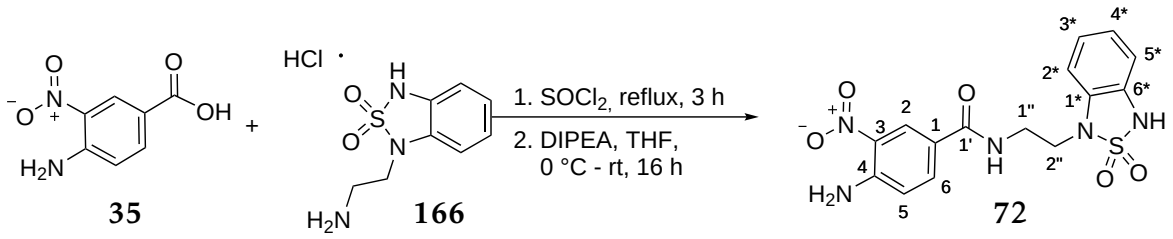

Dry solvents were used and the reaction was carried out under Ar atmosphere.
In a 10 mL Schlenck-tube, 4-amino-3-nitrobenzoic acid (**35**) (164 mg, 0.83 mmol, 1.00 eq) was suspended in thionyl chloride (4 mL) and heated to reflux for 3 h. Excess thionyl chloride was removed by distillation and the residue was dried *in vacuo*. Afterwards, it was dissolved in THF (5 mL) and the solution was cooled to 0 °C. At this temperature, 1-(2-aminoethyl)-1,3-dihydrobenzo[c][1,2,5]thiadiazole 2,2-dioxide · HCl (250 mg, 1.00 mmol, 1.20 eq) and DIPEA (0.50 mL, 3.00 mmol, 3.00 eq) were added. Complete conversion was achieved by stirring for 16 h at room temperature (determined via TLC). The reaction mixture was washed with HCl-solution (0.5 M, aq, 30 mL) and the aqueous layer extracted with EtOAc (3x 25 mL). The combined organic layers were washed with sat. NaCl-solution, dried over $MgSO_4$, filtered and evaporated to dryness. The residue was adsorbed onto silica and purification was performed via column chromatography (silica, DCM/MeOH (+NH_3) 99:1 → 95:5), which afforded 4-amino-*N*-(2-(2,2-dioxidobenzo[c][1,2,5]thiadiazol-1(3*H*)-yl)ethyl)-3-nitrobenzamide (**72**) as a yellow solid (156 mg, 0.41 mmol, 50%).

^{1}H-NMR: 500 MHz, DMSO-d_6, δ_H = 3.56 (dt, $^3J_{H,H}$=6.6 Hz, 6.0 Hz, 2H, H-C1"), 3.82 (t, $^3J_{H,H}$=6.6 Hz, 2H, H-C2"), 6.85 (dd, $^3J_{H,H}$=7.7 Hz, $^4J_{H,H}$=1.2 Hz, 1H, H-C2* or H-C5*), 6.91 (ddd, $^3J_{H,H}$=7.5 Hz, 7.5 Hz, $^4J_{H,H}$=1.4 Hz, 1H, H-C4* or H-C3*), 6.97 (ddd, $^3J_{H,H}$=7.7 Hz, 7.7 Hz, $^4J_{H,H}$=1.4 Hz, 1H, H-C4* or H-C3*), 7.01 (dd, $^3J_{H,H}$=7.5 Hz, $^4J_{H,H}$=1.2 Hz, 1H, H-C2* or H-C5*), 7.03 (d, $^3J_{H,H}$=8.9 Hz, 1H, H-C5), 7.75 (br, s, 2H, NH_2), 7.84 (dd, $^3J_{H,H}$=8.9 Hz, $^4J_{H,H}$=2.0 Hz, 1H, H-C6), 8.56 (d, $^4J_{H,H}$=2.3 Hz, 1H, H-C2), 8.67 (t, $^3J_{H,H}$=5.7 Hz, 1H, CONH), 11.35 (br, s, 1H, SO_2NH) ppm.

^{13}C-NMR: 125 MHz, DMSO-d_6, δ_C = 37.3 (1C, C1"), 40.6 (1C, C2"), 107.8 (1C, C5), 110.4 (1C, C4* or C5*), 118.8 (1C, C4* or C5*), 121.1 (1C, C2* or C3*), 121.6 (1C, C2* or C3*), 125.3 (1C, C2), 127.5 (1C, C6*), 129.5 (1C, C1), 130.5 (1C, C1*), 133.9 (1C, C6), 147.8 (1C, C4), 164.9 (1C, C1') ppm, C3 is missing.

HR-MS: ESI(+), *m/z* = 378.0877 ($[M+H]^+$, calcd. for $C_{15}H_{16}N_5O_5S$: 378.0867).

EA-CHN: 47.53% C, 4.02% H, 18.47% N (calcd. for $C_{15}H_{15}N_5O_5S$: 47.74% C, 4.01% H, 18.56% N).

M.P.: 207.6 °C.

5.2.37 Synthesis of 4-amino-*N*-benzyl-3-nitrobenzamide (73)

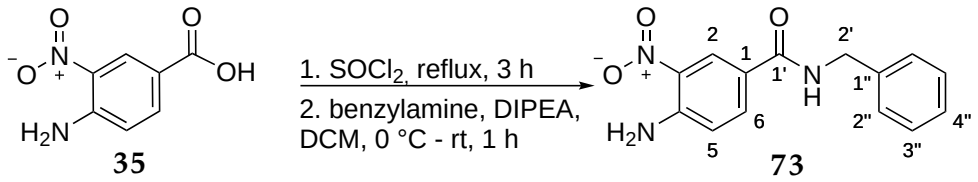

35 73

Dry solvents were used and the reaction was carried out under Ar atmosphere.
A 10 mL N_2-flask was charged with 4-amino-3-nitrobenzoic acid (**35**) (150 mg, 0.75 mmol, 1.00 eq) and thionyl chloride (3 mL). The suspension was refluxed for 3 h and the excess thionyl chloride was removed under reduced pressure afterwards and subsequently the acid chloride was dried *in vacuo*. In the following step, DCM (5 mL) was added and the resulting solution was cooled to 0 °C before adding benzylamine (96 mg, 0.90 mmol, 1.20 eq) and DIPEA (194 mg, 1.50 mmol, 2.00 eq). After stirring for 1 h at room temperature, complete conversion was observed via TLC. The solvent was removed under reduced pressure and the residue was taken up in water (40 mL) and extracted with EtOAc (3x 30 mL). The combined organic layers were washed with sat. NaCl-solution, dried over $MgSO_4$, filtered and the solvent was removed under reduced pressure. The crude material was adsorbed onto silica and purified by column chromatography (silica, Cyhex/EtOAc 60:40). The desired 4-amino-*N*-benzyl-3-nitrobenzamide (**73**) (137 mg, 0.50 mmol, 67%) was obtained as a yellow solid.

^{1}H-NMR: 500 MHz, DMSO-d_6, δ_H = 4.45 (d, $^3J_{H,H}$=6.0 Hz, 2H, H-C2'), 7.04 (d, $^3J_{H,H}$=8.9 Hz, 1H, H-C5), 7.22-7.36 (m, 5H, H-C2" - H-C6"), 7.74 (br, s, 2H, NH_2), 7.90 (dd, $^3J_{H,H}$=8.9 Hz, $^4J_{H,H}$=2.0 Hz, 1H, H-C6), 8.62 (d, $^4J_{H,H}$=2.0 Hz, H-C2), 8.99 (t, $^3J_{H,H}$=6.0 Hz, 1H, CONH) ppm.

^{13}C-NMR: 125 MHz, DMSO-d_6, δ_C = 42.5 (1C, C2'), 118.8 (1C, C5), 121.1 (1C, C1), 125.4 (1C, C2), 126.7 (1C, C4"), 127.2 (2C, C2"), 128.2 (2C, C3"), 129.6 (1C, C1"), 133.9 (1C, C6), 139.7 (1C, C3), 147.7 (1C, C4), 164.4 (1C, C1') ppm.

HR-MS: ESI(+), *m/z* = 272.1027 ($[M+H]^+$, calcd. for $C_{14}H_{14}N_3O_3$: 272.1030).

EA-CHN: 62.00% C, 4.91% H, 15.37% N
(calcd. for $C_{14}H_{13}N_3O_3$: 61.99% C, 4.83% H, 15.49% N).

M.P.: 174.2 °C.

5.2.38 Synthesis of 5-(3-fluorobenzyl)-1,3,4-thiadiazol-2-amine (102)

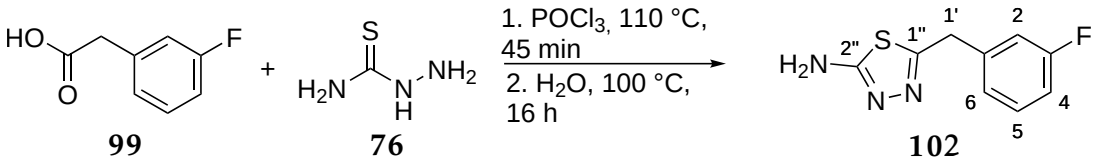

The reaction was carried out under Ar atmosphere.

A 50 mL three-necked-flask was charged with 3-fluorophenylacetic acid (**99**) (1.15 g, 7.50 mmol, 1.00 eq) and thiosemicarbazide (**76**) (683 mg, 7.50 mmol, 1.00 eq). After addition of $POCl_3$ (4 mL), the resulting suspension was heated to reflux for 45 min, upon which the solids dissolved completely. After the given time, the solution was cooled to 0 °C and water (11 mL) was slowly added. After stirring for 30 min at 0 °C, the reaction mixture was heated again to reflux for 16 h. Afterwards, the hot suspension was filtered and the filtrate was adjusted to pH=11-12, whereupon a white solid precipitated. The solid was collected by filtration and washed with water and DEE. Drying *in vacuo* afforded 5-(3-fluorobenzyl)-1,3,4-thiadiazol-2-amine (**114**) (940 mg, 4.49 mmol, 60%) as a white solid.

^{1}**H-NMR:**	400 MHz, DMSO-d_6, δ_H = 4.18 (s, 2H, H-C1'), 7.03 (br, s, 2H, NH_2), 7.08-7.13 (m, 3H, H-C2, H-C4, H-C6) 7.37 (sm, 1H, H-C5) ppm.
^{13}**C-NMR:**	100 MHz, DMSO-d_6, δ_C = 34.8 (1C, C1'), 113.6 (d, $^{2}J_{C,F}$=21.1 Hz, 1C, C4), 115.4 (d, $^{2}J_{C,F}$=22.0 Hz, 1C, C2), 124.8 (d, $^{4}J_{C,F}$=1.9 Hz, 1C, C6), 130.5 (d, $^{3}J_{C,F}$=7.7 Hz, 1C, C5), 140.8 (d, $^{3}J_{C,F}$=7.7 Hz, 1C, C1), 156.6 (1C, C1"), 162.1 (d, $^{1}J_{C,F}$=244.4 Hz, 1C, C3), 168.8 (1C, C2") ppm.
^{19}**F-NMR:**	377 MHz, DMSO-d_6, δ_F = -113.08 ppm.
HR-MS:	ESI(+), *m/z* = 210.0503 ([M+H]$^+$, calcd. for $C_9H_9FN_3S$: 210.0496).
M.P.:	197.6 °C.

All recorded spectral data are in accordance to literature.[90]

5.2.39 Synthesis of 4-amino-*N*-(5-(3-fluorobenzyl)-1,3,4-thiadiazol-2-yl)-3-nitrobenzamide (96)

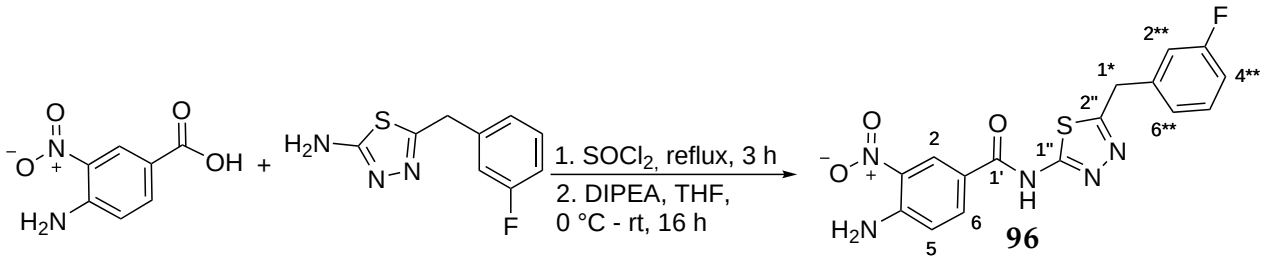

35 **102** **96**

Dry solvents were used and the reaction was carried out under Ar atmosphere.
In a 25 mL N_2-flask, 4-amino-3-nitrobenzoic acid (**35**) (365 mg, 2.00 mmol, 1.00 eq) was suspended in thionyl chloride (6 mL) and heated to reflux for 3 h. Thionyl chloride was removed by distillation and the residue was dried *in vacuo*. Afterwards, it was dissolved in THF (10 mL) and the solution was cooled to 0 °C. At this temperature, compound **114** (503 mg, 2.40 mmol, 1.20 eq) and DIPEA (0.68 mL, 4.00 mmol, 2.00 eq) were added. Complete conversion could be obtained after stirring for 16 h at room temperature (determined via TLC). The reaction mixture was washed with water (30 mL) and the aqueous layer extracted with EtOAc (3x 30 mL). The combined organic layers were dried over $MgSO_4$, filtered and evaporated to dryness. The residue was adsorbed onto silica and purification was performed via column chromatography (silica, DCM/MeCN 80:20 → 20:80). The desired 4-amino-*N*-(5-(3-fluorobenzyl)-1,3,4-thiadiazol-2-yl)-3-nitrobenzamide (**96**) (514 mg, 1.38 mmol, 69%) was obtained as a yellow solid.

^{1}H-NMR: 500 MHz, DMSO-d_6, δ_H = 4.40 (s, 2H, H-C1*), 7.08 (d, $^3J_{H,H}$=9.2 Hz, 1H, H-C5), 7.09-7.13 (m, 1H, H-C2**), 7.19-7.22 (m, 2H, H-C4** + H-C6**), 7.38-7.43 (m, 1H, H-C5**), 7.95 (br, s, 2H, NH_2), 8.04 (dd, $^3J_{H,H}$=8.9 Hz, $^4J_{H,H}$=2.3 Hz, 1H, H-C6), 8.89 (d, $^4J_{H,H}$=2.3 Hz, 1H, H-C2), 12.89 (br, s, 1H, CONH) ppm.

^{13}C-NMR: 125 MHz, DMSO-d_6, δ_C = 34.4 (1C, C1*), 113.8 (d, $^2J_{C,F}$=21.6 Hz, 1C, C4**), 115.6 (d, $^2J_{C,F}$=21.6 Hz, 1C, C2**), 118.0 (1C, C5), 119.1 (1C, C2), 125.0 (d, $^4J_{C,F}$=2.4 Hz, 1C, C6**), 127.5 (1C, C1), 129.7 (1C, C6), 130.6 (d, $^3J_{C,F}$=8.4 Hz, 1C, C5**), 134.3 (1C, C3), 140.4 (d, $^3J_{C,F}$=7.2 Hz, 1C, C1**), 148.6 (1C, C4), 159.8 (1C, C1''), 162.2 (d, $^1J_{C,F}$=244.4 Hz, 1C, C3**), 162.7 (1C, C2''), 163.8 (1C, C1') ppm.

^{19}F-NMR: 470 MHz, DMSO-d_6, δ_F = -112.89 ppm.

HR-MS: ESI(+), *m/z* = 374.0727 ($[M+H]^+$, calcd. for $C_{16}H_{13}FN_5O_3S$: 374.0718).

EA-CHN: 51.71% C, 3.46% H, 19.06% N (calcd. for $C_{16}H_{12}FN_5O_3S$: 51.47% C, 3.24% H, 18.76% N).

M.P.: 245.7 °C.

5.2.40 Synthesis of 5-(3-bromobenzyl)-1,3,4-thiadiazol-2-amine (103)

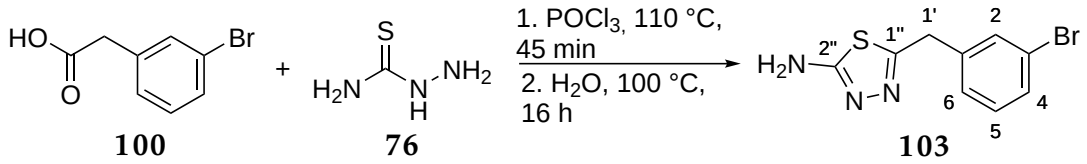

The reaction was carried out under Ar atmosphere.

A 50 mL three-necked-flask was charged with 3-bromophenylacetic acid (**100**) (860 mg, 4.00 mmol, 1.00 eq) and thiosemicarbazide (**76**) (366 mg, 4.00 mmol, 1.00 eq). The solids were suspended in $POCl_3$ (2 mL) and heated to reflux for 45 min. During this time, the solids dissolved completely. After the given time, the reaction mixture was cooled to 0 °C and water (6 mL) was slowly added. After stirring for 30 min at 0 °C, the reaction mixture was heated to reflux for 16 h. Afterwards, the suspension was filtered hot and the filtrate was adjusted to pH=11-12, whereupon a white solid precipitated, which was collected by filtration and washed with water and MTBE. Drying *in vacuo* afforded 5-(3-bromobenzyl)-1,3,4-thiadiazol-2-amine (**103**) (695 g, 2.57 mmol, 64%) as a white solid.

^{1}H-NMR: 500 MHz, DMSO-d_6, δ_H = 4.17 (s, 2H, H-C1'), 7.05 (br, s, 2H, NH_2), 7.29-7.30 (m, 2H, H-C5, H-C6), 7.44-7.49 (7.49 (m, 1H, H-C2), 7.50 (sm, 1H, H-C4) ppm.

^{13}C-NMR: 125 MHz, DMSO-d_6, δ_C = 34.7 (1C, C1'), 121.7 (1C, C3), 127.8 (1C, C6), 129.7 (1C, C4), 130.7 (1C, C5), 131.3 (1C, C2), 140.7 (1C, C1), 156.5 (1C, C1''), 168.8 (1C, C2'') ppm.

HR-MS: ESI(+), *m/z* = 269.9694 ($[M+H]^+$, calcd. for $C_9H_9BrN_3S$: 269.9695).

M.P.: 186.4 °C.

5.2.41 Synthesis of 4-amino-*N*-(5-(3-bromobenzyl)-1,3,4-thiadiazol-2-yl)-3-nitro-benzamide(97)

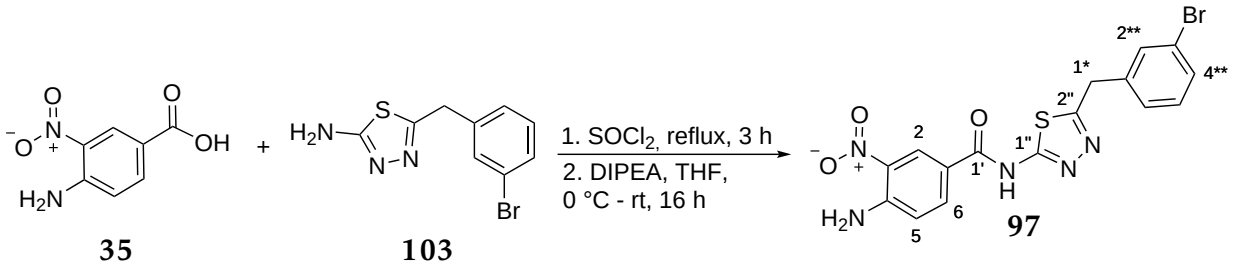

35 **103** **97**

Dry solvents were used and the reaction was carried out under Ar atmosphere.
In a 50 mL N_2-flask, 4-amino-3-nitrobenzoic acid (**35**) (392 mg, 2.00 mmol, 1.00 eq) was suspended in thionyl chloride (6 mL) and heated to reflux for 3 h. Excess thionyl chloride was removed by distillation and the residue was dried *in vacuo*. Afterwards, it was dissolved in THF (10 mL) and the solution was cooled to 0 °C. At this temperature, compound **103** (594 mg, 2.20 mmol, 1.10 eq) and DIPEA (1.02 mL, 6.00 mmol, 3.00 eq) were added. Complete conversion was achieved by stirring for 16 h at room temperature (determined via TLC). The reaction mixture was washed with sat. K_2CO_3-solution (30 mL) and the aqueous layer extracted with EtOAc (3x 20 mL). The combined organic layers were washed with sat. NaCl-solution, dried over $MgSO_4$, filtered and evaporated to dryness. The residue was adsorbed onto Celite® and purification was performed via column chromatography (silica, DCM/MeOH (+NH_3) 96:4). The resulting product was recrystallized from ^{i}PrOH/acetone (1:1), which afforded 4-amino-*N*-(5-(3-bromobenzyl)-1,3,4-thiadiazol-2-yl)-3-nitro-benzamide(**97**) (612 mg, 1.60 mmol, 80%) as a yellow solid.

^{1}H-NMR: 500 MHz, DMSO-d_6, δ_H = 4.39 (s, 2H, H-C1*), 7.08 (d, $^{3}J_{H,H}$=8.9 Hz, 1H, H-C5), 7.32 (dd, $^{3}J_{H,H}$=7.7 Hz, 7.7 Hz, 1H, H-C5**), 7.37 (d, $^{3}J_{H,H}$=7.7 Hz, 1H, H-C6**), 7.48 (ddd, $^{3}J_{H,H}$= 8.0 Hz, $^{4}J_{H,H}$=1.6 Hz, 1.6 Hz, 1H, H-C4**), 7.59 (dd, $^{4}J_{H,H}$=1.4 Hz, 1.4 Hz, 1H, H-C2**), 7.95 (br, s, 2H, NH_2), 8.04 (dd, $^{3}J_{H,H}$=9.0 Hz, $^{4}J_{H,H}$=2.1 Hz, 1H, H-C6), 8.89 (d, $^{4}J_{H,H}$=2.3 Hz, 1H, H-C2), 12.91 (br, s, 1H, CONH) ppm.

^{13}C-NMR: 125 MHz, DMSO-d_6, δ_C = 34.2 (1C, C1*), 117.9 (br, 1C, C3), 119.1 (1C, C5), 121.8 (1C, C3**), 127.5 (1C, C2), 128.0 (1C, C6**), 129.7 (1C, C1), 129.3 (1C, C5**), 130.8 (1C, C4**), 131.5 (1C, C2**), 134.3 (1C, C6), 140.4 (1C, C1**), 148.6 (1C, C4), 159.7 (br, 1C, C1”), 162.6 (br, 1C, C2”), 163.2 (br, 1C, C1’) ppm.

HR-MS: ESI(+), *m/z* = 435.9891([M+H]$^+$, calcd. for $C_{16}H_{13}BrN_5O_3S$: 435.9897).

EA-CHN: 44.17% C, 2.96% H, 15.58% N (calcd. for $C_{16}H_{12}BrN_5O_3S \cdot 0.25\ H_2O$: 43.80% C, 2.87% H, 15.96% N).

M.P.: 267.5 °C.

5.2.42 Synthesis of 5-(3-iodobenzyl)-1,3,4-thiadiazol-2-amine (104)

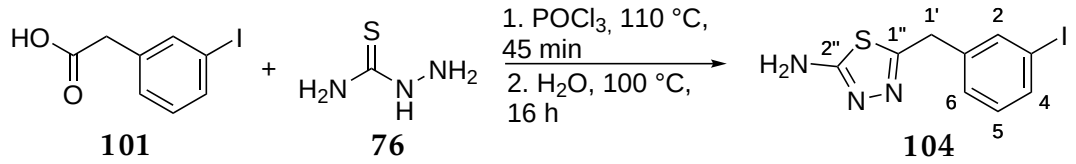

101 **76** **104**

The reaction was carried out under Ar atmosphere.

A 50 mL three-necked-flask was charged with 3-iodophenylacetic acid (**167**) (1000 mg, 3.82 mmol, 1.00 eq) and thiosemicarbazide (**76**) (348 mg, 3.82 mmol, 1.00 eq). The solids were suspended in $POCl_3$ (2 mL) and heated to reflux for 45 min. During this time, the solids dissolved completely. After the given time, the reaction mixture was cooled to 0 °C and water (8 mL) was added slowly. After stirring for 30 min at 0 °C, the reaction mixture was heated to reflux for 3 h. Afterwards, the suspension was filtered hot and the filtrate was adjusted with sat. NaOH solution to pH=10-11, whereupon a white solid precipitated, which was collected by filtration and washed with water and cyclohexane. Drying *in vacuo* afforded 5-(3-iodobenzyl)-1,3,4-thiadiazol-2-amine (**104**) (530 mg, 1.67 mmol, 44%) as a white solid.

^{1}H-NMR: 500 MHz, DMSO-d_6, δ_H = 4.13 (s, 2H, H-C1'), 7.03 (br, s, 2H, NH_2), 7.14 (dd, $^3J_{H,H}$=7.7 Hz, 7.7 Hz, 1H, H-C5), 7.30 (d, $^3J_{H,H}$=8.0 Hz, 1H, H-C6), 7.62 (d, $^3J_{H,H}$=7.7 Hz, 1H, H-C4), 7.67 (s, 1H, H-C2) ppm.

^{13}C-NMR: 125 MHz, DMSO-d_6, δ_C = 34.6 (1C, C1'), 94.9 (1C, C3), 128.1 (1C, C6), 130.7 (1C, C5), 135.5 (1C, C4), 137.2 (1C, C1), 140.6 (1C, C2), 156.6 (1C, C1''), 168.8 (1C, C2'') ppm.

HR-MS: ESI(+), *m/z* = 317.9554 ([M+H]$^+$, calcd. for $C_9H_9IN_3S$: 317.9556).

M.P.: 198.2 °C.

5.2.43 Synthesis of 4-amino-*N*-(5-(3-iodobenzyl)-1,3,4-thiadiazol-2-yl)-3-nitrobenzamide (98)

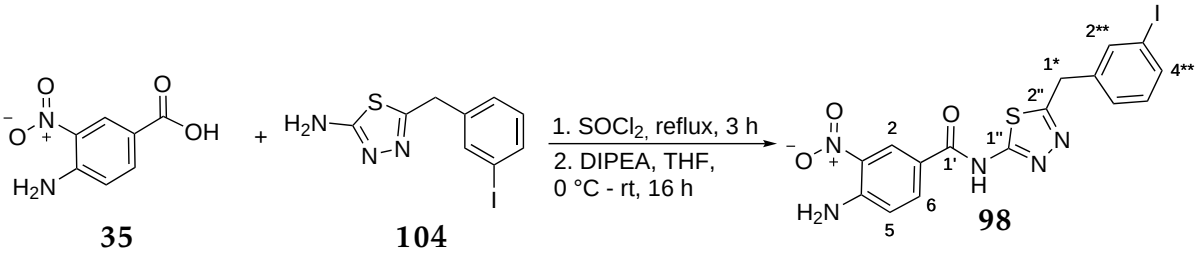

35 **104** **98**

Dry solvents were used and the reaction was carried out under Ar atmosphere.
In a 50 mL N_2-flask, 4-amino-3-nitrobenzoic acid (**35**) (235 mg, 1.29 mmol, 1.00 eq) was suspended in thionyl chloride (5 mL) and heated to reflux for 3 h. The excess thionyl chloride was removed by distillation and the residue was dried *in vacuo*. Afterwards, it was dissolved in THF (10 mL) and the solution was cooled to 0 °C. At this temperature, compound **104** (450 mg, 1.42 mmol, 1.10 eq) and DIPEA (0.66 mL, 3.87 mmol,32.00 eq) were added. Since **104** did not dissolve completely, DMSO (5 mL) was added. Complete conversion was achieved by stirring for 16 h at room temperature (determined via TLC). The reaction mixture was washed with sat. K_2CO_3-solution (30 mL) and the aqueous layer extracted with EtOAc (3x 20 mL). The combined organic layers were dried over $MgSO_4$, filtered and evaporated to dryness. The residue was adsorbed onto Celite® and purification was performed via column chromatography (silica, DCM/MeOH (+NH_3) 98:2 → 96:4). The resulting product was recrystallized from ^{i}PrOH, which afforded 4-amino-*N*-(5-(3-iodobenzyl)-1,3,4-thiadiazol-2-yl)-3-nitrobenzamide (**98**) (249 mg, 0.52 mmol, 40%) as a yellow solid.

^{1}H-NMR: 500 MHz, DMSO-d_6, δ_H = 4.35 (s, 2H, H-C1*), 7.08 (d, $^{3}J_{H,H}$=8.9 Hz, 1H, H-C5), 7.17 (dd, $^{3}J_{H,H}$=7.8 Hz, 7.8 Hz, 1H, H-C5**), 7.38 (d, $^{3}J_{H,H}$=7.8 Hz, 1H, H-C6**), 7.65 (d, $^{3}J_{H,H}$=8.0 Hz, 1H, H-C4**), 7.76 (s, 1H, H-C2**), 7.96 (br, s, 2H, NH_2), 8.04 (dd, $3J_{H,H}$=9.0 Hz, $4J_{H,H}$=2.1 Hz, 1H, H-C6), 8.89 (d, $^{4}J_{H,H}$=2.1 Hz, 1H, H-C2), 12.90 (br, s, 1H, CONH) ppm.

^{13}C-NMR: 125 MHz, DMSO-d_6, δ_C = 34.1 (1C, C1*), 95.0 (1C, C3**), 118.4 (br, 1C, C3), 119.1 (1C, C5), 127.5 (1C, C2), 128.3 (1C, C6**), 129.7 (1C, C1), 130.8 (1C, C5**), 134.3 (1C, C6), 135.7 (1C, C4**), 137.3 (1C, C2**), 140.3 (1C, C1**), 148.6 (1C, C4), 159.8 (br, 1C, C1''), 160.9 (br, 1C, C2''), 162.8 (br, 1C, C1') ppm.

HR-MS: APCI(+), *m/z* = 481.9775 ($[M+H]^+$, calcd. for $C_{16}H_{13}IN_5O_3S$: 481.9778).

EA-CHN: 40.29% C, 2.68% H, 14.32% N (calcd. for $C_{16}H_{12}IN_5O_3S$: 39.93% C, 2.51% H, 14.55% N).

M.P.: 276.3 °C.

5.2.44 Synthesis of 5-(3-methylbenzyl)-1,3,4-thiadiazol-2-amine (113)

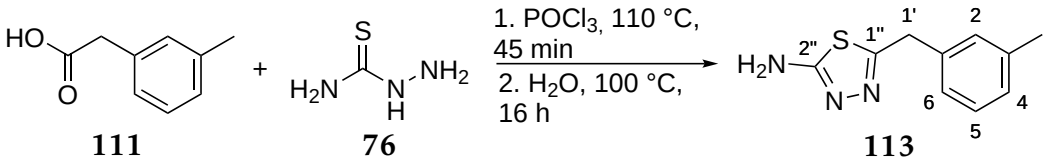

111 **76** **113**

The reaction was carried out under Ar atmosphere.

A 50 mL three-necked-flask was charged with 3-methylphenylacetic acid (**111**) (1.13 g, 7.50 mmol, 1.00 eq) and thiosemicarbazide (**76**) (683 mg, 7.50 mmol, 1.00 eq). The solids were suspended in $POCl_3$ (4 mL) and heated to reflux for 45 min. During this time, the solids dissolved completely. After the given time, the reaction mixture was cooled to 0 °C and water (12 mL) was slowly added. After stirring for 30 min at 0 °C, the reaction mixture was heated to reflux for 16 h. Afterwards, the suspension was filtered hot and the filtrate was adjusted to pH=11-12, whereupon a white solid precipitated, which was collected by filtration and washed with water and DEE. Drying *in vacuo* afforded 5-(3-methylbenzyl)-1,3,4-thiadiazol-2-amine (**113**) (1.49 g, 7.23 mmol, 96%) as a white solid.

^{1}H-NMR: 500 MHz, DMSO-d_6, δ_H = 2.29 (s, 3H, Me), 4.15 (s, 2H, H-C1'), 7.08-7.11 (m, 3H, H-C2, H-C4, H-C6), 7.23 (dd, $^3J_{H,H}$=7.23 Hz, 7.1 Hz, 1H, H-C5), 8.53 (br, s, 2H, NH_2) ppm.

^{13}C-NMR: 125 MHz, DMSO-d_6, δ_C = 20.9 (1C, Me), 35.2 (1C, C1'), 125.8 (1C, C4 or C6), 127.8 (1C, C4 or C6), 128.6 (1C, C5), 129.3 (1C, C2), 136.8 (1C, C1), 137.9 (1C, C3), 158.0 (1C, C1"), 169.1 (1C, C2") ppm.

HR-MS: ESI(+), *m/z* = 206.0752 ($[M+H]^+$, calcd. for $C_{10}H_{12}N_3S$: 206.0746).

M.P.: 147.0 °C.

All recorded spectral data are in accordance to literature.[66]

5.2.45 Synthesis of 4-amino-*N*-(5-(3-methylbenzyl)-1,3,4-thiadiazol-2-yl)-3-nitrobenzamide (109)

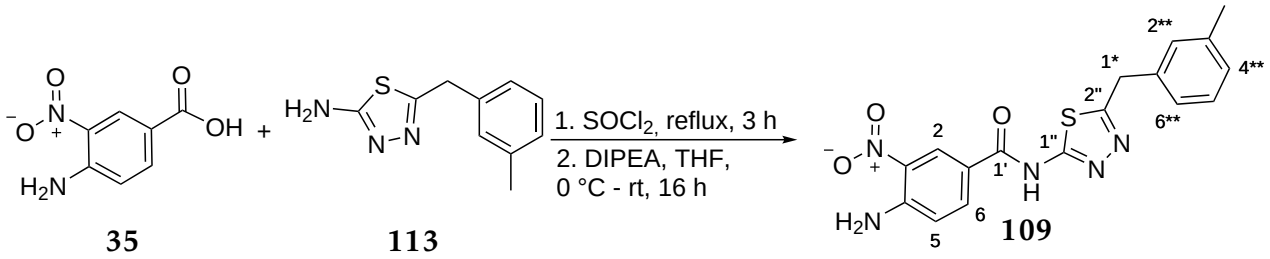

35 **113** **109**

Dry solvents were used and the reaction was carried out under Ar atmosphere.
In a 50 mL N_2-flask, 4-amino-3-nitrobenzoic acid (**35**) (455 mg, 2.50 mmol, 1.00 eq) was suspended in thionyl chloride (10 mL) and heated to reflux for 3 h. Excess thionyl chloride was removed by distillation and the residue was dried *in vacuo*. Afterwards, it was dissolved in THF (10 mL) and the solution was cooled to 0 °C. At this temperature, compound **113** (616 mg, 3.00 mmol, 1.20 eq) and DIPEA (1.30 mL, 7.50 mmol, 3.00 eq) were added. Complete conversion was achieved by stirring for 16 h at room temperature (determined via TLC). The reaction mixture was washed with water (45 mL) and the aqueous layer extracted with EtOAc (3x 30 mL). The combined organic layers were washed with sat. NaCl-solution, dried over $MgSO_4$, filtered and evaporated to dryness. The residue was adsorbed onto Celite® and purification was performed via column chromatography (silica, DCM/MeOH (+NH_3) 100:0 → 90:10). The desired 4-amino-*N*-(5-(3-methylbenzyl)-1,3,4-thiadiazol-2-yl)-3-nitrobenzamide (**109**) (635 mg, 1.72 mmol, 69%) was obtained as a yellow solid.

^{1}H-NMR: 500 MHz, DMSO-d_6, δ_H = 2.29 (s, 3H, Me), 4.31 (s, 2H, H-C1*), 7.06-7.16 (m, 4H, H-C5, H-C2**, H-C4**, H-C6**), 7.24 (sm, 1H, H-C5**), 7.95 (br, s, 2H, NH_2), 8.03 (dd, $^3J_{H,H}$=9.0 Hz, $^4J_{H,H}$=2.3 Hz, 1H, H-C6), 8.89 (d, $^4J_{H,H}$=2.1 Hz, 1H, H-C2), 12.91 (br, s, 1H, CONH) ppm.

^{13}C-NMR: 125 MHz, DMSO-d_6, δ_C = 20.9 (1C, Me), 34.9 (1C, C1*), 118.0 (br, 1C, C3), 119.1 (1C, C5), 125.8 (1C, C2** or C6**), 127.5 (1C, C2), 127.6 (1C, C4**), 128.6 (1C, C5**), 129.3 (1C, C2** or C6**), 129.7 (1C, C1), 134.3 (1C, C6), 137.6 (1C, C1**), 137.9 (1C, C3**), 148.6 (1C, C4), 160.2 (br, 1C, C1''), 162.5 (br, 1C, C2''), 163.6 (br, 1C, C1') ppm.

HR-MS: ESI(-), *m/z* = 368.0832 ([M-H]$^-$, calcd. for $C_{17}H_{14}N_5O_3S$: 368.0823).

EA-CHN: 55.49% C, 4.14% H, 18.56% N (calcd. for $C_{17}H_{15}N_5O_3S$: 55.28% C, 4.09% H, 18.96% N).

M.P.: 209.1 °C.

5.2.46 Synthesis of 5-(3-(trifluoromethyl)benzyl)-1,3,4-thiadiazol-2-amine (114)

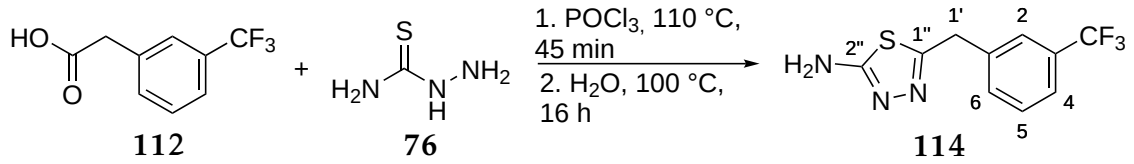

112 **76** **114**

The reaction was carried out under Ar atmosphere.

A 50 mL three-necked-flask was charged with 3-(trifluoromethyl)phenylacetic acid (**112**) (1.53 g, 7.50 mmol, 1.00 eq) and thiosemicarbazide (**76**) (683 mg, 7.50 mmol, 1.00 eq). After addition of $POCl_3$ (4 mL), the resulting suspension was heated to reflux for 45 min, upon which the solids dissolved completely. After the given time, the solution was cooled to 0 °C and water (11 mL) was slowly added. After stirring for 30 min at 0 °C, the reaction mixture was heated again to reflux for 16 h. Afterwards, the hot suspension was filtered and the filtrate was adjusted to pH=11-12, whereupon a white solid precipitated. The solid was collected by filtration and washed with water and DEE. Drying *in vacuo* afforded 5-(3-(trifluoromethyl)benzyl)-1,3,4-thiadiazol-2-amine (**102**) (1.50 g, 5.79 mmol, 77%) as a white solid.

^{1}**H-NMR:**	400 MHz, DMSO-d_6, δ_H = 4.28 (s, 2H, H-C1'), 7.05 (br, s, 2H, NH_2), 7.55-7.66 (m, 4H, H-C2, H-C4 - H-C6) ppm.
^{13}**C-NMR:**	100 MHz, DMSO-d_6, δ_C = 34.8 (1C, C1'), 123.5 (q, $^{3}J_{C,F}$=2.9 Hz, 1C, C4), 124.1 (q, $^{1}J_{C,F}$=278.0 Hz, 1C, CF_3), 125.1 (q, $^{3}J_{C,F}$=3.8 Hz, 1C, C2), 129.2 (q, $^{2}J_{C,F}$=31.6 Hz, 1C, C3), 129.7 (1C, C5), 139.4 (1C, C6), 132.9 (1C, C1), 156.4 (1C, C1"), 168.9 (1C, C2") ppm.
^{19}**F-NMR:**	377 MHz, DMSO-d_6, δ_F = -61.00 ppm.
HR-MS:	ESI(+), *m/z* = 260.0472 ($[M+H]^+$, calcd. for $C_{10}H_8F_3N_3S$: 260.0464).
M.P.:	174.5 °C.

All recorded spectral data are in accordance to literature.[91]

5.2.47 Synthesis of 4-amino-3-nitro-*N*-(5-(3-(trifluoromethyl)benzyl)-1,3,4-thiadiazol-2-yl)benzamide (110)

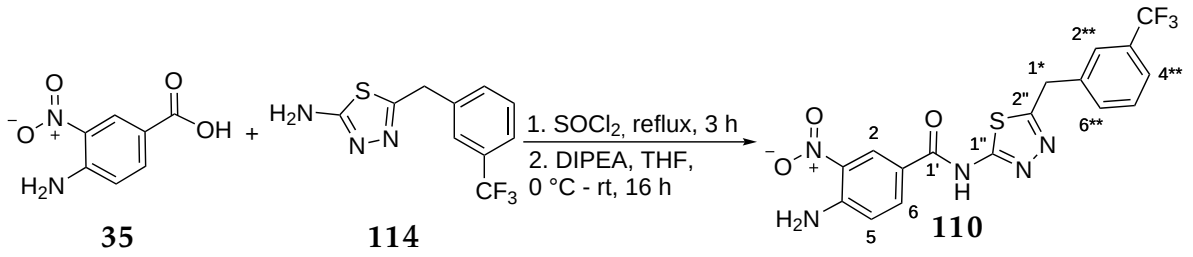

35 **114** **110**

Dry solvents were used and the reaction was carried out under Ar atmosphere.
In a 25 mL N_2-flask, 4-amino-3-nitrobenzoic acid (**35**) (293 mg, 1.61 mmol, 1.00 eq) was suspended in thionyl chloride (6 mL) and heated to reflux for 3 h. Thionyl chloride was removed by distillation and the residue was dried *in vacuo*. Afterwards, it was dissolved in THF (10 mL) and the solution was cooled to 0 °C. At this temperature, compound **102** (500 mg, 1.93 mmol, 1.20 eq) and DIPEA (0.42 mL, 3.20 mmol, 2.00 eq) were added. Complete conversion could be obtained after stirring for 16 h at room temperature (determined via TLC). The reaction mixture was washed with water (30 mL) and the aqueous layer extracted with EtOAc (3x 30 mL). The combined organic layers were dried over $MgSO_4$, filtered and evaporated to dryness. The residue was adsorbed onto silica and purification was performed via column chromatography (silica, DCM/MeCN 80:20 + 1% 7 N NH_3 in MeOH). The desired 4-amino-*N*-(5-(3-(trifluoromethyl)benzyl)-1,3,4-thiadiazol-2-yl)-3-nitrobenzamide (**110**) (412 mg, 0.97 mmol, 60%) was obtained as a yellow solid.

^{1}**H-NMR:** 500 MHz, DMSO-d_6, δ_H = 4.51 (s, 2H, H-C1*), 7.08 (d, $^3J_{H,H}$=9.2 Hz, 1H, H-C5), 7.58-7.68 (m, 3H, H-C4**, H-C5**, H-C6**), 7.76 (s, 1H, H-C2**), 7.95 (br, s, 2H, NH_2), 8.04 (dd, $^3J_{H,H}$=9.0 Hz, $^4J_{H,H}$=2.3 Hz, 1H, H-C6), 8.89 (d, $^4J_{H,H}$=2.3 Hz, 1H, H-C2), 12.90 (br, s, 1H, CONH) ppm.

^{13}**C-NMR:** 125 MHz, DMSO-d_6, δ_C = 34.3 (1C, C1*), 119.1 (1C, C5), 123.7 (q, $^3J_{C,F}$=3.6 Hz, 1C, C4**), 124.1 (q, $^1J_{C,F}$=272.3 Hz, 1C, CF_3), 125.4 ($^3J_{C,F}$=3.6 Hz, 1C, C2**), 127.5 (1C, C2), 129.3 (q, $^2J_{C,F}$=31.2 Hz, 1C, C3**), 129.7 (2C, C1 + C6**), 129.8 (1C, C5**), 133.1 (1C, C1**), 134.3 (1C, C6), 139.1 (1C, C3), 148.6 (1C, C4), 160.0 (1C, C1"), 162.5 (1C, C2"), 163.3 (1C, C1') ppm.

^{19}**F-NMR:** 470 MHz, DMSO-d_6, δ_F = -60.95 ppm.

HR-MS: ESI(+), *m/z* = 446.0517 ([M+Na]$^+$, calcd. for $C_{17}H_{12}F_3N_5O_3SNa$: 446.0505).

EA-CHN: 48.36% C, 2.95% H, 16.35% N (calcd. for $C_{17}H_{12}F_3N_5O_3S$: 48.23% C, 2.86% H, 16.54% N).

M.P.: 230.9 °C.

5.2.48 Synthesis of 5-(3,5-dichlorobenzyl)-1,3,4-thiadiazol-2-amine (119)

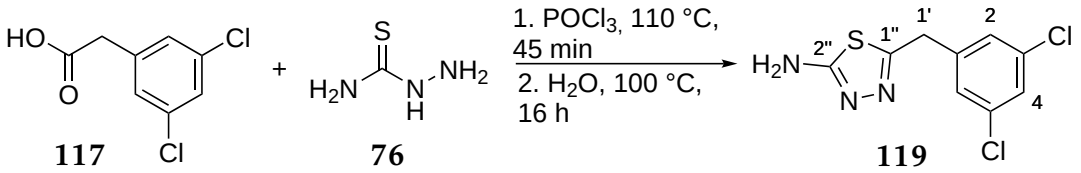

The reaction was carried out under Ar atmosphere.

A 50 mL three-necked-flask was charged with 3,5-dichlorophenylacetic acid (**117**) (820 mg, 4.00 mmol, 1.00 eq) and thiosemicarbazide (**76**) (366 mg, 4.00 mmol, 1.00 eq). The solids were suspended in $POCl_3$ (4 mL) and heated to reflux for 45 min. During this time, the solids dissolved completely. After the given time, the reaction mixture was cooled to 0 °C and water (8 mL) was slowly added. After stirring for 30 min at 0 °C, the reaction mixture was heated to reflux for 16 h. Afterwards, the suspension was filtered hot and the filtrate was adjusted to pH=11-12, whereupon a white solid precipitated, which was collected by filtration and washed with water and cyclohexane. Drying *in vacuo* afforded 5-(3,5-dichlorobenzyl)-1,3,4-thiadiazol-2-amine (**119**) (740 mg, 2.84 mmol, 71%) as a white solid.

^{1}H-NMR: 500 MHz, 130 °C, DMSO-d_6, δ_H = 4.21 (s, 2H, H-C1'), 6.65 (br, s, 2H, NH_2), 7.33 (d, $^4J_{H,H}$=1.8 Hz, 2H, H-C2), 7.40 (dd, $^4J_{H,H}$=1.8 Hz, 1.8 Hz, 1H, H-C4) ppm.

^{13}C-NMR: 125 MHz, 130 °C, DMSO-d_6, δ_C = 33.9 (1C, C1'), 125.8 (1C, C4), 126.8 (2C, C2), 133.6 (2C, C3), 141.5 (1C, C1), 155.3 (1C, C1''), 168.2 (1C, C2'') ppm.

HR-MS: ESI(+), *m/z* = 259.9811 ($[M+H]^+$, calcd. for $C_9H_8Cl_2N_3S$: 259.9810).

M.P.: 150.2 °C.

5.2.49 Synthesis of 4-amino-*N*-(5-(3,5-dichlorobenzyl)-1,3,4-thiadiazol-2-yl)-3-nitro-benzamide (115)

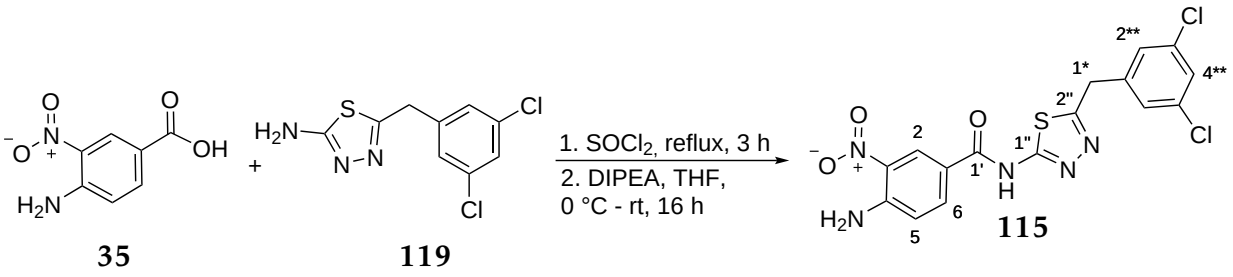

35 **119** **115**

Dry solvents were used and the reaction was carried out under Ar atmosphere.
In a 50 mL N_2-flask, 4-amino-3-nitrobenzoic acid (**35**) (392 mg, 2.00 mmol, 1.00 eq) was suspended in thionyl chloride (10 mL) and heated to reflux for 3 h. Excess thionyl chloride was removed by distillation and the residue was dried *in vacuo*. Afterwards, it was dissolved in THF (10 mL) and the solution was cooled to 0 °C. At this temperature, compound **119** (624 mg, 2.40 mmol, 1.20 eq) and DIPEA (0.68 mL, 4.00 mmol, 2.00 eq) were added. Complete conversion was achieved by stirring for 16 h at room temperature (determined via TLC). The reaction mixture was washed with water (30 mL) and the aqueous layer extracted with EtOAc (3x 30 mL). The combined organic layers were washed with sat. NaCl-solution, dried over $MgSO_4$, filtered and evaporated to dryness. The residue was adsorbed onto silica and purification was performed via column chromatography (silica, DCM/MeOH (+NH_3) 100:0 → 90:10). The resulting product was recrystallized from MeCN, which afforded 4-amino-*N*-(5-(3,5-dichlorobenzyl)-1,3,4-thiadiazol-2-yl)-3-nitro-benzamide (**115**) (288 mg, 0.68 mmol, 34%) as a yellow solid.

^{1}H-NMR: 500 MHz, DMSO-d_6, δ_H = 4.42 (s, 2H, H-C1*), 7.08 (d, $^3J_{H,H}$=9.2 Hz, 1H, H-C5), 7.46 (d, $^4J_{H,H}$=1.8 Hz, 2H, H-C2**), 7.53 (dd, $^4J_{H,H}$=1.8 Hz, 1.8 Hz, 1H, H-C4**), 7.96 (br, s, 2H, NH_2), 8.05 (dd, $^3J_{H,H}$=9.1 Hz, $^4J_{H,H}$=2.1 Hz, 1H, H-C6), 8.90 (d, $^4J_{H,H}$=2.1 Hz, 1H, H-C2), 12.98 (br, s, 1H, CONH) ppm.

^{13}C-NMR: 125 MHz, DMSO-d_6, δ_C = 33.8 (1C, C1*), 118.1 (br, 1C, C3), 119.1 (1C, C5), 126.7 (1C, C4**), 127.5 (1C, C2), 127.8 (2C, C2**), 129.7 (1C, C1), 134.1 (2C, C3**), 134.3 (1C, C6), 141.8 (1C, C1**), 148.6 (1C, C4), 160.2 (br, 1C, C1''), 161.8 (br, 1C, C2''), 163.5 (br, 1C, C1') ppm.

HR-MS: ESI(-), *m/z* = 421.9898 ([M-H]$^-$, calcd. for $C_{16}H_{10}Cl_2N_5O_3S$: 421.9887).

EA-CHN: 44.38% C, 2.83% H, 16.19% N (calcd. for $C_{16}H_{11}Cl_2N_5O_3S \cdot 0.5\ H_2O$: 44.35% C, 2.79% H, 16.16% N).

M.P.: 247.3 °C.

5.2.50 Synthesis of 5-(3,5-dibromobenzyl)-1,3,4-thiadiazol-2-amine (120)

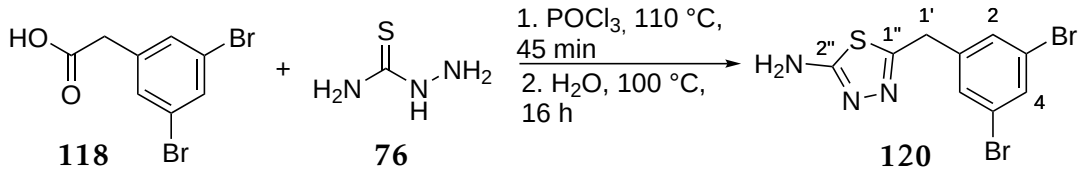

The reaction was carried out under Ar atmosphere.

A 50 mL three-necked-flask was charged with 3,5-dibromophenylacetic acid (**118**) (1176 mg, 4.00 mmol, 1.00 eq) and thiosemicarbazide (**76**) (366 mg, 4.00 mmol, 1.00 eq). The solids were suspended in $POCl_3$ (4 mL) and heated to reflux for 45 min. During this time, the solids dissolved completely. After the given time, the reaction mixture was cooled to 0 °C and water (8 mL) was slowly added. After stirring for 30 min at 0 °C, the reaction mixture was heated to reflux for 16 h. Afterwards, the suspension was filtered hot and the filtrate was adjusted to pH=11-12, whereupon a white solid precipitated, which was collected by filtration and washed with water and cyclohexane. Drying *in vacuo* afforded 5-(3,5-dibromobenzyl)-1,3,4-thiadiazol-2-amine (**120**) (1020 mg, 2.92 mmol, 73%) as a white solid.

^{1}H-NMR: 500 MHz, DMSO-d_6, δ_H = 4.19 (s, 2H, H-C1'), 7.08 (br, s, 2H, NH_2), 7.53 (d, $^4J_{H,H}$=1.6 Hz, 2H, H-C2), 7.73 (dd, $^4J_{H,H}$=1.6 Hz, 1.6 Hz, 1H, H-C4) ppm.

^{13}C-NMR: 125 MHz, DMSO-d_6, δ_C = 34.1 (1C, C1'), 122.4 (2C, C3), 130.7 (2C, C2), 131.8 (1C, C4), 142.6 (1C, C1), 155.8 (1C, C1"), 168.9 (1C, C2") ppm.

HR-MS: ESI(+), *m/z* = 349.8780 ($[M+H]^+$, calcd. for $C_9H_8Br_2N_3S$: 349.8779).

M.P.: 224.7 °C.

5.2.51 Synthesis of 4-amino-*N*-(5-(3,5-dibromobenzyl)-1,3,4-thiadiazol-2-yl)-3-nitrobenzamide (116)

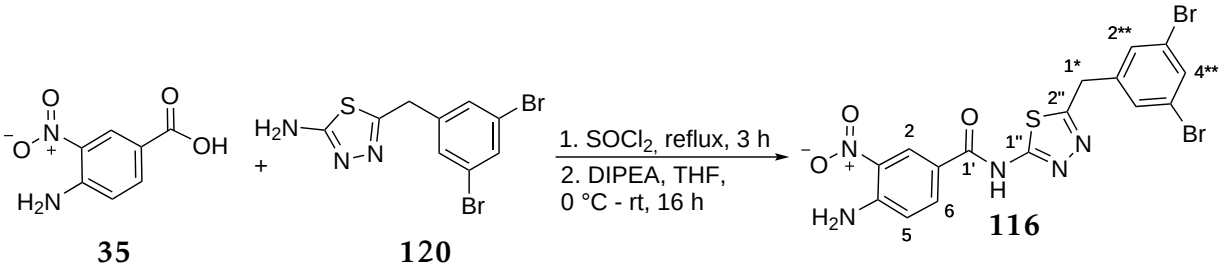

35 **120** **116**

Dry solvents were used and the reaction was carried out under Ar atmosphere.
In a 50 mL N_2-flask, 4-amino-3-nitrobenzoic acid (**35**) (392 mg, 2.00 mmol, 1.00 eq) was suspended in thionyl chloride (6 mL) and heated to reflux for 3 h. The excess thionyl chloride was removed by distillation and the residue was dried *in vacuo*. Afterwards, it was dissolved in THF (10 mL) and the solution was cooled to 0 °C. At this temperature, compound **120** (838 mg, 2.40 mmol, 1.20 eq) and DIPEA (0.68 mL, 4.00 mmol, 2.00 eq) were added. Complete conversion was achieved by stirring for 16 h at room temperature (determined via TLC). The reaction mixture was washed with sat. K_2CO_3-solution (50 mL) and the aqueous layer extracted with EtOAc (3x 50 mL). The combined organic layers were washed with sat. NaCl-solution, dried over $MgSO_4$, filtered and evaporated to dryness. The residue was adsorbed onto silica and purification was performed via column chromatography (silica, DCM/MeCN 85:15 → 80:20). The resulting product was recrystallized from MeCN, which afforded 4-amino-*N*-(5-(3,5-dibromobenzyl)-1,3,4-thiadiazol-2-yl)-3-nitro-benzamide (**116**) (420 mg, 0.82 mmol, 41%) as a yellow solid.

^{1}H-NMR: 500 MHz, DMSO-d_6, δ_H = 4.41 (s, 2H, H-C1*), 7.08 (d, $^3J_{H,H}$=8.9 Hz, 1H, H-C5), 7.62 (d, $^4J_{H,H}$=1.8 Hz, 2H, H-C2**), 7.75 (dd, $^4J_{H,H}$=1.8 Hz, 1.8 Hz, 1H, H-C4**), 7.96 (br, s, 2H, NH_2), 8.05 (dd, $^3J_{H,H}$=9.1 Hz, $^4J_{H,H}$=2.1 Hz, 1H, H-C6), 8.90 (d, $^4J_{H,H}$=2.3 Hz, 1H, H-C2), 12.95 (br, s, 1H, CONH) ppm.

^{13}C-NMR: 125 MHz, DMSO-d_6, δ_C = 33.7 (1C, C1*), 118.0 (br, 1C, C3), 119.1 (1C, C5), 122.5 (1C, C3**), 127.5 (1C, C2), 129.7 (1C, C1), 130.9 (2C, C2**), 132.0 (1C, C4**), 134.3 (1C, C6), 142.3 (1C, C1**), 148.6 (1C, C4), 160.0 (br, 1C, C1''), 161.9 (br, 1C, C2''), 163.4 (br, 1C, C1') ppm.

HR-MS: ESI(-), *m/z* = 511.8864 ($[M-H]^-$, calcd. for $C_{16}H_{10}Br_2N_5O_3S$: 511.8856).

EA-CHN: 36.45% C, 2.96% H, 11.71% N (calcd. for $C_{16}H_{11}Br_2N_5O_3S \cdot$ DMSO: 36.56% C, 2.90% H, 11.84% N).

M.P.: 220.1 °C.

5.2.52 Synthesis of 1-(3-fluorobenzyl)-4-nitro-1*H*-pyrazole (125)

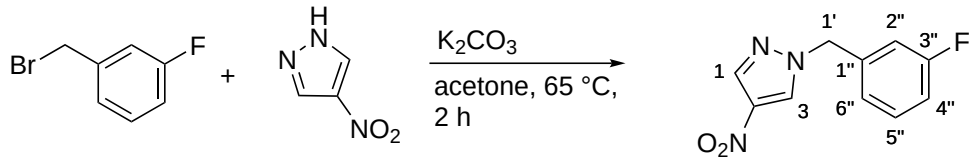

124 **78** **125**

A 100 mL two-necked flask was charged with 4-nitro-1*H*-pyrazole (**78**) (1.50 g, 13.30 mmol, 1.00 eq) and K_2CO_3 (11.52 g, 83.35 mmol, 5.00 eq). The solids were suspended in acetone (50 mL) and 3-fluorobenzylbromide (**124**) (1.63 mL, 13.30 mmol, 1.00 eq) was added dropwise. Afterwards, the mixture was heated to 65 °C for 2 h. After detection of complete conversion by TLC, the mixture was washed with water (40 mL) and the aqueous layer extracted with DCM (3x 35 mL). The combined organic layers were dried over $MgSO_4$, filtered and evaporated to dryness, which afforded 1-(3-fluorobenzyl)-4-nitro-1*H*-pyrazole (**125**) as a colorless oil (2.75 g, 12.43 mmol, 93%).

^{1}H-NMR: 500 MHz, DMSO-d_6, δ_H = 5.43 (s, 2H, H-C1'), 7.15-7.19 (m, 3H, H-C4" - H-C6"), 7.39-7.43 (m, 1H, H-C2"), 8.28 (s, 1H, H-C1), 9.04 (s, 1H, H-C3) ppm.

^{13}C-NMR: 125 MHz, DMSO-d_6, δ_C = 55.1 (1C, C1'), 114.8 (d, $^2J_{C,F}$=25.8 Hz, 1C, C2" or C4"), 115.0 (d, $^2J_{C,F}$=21.1 Hz, 1C, C2" or C4"), 124.0 (d, $^4J_{C,F}$=2.9 Hz, 1C, C6"), 130.7 (1C, C3), 130.8 (d, $^3J_{C,F}$=8.6 Hz, 1C, C5"), 135.1 (1C, C1 or C2), 136.0 (1C, C1 or C2), 138.4 (d, $^3J_{C,F}$=7.7 Hz, 1C, C1"), 162.1 (d, $^1J_{C,F}$=244.4 Hz, 1C, C3") ppm.

^{19}F-NMR: 377 MHz, DMSO-d_6, δ_F = -112.72 ppm.

HR-MS: APCI(+), *m/z* = 222.0675 ($[M+H]^+$, calcd. for $C_{10}H_9FN_3O_2$: 222.0673).

M.P.: Liquid at RT.

All recorded spectral data are in accordance to literature.[92]

5.2.53 Synthesis of 1-(3-fluorobenzyl)-1*H*-pyrazol-4-amine (127)

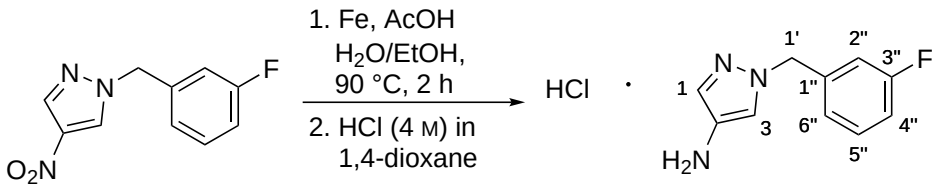

125 **127**

The reaction was carried out under Ar atmosphere.
In a 100 mL two-necked flask, compound **127** (1.22 g, 5.53 mmol, 1.00 eq) and iron powder (927 mg, 16.6 mmol, 3.00 eq) were suspended in ethanol (25 mL) and water (20 mL). Acetic acid (0.32 mL, 5.51 mmol, 1.00 eq) was added and the suspension was heated to reflux for 2 h. After this time, complete conversion was detected by TLC. The solids were removed by filtration and NaOH-solution (0.5 M, 100 mL) was added to the filtrate. Afterwards, the filtrate was extracted with EtOAc (3x 60 mL), the combined organic layers washed with sat. NaCl-solution, dried over $MgSO_4$, filtered and evaporated to dryness. The residue was dissolved in 1,4-dioxane (20 mL) and HCl-solution (4 M in 1,4-dioxane, 2.8 mL, 2.00 eq) was added. The obtained solid was collected by filtration, washed with 1,4-dioxane and DEE and dried *in vacuo* to afford 1-(3-fluorobenzyl)-1*H*-pyrazol-4-amine (**127**) · HCl as a beige solid (776 mg, 3.41 mmol, 62%).

^{1}**H-NMR:**	500 MHz, DMSO-d_6, δ_H = 5.38 (s, 2H, H-C1'), 7.05-7.15 (m, 3H, H-C4" - H-C6"), 7.37-7.41 (m, 1H, H-C2"), 7.58 (s, 1H, H-C1), 8.12 (s, 1H, H-C3), 10.28 (br, s, 3H, NH_3^+) ppm.
^{13}**C-NMR:**	125 MHz, DMSO-d_6, δ_C = 54.43 (1C, C1'), 113.4 (1C, C3), 114.4 (d, $^2J_{C,F}$=21.1 Hz, 1C, C2" or C4"), 114.6 (d, $^2J_{C,F}$=20.1 Hz, 1C, C2" or C4"), 123.7 (d, $^4J_{C,F}$=2.9 Hz, 1C, C6"), 125.6 (1C, C1), 130.6 (d, $^3J_{C,F}$=8.6 Hz, 1C, C5"), 134.0 (1C, C2), 139.8 (d, $^3J_{C,F}$=7.7 Hz, 1C, C1"), 162.0 (d, $^1J_{C,F}$=244.4 Hz, 1C, C3") ppm.
^{19}**F-NMR:**	377 MHz, DMSO-d_6, δ_F = -112.93 ppm.
HR-MS:	ESI(+), *m/z* = 192.0932 ([M+H]$^+$, calcd. for $C_{10}H_{11}FN_3$: 192.0932).
M.P.:	Decomposition at 210 °C.

All recorded spectral data are in accordance to literature.[92]

5.2.54 Synthesis of 4-amino-*N*-(1-(3-fluorobenzyl)-1*H*-pyrazol-4-yl)-3-nitro-benzamide (121)

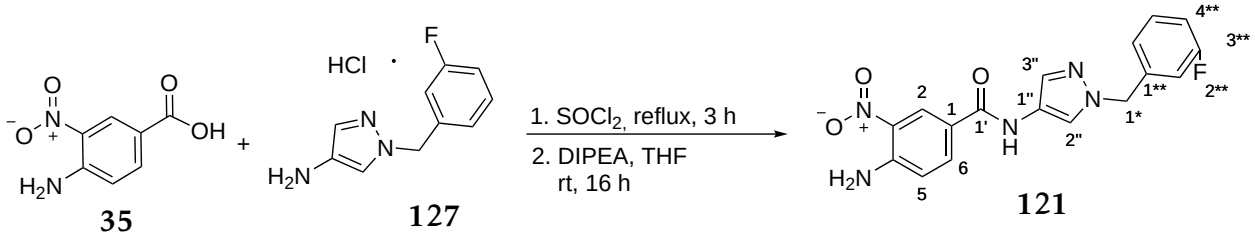

35 **127** **121**

Dry solvents were used and the reaction was carried out under Ar atmosphere.
In a 25 mL N_2-flask, 4-amino-3-nitrobenzoic acid (**35**) (392 mg, 2.00 mmol, 1.00 eq) was suspended in thionyl chloride (6 mL) and heated to reflux for 3 h. Excess thionyl chloride was removed by distillation and the residue was dried *in vacuo*. Afterwards, it was dissolved in THF (10 mL) and the solution was cooled to 0 °C. At this temperature, compound **127** · HCl (459 mg, 2.40 mmol, 1.20 eq) and DIPEA (2.04 mL, 12.00 mmol, 6.00 eq) were added. Complete conversion was achieved by stirring for 16 h at room temperature (determined via TLC). The reaction mixture was washed with sat. K_2CO_3-solution (40 mL) and the aqueous layer extracted with EtOAc (3x 30 mL). The combined organic layers were washed with sat. NaCl-solution, dried over $MgSO_4$, filtered and evaporated to dryness. The residue was adsorbed onto silica and purification was performed via column chromatography (silica, Cyhex/EtOAC (+NH_3 in MeOH) 75:25 → 50:50), which afforded 4-amino-*N*-(1-(3-fluorobenzyl)-1*H*-pyrazol-4-yl)-3-nitro-benzamide (**121**) (452 mg, 1.27 mmol, 63%) as a yellow solid.

^{1}H-NMR: 500 MHz, DMSO-d_6, δ_H = 5.34 (s, 2H, H-C1*), 7.03-7.14 (m, 4H, H-C5, H-C4** - H-C6**), 7.54 (ddd, $^3J_{H,F}$=8.0 Hz, $^4J_{H,H}$=1.7 Hz, 1.7 Hz, 1H, H-C2**), 7.63 (s, 1H, H-C2"), 7.81 (br, s, 2H, NH_2), 7.95 (dd, $^3J_{H,H}$=8.9 Hz, $^4J_{H,H}$=2.3 Hz, 1H, H-C6), 8.15 (s, 1H, H-C3"), 8.69 (d, $^4J_{H,H}$=2.0 Hz, 1H, H-C2), 10.39 (br, s, 1H, CONH) ppm.

^{13}C-NMR: 125 MHz, DMSO-d_6, δ_C = 54.2 (1C, C1*), 114.2 (d, $^2J_{C,F}$=21.6 Hz, 1C, C2** or C4**), 114.3 (d, $^2J_{C,F}$=20.4 Hz, 1C, C2** or C4**), 119.0 (1C, C5), 120.8 (1C, C2), 121.2 (1C, C2"), 122.1 (1C, C3), 123.5 (d, $^4J_{C,F}$=2.4 Hz, 1C, C6**), 125.5 (1C, C1), 129.6 (1C, C1"), 130.5 (d, $^3J_{C,F}$=8.4 Hz, 1C, C5**), 130.9 (1C, C3"), 134.0 (1C, C6), 140.5 (d, $^3J_{C,F}$=7.2 Hz, 1C, C1**), 147.8 (1C, C4), 161.7 (1C, C1'), 162.1 (d, $^1J_{C,F}$=244.8 Hz, 1C, C3**) ppm.

^{19}F-NMR: 377 MHz, DMSO-d_6, δ_F = -113.11 ppm.

HR-MS: ESI(+), *m/z* = 356.1152 ($[M+H]^+$, calcd. for $C_{17}H_{15}FN_5O_3$: 356.1157).

EA-CHN: 57.02% C, 4.12% H, 19.28% N (calcd. for $C_{17}H_{14}FN_5O_3 \cdot 0.25\ H_2O$: 56.75% C, 4.06% H, 19.46% N).

M.P.: 238.4 °C.

5.2.55 Synthesis of 3,5-dichlorobenzyl bromide (123)

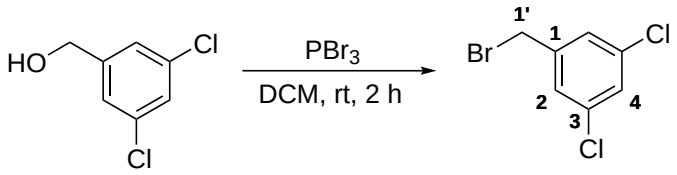

168 **123**

Dry solvents were used and the reaction was carried out under Ar atmosphere.
In a 100 mL N_2-flask, 3,5-dichlorobenzyl alcohol (**168**) (5.00 g, 28.2 mmol, 1.00 eq) was dissolved in DCM (50 mL). Afterwards, PBr_3 (2.68 mL, 28.2 mmol, 1.00 eq) was added dropwise and the resulting solution stirred at RT for 2 h. After this time, complete conversion was detected by TLC and the reaction was quenched by addition of water (75 mL). The aqueous layer was extracted with DCM (3x50 mL), the combined organic layers were washed with sat. NaCl-solution, dried over $MgSO_4$, filtered and evaporated to dryness. The desired 3,5-dichlorobenzyl bromide (**123**) was obtained as a beige solid (6.56 g, 27.34 mmol, 97%).

^{1}**H-NMR:**	500 MHz, $CDCl_3$, δ_H = 4.38 (s, 2H, H-C1'), 7.28 (d, $^4J_{H,H}$=1.8 Hz, 2H, H-C2), 7.30 (t, $^4J_{H,H}$=1.8 Hz, 1H, H-C4) ppm.
^{13}**C-NMR:**	125 MHz, $CDCl_3$, δ_C = 31.1 (1C, C1'), 127.6 (2C, C2), 128.7 (1C, C4), 135.3 (2C, C3), 140.9 (1C, C1) ppm.
HR-MS:	EI(+), *m/z* = 237.89539 ([M]$^+$, calcd. for $C_7H_5^{79}Br^{35}Cl_2$: 237.89517).
M.P.:	60.8 °C.

All recorded spectral data are in accordance to literature.[93]

5.2.56 Synthesis of 1-(3,5-dichlorobenzyl)-4-nitro-1*H*-pyrazole (126)

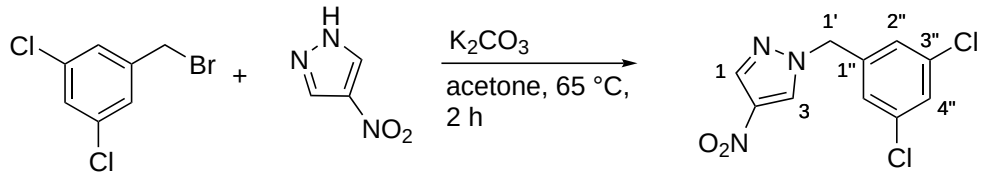

123 **78** **126**

A 100 mL two-necked flask was charged with 4-nitro-1*H*-pyrazole (**78**) (1.89 g, 16.67 mmol, 1.00 eq), compound **123** (4.00 g, 16.67 mmol, 1.00 eq) and K_2CO_3 (11.52 g, 83.35 mmol, 5.00 eq). The solids were suspended in acetone (50 mL) and the mixture heated to 65 °C for 2 h. Afterwards, complete conversion was detected by TLC, so that EtOAc (50 mL) was added and the mixture was washed with water (75 mL) and the aqueous layer extracted with EtOAc (3x 50 mL). The combined organic layers were dried over $MgSO_4$, filtered and evaporated to dryness. The residue was adsorbed onto silica and purified by column chromatography (Cyhex/EtOAc 85:15 → 75:25), which afforded 1-(3,5-dichlorobenzyl)-4-nitro-1*H*-pyrazole (**126**) as a white solid (3.24 g, 11.91 mmol, 71%).

^{1}H-NMR: 500 MHz, DMSO-d_6, δ_H = 5.42 (s, 2H, H-C1'), 7.42 (d, $^4J_{H,H}$=1.8 Hz, 2H, H-C2"), 7.59 (dd, $^4J_{H,H}$=1.8 Hz, 1.8 Hz, 1H, H-C4"), 8.29 (s, 1H, H-C1), 9.04 (s, 1H, H-C2) ppm.

^{13}C-NMR: 125 MHz, DMSO-d_6, δ_C = 54.4 (1C, C1'), 127.0 (2C, C2"), 127.8 (1C, C4"), 131.1 (1C, C3), 134.2 (1C, C1), 135.2 (1C, C2), 136.2 (2C, C3"), 139.6 (1C, C1") ppm.

HR-MS: APCI(+), *m/z* = 271.9985 ([M+H]$^+$, calcd. for $C_{10}H_8^{35}Cl_2N_3O_2$: 271.9988).

M.P.: 95.6 °C.

5.2.57 Synthesis of 1-(3,5-dichlorobenzyl)-1*H*-pyrazol-4-amine (128)

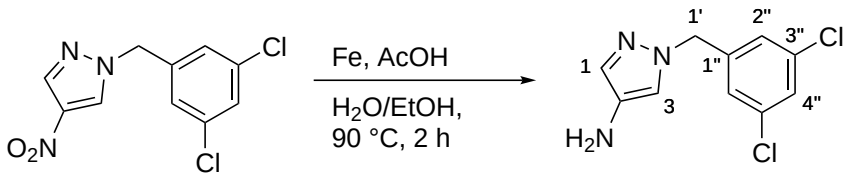

126 **128**

The reaction was carried out under Ar atmosphere.
In a 100 mL two-necked flask, compound **126** (1.50 g, 5.51 mmol, 1.00 eq) and iron powder (927 mg, 16.6 mmol, 3.00 eq) were suspended in ethanol (25 mL) and water (20 mL). Acetic acid (0.32 mL, 5.51 mmol, 1.00 eq) was added and the suspension was heated to reflux for 2 h. After this time, complete conversion was detected by TLC. The solids were removed by filtration and sat. K_2CO_3-solution (60 mL) was added to the filtrate. Afterwards, the filtrate was extracted with EtOAc (3x 40 mL), the combined organic layers washed with sat. NaCl-solution, dried over $MgSO_4$, filtered and evaporated to dryness. The residue was dissolved in EtOAc (30 mL) and HCl-solution (2 M in DEE, 5.5 mL, 2.00 eq) was added. The obtained solid was collected by filtration, washed with EtOAc and DEE and dried *in vacuo*. Finally, it was further purified by prep-HPLC (Water/MeCN 80:20 → 5:95) to afford 1-(3,5-dichlorobenzyl)-1*H*-pyrazol-4-amine (**128**) as a beige solid (967 mg, 3.99 mmol, 72%).

^{1}H-NMR: 500 MHz, DMSO-d_6, δ_H = 4.06 (br, s, 2H, NH_2), 5.17 (s, 2H, H-C1'), 7.00 (d, $^4J_{H,H}$=0.9 Hz, 1H, H-C3), 7.16-7.17 (m, 3H, H-C2", H-C1), 7.50 (dd, $^4J_{H,H}$=1.8 Hz, 1.8 Hz, 1H, H-C4") ppm.

^{13}C-NMR: 125 MHz, DMSO-d_6, δ_C = 53.3 (1C, C1'), 117.0 (1C, C3), 125.9 (2C, C2"), 126.9 (1C, C4), 130.4 (1C, C1), 131.2 (1C, C2), 134.0 (2C, C3"), 142.6 (1C, C1") ppm.

HR-MS: ESI(+), *m/z* = 242.0246 ([M+H]$^+$, calcd. for $C_{10}H_{10}^{35}Cl_2N_3$: 242.0246).

M.P.: Decomposition at 213 °C.

5.2.58 Synthesis of 4-amino-*N*-(1-(3,5-dichlorobenzyl)-1*H*-pyrazol-4-yl)-3-nitrobenzamide (122)

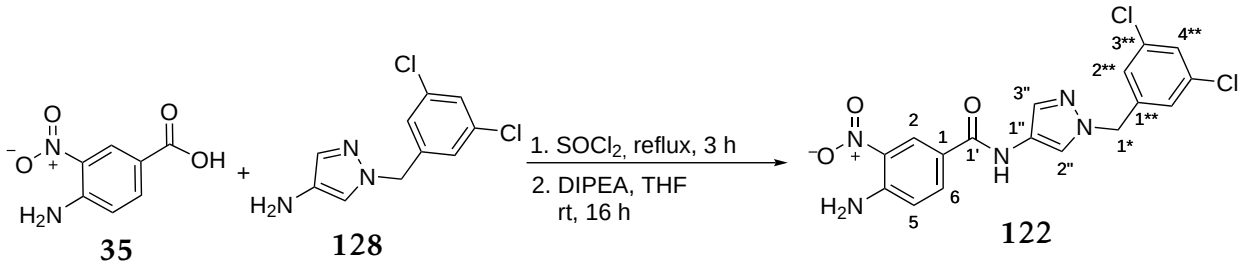

35 128 122

Dry solvents were used and the reaction was carried out under Ar atmosphere.
In a 50 mL N_2-flask, 4-amino-3-nitrobenzoic acid (**35**) (297 mg, 1.63 mmol, 1.00 eq) was suspended in thionyl chloride (5 mL) and heated to reflux for 3 h. Excess thionyl chloride was removed by distillation and the residue was dried *in vacuo*. Afterwards, it was dissolved in THF (8 mL) and the solution was cooled to 0 °C. At this temperature, compound **128** (500 mg, 1.79 mmol, 1.10 eq) and DIPEA (1.10 mL, 6.52 mmol, 4.00 eq) were added. Complete conversion was achieved by stirring for 16 h at room temperature (determined via TLC). The reaction mixture was washed with sat. K_2CO_3-solution (30 mL) and the aqueous layer extracted with EtOAc (3x 30 mL). The combined organic layers were washed with sat. NaCl-solution, dried over $MgSO_4$, filtered and evaporated to dryness. The residue was adsorbed onto Celite® and purification was performed via column chromatography (silica, DCM/MeOH (+NH_3) 97:3 → 93:7), which afforded 4-amino-*N*-(1-(3,5-dichlorobenzyl)-1*H*-pyrazol-4-yl)-3-nitrobenzamide (**122**) (425 mg, 1.04 mmol, 64%) as a yellow solid.

^{1}H-NMR: 500 MHz, DMSO-d_6, δ_H = 5.35 (s, 2H, H-C1*), 7.08 (d, $^3J_{H,H}$=8.9 Hz, 1H, H-C5), 7.26 (d, $^4J_{H,H}$=1.7 Hz, 2H, H-C2**), 7.54 (dd, $^4J_{H,H}$=1.7 Hz, 1.7 Hz, 1H, H-C4**), 7.65 (d, $^4J_{H,H}$=0.6 Hz, 1H, H-C2"), 7.81 (br, s, 2H, NH_2), 7.95 (dd, $^3J_{H,H}$=8.9 Hz, $^4J_{H,H}$=2.0 Hz, 1H, H-C6), 8.20 (d, $^4J_{H,H}$=0.6 Hz, 1H, H-C3"), 8.62 (d, $^4J_{H,H}$=2.3 Hz, 1H, H-C2), 10.41 (br, s, 1H, CONH) ppm.

^{13}C-NMR: 125 MHz, DMSO-d_6, δ_C = 53.5 (1C, C1*), 119.0 (1C, C5), 120.7 (1C, C2), 121.4 (1C, C2"), 122.1 (1C, C3), 125.5 (1C, C5), 126.3 (2C, C2**), 127.2 (1C, C4**), 129.6 (1C, C1"), 131.3 (1C, C3"), 134.0 (2C, C3**), 134.0 (1C, C6), 141.9 (1C, C1**), 147.8 (1C, C4), 161.7 (1C, C1') ppm.

HR-MS: ESI(-), *m/z* = 404.0328 ($[M-H]^-$, calcd. for $C_{17}H_{12}^{35}Cl_2N_5O_3$: 404.0312).

EA-CHN: 50.08% C, 3.40% H, 16.96% N (calcd. for $C_{17}H_{13}Cl_2N_5O_3$: 50.26% C, 3.23% H, 17.24% N).

M.P.: 245.3 °C.

5.2.59 Synthesis of 5-(3-chlorobenzyl)-1,3,4-oxadiazol-2-amine (131)

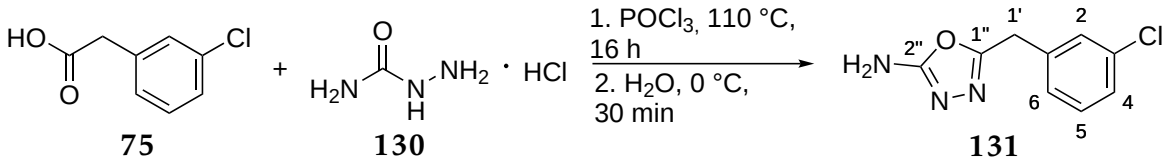

75 **130** **131**

The reaction was carried out under Ar atmosphere.

In a 25 mL N_2-flask, 3-chlorophenylacetic acid (**75**) (1.50 g, 8.79 mmol, 1.00 eq) was dissolved in $POCl_3$ (4 mL). Semicarbazide · HCl (**130**) (1.96 g, 17.59 mmol, 2.00 eq) was added and the solution was stirred at reflux for 16 h. After this time, the solution was cooled to 0 °C and water (10 mL) was cautiously added. After stirring for 30 min at this temperature, the solution was adjusted to pH=7 (NaOH-solution, 4 M), upon which a white solid precipitated, which was collected by filtration and washed with $NaHCO_3$-solution and water and afterwards dried *in vacuo*. The desired 5-(3-chlorobenzyl)-1,3,4-oxadiazol-2-amine (**131**) (1.82 g, 8.65 mmol, 98%) was obtained as a white solid.

^{1}H-NMR: 500 MHz, DMSO-d_6, δ_H = 4.07 (s, 2H, H-C1'), 6.90 (br, s, 2H, NH_2), 7.24-7.39 (m, 4H, H-C2, H-C4 - H-C6) ppm.

^{13}C-NMR: 125 MHz, DMSO-d_6, δ_C = 30.3 (1C, C1'), 127.0 (1C, C4), 127.4 (1C, C6), 128.6 (1C, C2), 130.4 (1C, C5), 133.1 (1C, C3), 137.7 (1C, C1), 157.5 (1C, C1"), 163.9 (1C, C2") ppm.

HR-MS: ESI(+), *m/z* = 210.0435 ($[M+H]^+$, calcd. for $C_9H_9ClN_3O$: 210.0429).

M.P.: 174.3 °C.

5.2.60 Synthesis of 4-amino-*N*-(5-(3-chlorobenzyl)-1,3,4-oxadiazol-2-yl)-3-nitrobenzamide (129)

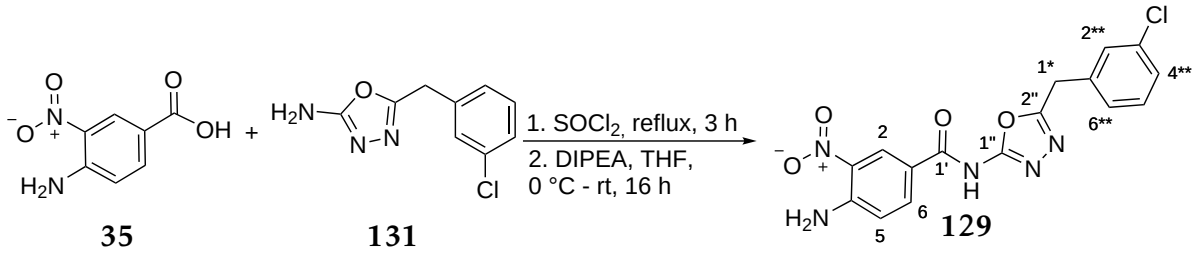

35 **131** **129**

Dry solvents were used and the reaction was carried out under Ar atmosphere.
In a 25 mL N_2-flask, 4-amino-3-nitrobenzoic acid (**35**) (365 mg, 2.00 mmol, 1.00 eq) was suspended in thionyl chloride (6 mL) and heated to reflux for 3 h. Excess thionyl chloride was removed by distillation and the residue was dried *in vacuo*. Afterwards, it was dissolved in THF (10 mL) and the solution was cooled to 0 °C. At this temperature, compound **131** (504 mg, 2.40 mmol, 1.20 eq) and DIPEA (0.68 mL, 4.00 mmol, 2.00 eq) were added. Complete conversion could be obtained after stirring for 16 h at room temperature (determined via TLC). The reaction mixture was washed with water (30 mL) and the aqueous layer extracted with EtOAc (3x 30 mL). The combined organic layers were dried over $MgSO_4$, filtered and evaporated to dryness. The residue was adsorbed onto silica and purification was performed via column chromatography (silica, DCM/MeCN (+ HCOOH) 50:50). Since the product still contained impurities, it was recrystallized from MeCN. The desired 4-amino-*N*-(5-(3-chlorobenzyl)-1,3,4-oxadiazol-2-yl)-3-nitrobenzamide (**129**) (120 mg, 0.32 mmol, 16%) was obtained as a yellow solid.

^{1}H-NMR: 500 MHz, DMSO-d_6, δ_H = 4.29 (s, 2H, H-C1*), 7.07 (d, $^3J_{H,H}$=8.9 Hz, 1H, H-C5), 7.33-7.45 (m, 4H, H-C2**, H-C4** - H-C6**), 7.94-7.96 (m, 3H, H-C6, NH_2), 8.76 (d, $^4J_{H,H}$=2.0 Hz, 1H, H-C2), 11.87 (br, s, 1H, CONH) ppm.

^{13}C-NMR: 125 MHz, DMSO-d_6, δ_C = 30.3 (1C, C1*), 118.8 (1C, C3), 119.1 (1C, C5), 127.2 (1C, C2** or C6**), 127.3 (1C, C2), 127.7 (1C, C4** or C5**), 128.8 (1C, C2** or C6**), 129.5 (1C, C1), 130.5 (1C, C4** or C5**), 133.2 (1C, C3**), 134.4 (1C, C6), 136.8 (1C, C1**), 148.6 (1C, C4), 158.3 (1C, C1"), 162.1 (1C, C2"), 163.5 (1C, C1') ppm.

HR-MS: ESI(-), *m/z* = 372.0509 ($[M-H]^-$, calcd. for $C_{16}H_{11}ClN_5O_4$: 372.0505).

q-^{1}H-NMR: 500 MHz, DMSO-d_6, maleic acid as internal standard: 95.4% ± 0.16% purity.

M.P.: 180.2 °C.

5.2.61 Synthesis of *tert*-butyl (*tert*-butoxycarbonyl)(2-chloropyrimidin-4-yl) carbamate (139)

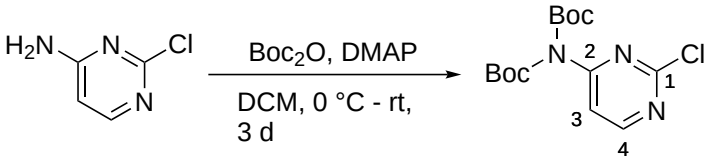

138 **139**

Dry solvents were used and the reaction was carried out under Ar atmosphere.
In a 250 mL N_2-flask, 4-amino-2-chloro-pyrimidine (**138**) (1.94 g, 15.0 mmol, 1.00 eq) was dissolved in DCM (120 mL) and cooled to 0 °C. At this temperature, Boc_2O (7.20 g, 33.0 mmol, 2.20 eq) and DMAP (366 mg, 3.00 mmol, 0.20 eq) were added. Over night, the reaction mixture was allowed to warm up to room temperature and after 3 d of stirring at RT, complete conversion was detected by TLC. The reaction mixture was washed with sat. NH_4Cl-solution (80 mL) and the aqueous layer extracted with DCM (3x 80 mL). The combined organic layers were dried over $MgSO_4$, filtered and the solvent removed under reduced pressure. The crude material was adsorbed onto silica and purified via column chromatography (Cyhex/EtOAc 95:5 → 75:25) to afford *tert*-butyl (*tert*-butoxycarbonyl)(2-chloropyrimidin-4-yl)carbamate (**139**) as a white solid (4.12 g, 12.50 mmol, 83%).

^{1}H-NMR: 500 MHz, DMSO-d_6, δ_H = 1.49 (s, 18H, ^{t}Bu), 7.73 (d, $^3J_{H,H}$=5.7 Hz, 1C, H-C3), 8.72 (d, $^3J_{H,H}$=5.7 Hz, 1C, H-C4) ppm.

^{13}C-NMR: 125 MHz, DMSO-d_6, δ_C = 27.2 (6C, ^{t}Bu), 84.9 (2C, $C(CH_3)_3$), 111.2 (1C, C3), 149.0 (1C, C4), 158.6 (1C, C1), 159.3 (1C, C2), 161.4 (2C, COON) ppm.

HR-MS: ESI(+), *m/z* = 352.1041 ($[M+Na]^+$, calcd. for $C_{14}H_{20}ClN_3O_4Na$: 352.1035).

M.P.: 71.9 °C.

5.2.62 Synthesis of *tert*-butyl (*tert*-butoxycarbonyl)(2-(3-methylbenzyl)pyrimidin-4-yl)carbamate (142)

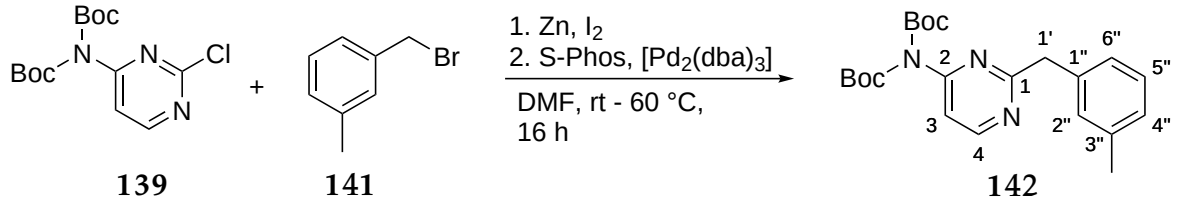

139 **141** **142**

Dry solvents were used and the reaction was carried out under Ar atmosphere.
In a 100 mL three-necked flask, zinc powder (2.38 g, 36.36 mmol, 6.00 eq) and iodine (386 mg, 1.52 mmol, 0.25 eq) were suspended in DMF (11 mL) and 3-methylbenzylbromide (**141**) (1.64 mL, 12.12 mmol, 2.00 eq) was added. After stirring for 1 h at RT, compound **139** (2.00 g, 6.06 mmol, 1.00 eq), S-Phos (250 mg, 0.61 mmol, 0.10 eq) and $[Pd_2(dba)_3]$ (284 mg, 0.31 mmol, 0.05 eq) were added. The reaction mixture was stirred at 60 °C until complete conversion was detected by TLC (16 h). Afterwards, the reaction mixture was filtered over Celite® and the filtrate concentrated to $\frac{1}{3}$ residual volume. 50 mL DCM were added and the solution was washed with LiCl-solution (5% (m/m), 50 mL). The aqueous layer was extracted with DCM (3x 50 mL) and the combined organic layers washed with LiCl-solution (5% (m/m), 50 mL), dried over $MgSO_4$, filtered and the solvent removed under reduced pressure. The crude product was adsorbed onto silica and purified via column chromatography (Cyhex/EtOAc 88:12), which afforded *tert*-butyl (*tert*-butoxycarbonyl)(2-(3-methylbenzyl)pyrimidin-4-yl)carbamate (**142**) as a yellow oil (1.15 g, 2.87 mmol, 47%).

^{1}H-NMR: 500 MHz, DMSO-d_6, δ_H = 1.42 (s, 18H, ^{t}Bu), 2.25 (2, 3H, Me), 4.07 (s, 2H, H-C1'), 7.00-7.06 (m, 3H, H-C4" - H-C6"), 7.15 (dd, $^3J_{H,H}$=7.7 Hz, 7.7 Hz, 1H, H-C2"), 7.49 (d, $^3J_{H,H}$=5.7 Hz, 1H, H-C3), 8.69 (d, $^3J_{H,H}$=5.7 Hz, 1H, H-C4) ppm.

^{13}C-NMR: 125 MHz, DMSO-d_6, δ_C = 20.9 (1C, Me), 27.1 (6C, ^{t}Bu), 44.8 (1C, C1'), 83.9 (1C, $C(CH_3)_3$)), 110.7 (1C, C3), 125.9 (1C, C4" or C6"), 127.0 (1C, C4" or C6"), 128.2 (1C, C5"), 129.4 (1C, C2"), 137.3 (1C, C1" or C3"), 137.9 (1C, C1" or C3"), 149.6 (1C, C4), 157.9 (1C, C1), 158.8 (2C, CON), 168.8 (1C, C2) ppm.

HR-MS: APCI(+), *m/z* = 422.2047 ($[M+Na]^+$, calcd. for $C_{22}H_{29}N_3O_4Na$: 422.2050).

M.P.: Liquid at RT.

5.2.63 Synthesis of 2-(3-methylbenzyl)pyrimidin-4-amine (143)

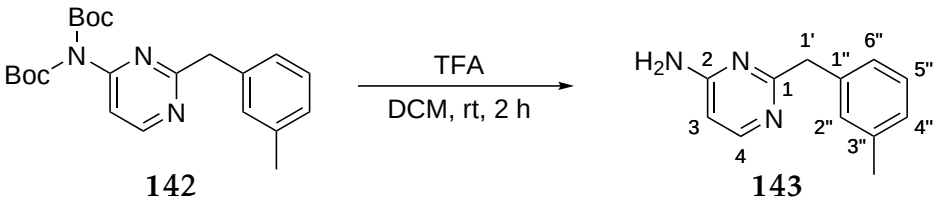

142 **143**

In a 100 mL round-bottomed flask, compound **142** (1.10 g, 2.75 mmol, 1.00 eq) was dissolved in DCM (12 mL). Trifluoroacetic acid (4.0 mL) was added dropwise, where upon the colorless solution turned orange. After 2 h stirring at RT, complete conversion was detected by LC-MS. The reaction mixture was washed with sat. K_2CO_3-solution (30 mL) and the aqueous layer extracted with DCM (3x 30 mL). The combined organic layers were washed with water (30 mL), dried over $MgSO_4$, filtered and the solvent removed under reduced pressure. The crude material was adsorbed onto silica and purified via column chromatography (Cyhex/EtOAc 40:60 → 0:100). The desired compound 2-(3-methylbenzyl)pyrimidin-4-amine (**143**) was obtained as a white solid (435 mg, 2.19 mmol, 80%).

^{1}H-NMR: 500 MHz, DMSO-d_6, δ_H = 2.51 (s, 3H, Me), 3.81 (s, 2H, H-C1'), 6.24 (d, $^3J_{H,H}$=5.7 Hz, 1H, H-C3), 6.75 (br, s, 2H, NH_2), 6.97-7.06 (m, 3H, H-C4" - H-C6"), 7.14 (dd, $^3J_{H,H}$=7.7 Hz, 7.7 Hz, 1H, H-C2"), 7.98 (d, $^3J_{H,H}$=5.7 Hz, 1H, H-C4") ppm.

^{13}C-NMR: 125 MHz, DMSO-d_6, δ_C = 21.0 (1C, Me), 45.2 (1C, C1'), 102.4 (1C, C3), 125.9 (1C, C4" or C6"), 126.6 (1C, C4" or C6"), 128.0 (1C, C5"), 129.5 (1C, C2"), 137.1 (1C, C1"), 138.9 (1C, C3"), 155.0 (1C, C4), 163.6 (1C, C2), 168.5 (1C, C1) ppm.

HR-MS: ESI(+), *m/z* = 200.1181 ($[M+H]^+$, calcd. for $C_{12}H_{14}N_3$: 200.1181).

M.P.: 75.4 °C.

5.2.64 Synthesis of 4-amino-*N*-(2-(3-methylbenzyl)pyrimidin-4-yl)-3-nitro-benzamide (140)

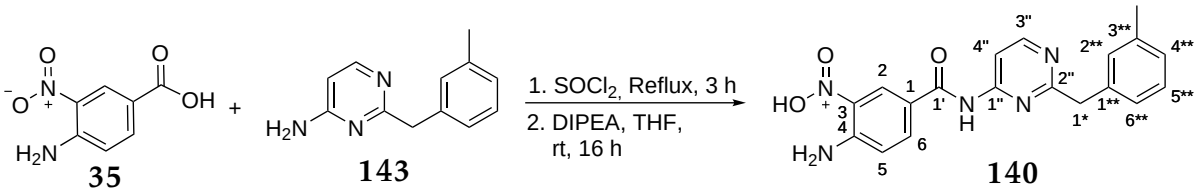

35 **143** **140**

Dry solvents were used and the reaction was carried out under Ar atmosphere.
In a 50 mL N_2-flask, 4-amino-3-nitrobenzoic acid (**35**) (332 mg, 1.82 mmol, 1.00 eq) was suspended in thionyl chloride (5 mL) and heated to reflux for 3 h. Excess thionyl chloride was removed by distillation and the residue was dried *in vacuo*. Afterwards, it was dissolved in THF (8 mL) and the solution was cooled to 0 °C. At this temperature, compound **143** (400 mg, 2.00 mmol, 1.10 eq) and DIPEA (0.93 mL, 5.46 mmol, 3.00 eq) were added. Complete conversion was achieved by stirring for 16 h at room temperature (determined via TLC). The reaction mixture was washed with sat. K_2CO_3-solution (40 mL) and the aqueous layer extracted with EtOAc (3x 30 mL). The combined organic layers were washed with HCl-solution (0.5 M), dried over $MgSO_4$, filtered and evaporated to dryness. The residue was adsorbed onto Celite® and purification was performed via column chromatography (silica, DCM/MeOH (+NH_3) 98:2 → 95:5). The obtained product was recrystallized from ^{i}PrOH, which afforded 4-amino-*N*-(2-(3-methylbenzyl)pyrimidin-4-yl)-3-nitro-benzamide (**140**) (404 mg, 1.11 mmol, 61%) as a yellow solid.

^{1}H-NMR: 500 MHz, DMSO-d_6, δ_H = 2.26 (s, 3H, Me), 4.09 (s, 2H, H-C1*), 7.06-7.19 (m, 5H, H-C5, H-C2**, H-C4** - H-C6**), 7.90 (br, s, 2H, NH_2), 8.01 (sm, 2H, H-C6, H-C4"), 8.61 (d, $^{3}J_{H,H}$=7.6 Hz, 1H, H-C3"), 8.79 (d, $^{4}J_{H,H}$=2.0 Hz, 1H, H-C2), 11.15 (s, 1H, CONH) ppm.

^{13}C-NMR: 125 MHz, DMSO-d_6, δ_C = 20.9 (1C, Me), 44.9 (1C, C1*), 108.0 (1C, C4"), 118.8 (1C, C5), 125.9 (1C, C2** or C4** or C5** or C6**), 126.9 (1C, C2** or C4** or C5** or C6**), 127.5 (1C, C2), 128.2 (1C, C2** or C4** or C5** or C6**), 129.5 (1C, C2** or C4** or C5** or C6**), 129.5 (1C, C1), 134.5 (1C, C6), 137.3 (1C, C1**), 138.3 (1C, C3**), 148.4 (1C, C4), 158.5 (1C, C3"), 158.6 (1C, C1"), 165.1 (1C, C2"), 168.8 (1C, C1') ppm.

HR-MS: APCI(+), *m/z* = 364.1398 ($[M+H]^+$, calcd. for $C_{19}H_{18}N_5O_3$: 364.1404).

EA-CHN: 60.93% C, 4.88% H, 18.31% N (calcd. for $C_{19}H_{17}N_5O_3 \cdot 0.5\ H_2O$: 61.28% C, 4.87% H, 18.71% N).

M.P.: 90.8 °C.

5.2.65 Synthesis of 4-amino-*N*-(1-benzylpiperidin-4-yl)-3-nitrobenzamide (144)

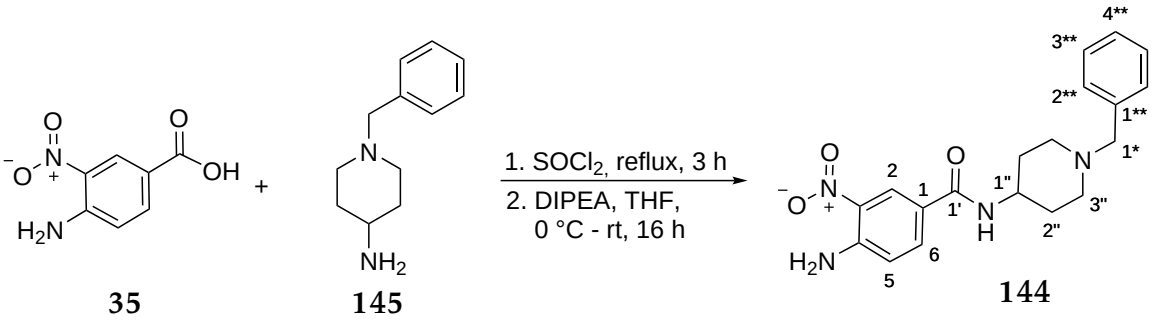

35 **145** **144**

Dry solvents were used and the reaction was carried out under Ar atmosphere.
In a 50 mL N_2-flask, 4-amino-3-nitrobenzoic acid (**35**) (455 mg, 2.50 mmol, 1.00 eq) was suspended in thionyl chloride (10 mL) and heated to reflux for 3 h. Excess thionyl chloride was removed by distillation and the residue was dried *in vacuo*. Afterwards, it was dissolved in THF (10 mL) and the solution was cooled to 0 °C. At this temperature, 4-amino-1-benzyl piperidine (0.61 mL, 3.00 mmol, 1.20 eq) and DIPEA (1.30 mL, 7.50 mmol, 3.00 eq) were added. Complete conversion was achieved by stirring for 16 h at room temperature (determined via TLC). The reaction mixture was washed with sat. K_2CO_3-solution (30 mL) and the aqueous layer extracted with EtOAc (3x 30 mL). The combined organic layers were washed with sat. NaCl-solution, dried over $MgSO_4$, filtered and evaporated to dryness. The residue was adsorbed onto silica and purification was performed via column chromatography (silica, DCM/MeOH (+NH_3) 93:7). The resulting product was recrystallized from ^{i}PrOH, which afforded 4-amino-*N*-(1-benzylpiperidin-4-yl)-3-nitrobenzamide (**144**) (789 mg, 2.23 mmol, 89%) as a yellow solid.

^{1}**H-NMR:** 500 MHz, DMSO-d_6, δ_H = 1.57 (sm, 2H, H-C2”), 1.76 (sm, 2H, H-C2”), 2.01 (sm, 2H, H-C3”), 2.82 (sm, 2H, HC3”), 3.47 (s, 2H, H-C1*), 3.74 (sm, 1H, H-C1”), 7.02 (d, $^{3}J_{H,H}$=8.9 Hz, 1H, H-C5), 7.22-7.34 (m, 5H, H-C2** - H-C4**), 7.71 (br, s, 2H, NH_2), 7.86 (dd, $^{3}J_{H,H}$=8.9 Hz, $^{4}J_{H,H}$=2.3 Hz, 1H, H-C6), 8.21 (d, $^{3}J_{H,H}$=7.7 Hz, 1H, CONH), 8.56 (d, $^{4}J_{H,H}$=2.3 Hz, 1H, H-C2) ppm.

^{13}**C-NMR:** 125 MHz, DMSO-d_6, δ_C = 31.5 (2C, C2”), 46.9 (1C, C1”), 52.2 (2C, C3”), 62.0 (1C, C1*), 118.7 (1C, C5), 121.5 (1C, C2), 125.3 (1C, C1), 124.8 (1C, C4**), 128.1 (2C, C3**), 128.7 (2C, C2**), 129.5 (1C, C1**), 134.0 (1C, C6), 138.5 (1C, C3), 147.6 (1C, C4), 163.7 (1C, C1’) ppm.

HR-MS: ESI(+), *m/z* = 355.1759 ($[M+H]^+$, calcd. for $C_{19}H_{23}N_4O_3$: 355.1765).

EA-CHN: 64.64% C, 6.35% H, 15.41% N (calcd. for $C_{19}H_{22}N_4O_3$: 64.39% C, 6.26% H, 15.81% N).

M.P.: 190.3 °C.

5.2.66 Synthesis of 5-(3-chlorophenethyl)-1,3,4-thiadiazol-2-amine (149)

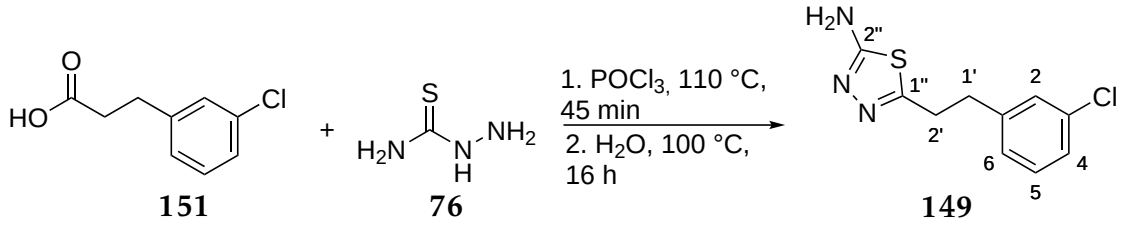

151 **76** **149**

The reaction was carried out under Ar atmosphere.
A 50 mL three-necked-flask was charged with 3-chlorophenylpropionic acid (**151**) (738 mg, 4.00 mmol, 1.00 eq) and thiosemicarbazide (**76**) (366 mg, 4.00 mmol, 1.00 eq). The solids were suspended in $POCl_3$ (4 mL) and heated to reflux for 45 min. During this time, the solids dissolved completely. After the given time, the reaction mixture was cooled to 0 °C and water (8 mL) was slowly added. After stirring for 30 min at 0 °C, the reaction mixture was heated to reflux for 16 h. Afterwards, the suspension was filtered hot and the filtrate was adjusted to pH=11-12, whereupon a white solid precipitated, which was collected by filtration and washed with water and DEE. Drying *in vacuo* afforded 5-(3-chlorophenethyl)-1,3,4-thiadiazol-2-amine (**149**) (696 mg, 2.90 mmol, 73%) as a white solid.

^{1}**H-NMR:**	500 MHz, DMSO-d_6, δ_H = 2.95 (t, $^3J_{H,H}$=7.8 Hz, 2H, H-C1'), 3.12 (t, $^3J_{H,H}$=7.8 Hz, 2H, H-C2'), 7.04 (br, s, 2H, NH_2), 7.21-7.35 (m, 4H, H-C2, H-C4 - H-C6) ppm.
^{13}**C-NMR:**	125 MHz, DMSO-d_6, δ_C = 30.6 (1C, C2'), 34.0 (1C, C1'), 126.1 (1C, C4 or C6), 127.2 (1C, C4 or C6), 128.3 (1C, C2), 130.0 (1C, C5), 132.8 (1C, C3), 142.9 (1C, C1), 157.0 (1C, C2"), 168.2 (1C, C1") ppm.
HR-MS:	ESI(+), *m/z* = 240.0356 ([M+H]$^+$, calcd. for $C_{10}H_{11}ClN_3S$: 240.0357).
M.P.:	173.2 °C.

All recorded spectral data are in accordance to literature.[94]

5.2.67 Synthesis of 4-amino-*N*-(5-(3-chlorophenethyl)-1,3,4-thiadiazol-2-yl)-3-nitrobenzamide (146)

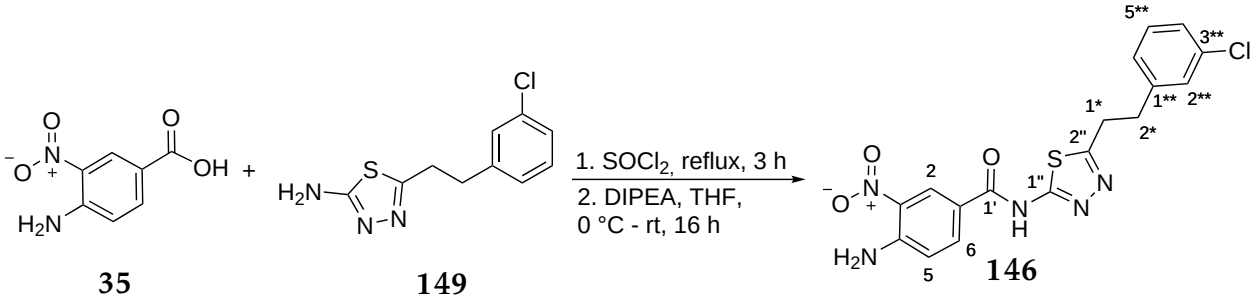

35 **149** **146**

Dry solvents were used and the reaction was carried out under Ar atmosphere.
In a 50 mL N_2-flask, 4-amino-3-nitrobenzoic acid (**35**) (346 mg, 1.90 mmol, 1.00 eq) was suspended in thionyl chloride (6 mL) and heated to reflux for 3 h. The excess thionyl chloride was removed by distillation and the residue was dried *in vacuo*. Afterwards, it was dissolved in THF (10 mL) and the solution was cooled to 0 °C. At this temperature, compound **149** (479 mg, 2.00 mmol, 1.05 eq) and DIPEA (0.68 mL, 4.00 mmol, 2.10 eq) were added. Complete conversion was achieved by stirring for 16 h at room temperature (determined via TLC). The reaction mixture was washed with sat. K_2CO_3-solution (40 mL) and the aqueous layer extracted with EtOAc (3x 30 mL). The combined organic layers were washed with sat. NaCl-solution, dried over $MgSO_4$, filtered and evaporated to dryness. The residue was adsorbed onto Celite® and purification was performed via column chromatography (silica, DCM/MeOH (+NH_3) 96:4 → 90:10), which afforded 4-amino-*N*-(5-(3-chlorophenethyl)-1,3,4-thiadiazol-2-yl)-3-nitrobenzamide (**146**) (424 mg, 1.05 mmol, 55%) as a yellow solid.

^{1}H-NMR: 500 MHz, DMSO-d_6, δ_H = 3.08 (t, $^3J_{H,H}$=7.5 Hz, 2H, H-C2*), 3.33 (t, $^3J_{H,H}$=7.5 Hz, 2H, H-C1*), 7.08 (d, $^3J_{H,H}$=8.9 Hz, 1H, H-C5), 7.24-33 (m, 3H, H-C4** - H-C6**), 7.39 (dd, $^4J_{H,H}$=1.4 Hz, 1.4 Hz, 1H, H-C2**), 7.95 (br, s, 2H, NH_2), 8.05 (dd, $^3J_{H,H}$=9.0 Hz, $^4J_{H,H}$=2.2 Hz, 1H, H-C6), 8.90 (d, $^4J_{H,H}$=2.3 Hz, 1H, H-C2), 12.85 (br, s, 1H, CONH) ppm.

^{13}C-NMR: 125 MHz, DMSO-d_6, δ_C = 30.2 (1C, C1*), 33.9 (1C, C2*), 118.2 (br, 1C, C3), 119.1 (1C, C5), 126.2 (1C, C4** or C6**), 127.2 (1C, C4** or C6**), 127.5 (1C, C2), 128.3 (1C, C2**), 129.7 (1C, C1), 130.0 (1C, C5**), 133.1 (1C, C3**), 134.3 (1C, C6), 142.8 (1C, C1**), 148.6 (1C, C4), 159.4 (br, 1C, C1''), 162.8 (br, 1C, C2''), 163.4 (br, 1C, C1') ppm.

HR-MS: ESI(-), *m/z* = 402.0436 ([M-H]$^-$, calcd. for $C_{17}H_{13}ClN_5O_3S$: 402.0433).

EA-CHN: 47.52% C, 4.08% H, 14.42% N (calcd. for $C_{17}H_{14}ClN_5O_3S \cdot DMSO$: 47.35% C, 4.18% H, 14.53% N).

M.P.: 145.2 °C.

5.2.68 Synthesis of 5-(3,5-dibromophenethyl)-1,3,4-thiadiazol-2-amine (150)

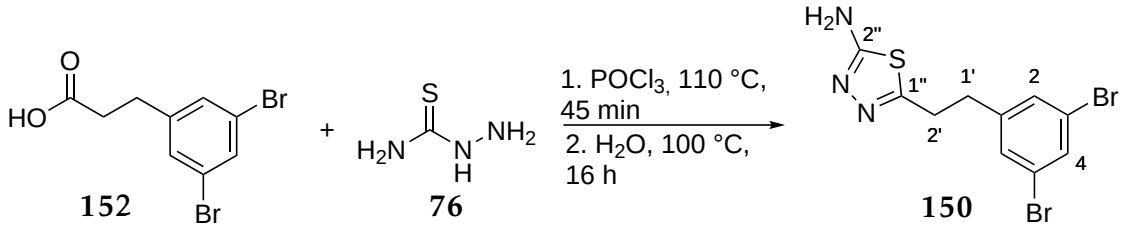

The reaction was carried out under Ar atmosphere.

A 50 mL three-necked-flask was charged with 3,5-dibromophenylpropionic acid (**152**) (1.00 g, 3.25 mmol, 1.00 eq) and thiosemicarbazide (**76**) (296 mg, 3.25 mmol, 1.00 eq). The solids were suspended in $POCl_3$ (4 mL) and heated to reflux for 45 min. During this time, the solids dissolved completely. After the given time, the reaction mixture was cooled to 0 °C and water (8 mL) was slowly added. After stirring for 30 min at 0 °C, the reaction mixture was heated to reflux for 16 h. Afterwards, the suspension was filtered hot and the filtrate was adjusted to pH=11-12, whereupon a white solid precipitated, which was collected by filtration and washed with water and MTBE. Drying *in vacuo* afforded 5-(3,5-dibromophenethyl)-1,3,4-thiadiazol-2-amine (**150**) (891 mg, 2.45 mmol, 76%) as a white solid.

^{1}H-NMR: 500 MHz, DMSO-d_6, δ_H = 2.96 (t, $^3J_{H,H}$=7.7 Hz, 2H, H-C1'), 3.13 (t, $^3J_{H,H}$=7.7 Hz, 2H, H-C2'), 6.97 (br, s, 2H, NH_2), 7.52 (d, $^4J_{H,H}$=1.7 Hz, 2H, H-C2), 7.65 (dd, $^4J_{H,H}$=1.7 Hz, 1.7 Hz, 1H, H-C4) ppm.

^{13}C-NMR: 125 MHz, DMSO-d_6, δ_C = 30.3 (1C, C2'), 33.4 (1C, C1'), 122.2 (2C, C3), 130.6 (2C, C2), 131.1 (1C, C2), 145.3 (1C, C1), 156.8 (1C, C2"), 168.2 (1C, C1") ppm.

HR-MS: ESI(+), *m/z* = 385.8763 ([M+Na]$^+$, calcd. for $C_{10}H_9Br_2N_3SNa$: 385.8766).

M.P.: 178.2 °C.

5.2.69 Synthesis of 4-amino-*N*-(5-(3,5-dibromophenethyl)-1,3,4-thiadiazol-2-yl)-3-nitrobenzamide (147)

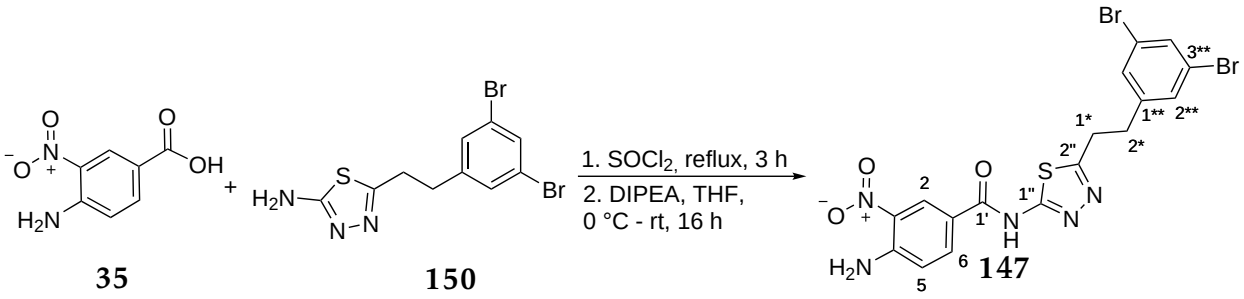

35 **150** **147**

Dry solvents were used and the reaction was carried out under Ar atmosphere.
In a 50 mL N_2-flask, 4-amino-3-nitrobenzoic acid (**35**) (120 mg, 0.66 mmol, 1.00 eq) was suspended in thionyl chloride (3 mL) and heated to reflux for 3 h. The excess thionyl chloride was removed by distillation and the residue was dried *in vacuo*. Afterwards, it was dissolved in THF (5 mL) and the solution was cooled to 0 °C. At this temperature, compound **150** (250 mg, 0.69 mmol, 1.05 eq) and DIPEA (0.25 mL, 1.32 mmol, 2.00 eq) were added. Complete conversion was achieved by stirring for 16 h at room temperature (determined via TLC). The reaction mixture was washed with sat. K_2CO_3-solution (30 mL) and the aqueous layer extracted with EtOAc (3x 25 mL). The combined organic layers were washed with sat. NaCl-solution, dried over $MgSO_4$, filtered and evaporated to dryness. The residue was adsorbed onto silica and purification was performed via column chromatography (silica, DCM/MeOH (+NH_3) 100:0 → 80:20). The resulting product was recrystallized from DMSO/Water, which afforded 4-amino-*N*-(5-(3,5-dibromophenethyl)-1,3,4-thiadiazol-2-yl)-3-nitrobenzamide (**147**) (224 mg, 0.42 mmol, 64%) as a yellow solid.

^{1}H-NMR: 500 MHz, DMSO-d_6, δ_H = 3.08 (t, $^3J_{H,H}$=8.0 Hz, 2H, H-C2*), 3.33 (t, $^3J_{H,H}$=7.7 Hz, 2H, H-C1*), 7.08 (d, $^3J_{H,H}$=9.2 Hz, 1H, H-C5), 7.57 (d, $^4J_{H,H}$=1.7 Hz, 2H, H-C2**), 7.66 (dd, $^4J_{H,H}$=1.7 Hz, 1.7 Hz, 1H, H-C4**), 7.96 (br, s, 2H, NH_2), 8.06 (dd, $^3J_{H,H}$=9.0 Hz, $^4J_{H,H}$=2.2 Hz, 1H, H-C6), 8.90 (d, $^4J_{H,H}$=2.0 Hz, 1H, H-C2), 12.84 (br, s, 1H, CONH) ppm.

^{13}C-NMR: 125 MHz, DMSO-d_6, δ_C = 29.9 (1C, C1*), 33.4 (1C, C2*), 118.1 (br, 1C, C3), 119.1 (1C, C5), 122.3 (2C, C3**), 127.5 (1C, C2), 129.7 (1C, C1), 130.6 (2C, C2**), 131.2 (1C, C4**), 134.3 (1C, C6), 145.2 (1C, C1**), 148.6 (1C, C4), 159.3 (br, 1C, C1''), 162.9 (br, 1C, C2''), 162.9 (br, 1C, C1') ppm.

HR-MS: ESI(-), *m/z* = 525.8994 ([M-H]$^-$, calcd. for $C_{17}H_{12}Br_2N_5O_3S$: 525.9013).

EA-CHN: 38.43% C, 2.68% H, 12.77% N (calcd. for $C_{17}H_{13}Br_2N_5O_3S \cdot 0.25$ DMSO: 38.45% C, 2.67% H, 12.81% N).

M.P.: 285.5 °C.

5.2.70 Synthesis of *tert*-butyl (1-phenethylpiperidin-4-yl)carbamate (155)

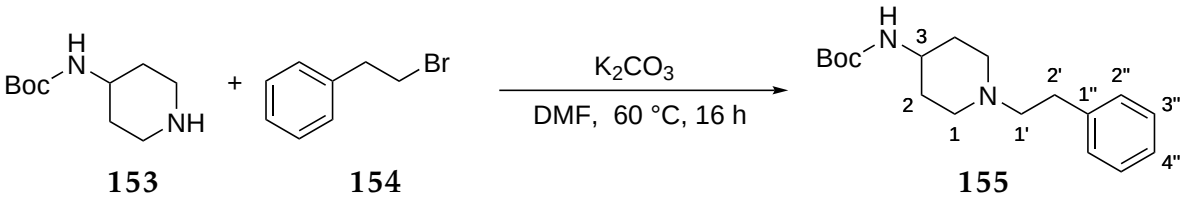

153 **154** **155**

In a 250 mL round-bottomed flask, *tert*-butyl-piperidin-4-yl-carbamate (**153**) (2.50 g, 12.50 mmol, 1.00 eq) and K_2CO_3 (5.18 g, 37.50 mmol, 3.00 eq) were suspended in DMF (150 mL). (2-Bromoethyl)benzene (**154**) (2.04 mL, 15.00 mmol, 1.20 eq) was added dropwise and the suspension was heated to 60 °C for 16 h. After the given time, complete conversion was detected by TLC, so that the reaction mixture was poured onto ice-cold water (300 mL). The resulting solid was collected by filtration, washed with water and cyclohexane and dried *in vacuo* to afford *tert*-butyl (1-phenethylpiperidin-4-yl)carbamate (**155**) as a white solid (2.46 g, 8.08 mmol, 65%).

^{1}H-NMR: 500 MHz, $CDCl_3$, δ_H = 1.44 (s, 9H, ^{t}Bu), 1.53-1.56 (m, 2H, H-C2), 1.98 (d, $^2J_{H,H}$=12.0 Hz, 2H, H-C2), 2.22 (t, $^2J_{H,H}$=10.6 Hz, 2H, H-C1), 2.63 (sm, 2H, H-C1), 2.84 (sm, 2H, H-C2'), 2.98 (sm, 2H, H-C1'), 3.51 (br, s, 1H, H-C3), 4.47 (d, $^4J_{H,H}$=5.4 Hz, 1H, NH), 7.18-7.21 (m, 3H, H-C3", H-C4"), 7.26-7.30 (m, 2H, H-C2") ppm.

^{13}C-NMR: 125 MHz, $CDCl_3$, δ_C = 28.5 (3C, CH_3), 32.4 (1C, C2'), 33.6 (1C, C2), 47.7 (1C, C3), 52.5 (1C, C1), 60.5 (1C, C1'), 79.5 (1C, $C(CH_3)_3$), 126.3 (1C, C4"), 128.6 (2C, C2" or C3"), 128.8 (2C, C2" or C3"), 140.0 (1C, C1"), 155.3 (1C CONH) ppm.

HR-MS: ESI(+), *m/z* = 305.2223 ($[M+H]^+$, calcd. for $C_{18}H_{29}N_2O_2$: 305.2224).

M.P.: 105.2 °C.

All recorded spectral data are in accordance to literature.[95]

5.2.71 Synthesis of 1-phenethylpiperidin-4-amine (156)

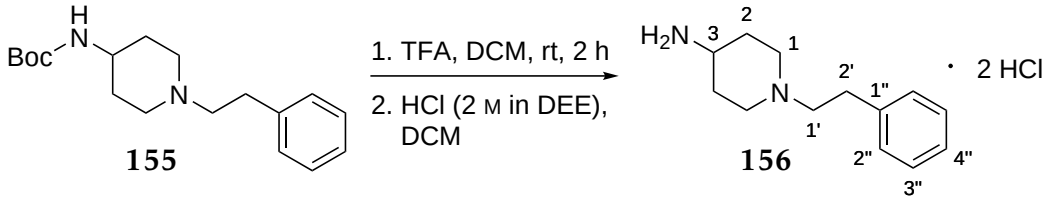

In 100 mL round-bottomed flask, compound **155** (1.50 g, 4.93 mmol, 1.00 eq) was dissolved in DCM (24 mL). Trifluoroacetic acid (4.00 mL) was added and the solution was stirred at RT for 3 h, after which complete conversion was detected by LC-MS. The reaction mixture was washed with sat. K_2CO_3-solution (50 mL) and the aqueous layer extracted with DCM (3x 40 mL). The combined organic layers were washed with water (40 mL), dried over $MgSO_4$, filtered and the solvent removed under reduced pressure. The resulting product was adsorbed onto silica and purified by column chromatography (DCM/MeOH (+NH_3), 10:1). Afterwards, it was dissolved in DCM (30 mL) and HCl-solution (2 M in DEE, 2 mL, 2.00 eq) was added dropwise. The resulting solid was collected by filtration, washed with DCM and dried *in vacuo* to afford 1-phenethylpiperidin-4-amine · 2 HCl (**156**) as a white solid (401 mg, 1.45 mmol, 29%).

^{1}**H-NMR:**	500 MHz, D_2O, δ_H = 2.04 (sm, 2H, H-C2), 2.42 (sm, 2H, H-C2), 3.15-3.28 (m, 4H, H-C2', H-C1), 3.49 (sm, 2H, H-C1), 3.62-3.68 (m, 1H, H-C3), 3.81 (d, $^3J_{H,H}$=11.4 Hz, 2H, H-C1'), 4.80 (d, $^3J_{H,H}$=6.0 Hz, 4H, NH_3^+, NH^+), 7.42-7.51 (m, 5H, H-C2" - H-C4") ppm.
^{13}**C-NMR:**	125 MHz, D_2O, δ_C = 26.9 (1C, C2'), 30.0 (2C, C2), 45.5 (2C, C1), 50.7 (1C, C3), 57.5 (1C, C1'), 127.5 (1C, C4"), 128.9 (2C, C2"), 129.2 (2C, C3"), 136.3 (1C, C1") ppm.
HR-MS:	ESI(+), *m/z* = 205.1698 ($[M+H]^+$, calcd. for $C_{13}H_{21}N_2$: 205.1699).
M.P.:	Decomposition at 285 °C.

All recorded spectral data are in accordance to literature.[95]

5.2.72 Synthesis of 4-amino-3-nitro-*N*-(1-phenethylpiperidin-4-yl) benzamide (148)

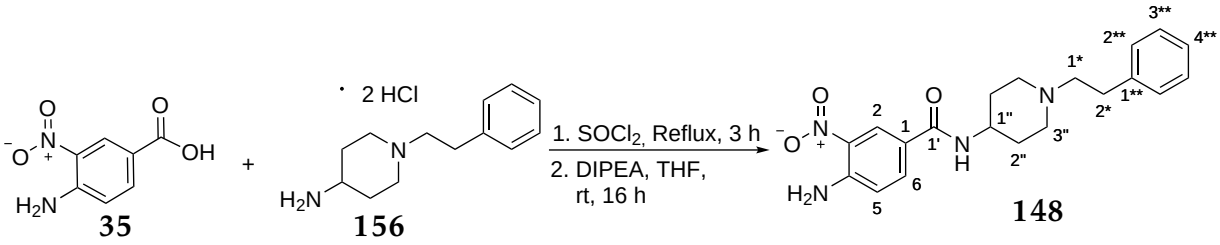

Dry solvents were used and the reaction was carried out under Ar atmosphere.
In a 25 mL N_2-flask, 4-amino-3-nitrobenzoic acid (**35**) (182 mg, 1.00 mmol, 1.00 eq) was suspended in thionyl chloride (4 mL) and heated to reflux for 3 h. Thionyl chloride was removed by distillation and the residue was dried *in vacuo*. Afterwards, it was dissolved in THF (6 mL) and the solution was cooled to 0 °C. At this temperature, compound **156** · 2 HCl (300 mg, 1.08 mmol, 1.10 eq) and DIPEA (0.85 mL, 5.00 mmol, 5.00 eq) were added. Since compound **156** did not dissolve completely, DMSO (2 mL) was added. Complete conversion could be obtained after stirring for 16 h at room temperature (determined via TLC). The reaction mixture was washed with sat. K_2CO_3-solution (40 mL) and the aqueous layer extracted with EtOAc (3x 30 mL). The combined organic layers were washed with sat. NaCl-solution, dried over $MgSO_4$, filtered and evaporated to dryness. The residue was adsorbed onto Celite® and purification was performed via column chromatography (silica, DCM/MeOH (+NH_3) 97:3 → 93:7), which afforded 4-amino-3-nitro-*N*-(1-phenethylpiperidin-4-yl)benzamide (**148**) (130 mg, 0.35 mmol, 35%) as a yellow solid.

^{1}H-NMR: 500 MHz, DMSO-d_6, δ_H = 1.56 (sm, 2H, H-C2''), 1.77 (sm, 2H, H-C2''), 2.05 (sm, 2H, H-C3''), 2.51 (dd, $^3J_{H,H}$=7.7 Hz, 7.7 Hz, 2H, H-C2*), 2.74 (dd, $^3J_{H,H}$=7.5 Hz, 7.7 Hz, 2H, H-C1*), 2.95 (sm, 2H, H-C3''), 3.74 (sm, 1H, H-C1''), 7.02 (d, $^3J_{H,H}$=9.2 Hz, 1H, H-C5), 7.16-7.29 (m, 5H, H-C2** - H-C4**), 7.71 (br, s, 2H, NH_2), 7.87 (dd, $^3J_{H,H}$=8.9 Hz, $^4J_{H,H}$=2.0 Hz, 1H, H-C6), 8.21 (d, $^3J_{H,H}$=7.7 Hz, 1H, CONH), 8.57 (d, $^4J_{H,H}$=2.0 Hz, 1H, H-C2) ppm.

^{13}C-NMR: 125 MHz, DMSO-d_6, δ_C = 31.5 (2C, C2''), 32.9 (1C, C2*), 46.9 (1C, C1''), 52.3 (2C, C3''), 59.9 (1C, C1*), 118.7 (1C, C5), 121.5 (1C, C2), 125.3 (1C, C1), 124.8 (1C, C4**), 128.1 (2C, C3**), 128.6 (2C, C2**), 129.5 (1C, C1**), 134.0 (1C, C6), 140.5 (1C, C3), 147.6 (1C, C4), 163.7 (1C, C1') ppm.

HR-MS: ESI(+), *m/z* = 369.1920 ($[M+H]^+$, calcd. for $C_{20}H_{25}N_4O_3$: 369.1921).

EA-CHN: 64.33% C, 6.42% H, 14.85% N (calcd. for $C_{20}H_{24}N_4O_3 \cdot 0.25\ H_2O$: 64.41% C, 6.62% H, 15.02% N).

M.P.: 221.2 °C.

5.3 Biochemical Assays

5.3.1 General

Crystallization buffers: The DENV2 crystallization buffer consisted of 20 mM Tris-HCl, 50 mM NaCl, 5% glycerol, adjusted to pH 7.5 and the DENV3 crystallization buffer consisted of 20 mM Tris, 150 mM NaCl, 5% glycerol, adjusted to pH 8.5. The bZIKV crystallization buffer consisted of 20 mM Tris, 2 mM DTT, 10% glycerol, 0.01% Triton X-100, adjusted to pH 8.5 and for bDENV4 protease, the same buffer as for bZIKV protease was used.

Assay buffers: The assay buffer used for the affinity determination utilizing DENV2 and DENV3 protease consisted of 50 mM Tris-HCl and 1 mM Chaps, adjusted to pH 9.0 and the assay buffer utilizing the binary protease constructs (bDENV4 and ZIKV) consisted of 20 mM Tris, 1 mM Chaps, 2 mM DTT, 10% glycerol and was adjusted to pH 8.5.

Flaviviral proteases: DENV2 and DENV3 proteases were over expressed and purified by W. Scanlan. The bDENV4 protease as well as the DENV3-I123F and DENV3-I123W mutants were over expressed and purified by Dr. A. Nguyen and the bZIKV protease was kindly provided by the Steinmetzer research group. All proteases were stored as solutions in the appropriate crystallization buffer at -80 °C.

Peptide substrates for fluorescence-based assays: All peptide substrates for fluorescence-based assays were kindly provided as lyophilized solids by the Steinmetzer research group. The tripeptide PhAc-Lys-Arg-Arg-AMC (MI-0084) was used for measurements with the DENV2, DENV3, and bDENV4 protease, and the tetrapeptide PhAc-Leu-Lys-Lys-Arg-AMC (MI-624) for measurements with the bZIKV protease. Substrate stock solutions were prepared by dissolving a given amount of solid in dist. H_2O, resulting in a 100 mM concentration. The stock solutions were stored at -20 °C.

Small molecule compounds: Stock solutions of small molecule compounds were prepared by dissolving a given amount of solid in DMSO, resulting in a 100 mM concentration and were stored at -20 °C.

Measurements of fluorescence emission: Experiments, in which a fluorescence emission signal was measured were conducted in black 96-well plates (Nunc™, Thermo Scientific™) on a Tecan Saphire^2 plate reader (Tecan, Männedorf, Switzerland). All data points were measured as technical triplicates.

5.3.2 Determination of Enzyme Kinetic Parameters

Enzyme kinetic parameters (K_M and v_{max}) for the DENV3-I123F and DENV-I123W mutants and for the bDENV4 protease were determined by measuring the increase in fluorescence emission upon cleavage of the fluorogenic substrate over time (λ_{ex} = 380 nm, λ_{em} = 460 nm). Measurements were performed at 37 °C for 20 cycles, each cycle consisting of a 20 s measurement and 5 s shaking. The composition of each well was as follows: 125 μL assay buffer, 25 μL protein solution and 50 μL substrate solution. For DENV3-I123F and DENV3-I123W, the final protein concentration in the well was 50 nM, whereas for bDENV4, the final protein concentration was 30 nM. Fluorescence emission was measured at six different substrate concentrations, namely 5, 10, 15, 20, 25, and 50 μM for both DENV3 mutants and 2.5, 5.0, 7.5, 10, 15, and 20 μM for the bDENV4 protease. The experiments were started by addition of the protease solution with a 8-channel pipette (Xplorer®, Eppendorf). The reaction rate for each concentration was determined by plotting the increase in fluorescence signal versus time and linear regression of the obtained data (MS Excel). The enzyme kinetic parameters were then determined by Lineweaver-Burk plot analysis, plotting the reciprocal reaction rate vs. the concentration and linear regression of the obtained data (MS Excel).

5.3.3 Determination of Inhibition Values and IC_{50} Values

In order to determine the percentage inhibition values of small molecule inhibitors, the increase in fluorescence emission upon cleavage of the fluorogenic substrate was measured over time for a given inhibitor concentration (λ_{ex} = 380 nm, λ_{em} = 460 nm). Measurements were performed at 37 °C for 60 cycles, each cycle consisting of a 20 s measurement and 5 s shaking. The composition of each well was as follows: 168 μL assay buffer, 10 μL protein solution, 20 μL substrate solution and 2 μL inhibitor solution (in DMSO) or DMSO. For DENV2 and DENV3 protease, the final protein concentration in each well was 50 nM, whereas for bDENV4 and bZIKV protease, the final protein concentration was 30 nM. For DENV2 and bDENV4 protease, the final substrate concentration in each well was 20 μM, for DENV3 protease 40 μM and for bZIKV protease 10 μM. Before addition of the substrate, the protein-inhibitor mixture was incubated at RT for 30 min. Then, the measurement was started by adding the substrate solution using a 8-channel pipette (Xplorer®, Eppendorf). The reaction rate for each inhibitor concentration was determined by plotting the increase in fluorescence signal against time and linear regression of the obtained data (GraphPad Prism 7.0). The percentage inhibition was then calculated as the quotient of the reaction rate for a given concentration and the reaction rate of the DMSO control.

In order to determine the IC_{50} value of a small molecule inhibitor, the respective percentage inhibition was measured for at least eight different concentrations covering the entire possible range of inhibition for the respective inhibitor. The obtained data were then plotted as log(concentration) vs. remaining activity (100% - percentage inhibition) and fitted with GraphPad Prism 7.0 using the option "log(inhibitor) vs. normalized response - variable slope".

5.3.4 Tryptophan Quenching Assay

In the tryptophan quenching assay, fluorescence emission from the tryptophan residues of DENV3 protease was measured at λ_{ex} = 280 nm and λ_{em} = 340 nm. Five cycles, each consisting of 10 s measurement and 5 s shaking, were recorded at RT, and the respective value was calculated as the average of these five data points. The composition of each well was as follows: 186 μL assay buffer, 10 μL protein solution, 2 μL inhibitor solution (in DMSO) or DMSO and 2 μL aprotinin solution (in H_2O). The final protein concentration in each well was 20 μM, as was the final aprotinin concentration. Fluorescence quenching was determined for four different inhibitor concentrations, namely 0, 5, 50, and 100 μM. Before the measurement started, the protein-inhibitor mixture was incubated at RT for 30 min. Then the fluorescence emission was determined and subsequently aprotinin was added and the fluorescence emission was measured again. The relative fluorescence quenching for each inhibitor concentration was determined as the quotient of the fluorescence emission at the respective concentration and the DMSO control.

6 Bibliography

[1] M. A. M. Behnam, C. Nitsche, V. Boldescu, C. D. Klein, *J. Med. Chem.* **2016**, *59*, 5622–5649.

[2] M. S. Diamond, T. C. Pierson, *Cell* **2015**, *162*, 488–492.

[3] C. Nitsche, S. Holloway, T. Schirmeister, C. D. Klein, *Chem. Rev.* **2014**, *114*, 11348–11381.

[4] S. M. Best, *Curr. Biol.* **2016**, *26*, R1258–R1260.

[5] A. T. Bäck, A. Lundkvist, *Infect. Ecol. Epidemiol.* **2013**, *3*, 19839.

[6] S. Nasar, N. Rashid, S. Iftikhar, *J. Med. Virol.* **2020**, *92*, 941–955.

[7] S. B. Halstead, *Lancet* **2007**, *370*, 1644–1652.

[8] K. Fatima, N. I. Syed, *J. Glob. Health* **2018**, *8*, 010312.

[9] M. A. M. Behnam, C. D. Klein, *Biochimie* **2020**, *174*, 117–125.

[10] E. Di Cera, *IUBMB life* **2009**, *61*, 510–515.

[11] L. Hedstrom, *Chem. Rev.* **2002**, *102*, 4501–4524.

[12] C. Nitsche, V. N. Schreier, M. A. M. Behnam, A. Kumar, R. Bartenschlager, C. D. Klein, *J. Med. Chem.* **2013**, *56*, 8389–8403.

[13] K.-H. Lin, A. Ali, L. Rusere, D. I. Soumana, N. Kurt Yilmaz, C. A. Schiffer, *J. Virol.* **2017**, *91*, e00045–17.

[14] J. Li, S. P. Lim, D. Beer, V. Patel, D. Wen, C. Tumanut, D. C. Tully, J. A. Williams, J. Jiricek, J. P. Priestle, J. L. Harris, S. G. Vasudevan, *J. Biol. Chem.* **2005**, *280*, 28766–28774.

[15] A. E. Shannon, M. M. Pedroso, K. J. Chappell, D. Watterson, S. Liebscher, W. M. Kok, D. P. Fairlie, G. Schenk, P. R. Young, *Scient. Rep.* **2016**, *6*, 37539.

[16] P. Erbel, N. Schiering, A. D'Arcy, M. Renatus, M. Kroemer, S. P. Lim, Z. Yin, T. H. Keller, S. G. Vasudevan, U. Hommel, *Nature Struct. Mol. Biol.* **2006**, *13*, 372–373.

[17] C. G. Noble, C. C. Seh, A. T. Chao, P. Y. Shi, *J. Virol.* **2012**, *86*, 438–446.

[18] S. Chandramouli, J. S. Joseph, S. Daudenarde, J. Gatchalian, C. Cornillez-Ty, P. Kuhn, *J. Virol.* **2010**, *84*, 3059–3067.

[19] M. Yildiz, S. Ghosh, J. A. Bell, W. Sherman, J. A. Hardy, *ACS Chem. Biol.* **2013**, *8*, 2744–2752.

[20] Y. Yao, T. Huo, Y.-L. Lin, S. Nie, F. Wu, Y. Hua, J. Wu, A. R. Kneubehl, M. B. Vogt, R. Rico-Hesse, Y. Song, *J. Am. Chem. Soc.* **2019**, *141*, 6832–6836.

[21] D. Luo, T. Xu, C. Hunke, G. Grüber, S. G. Vasudevan, J. Lescar, *J. Virol.* **2008**, *82*, 173–183.

[22] D. Luo, N. Wei, D. N. Doan, P. N. Paradkar, Y. Chong, A. D. Davidson, M. Kotaka, J. Lescar, S. G. Vasudevan, *J. Biol. Chem.* **2010**, *285*, 18817–18827.

[23] A. C. Gibbs, R. Steele, G. Liu, B. A. Tounge, G. T. Montelione, *Biochemistry* **2018**, *57*, 1591–1602.

[24] L. de La Cruz, W.-N. Chen, B. Graham, G. Otting, *FEBS* **2014**, *281*, 1517–1533.

[25] Y. M. Kim, S. Gayen, C. Kang, J. Joy, Q. Huang, A. S. Chen, J. L. K. Wee, M. J. Y. Ang, H. A. Lim, A. W. Hung, R. Li, C. G. Noble, T. Le Lee, A. Yip, Q.-Y. Wang, C. S. B. Chia, J. Hill, P.-Y. Shi, T. H. Keller, *J. Biol. Chem.* **2013**, *288*, 12891–12900.

[26] M. E. Hill, M. Yildiz, J. A. Hardy, *Biochemistry* **2019**, *58*, 776–787.

[27] H. Wu, S. Bock, M. Snitko, T. Berger, T. Weidner, S. Holloway, M. Kanitz, W. E. Diederich, H. Steuber, C. Walter, D. Hofmann, B. Weißbrich, R. Spannaus, E. G. Acosta, R. Bartenschlager, B. Engels, T. Schirmeister, J. Bodem, *Antimicrob. Agents Chemother.* **2015**, *59*, 1100–1109.

[28] M. Brecher, Z. Li, B. Liu, J. Zhang, C. A. Koetzner, A. Alifarag, S. A. Jones, Q. Lin, L. D. Kramer, H. Li, *PLoS pathogens* **2017**, *13*, e1006411.

[29] R. Grinter, *Questionable Ligand Density: 6MO0, 6MO1, 6MO2*, **08.04.2021**, https://www.mail-archive.com/ccp4bb@jiscmail.ac.uk/msg47072.html.

[30] T. J. Green, *Re: Questionable Ligand Density: 6MO0, 6MO1, 6MO2*, **08.04.2021**, https://www.mail-archive.com/ccp4bb@jiscmail.ac.uk/msg47086.html.

[31] Aleshin, A.E., Shiryaev, S.A., Liddington, R.C., *Structure of Zika virus NS2b-NS3 protease mutant stabilizing the super-open conformation*, **08.04.2021**, https://www.rcsb.org/structure/6UM3.

[32] D. Leung, K. Schroder, H. White, N. X. Fang, M. J. Stoermer, G. Abbenante, J. L. Martin, P. R. Young, D. P. Fairlie, *J. Biol. Chem.* **2001**, *276*, 45762–45771.

[33] K. Vashisht, C. Prashar, Tyagi S., G. Rawat, Kumari P., K. C. Pandey, *Dengue Bulletin* **2021**, *41*, 31–38.

[34] S. Robert, B. K. Wagner, M. Boulanger, M. Richer, *The Annals of pharmacotherapy* **1996**, *30*, 372–380.

[35] S. Chanprapaph, P. Saparpakorn, C. Sangma, P. Niyomrattanakit, S. Hannongbua, C. Angsuthanasombat, G. Katzenmeier, *Biochem. Biophys. Res. Com.* **2005**, *330*, 1237–1246.

[36] Z. Yin, S. J. Patel, W.-L. Wang, G. Wang, W.-L. Chan, K. R. R. Rao, J. Alam, D. A. Jeyaraj, X. Ngew, V. Patel, D. Beer, S. P. Lim, S. G. Vasudevan, T. H. Keller, *Bioorg. Med. Chem. Lett.* **2006**, *16*, 36–39.

[37] S. Xu, H. Li, X. Shao, C. Fan, B. Ericksen, J. Liu, C. Chi, C. Wang, *J. Med. Chem.* **2012**, *55*, 6881–6887.

[38] M. A. M. Behnam, C. Nitsche, S. M. Vechi, C. D. Klein, *ACS Med. Chem. Lett.* **2014**, *5*, 1037–1042.

[39] M. A. M. Behnam, D. Graf, R. Bartenschlager, D. P. Zlotos, C. D. Klein, *J. Med. Chem.* **2015**, *58*, 9354–9370.

[40] J. Kouretova, M. Z. Hammamy, A. Epp, K. Hardes, S. Kallis, L. Zhang, R. Hilgenfeld, R. Bartenschlager, T. Steinmetzer, *J. Enzym. Inhib. Med. Chem.* **2017**, *32*, 712–721.

[41] N. J. Braun, J. P. Quek, S. Huber, J. Kouretova, D. Rogge, H. Lang-Henkel, E. Z. K. Cheong, B. L. A. Chew, A. Heine, D. Luo, T. Steinmetzer, *ChemMedChem* **2020**, *15*, 1439–1452.

[42] V. K. Ganesh, N. Muller, K. Judge, C.-H. Luan, R. Padmanabhan, K. H. M. Murthy, *Bioorg. Med. Chem.* **2005**, *13*, 257–264.

[43] X. Koh-Stenta, J. Joy, S. F. Wang, P. Z. Kwek, J. L. K. Wee, K. F. Wan, S. Gayen, A. S. Chen, C. Kang, M. A. Lee, A. Poulsen, S. G. Vasudevan, J. Hill, K. Nacro, *Drug Des. Dev. Ther.* **2015**, *9*, 6389–6399.

[44] H. Lai, G. Sridhar Prasad, R. Padmanabhan, *Antiv. Res.* **2013**, *97*, 74–80.

[45] H. N. Saleem, F. Batool, H. J. Mansoor, S. Shahzad-ul Hussan, M. Saeed, *ACS Omega* **2019**, *4*, 1525–1533.

[46] M. Hariono, S. B. Choi, R. F. Roslim, M. S. Nawi, M. L. Tan, E. E. Kamarulzaman, N. Mohamed, R. Yusof, S. Othman, N. Abd Rahman, R. Othman, H. A. Wahab, *PloS one* **2019**, *14*, e0210869.

[47] S. Pach, T. M. Sarter, R. Yousef, D. Schaller, S. Bergemann, C. Arkona, J. Rademann, C. Nitsche, G. Wolber, *ACS Med. Chem. Lett.* **2020**, *11*, 514–520.

[48] C.-C. Yang, Y.-C. Hsieh, S.-J. Lee, S.-H. Wu, C.-L. Liao, C.-H. Tsao, Y.-S. Chao, J.-H. Chern, C.-P. Wu, A. Yueh, *Antimicrob. Agents Chemother.* **2011**, *55*, 229–238.

[49] J. Deng, N. Li, H. Liu, Z. Zuo, O. W. Liew, W. Xu, G. Chen, X. Tong, W. Tang, J. Zhu, J. Zuo, H. Jiang, C.-G. Yang, J. Li, W. Zhu, *J. Med. Chem.* **2012**, *55*, 6278–6293.

[50] B. Millies, F. von Hammerstein, A. Gellert, S. Hammerschmidt, F. Barthels, U. Göppel, M. Immerheiser, F. Elgner, N. Jung, M. Basic, C. Kersten, W. Kiefer, J. Bodem, E. Hildt, M. Windbergs, U. A. Hellmich, T. Schirmeister, *J. Med. Chem.* **2019**, *62*, 11359–11382.

[51] Z. Li, M. Brecher, Y.-Q. Deng, J. Zhang, S. Sakamuru, B. Liu, R. Huang, C. A. Koetzner, C. A. Allen, S. A. Jones, H. Chen, N.-N. Zhang, M. Tian, F. Gao, Q. Lin, N. Banavali, J. Zhou, N. Boles, M. Xia, L. D. Kramer, C.-F. Qin, H. Li, *Cell Res.* **2017**, *27*, 1046–1064.

[52] G. M. Morris, M. Lim-Wilby, *Methods Mol. Biol.* **2008**, *443*, 365–382.

[53] N. S. Pagadala, K. Syed, J. Tuszynski, *Biophys. Rev.* **2017**, *9*, 91–102.

[54] O. Trott, A. J. Olson, *J. Comput. Chem.* **2010**, *31*, 455–461.

[55] G. M. Morris, R. Huey, W. Lindstrom, M. F. Sanner, R. K. Belew, D. S. Goodsell, A. J. Olson, *J. Comput. Chem.* **2009**, *30*, 2785–2791.

[56] J. Gasteiger, M. Marsili, *Tetrahedron Lett.* **1978**, *19*, 3181–3184.

[57] J. Gasteiger, M. Marsili, *Tetrahedron* **1980**, *36*, 3219–3228.

[58] T. Sterling, J. J. Irwin, *J. Chem. Inf. Mod.* **2015**, *55*, 2324–2337.

[59] M. Dixon, *Biochem. J.* **1953**, *55*, 170–171.

[60] M. D. Shultz, *ACS Med. Chem. Lett.* **2014**, *5*, 2–5.

[61] K. Nepali, H.-Y. Lee, J.-P. Liou, *J. Med. Chem.* **2019**, *62*, 2851–2893.

[62] P. Champagne, J. Desroches, J.-F. Paquin, *Synthesis* **2015**, *47*, 306–322.

[63] A. Lee-Dutra, D. K. Wiener, K. L. Arienti, J. Liu, N. Mani, M. K. Ameriks, F. U. Axe, D. Gebauer, P. J. Desai, S. Nguyen, M. Randal, R. L. Thurmond, S. Sun, L. Karlsson, J. P. Edwards, T. K. Jones, C. A. Grice, *Bioorg. Med. Chem. Lett.* **2010**, *20*, 2370–2374.

[64] N. M. O'Boyle, M. Banck, C. A. James, C. Morley, T. Vandermeersch, G. R. Hutchison, *J. Cheminform.* **2011**, *3*, 33.

[65] F. Chevillard, H. Rimmer, C. Betti, E. Pardon, S. Ballet, N. van Hilten, J. Steyaert, W. E. Diederich, P. Kolb, *J. Med. Chem.* **2018**, *61*, 1118–1129.

[66] S. Wickham, N. Regan, M. B. West, V. P. Kumar, J. Thai, P. K. Li, P. F. Cook, M. H. Hanigan, *J. Enzym. Inhib. Med. Chem.* **2012**, *27*, 476–489.

[67] I. Çoruh, S. Rollas, S. Ö. Turan, J. Akbuğa, *Marmara Pharm. J.* **2012**, *16*, 56–63.

[68] C. Sambiagio, S. P. Marsden, A. J. Blacker, P. C. McGowan, *Chem. Soc. Rev.* **2014**, *43*, 3525–3550.

[69] P. L. López-Tudanca, L. Labeaga, A. Innerárity, L. Alonso-Cires, I. Tapia, R. Mosquera, A. Orjales, *Bioorg. Med. Chem.* **2003**, *11*, 2709–2714.

[70] S. Kodumuri, S. Peraka, N. Mameda, D. Chevella, R. Banothu, N. Nama, *RSC Adv.* **2016**, *6*, 6719–6723.

[71] B. Brandhuber, Y. Jiang, G. Kolakowski, S. Winski, *Array Biopharma Inc. (US)* **2014**, WO 2014/078322 A1.

[72] B. H. Lipshutz, R. W. Hungate, K. E. McCarthy, *J. Am. Chem. Soc.* **1983**, *105*, 7703–7713.

[73] C. Elschenbroich, *Organometallchemie*, Teubner, Wiesbaden, 5th ed., **2005**.

[74] H. Lineweaver, D. Burk, *J. Am. Chem. Soc.* **1934**, *56*, 658–666.

[75] M. Kanitz, *Dissertation*, Philipps-University Marburg, Marburg/Lahn, **2016**.

[76] M. Kuhnert, H. Köster, R. Bartholomäus, A. Y. Park, A. Shahim, A. Heine, H. Steuber, G. Klebe, W. E. Diederich, *Angew. Chem. Int. Ed.* **2015**, *54*, 2849–2853.

[77] A. Yammine, J. Gao, A. H. Kwan, *Bio-protocol* **2019**, *9*, e3253.

[78] T. Förster, *Ann. Phys.* **1948**, *437*, 55–75.

[79] C. Bodenreider, D. Beer, T. H. Keller, S. Sonntag, D. Wen, L. Yap, Y. H. Yau, S. G. Shochat, D. Huang, T. Zhou, A. Caflisch, X.-C. Su, K. Ozawa, G. Otting, S. G. Vasudevan, J. Lescar, S. P. Lim, *Analyt. Biochem.* **2009**, *395*, 195–204.

[80] J. Kramer, V. Désor, S. Brunst, S. K. Wittmann, J. Lausen, J. Heering, A. Proschak, E. Proschak, *Analyt. Biochem.* **2018**, *547*, 7–13.

[81] N. Kühl, M. M. Leuthold, M. A. M. Behnam, C. D. Klein, *J. Med. Chem.* **2021**, *64*, 4567–4587.

[82] T. Mosmann, *JIM* **1983**, *65*, 55–63.

[83] M. V. Berridge, A. S. Tan, *ABB* **1993**, *303*, 474–482.

[84] J. C. Stockert, A. Blázquez-Castro, M. Cañete, R. W. Horobin, A. Villanueva, *Acta histochemica* **2012**, *114*, 785–796.

[85] G. R. Fulmer, A. J. M. Miller, N. H. Sherden, H. E. Gottlieb, A. Nudelman, B. M. Stoltz, J. E. Bercaw, K. I. Goldberg, *Organometallics* **2010**, *29*, 2176–2179.

[86] R. C. Lang, C. M. Williams, M. J. Garson, *Org. Prep. Proc. Int.* **2003**, *35*, 520–524.

[87] N. Charrier, E. Demont, R. Dunsdon, G. Maile, A. Naylor, A. O'Brien, S. Redshaw, P. Theobald, D. Vesey, D. Walter, *Synthesis* **2006**, *2006*, 3467–3477.

[88] C. M. Marson, C. J. Matthews, E. Yiannaki, S. J. Atkinson, P. E. Soden, L. Shukla, N. Lamadema, N. S. B. Thomas, *J. Med. Chem.* **2013**, *56*, 6156–6174.

[89] N. Kinarivala, R. Patel, R.-M. Boustany, A. Al-Ahmad, P. C. Trippier, *J. Med. Chem.* **2017**, *60*, 9739–9756.

[90] M. Er, H. Tahtaci, T. Karakurt, A. Onaran, *J. Heterocyclic Chem.* **2019**, *56*, 2555–2570.

[91] J. Westman, *BE-TAGENON AB (Sweden)* **2010**, WO 2010/073011 A2.

[92] I. Wrona, P. Tivitmahaisoon, B. Pandy, K. Ozboya, M. Lucas, B. Le Bourdonnec, *Yumanity Therapeutics Inc. (US)* **2019**, WO 2019/209962 A1.

[93] T. Lübbers, P. Angehrn, H. Gmünder, S. Herzig, J. Kulhanek, *Bioorg. Med. Chem. Lett.* **2000**, *10*, 821–826.

[94] N. Suzuki, T. Miwa, S. Aibara, H. Kanno, H. Takamori, M. Tsubokawa, Y. Ryokawa, W. Tsukada, S. Isoda, *Chem. Pharm. Bull.* **1992**, *40*, 357–363.

[95] R. W. Carling, K. W. Moore, C. R. Moyes, E. A. Jones, K. Bonner, F. Emms, R. Marwood, S. Patel, A. E. Fletcher, M. Beer, B. Sohal, A. Pike, P. D. Leeson, *J. Med. Chem.* **1999**, *42*, 2706–2715.

7 Appendix

Erklärung

Ich versichere, dass ich die beiliegende Dissertation mit dem Titel „Design and Synthesis of Allosteric Inhibitors against Dengue Virus Protease“ selbständig ohne unerlaubte Hilfe angefertigt und mich dabei keiner anderen als der von mir ausdrücklich bezeichneten Quellen bedient habe. Alle vollständig oder sinngemäß übernommenen Zitate sind als solche gekennzeichnet.

Die Dissertation wurde in der jetzigen oder einer ähnlichen Form noch bei keiner anderen Hochschule eingereicht und hat noch keinen sonstigen Prüfungszwecken gedient.

Marburg, den 21. Oktober 2021

_____

Kerstin Mark